Deciphering the Relationship Among Nutrition, Host and Microbe

Denise Chac

A dissertation

submitted in partial fulfillment of the

requirements for the degree of

Doctor of Philosophy

University of Washington

2019

Reading Committee:

William DePaolo, Chair

Mohamed Oukka

Patricia Pavlinac

Program Authorized to Offer Degree:

Pathology

University of Washington

Abstract

Deciphering the relationship among nutrition, host and microbe

Denise Chac

Chair of the Supervisory Committee:

R. William DePaolo

Department of Medicine

Within the human gastrointestinal tract, there are trillions of resident microbes collectively known as the gut microbiota. These organisms have a profound impact on host physiology, particularly the immune system. Upon birth, the gut microbiota begins to take shape with input from various influences including genetics and environmental factors such as dietary habits, antibiotic use, and stress. While the gut microbiota has been shown to be necessary for proper development and immunity, it has also been implicated in the development of several environment linked diseases including non-alcoholic fatty liver disease (NAFLD), inflammatory bowel disease (IBD) and colorectal cancer (CRC). The consequences of the changing microbiota in these disease states and how the microbiota can be used therapeutically has yet to be fully explored. In this body of research, alterations to the microbiota due to diet (Chapter 2) and host genetics (Chapter 5 and 6) in the context of disease are analyzed. Environmental factors that influence the gut microbiota are also explored in the context of individual species (Chapter 3 and 4).

One of the key players in shaping the gut microbiota is diet. To study how dietary fats could alter host microbiota and liver pathology, various diets were used in a model of NAFLD. A NAFLD-inducing diet high in cholesterol and sucrose was used to induced steatosis and liver inflammation while two intervention diets of either low fat and low fiber or a high fish oil diet were developed. While switching from the NAFLD-inducing diet to either of the intervention diets drastically reduced the steatosis and

improved liver pathology, the corresponding microbiotas from the intervention diets were not sufficient to resolve hepatic steatosis and may even exacerbate the liver inflammation in the absence of dietary change (Chapter 2).

To study the effects of dietary factors directly on the microbes, dietary fatty acids were applied directly to the enteric pathogen, *Yersinia enterocolitica*. Arachidonic acid is an omega-6 fatty acid that is found in high concentrations in the Western diet and has been associated with inflammation. Therefore, this study analyzed how arachidonic acid altered the protein signature using a technique of matrix-assisted laser desorption/ionization time-of-flight mass spectrometry (MALDI-TOF MS) (Chapter 3) and virulence through both *in vitro* and *in vivo* assays. Following exposure to physiological levels of arachidonic acid, Y. enterocolitica became highly virulent with increased invasion into colonic epithelial cells and rapid systemic infection of mice (Chapter 4).

Another factor influencing the gut microbiota and, therefore the host immune response, is genetics. Development of the human immune system depends on various receptors capable of recognizing and responding to pathogens and commensals. These receptors include toll-like receptors (TLRs) found on macrophages, dendritic cells, and intestinal epithelial cells. Using TLR1 and TLR6 knockout mice, these studies aim to understand how disruption in host recognition of the microbiota can exacerbate disease. In Chapter 5, aberrant TLR1 signaling led to increased mucosal-adherent microbes and defective mucosal immunity. These changes consequently exacerbated the host response to a model of colonic injury and recovery. On the other hand, defective TLR6 signaling worsens the host susceptibility to inflammation associated colorectal cancer (Chapter 6). Within the same study, analyze of the microbiota revealed a potential therapeutic by restoring microbial ecology.

By investigating the various influences on the microbiota and the host in the context of nutrition and disease we can begin to understand the complexity of the microbiome and develop therapeutics. The diverse studies in this body of research ultimately reveal how environmental stimuli and disrupted sensing of the microbiota can have prolonged immunological impact.

Dedication

To my family and friends.

Acknowledgements

When I first applied to graduate school, I never expected I would end up here. The last five years have been an adventure with no shortage of obstacles and daring decisions. This journey would not have been successful without the many talented scientists I am extremely grateful for. Thanks to Amy Merrill for a wonderful first year rotation experience at the University of Southern California. Many thanks to Merrill lab members Cynthia Neben, Joanna Salva and Ryan Roberts. Thanks to Kian Kani for the wonderful mentorship and support during my first years at USC. Thanks to Andre Ouellette for the mentorship through my first PhD candidate qualifying exam at USC. Special thanks to the many researchers of the USC Program in Biomedical and Biological Sciences including Andrea Gadon, Tracy Tran, Sonya Liu and Priya Rangan for the support and friendship. Thanks to the directors of Molecular medicine and mechanisms of diseases including Nancy Maizels, Daniel Promislow and Conrad Liles for allowing my transfer from USC to UW and helping me keep the momentum throughout this transition. Thanks to the members of my doctoral supervisory committee including Mohamed Oukka and Lisa Strate for their time and guidance. Special thanks to Bill Mahoney and Patricia Pavlinac for their mentorship on my committee and support through the PhD process.

Thanks to all the members of the DePaolo lab that I have had the pleasure of working with and learning from. Thanks to Tania Mitsinikos for being an outstanding role model and mentorship on non-alcoholic fatty liver disease and gastroenterology. Thanks to Andrew Johnson for the guidance and support. Thanks to volunteers Kelly Crebs and Cara Lee for the assistance and enthusiasm for science. Thanks to Arushi Verma and Marion Avril for the support in the DePaolo Lab. Special thanks to Leandra Brettner and Melissa Kordahi for the continuous support and guidance through the PhD process. Finally, huge thanks to William DePaolo for accepting me as a graduate student and providing me the opportunity to become a researcher.

Thanks to my family and friends for their unconditional love and support. Thanks to Yin for being understanding of the crazy PhD hours. Thanks to my cousin Wynne for initiating my pursuit of a PhD in biomedical. Thanks to my sister Sylvia for 24/7 emotional support and being my personal physical therapist. Special thanks to my parents for being extremely understanding as I continued my career as a student.

Table of Contents

Abstract iii

Dedication v

Acknowledgements vi

List of Figures xi

Chapter 1. Introduction 1

1.1 Nutrition 1

1.1.A The dietary trends and diseases of hunter-gatherers 1

1.1.B The dietary trends and diseases of Western Civilization 2

1.2 Mucosal Immunology 2

1.2.A Specialized Intestinal epithelial cells 4

1.2.B Mucosal barrier 4

1.2.C Secretory Immunoglobulins 5

1.2.D Immune cells of the mucosal associated lymphoid tissue 5

1.3 Microbiome 11

1.3.A The Dynamic Microbial Landscape of the Intestine 11

1.3.B Microbiota: Initiator of disease and target of treatment 14

1.4 Dynamics concerning host, nutrition and microbes 20

1.5 References 22

Chapter 2. Modifying Macronutrients is Superior to Microbial Transplants in Reversing the Progression of Non-Alcoholic Fatty Liver Disease 34

2.1 Abstract 34

2.2 Introduction 35

2.3 Results 36

Non-alcoholic fatty liver disease (NAFLD)-inducing diet in rodent model can mimic liver pathology 36

Dietary intervention suppresses weight gain and reverses fat accumulation in the liver 39

Dietary intervention improves liver enzymes and cytokine levels 41

Fecal microbial communities from dietary interventions shift to more organized and central microbiotas *41*

Microbiota transplantation fails to relieve NAFLD symptoms and liver inflammation *44*

2.4 Discussion **47**

2.5 Materials and Methods **51**

2.6 Supplemental Tables and Figures **55**

2.7 References **62**

Chapter 3. Detection of Physiological Changes from Environmental Conditions through Matrix-Assisted Laser Desorption/Ionization – Time of Flight (MALDI-TOF) Mass Spectrometry **65**

3.2 Introduction **66**

3.3 Results & Discussion **68**

Peptide mass fingerprints distinguish genetic differences within microbial species *68*

PMFs distinguish phenotypic differences within genetically identical strains *72*

PMFs identify metabolic states of Y. enterocolitica during in vitro adhesion and invasion assay *74*

PMFs distinguish between fresh and frozen clinical isolates of the same species *76*

3.4 Conclusion **77**

3.5 Materials and Methods **78**

3.5 References **82**

Chapter 4. Polyunsaturated fatty acid arachidonic acid increases the virulence of gut pathogen, *Yersinia enterocolitica* **86**

4.2 Introduction **87**

4.3 Results **88**

Polyunsaturated fatty acids differentially affect proliferation of Yersinia enterocolitica *88*

Arachidonic acid increases intracellular invasion of Yersinia enterocolitica in vitro *90*

Arachidonic acid alters the peptide mass fingerprint of Yersinia enterocolitica *90*

Arachidonic acid induces a virulent state in Yersinia enterocolitica *91*

Y. enterocolitica becomes more virulent in vivo after exposure to arachidonic acid *92*

4.4 Discussion **93**

4.5 Materials and Methods 96

4.6 Supplemental Material 100

4.7 References 104

Chapter 5. Innate Recognition of the Microbiota by TLR1 Promotes Epithelial Homeostasis and Prevents Chronic Inflammation 108

5.1 Abstract 108

5.2 Introduction 109

5.3 Results 110

TLR1-deficiency is associated with mucosal-associated bacteria, gut permeability, and systemic bacteria 110

Elevated innate immune responses in TLR1-deficient mice 112

TLR1-sensing of the microbiota by nonhematopoietic cells restrains innate immune responses 114

TLR1 signaling contributes to homeostasis of the colonic epithelium 117

TLR1 signaling restrains microbiota-induced epithelial cell proliferation 120

TLR1 deficiency exacerbates tissue injury and prevents epithelial healing 122

5.4 Discussion 126

5.5 Materials and Methods 130

5.7 Supplemental Materials 135

5.6 References 138

Chapter 6. TLR6 Signaling Prevents Inflammation and Impacts Composition of the Microbiota During Inflammation-Induced Colorectal Cancer 143

6.1 Abstract 143

6.2 Introduction 144

6.3 Results 145

TLR6 deficiency exacerbates inflammation-associated CRC, while co-housing protects WT mice 145

Both genotype and housing influence dysbiosis associated with AOM/DSS 149

Restoring commensals ameliorates disease and reduces inflammatory cytokines in WT mice via a TLR6-dependent mechanism. 152

IL-10 is responsible for the partial reduction in tumor number but is dispensable for changes in the microbiota *155*

Impaired apoptosis during AOM/DSS in TLR6-deficient mice *158*

6.4 Discussion **160**

6.5 Materials and Methods **162**

6.6 Supplemental Materials **168**

6.7 References **169**

Chapter 7. Conclusions and Perspectives **173**

List of Figures

Figure 2.1: Liver inflammation and steatosis induced by a diet high in fructose, cholesterol and low in fiber....37

Figure 2.2: Both a high fat/high fiber and a low fat/low fiber diet can reverse the progression of NAFLD. 40

Figure 2.3: HFF and LFF diets cause distinct shifts in the composition of the microbiota following dietary intervention....43

Figure 2.4: HFF or LFF diet-educated microbiota alone is not sufficient to reverse NAFLD. 46

Figure 3.1: Differentiation of bacterial genetic mutants on MALDI-TOF MS....70

Figure 3.2: Differentiation of bacterial biological environments on MALDI-TOF MS....74

Figure 3.3: PMF Analysis of Y. enterocolitica virulence states....75

Figure 3.4: PMF analysis of fresh and frozen clinical isolates....76

Figure 4.1: Arachidonic acid increases proliferation and intracellular invasion of Y. enterocolitica....89

Figure 4.2: Exposure to AA alters invasion and PMF of Y. enterocolitica....91

Figure 4.3: AA alters the virulence state of Y. enterocolitica....92

Figure 4.4: Exposure to AA increases virulence of Y. enterocolitica in vivo 93

Figure 5.1: Expression of TLR1 prevents mucosal-associated bacteria and their translocation to the periphery 111

Figure 5.2: TLR1 deficiency is associated with disturbed immune homeostasis in the colonic LP. 113

Figure 5.3: The microbiota of the TLR1KO mice are required for homeostatic immune regulation.....115

Figure 5.4: Aberrant immune activation is due to loss of TLR1 signaling in the epithelium....117

Figure 5.5: Reduced mucus secretion and an increase in antibacterial peptides occur in the colonic crypt in the absence of TLR1 signaling....119

Figure 5.6: Endogenous TLR1 signaling regulates colonic crypt proliferation. 121

Figure 5.7: Loss of TLR1 exacerbates DSS-induced cytokine production and prevents colonic repair. .123

Figure 5.8: IFN-γ contributes to the mortality observed in the context of TLR1 deficiency.....125

Figure 6.1: TLR6 signaling reduces the severity of inflammation-associated colorectal cancer 146

Figure 6.2: Colonic lysates from co-housed mice are less inflammatory and induce IL-10 in a TLR6-dependent manner. 148

Figure 6.3: Compositional changes within the microbiota are influenced by TLR6 expression and housing status. 150

Figure 6.4: Restoration of Lactobacillus reduces tumor burden and suppresses inflammation in a TLR-6 dependent and independent manner. 153

Figure 6.5: Requirement for IL-10 dissociates Lactobacillus effects on inflammation and composition. 157

Figure 6.6: Proliferation and apoptosis of colonocytes are altered in TLR6KO mice. 159

List of Diagrams

Diagram 1.1: Protective factors in the intestines 3

Diagram 1.2: Navigating the complex landscape of the microbiome 19

Diagram 3.1: MALDI-TOF MS methodology 68

List of Tables

Table 1.1: Studies of PRR impact on microbiota 8

Table 3.1: Environmental influences on MALDI-TOF MS analyses 71

List of Supplemental Figures

Supplemental Figure 2.1: Phylum abundance of NAFLD and intervention diet microbiota 58

Supplemental Figure 2.2: Heat map of family abundance of ileal microbiota of NAFLD and intervention diet mice 59

Supplemental Figure 2.3: Adipose tissue weight of mice following microbiota transplant 60

Supplemental Figure 2.4: Heat map of family abundance of fecal microbiota of microbiota transplant mice 61

Supplemental Figure 4.1: Growth of Y. enterocolitica with PUFAs at 37C 100

Supplemental Figure 4.2: Invasion of Y. enterocolitica with altered ratios of AA and EPA 101

Supplemental Figure 4.3: Dendrogram of Y. enterocolitica PMF with cellular assay 102

Supplemental Figure 4.4: Flow diagram of percentage and number of mice with Y. enterocolitica colonization 103

Supplemental Figure 5.1: Expression of claudin 2 and claudin 3 in colonic mucosal scrapings 135

Supplemental Figure 5.2: PCoA of colon mucosal-associated bacteria communities 136

Supplemental Figure 5.3: Expression of stem-cell and notch-signaling genes of colonic mucosa.....137

Supplemental Figure 6.1: TLR6 signaling impacts dysbiosis associated with AOM/DSS.....168

List of Supplemental Tables

Supplemental Table 2.1: Nutrient Breakdown of NAFLD and intervention Diets.....55

Supplemental Table 2.2: Relationship between Erysipelotrichaceae and Verrucomicrobiaceae.....56

Supplemental Table 2.3: Relationship among bacterial families and weight change 57

Chapter 1. Introduction

1.1 Nutrition

The U.S. and the rest of the world that has imported our dietary habits is eating itself into disease. Diet is the leading risk factor for mortality in the U.S with over 500,000 diet-related deaths, considerably surpassing mortality by tobacco use, high blood pressure and high BMI[1]. Globally, 11 million deaths, or 1 in 5 deaths, are associated with dietary risk factors[2,3]. These top deaths include cardiovascular disease, cancer, and type II diabetes from consuming too little whole grains and fruits with too much sodium[2]. Jared Diamond said it best with his 1987 article calling agriculture “the worst mistake in the history of the human race”[4].

According to Diamond’s infamous article, when the world began to domesticate plants and animals, our agricultural revolution scarified a varied, quality diet for cheap calories and quantity[4]. This idea has since bloomed as researchers note the marked rise of chronic diseases, so called “diseases of civilization”[5] or "Western diseases"[6,7]. According to the evolutionary discordance hypothesis, these diseases stem from the rapid change from the Paleolithic diets and lifestyles to the modern ones. Given the recent statistics of diet-related diseases, it is hard to argue with Diamond’s statement.

1.1.A The dietary trends and diseases of hunter-gatherers

Information regarding pre-agricultural diet compositions of hunter-gatherers relies on archeological evaluations of human remains through carbon isotype compositions and studies of the environmental resources. Diet is also studied through analysis of modern hunter-gatherers and foragers including the BaAka[8], Yanomami[9], and Hadza[10,11]. While diet composition is often reflective of the environment and can drastically alter macronutrient levels, the average macronutrients of hunter gatherer societies is 19-35% protein, 22-40% carbohydrates and 28-47% fats[12,13]. Despite relatively high fat, hunter-gatherers were free of cardiovascular diseases and had low levels of cholesterol[13]; this could be attributed to consumption of the more “good fats” such as monounsaturated and polyunsaturated fatty acids [13,14].

1.1.B The dietary trends and diseases of Western Civilization

Not only did the Agricultural Revolution limit the variety of foods and increase the availability of grains and dairy products, the Industrial Revolution introduced refined grains, refined vegetable oils, refined sugars (sucrose), high-fructose corn syrup and the "fast food" era[15,16]. The overall macronutrient composition of the average U.S. diet is 15.4% protein, 51.8% carbohydrates and 32.8% fats[15]. The nutrient trends of the Western diet include high glycemic load carbohydrates, increased sodium-potassium ratio, high saturated fats from animal products and refined seed oils, high omega-6 to omega-3 fatty acids, and low fiber intake. Diseases attributed to these dietary patterns include obesity[17], cardiovascular disease[18,19], type II diabetes[20,21], cancer[19,22], diverticulitis[23,24], non-alcoholic fatty liver disease[25,26], inflammatory bowel disease[27,28], and irritable bowel syndrome[29,30]. In conjunction to the epidemiological evidence of westernized diets leading to disease, the correlation between diet and disease has also been validated in mouse models of the same diseases [31-35]. To better understand how dietary trends can affect the health of the individual, nutritional status must be studied in the context of the multifaceted mucosal immune system and the commensal microbiota.

1.2 Mucosal Immunology

The gastrointestinal (GI) tract is one of the most complex organs in the human body. As the GI tract is constantly exposed to foreign antigens, it has a multitude of protective features to fight off infections and coexist with the millions of resident microbes known as the microbiota. With specialized epithelial cells, a physical barrier of mucus, gut-specific immunoglobulins and a pool of mixed immune cells in the lamina propria, intestinal homeostasis can be maintained through a concert of innate and adaptive responses (Diagram 1.1). The gut immune system has become well adapted to the relentless encounters with food antigens and potentially pathogenic microorganisms.

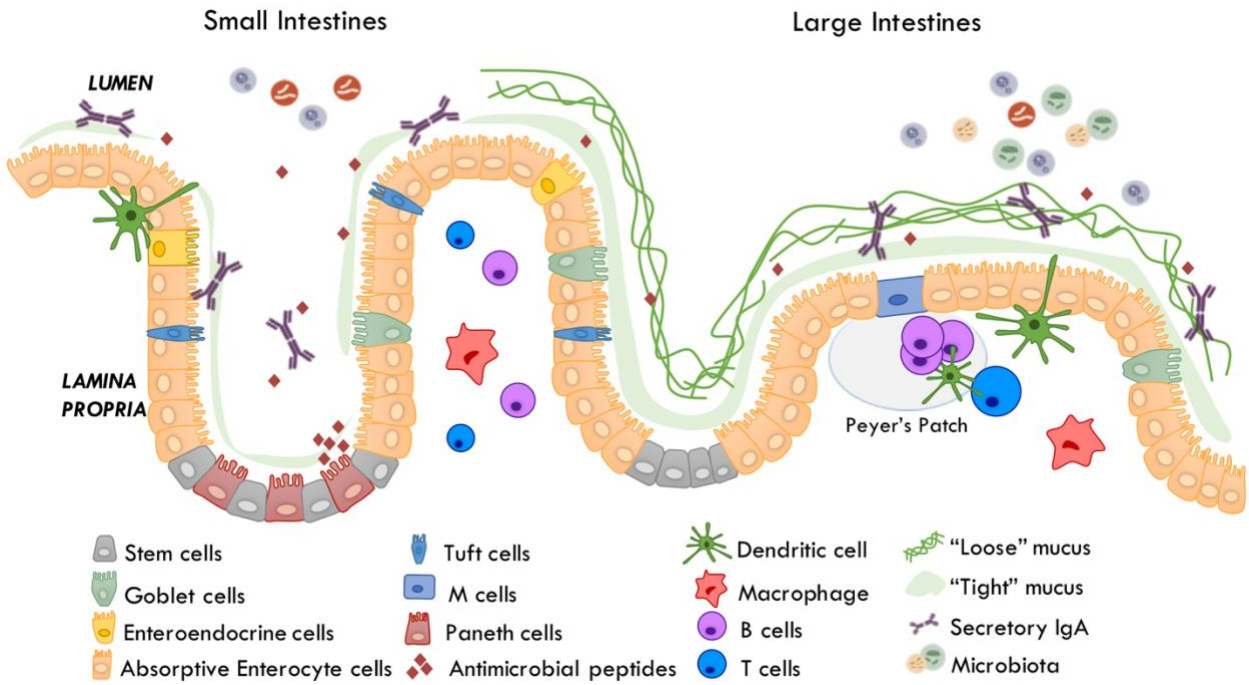

Diagram 1.1: Protective factors in the intestines

Within the intestines, the intestinal epithelial cells and mucosal barrier separate the external stimuli in the lumen from the various immune cells of the lamina propria. The specialized epithelial cells include (1) regenerative stem cells, (2) mucus-producing goblet cells, (3) hormone-releasing enteroendocrine cells, (4) absorptive enterocyte cells, (5) chemosensory tuft cells, (6) antigen-sampling "microfold" M cells and (7) antimicrobial peptide secreting Paneth cells. The mucosal layers provide physical and chemical barriers through the constant renewal and movement of mucus and trapping of antimicrobial peptides and secretory IgAs. Residing in the lumen on top of the mucus is the commensal microbiota. Within the lamina propria are T-cells, antibody producing B-cells, dendritic cells and macrophages.

1.2.A Specialized Intestinal epithelial cells

The GI tract starts at the mouth and ends with the anus. Throughout this open-ended tube, a single layer of epithelial cells separate the external environment from access to the host's immune cells. In addition to digesting foods, absorbing nutrients and expelling waste, the intestinal epithelium is populated with specialized cells that produce antimicrobial peptides, mucus and enteric hormones. Structurally, the small intestine is a tube of finger-like projections in the lumen called villi and the deep troughs between are the crypts. At the base of the crypts are a cluster of undifferentiated stem cells that regenerate and differentiate into the various cell types including absorptive enterocytes, enteroendocrine cells, goblet cells, M cells and Paneth cells. Comparatively, the large intestines (colon) lacks the long, projecting villi and Paneth cells but have more goblet cells.

Paneth cells are secretory cells that synthesize and secrete antimicrobial peptides (AMPs)[36]. Located between the small intestinal stem cells at the base of the crypt, these cells provide both grooming of the gut microbiota and protection from pathogens. Several *in vivo* studies altering the genes Paneth cell highlight its role in protection against pathogens[37–39], prevention of bacterial translocation[38] and maintenance of the microbiota[40].

Another type of specialized secretory cells are goblet cells. Rather than produce targeted molecules, goblet cells produce mucins and have largely been underappreciated as an immune cell until the last decade[41,42]. While present along the whole intestines, goblet cells secrete MUC2 mucins in the small intestines upon stimulation while mucin is continuously secreted in the colon. Layers of mucins blanket the intestinal epithelial cells, providing a buffer zone or a "demilitarized zone" that is devoid of microorganisms[43]. Disruption in the mucus layers can lead to increased bacterial translocation[44], intestinal permeability[45] and chemical damage from dextran sodium sulfate[44,46].

1.2.B Mucosal barrier

The intestinal mucus barrier acts as both a physical and chemical barrier. The physical layers of mucus vary location with one thick layer in the small intestines and an additional second loose layer in the colon. In the small intestines where there is nutrient absorption, the mucosal layer is loose and unattached[47] with

rapid mucus renewal by villi-associated goblet cells[48]. The rapid flow of mucus prevents bacterial adhesion[49]. Additionally, antimicrobial peptides secreted by the crypt-residing Paneth cells provide an additional protection[38,50,51].

Further down, the colon has a two-layered system with an attached inner layer and a loose outer layer. In addition to fast mucosal turn over [52,53], the mucosal layer acts as a filter and prevents penetration of molecules greater than 0.5 um[44]. While the colon does not have Paneth cells, AMPs can be readily found in the human[54,55] and murine colonic mucosa[56,57]. The colon is also home to the microbiota which is not only necessary for proper mucus production and development[53,58,59], but different microbiota compositions can alter the penetrability of the mucosal layer[60,61] and bacterial colonization[62].

1.2.C Secretory Immunoglobulins

In addition to the various anti-microbial molecules, the mucus is also home to secretory antibodies. The most abundant antibody in the intestines and other mucosal secretions is secretory IgA (sIgA), a dimeric antibody secreted by plasma cells and trancytosed into the lumen by intestinal epithelial cells after binding to the polymeric immunoglobulin receptor. Nested in the mucus, sIgA bind both commensal and pathogenic microbes. SIgA functions to regulate the host response to commensal microbes[63], carry pathogenic antigens to lymphoid cells [64,65] and neutralize microbes[65–67] and toxins[68,69].

1.2.D Immune cells of the mucosal associated lymphoid tissue

Underneath all the layers of the mucus and intestinal epithelial cells lies the lamina propria consisting of loose connective tissue harboring a pool of immune cells. At the crux of proper recognition and response are the pattern recognition receptors (TLRs, NLRs). The intestinal tract is a complex environment populated with gut commensal microbes and constant flow of external molecules in which the mucosal immune cells must constantly differentiate self from non-self and pathogenic from non-pathogenic antigens.

Pattern Recognition Receptors

Pattern recognition receptors (PRRs) are germline-encoded sensors heralding the first response to infections. By recognizing common structures of pathogens and commensal microbes, PPRs enable a quick

and broad response by macrophages and dendritic cells. PRRs recognize pathogen-associated molecular patterns (PAMPs) and can be grouped into 3 categories: Toll-like receptors (TLRs), NOD-like receptors (NLRs), and RIG-I-like receptors.

Toll-like receptors – There are 10 and 13 TLRs in human and mice, respectively. TLRs are composed of a large extracellular domain responsible for recognition, a short transmembrane region, and a short intracellular domain responsible for homo- or heterodimeric interactions and downstream signaling. They are expressed either on the cell surface (i.e. TLR1, TLR2, TLR4, TLR5, andTLR6), internally on endosomal membranes (TLR3, TLR7, TLR8, and TLR9). The location of TLRs enable their recognition of specific ligands. The extracellular TLRs recognize outer structural components of microorganism such as peptidoglycans by TLR1/2, tri- and di-acylated lipoproteins by TLR1/2 and TLR2/6, LPS and lipoteichoic acids by TLR4 and flagellin by TLR5. Endosomal-bound TLRs recognize internal viral and bacterial components such as double- and single-stranded RNA by TLR3 and TLR7, G-rich oligonucleotides by TLR8 and unmethylated CpG DNA by TLR9. While TLRs are expressed on phagocytic cells and lymphocytes, TLRs are also expressed on intestinal epithelial cells.

NOD-like receptors – Unlike the TLRs, NLRs are exclusively in the cytosol and sense intracellular molecules. The 23 NLRs found in humans are divided into the five subfamilies depending on effector domains. Of the NLR families, NLRC and NLRP families have important immune regulations within the intestinal mucosa. NLRC receptors contain a caspase recruitment domain (CARD) and include NOD1 and NOD2 that recognize bacteria peptidoglycan structures and motifs. NLRP have a pyrin domain and activate the inflammasomes following PAMP recognition.

RIG-like receptors – RLRs recognize viral pathogens through ligands of poly-uridine rich RNA motifs and long double-stranded RNAs.

The innate TLRs and NLRs preserve mucosal homeostasis through broad recognition of pathogens with a rapid response to eliminate pathogens. While we are still learning how these PRRs are regulated, studies

have shown that they are necessary for intestinal cell regulation. Signaling through PRRs are linked to expression of tight junction proteins[70,71], regulation of host metabolic genes[72–74], disruption of mucus layer[75], intestinal angiogenesis[76] and even intestinal hormone levels[77,78]. Defects in TLR and NLR signaling are also linked to chronic inflammatory diseases such as asthma[79–81], IBD[82–86] and colorectal cancer[87–92]. In addition to the role of innate sensors, the functional roles of PRRs need to be better studied especially in the context of shifting dietary trends and related microbiotas. There is undoubtedly an influence of TLRs and NLRs on the resident and passing microorganisms in the gut. However, it remains controversial if TLR or NLR signals are linked to specific microbiota compositions as there are several contradicting studies (Table 1.1)[72,

Table 1.1: Studies of PRR impact on microbiota

TLRs		Effect	Finding	Housing
Vijay-Kumar et al, 2010[94]	TLR5	Yes	• TLR5KO mice and WT littermates had similar levels of Firmicutes and Bacteroidetes but differed at the species-composition level. • TLR5KO microbiota also conferred metabolic syndrome in GF mice.	Samples were obtained post-weaning of multiple litters housed separately
Ubeda et al, 2012[98]	TLR2, TLR4, TLR5, TLR9	No	• No microbiota changes were observed in individually housed mice. Microbiota compositions were largely determined by maternal lineage. • Antibiotic treatment also did not differ between TLR-KOs.	Various litters were used and mice were housed separately
Chassaing et al, 2014[95]	TLR5, IEC specific	Yes	• IEC-TLR5KO microbiota was altered following 6 and 12 weeks single-housed by genotype but not at weaning. KO mice had increased Firmicutes/Bacteroidetes ratios. • Cohousing led to less distinction between microbiotas.	Single and cohousing
Chassaing et al, 2014[95]	TLR5, DC specific	No	• No effect on microbiota composition even with single-housing.	Single and cohousing
Zhang et al, 2016[99]	TLR5	No	• TLR5KO mice and WT did not vary in microbiota composition. These mice had equally high levels of Firmicutes. Compositional changes were compared to Vijay-Kumar 2010 results.	Single and cohousing
Lu et al, 2018[72]	TLR4, IEC specific	Yes	• IEC-TLR4KO led to decreased alpha-diversity with marked decreases in *Clostridiales, Turicibacter,* and increases of *Bacteroides, Deffibacteraceae, Odoribacteraceae,* and *Prevotella.* • Antibiotics and cohousing reduced TLR4KO-associated metabolic syndrome phenotypes in KO mice.	Single and cohousing affects observed but only single-housing microbiota analyzed
Kamdar et al, 2018[97]	TLR1	No	• TLR1KO mice and WT did not vary in microbiota composition or diversity.	Single and cohousing

Table 1.1 (continued): Studies of PPR impact on microbiota

TLRs		Effect	Finding	Housing
Xiao et al, 2019[96]	TLR4,	Yes	• TLR4KO mice had decreased *Bacteroides* and *Alloprevotella;* compositional changes were exasperated during Vitamin-A deficiency	Unsure if littermate controls were used and if there was cohousing
Kim et al, 2019	TLR6	Yes	• Single-housed TLR6KO mice had increased Lactobacillus • TLR6KO associated microbiota conferred protection against AOM/DSS induced colitis-associated CRC through cohousing	Single and cohousing
NLRs		**Effect**	**Finding**	**Housing**
Wen et al, 2008[105]	NOD Myd88	Yes	• NOD-MyD88 deficiency decreased ratio of firmicutes/bacteroidetes and high levels of sequences belonging to Porphyromonadaceae • Microbiota clustering was influenced by maternal lineage	Unsure if littermate controls were used and if there was cohousing
Petnicki-Ocwieja et al, 2009[101]	Nod2	Yes	• Nod2-/- mice had increased bacterial load and abundance of Bacteroidetes in the ileum.	Unsure if littermate controls were used and if there was cohousing
Elinav et al, 2011[102]	NLRP6	Yes	• Single-housed NLRP6-/- mice had increased Bacteroidetes and TM7 bacteria with reduced Lactobacilus • NLRP6-/- associated microbiota conferred susceptibility to DSS colitis in cohoused WT mice.	Single and cohousing
Couturier-Maillard et al, 2013[100]	Nod2	Yes	• Single-housed Nod2-/- mice had increased Bacteroidetes • Nod2-/- associated microbiota also conferred susceptibility to DSS colitis in cohoused WT mice and FMT with GF mice	Single and cohousing
Hu et al, 2013[103]	NLRP6	Yes	• NLRP6-/- associated microbiota conferred susceptibility to AOM/DSS induced colitis-associated CRC model through cohousing	Single and cohousing but microbiota not sequenced

Table 1.1 (continued): Studies of PPR impact on microbiota

NLRs		Effect	Finding	Housing
Robertson et al, 2013 [107]	Nod1 and Nod2	No	• Nod1-/-, Nod2-/-, and WT mice had similar microbiotas	Single and cohousing
Levy et al, 2015[104]	NLRP6	Yes	• NLRP6-/- and WT GF mice developed divergent microbiotas following spontaneous conventionalization.	Single and cohousing
Lemire et al, 2017[106]	NLRP6	No	• NLRP6-/- and WT mice have similar microbiotas and susceptibility to DSS colitis	Single and cohousing
Ringel-Scaia et al, 2019[108]	NLRP1b	Yes	• Single-housed NLRP1b-/- mice had increased Proteobacteria. Cohousing effects of maternal influences dominated genotype differences	Single and cohousing
Both		**Effect**	**Finding**	**Housing**
Larsson et al, 2012[93]	MyD88	Yes	• MyD88-deficienct mice had increasingly altered communities from the duodenum to the colon. These mice had marked increased segmented filamentous bacteria	Unsure if littermate controls were used and if there was cohousing
Ubeda et al, 2012[98]	MyD88	No	• No microbiota changes were observed in individually housed mice. Microbiota compositions were largely determined by maternal lineage. • Antibiotic treatment also did not differ between TLR-KOs	Various litters were used and mice were housed separately

1.3 Microbiome

Adapted from:

Chac *and DePaolo. 2016. The dynamic microbial landscape of the intestine and the impact of probiotic therapy.* Journal of Probiotics & Health 4:137.

A diverse, symbiotic ecosystem of microbes resides in our gut, contributing to the complexity of human health. As the most microbe-rich area of the human body, the gut microbiota provides a number of important physiological functions including metabolism, immunity, and protection from pathogens. Environmental factors, especially nutrition and dietary-components, can influence or even completely alter the microbial landscape and its functions. Currently, it is thought that under certain, but unknown, genetic and environmental contexts these changes can cause or exacerbate chronic inflammatory diseases. While using probiotics to treat disease seems like an easy solution, both basic and clinical data have demonstrated mixed results. Thus, it is imperative to re-examine probiotics in the complex context of both a healthy and diseased microbiome along with associated factors such as diet.

1.3.A The Dynamic Microbial Landscape of the Intestine

The human body is home to trillions of microorganisms, each with functions affecting the microenvironment of our bodies. From the different areas of the skin, to the start and finish of gastrointestinal (GI) tract, robust and vastly diverse communities of microbes thrive. While the human skin alone harbors microbes from 19 out of 100 different bacterial phyla[109,110], the human gut contains only 7[111], yet is home to 100 trillion microbes collectively referred to as our microbiota[112]. With these microbes, our GI tract represents a complex, multi- functional organ that is not only associated with digestion, but also with immunity, metabolism and resistance to pathogenic infection. The intestine contains multiple and unique physical, chemical, and structural features that define its anatomical landscape. These dramatically different, yet adjacent, geographies allow the colonization of microbes expressing certain genetic or virulence traits that allow them to survive. For those microbes not already expressing the necessary genes for colonization they will not survive or they will mutate and adapt to the microenvironment. Thus, the 9 million genes expressed by our microbiota[113] play important roles in helping to define the microbial diversity of our GI tract as well as contributing an enormous amount of to our own genetic

Early Microbiota

The gut microbiota interacting with the human host is a unified super-organism with stable yet evolving features. *In utero* we begin life as a sterile entity. Microbial colonization begins during birth, with one profound initial colonization event occurring during delivery (Figure 1). Studies have compared the microbial environments resulting from vaginal births to those resulting from Cesarean births, finding that infants via a vaginal birth acquire a microbial phenotype dominated by probiotic *Lactobacillus* species but have less overall diversity, or fewer bacterial types[114]. In contrast infants born via Cesarean section have a greater overall diversity as their intestinal colonization much more resembles the skin microbiome which also often has lower levels of *Lactobacilli*[114]. These early colonization events from a direct transfer of microbiota from the mother has important consequences for the overall health of the child[115].

Complicating these studies is the nutritional status of the infant and whether they received a formula-fed diet or were nursed on their mothers' breast milk. In the latter case, passive transfer of secretory immunoglobulin A (sIgA) not only helps to protect an infant from potentially infectious organisms, since the development of its own immune system takes many months, but sIgA also controls the interaction of the infants' cells with its newly acquired microorganisms[116]. Additionally, human breast milk contains essential ingredients for a healthy gut microbiota including carbohydrates, short chain fatty acids (SCFAs), and lactoferrin[117]. Breast milk may also contain viable microbes capable of influencing the colonization of the infant gut microbiome. In a study comparing the microbiota of 20 vaginally delivered infants and the composition of their mothers' breast milk, Solis et al.[118] report viable *Lactobacilli* and *Bifidobacteria* species capable of vertical transfer to the infant gut microbiota. A longitudinal study by Fallani et al.[119] further highlights the influences of infant feeding patterns on the intestinal microbiota. Breast-fed infants have a *Bifidobacteria* dominated microbiota while formula-fed infants have a more diverse microbiota including lower counts of Bifidobacterium and higher counts of *Bacteroides* and *Clostridium* [119]. Likewise, in a review by Thum et al. [120] the benefits and possibility of modifying infant microbiota and overall health through maternal diet are discussed.

While these studies demonstrate the influences of maternal probiotic bacteria and immunity on the infant microbiota, there remains a lack of understanding of the interplay between these factors in the short- and

long-term health of infants. For instance, comparing the evolution of the infant microbiota with the interaction of delivery mode with feeding conditions have not been well described as most studies compare only mode of birth or feeding practice with vaginally-delivered infants. By analyzing the changes in the microbiota of a child delivered vaginally and formula-fed to a child born by Cesarean fed breast milk could provide critically important data regarding the influence of the microbiota by environmental factors. Perhaps breast- feeding has a stronger influence on the microbiota, leading to a convergence of microbiota patterns despite mode of birth. Or maybe the initial mode of birth results in a lasting variation of the microbiota that may later influence the immune responses. Thus, it is important to consider how environmental factors including nutritional conditions and initial exposure to skin or vaginal microbiota communicate to develop the infant microbiota.

Adult Microbiota

During early colonization, the unique microbial composition of each child converges into the core microbiome of an adult[121]. Once established the microbial community is stable, but not fixed, influenced by environmental and genetic factors (Figure 1) [121]. These influences provide a variety of phylum proportions throughout the human body and variability among humans[122]. Similar to the influence of nutrition on an infants' microbiome, diet and antibiotic consumption are essential in shaping the adult microbiome. For example, mouse models with high fat diets and fecal microbiota transplants show clear evidence of the gut microbiota being indicative and causal of a physical phenotype such as obesity and leanness[123–126]. Among humans, one controlled-feeding study showed a strong microbiota profile, or enterotype, associated with long-term diets[126,127]. Mouse models clearly demonstrate that genetically obese individuals develop a unique gut microbiota[123]. In a pioneer study by Ley et al. [123] in which obese mice were shown to have a microbiota highly dominant in bacteria of the Firmicutes phylum, a more balanced ratio between Firmicutes and Bacteroidetes was observed in lean mice[123]. At the genus level, Bacteroidetes species have been positively associated with lean individuals,[128] while *Lactobacillus* has been negatively associated with lean individuals[128]. Even species-specific benefits have been shown to influence obesity. In a study analyzing *Lactobacillus* and *Bifidobacterium* species in obese individuals, Million et al.[129] identified an association of *B. animalis*, *L. paracasei* and *L. plantarum* with normal weight and *L. reuteri* with obesity. These studies

clearly outline a definitive microbiota in obese individuals capable of altering phenotypic, and possibly health, condition.

In addition to the environmental factors constantly contributing to shifts of the microbiome, the human host affects the microbiome through one's own genetic background. Genetic studies of both human twin subjects and mouse models reveal genes associated with specific bacterial abundances and composition. Goodrich et al.[130] establishes this connection using 416 twin-pairs and over 1,000 fecal samples; monozygotic twins had greater microbiota similarities than dizygotic twins. In another study, Davenport et al.[131] incorporates genome-wide association studies with microbiota sequencing using a founder population to limit variation in environmental exposure. Despite a small sample size, at least 8 bacterial taxa were significantly related to human genetic variation[131]. The mechanism of host- genetic modification of the microbiome remains unclear[132], however proposed models include alterations in levels of hormone production, energy availability, and immune system interaction[131]. Studying the genetic predisposition is crucial for understanding the evolving microbiota. While studies using adult twins or related family members provide a human model, these studies cannot control the variable environmental factors. Therefore, genetic influences are easily confounded by environmental influences. The use of genetically engineered mouse models manipulated under controlled environmental conditions can help us begin to understand the interplay between environment and genetics, but the translatability of these studies to humans still remains an issue.

1.3.B Microbiota: Initiator of disease and target of treatment

Most notably, changes within the gut microbiota have been associated with a number of chronic inflammatory diseases. These changes can occur in the composition, location, and/or function of the microbiota and are referred to as dysbiosis[133]. With over 60% of immune cells residing in the intestinal mucosa, the GI system and the microbiome is one of the leading influences on the immune system[134]. As the initial colonization of an infant's GI tract begins, so does the development of the immune system[135]. Furthermore, the gut microbiota is in constant contact with the human host and will continue to influence the immune system throughout life. Due to an association between microbiota shifts and diseases, the gut microbiota is connected to a range of conditions such as obesity, cardiovascular disease, and inflammatory

bowel disease[121]. In animal studies, the gut microbiota is shown to have important effects on metabolic diseases with causal effects being reported on glucose and lipid metabolism, adipose development, and insulin signaling[109,136].

The dynamic nature of the microbiome makes it a desirable target for potential therapies to prevent or treat disease. An obvious choice for such development is the administration of probiotics. Probiotics, as defined by the FAO and WHO, are “live microorganisms which when administered in adequate amounts confer a health benefit on the host”[137]. As the body is already populated with several millions of microbes, the idea of probiotic therapy would be to supplement the existing microbiota with “beneficial” bacteria. The health benefits of these bacteria would interact directly with the microbiota via the competition with potential opportunistic commensals (“pathobionts”) or infectious microorganisms for nutrients and/or anatomical niches. In fact, studies of the physicochemical and adhesive properties of Bifidobacterium and Lactobacillus species have been instrumental in revealing possible strains for probiotic use due to their ability to inhibit adherence of enteric pathogens such as Shigella, Staphylococcus, Salmonella, and Listeria[138,139].

Probiotic bacteria may also modulate the microbiota indirectly through inhibiting commensal translocation by decreasing intestinal permeability[134] or promoting anti-inflammatory activity of the immune system[133]. For example, Yan and Polk[140] observed decreased apoptosis and increased survival of colonic cells cultured with *L. rhamnosus GG*. *L. rhamnosus GG* produces two soluble proteins capable of regulating apoptosis and proliferation in intestinal epithelial cells[140]. The latter is accomplished through the production of SCFAs[141] and anti-inflammatory cytokines such as IL-10 and TGF-β[142]. In addition, dietary constituents influence whether the microenvironment of the GI tract is permissive for the establishment of pathobionts or the promotion of probiotic bacteria. For example, diets high in fiber have been shown to increase bacterial production of acetate and butyrate[143] which is beneficial for the host because butyrate produced through the fermentation by probiotic bacteria induces colonic regulatory T cell differentiation and enhances immune-suppression and tolerance[143]. On the other hand, diets high in fat create low grade inflammation[144] that promotes the expansion of pathobionts, reduces probiotic species[144], and has been suggested to affect commensal translocation[145]. While the presence of probiotic bacteria may inhibit the adherence of pathogenic bacteria, studies examining the relationship between nutritional status, pathogenic infection,

and probiotics have not been well studied. These results demonstrate the ability of probiotic species of the microbiota and their byproducts to directly and indirectly affect the intestinal microenvironment but currently lack mechanistic studies and translation to human disease.

Probiotic interventions

The interaction between nutritional status and probiotics is highlighted in research of metabolic diseases and associated syndromes. Several studies focusing on metabolic diseases have positive outcomes using probiotic therapy. One mouse study using high fat diet-induced diabetes found probiotic treatment highly effective in improving glucose tolerance, restoring insulin sensitivity, and reducing inflammatory cytokines in adipose tissue[145]. These results demonstrate clear evidence that a probiotic, capable of preventing bacterial adherence and translocation, can reverse a diet- induced intestinal disturbance and adipose inflammation[145]. In a double-blind human study of males with type 2 diabetes, use of a probiotic improved insulin sensitivity while baseline inflammatory markers remained the same[146]. Probiotic therapy has also shown success in a number of studies when used to treat chronic inflammatory diseases. For instance, clinical trials using *B. infantis* either mixed with a malted milk drink or in an encapsulated form both had promising results in relieving irritable bowel syndrome (IBS) symptoms, including decreased pain/discomfort, bloating, and bowel movement difficulty[147,148]. Molecularly, Pathmakanthan et al.[149] identified increases in IL-10 production and increases in the numbers of T cells and macrophage from the blood of healthy patients and colonic mucosa of active ulcerative colitis patients treated with *L. plantarum*. Another in vitro study using human monocyte-derived dendritic cells found that *L. rhamnosus* inhibits proliferation of T-cells and decreases IL-2, IL-4, and IL-10 production[150], results that were replicated in human subjects with Crohn's disease, indicating a potential *L. rhamnosus* derived treatment[151]. Probiotic therapy has also been used to improve both infectious disease and behavioral issues, indicating the potential breadth and therapeutic potential of probiotics.

On the other hand, the potential claims of probiotics in treating disease have been called into question by a number of reviews, citing the lack of evidence or controversial results[136]. Two clinical reviews found insufficient evidence supporting probiotic use for treating IBS, Crohn's disease, and necrotizing enterocolitis and sepsis in preterm infants[134,151]. Furthermore, studies have shown adverse effects when using probiotics

in humans or effects in animal models that do not translate well in humanized trials[152,153]. There is also a lack of scientific evidence supporting the widely-advertised functional foods containing probiotics[154]. Companies with products like yogurt widely advertise to the general public using attractive claims such as improving digestion or strengthening the body's natural defenses but cite questionable studies[154]. In a systematic review analyzing significance of studies containing *L. casei* and *B. lactis*, several of the studies were found linked to companies selling products containing those species through funding, company-supplied products, or a company-associated author[154].

Future of Probiotic Design

Given the new technological advances, cost effectiveness, and scale of the data generated by next-generation sequencing, we can analyze the relationship between the microbiome and probiotic-derived therapies. It is likely that given the proper knowledge of each individual's microbiome, diet, and lifestyle, accurate prescription of probiotics can be designed. In a human study of obese individuals, Korpela et al.[155] demonstrated that the microbiome, rather than weight status, can help determine the efficacy of treatments. Using fecal microbiota analysis at baseline and after dietary interventions, they were able to predict responsiveness of the host microbiota using microbial biomarkers[155]. Another human study profiling geriatric individuals revealed potential microbial biomarkers between probiotic respondents and non-respondents[156]. It was previously suggested that level of response depended on change in cholesterol; instead, the fecal microbiota provided a more clinically useful biomarker[156]. It is also important to note that the geriatric study identified a microbiota shift in non-respondents[156]; thus, it is pertinent to distinguish individuals that respond or do not respond to dietary interventions such as probiotics.

Due to the diverse results of probiotic studies, gut microbiota profiling could help tailor probiotic therapies per individual. With conditions highly dependent on glucose or insulin metabolism, personalized nutritional treatments have the greatest prospects. For example, probiotic therapy may be especially useful in cases where the identification of a "pre-diseased" microbiome is compared to a profile during disease or flare and specific probiotic bacterial species once lost are restored. This targeted microbiota therapy (TMT) would then be restoring species that have already been able to previously colonize and survive in an individual's particular intestinal landscape (Diagram 1.2). However, this therapy relies on understanding the various

healthy pre- diseased and diseased microbiome and, while the advent of stool banks and sequencing of the microbiome makes this information accessible to the general population, this knowledge will still be a limiting factor in such designs. A second and more intriguing notion is the idea of probiotic sensitization in which the intestinal microenvironment is somehow manipulated through drugs, prebiotics, or antibiotics in an effort to alter the topography of the intestine, making it more permissive for colonization and establishment of the specific probiotic.

The anatomical, immunological, and microbiological complexity of the GI tract has likely contributed to the variable results seen in clinical trials and human studies regarding probiotic therapy. Utilizing the technological and intellectual advances regarding the microbiome, we need to have a plan for the design and execution of a new generation of probiotics using TMT. We must spend more time and effort understanding traits that underlie the probiotic function. We need to identify the genes responsible for this given function through mutagenesis studies that will help to derive mutants, isolate genes, and/or identify proteins responsible for the probiotic function. Once identified, we will need to either design genetically modified microorganisms (GMM) or synthesize and test the probiotic-derived protein to establish a treatment not requiring the delivery of a live bacteria. Lastly, we must establish more standardized treatments and standardized strains in order to compare efficacy across clinical trials. Only when we start rigorous, cross-disciplinary, and holistic studies that consider the analysis of the microbiome, dietary, and lifestyle choices both pre- and post-probiotic treatment will we be able to create significant therapies utilizing probiotics or microbiome-derived products.

Humans are known for their diversity and complexity as a species and the identification of the microbiome, with its associated 9 million genes, have further increased our diversity and individuality. Here we discussed the numerous ways the uniquely tailored microbiome is formed, shaped, and altered throughout the human lifespan by genetic and environmental factors. As our knowledge of the microbiome continues to expand, the need to include microbiota analysis in conjunction with disease and treatment studies is crucial as the microbiome could confound our understanding of host and disease. Our current lack of understanding, especially in regards to probiotics, could be the cause of the contradicting results at the research and clinical trial level with probiotic treatments. Before proposing probiotic and nutritional interventions that induce

microbiome changes, we first need to acknowledge and incorporate our findings of the microbiota landscape. Only through the comprehensive approach of integrating our microbial ecosystem with nutritional and medical knowledge will we be able to advance the field of probiotics.

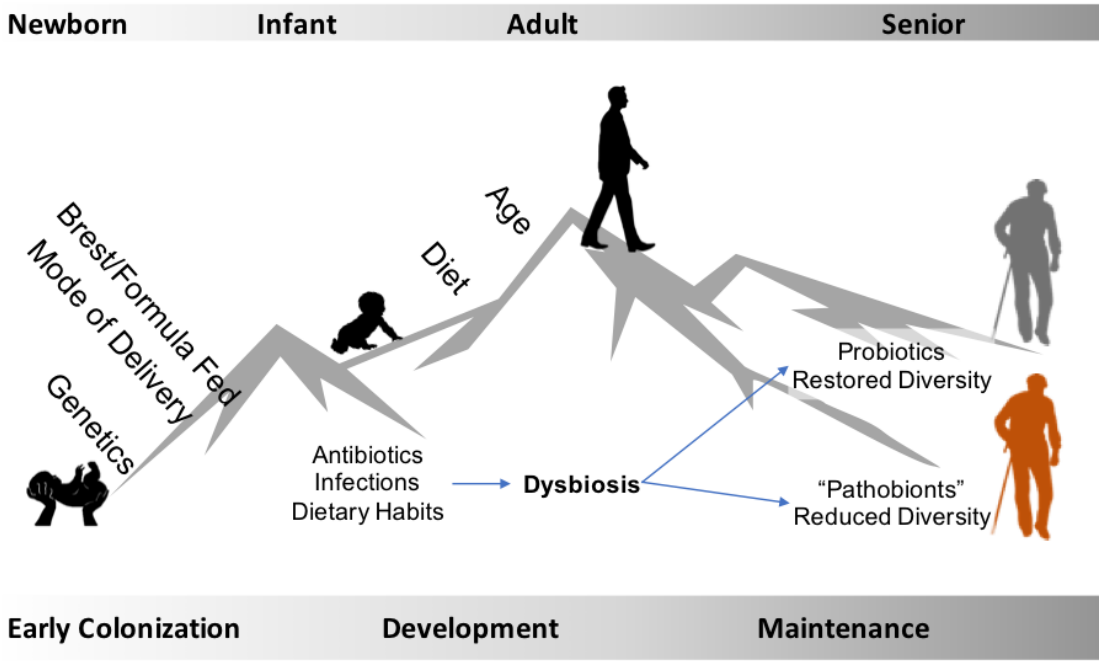

Diagram 1.2: Navigating the complex landscape of the microbiome
Throughout human development, several factors impact the composition, diversity and health of the gut microbiota. These factors include both environmental and genetic components continually interacting in a dynamic ecosystem of human and microbes. While the adult microbiota is considered stable and resilient, multiple elements can create a microbial imbalance known as dysbiosis. Our ability to treat the dysbiosis is limited due to lack of understand and consideration of the holistic nature of the microbiome.

1.4 Dynamics concerning host, nutrition and microbes

The interactions between host, nutrients and microbes are complex and intricate. When one component falters, the consequences on the others are vast. There is a lot to be learned of these interlacing factors so we can better understand diseases and develop therapeutics. This is especially true with environmentally linked diseases such as non-alcoholic fatty disease, spontaneous cases of CRC and general inflammation and susceptibility to infections. Therefore, this piece of work aims to holistically investigate the various relationships among nutrition, host and microbe.

Chapter 2 explores the interactions between host and nutrition using a model of diet-induced non-alcoholic fatty liver disease (NALFD) and comparing treatments of dietary intervention and microbiota transplants. Whereas dietary intervention completely reverses hepatic steatosis, microbiota transplants fail to resolve the fatty liver. This chapter highlights the dietary influences on the microbiota in both a disease and recovery model.

Chapter 3 evaluates the technique of matrix-assisted laser desorption/ionization – time of flight (MALDI-TOF) mass spectrometry (MS) with multiple environmental stressors. The MALDI-TOF MS is capable of reliably picking up physiological changes related to metabolic states. This chapter expands on the current MALDI-TOF MS uses to include metabolic and phenotypic screening within bacterial species and strains.

Chapter 4 studies the effects of polyunsaturated fatty acids on *Yersinia enterocolitica*. Pro-inflammatory omega-6 fatty acid – arachidonic acid (AA) – induces virulence proteins and alters metabolic signatures. Exposure to AA also increases pathogenicity within the host, leading to rapid systemic infection. This chapter investigates how nutrition can directly impact enteric pathogens.

Chapter 5 explores the role of TLR1 in intestinal barrier integrity during homeostasis and injury. Aberrant TLR1 signaling increases mucus-associated bacteria, produces a defective mucus layer and deregulates intestinal stem cell proliferation. These defects led to chronic inflammation following a model of intestinal injury and repair. This chapter focuses on understanding the complex, knit relationship between host and microbe.

Chapter 6 studies the role of TLR6 in a model of inflammation-associated colorectal cancer. TLR6 deficiency increased *Lactobacillus* retention during disease and conferred protection to wildtype hosts. Targeted treatment with *Lactobacillus* reduced disease burden and suppressed inflammation. This chapter investigates the role of host innate receptors in regulating microbiota composition and effectiveness of targeted microbiota treatments to restore microbial diversity.

1.5 References

1. US Burden of Disease Collaborators, Mokdad AH, Ballestros K, et al. The State of US Health, 1990-2016: Burden of Diseases, Injuries, and Risk Factors Among US States. *JAMA*. 2018;319(14):1444-1472. doi:10.1001/jama.2018.0158

2. Afshin A, Sur PJ, Fay KA, et al. Health effects of dietary risks in 195 countries, 1990–2017: a systematic analysis for the Global Burden of Disease Study 2017. *The Lancet*. 2019;393(10184):1958-1972. doi:10.1016/S0140-6736(19)30041-8

3. Wang DD, Li Y, Afshin A, et al. Global Improvement in Dietary Quality Could Lead to Substantial Reduction in Premature Death. *J Nutr*. 2019;149(6):1065-1074. doi:10.1093/jn/nxz010

4. Diamond J. The worst mistake in the history of the human race. *Discover*. 1987;8(5):64-66.

5. Eaton SB, Konner M, Shostak M. Stone agers in the fast lane: chronic degenerative diseases in evolutionary perspective. *Am J Med*. 1988;84(4):739-749. doi:10.1016/0002-9343(88)90113-1

6. Trowell HC, Burkitt DP. *Western Diseases, Their Emergence and Prevention*. Harvard University Press; 1981.

7. Quinn M. Origins of Western diseases. *J R Soc Med*. 2011;104(11):449-456. doi:10.1258/jrsm.2011.110014

8. Gomez A, Petrzelkova KJ, Burns MB, et al. Gut Microbiome of Coexisting BaAka Pygmies and Bantu Reflects Gradients of Traditional Subsistence Patterns. *Cell Rep*. 2016;14(9):2142-2153. doi:10.1016/j.celrep.2016.02.013

9. Clemente JC, Pehrsson EC, Blaser MJ, et al. The microbiome of uncontacted Amerindians. *Sci Adv*. 2015;1(3). doi:10.1126/sciadv.1500183

10. Schnorr SL, Candela M, Rampelli S, et al. Gut microbiome of the Hadza hunter-gatherers. *Nat Commun*. 2014;5. doi:10.1038/ncomms4654

11. Rampelli S, Schnorr SL, Consolandi C, et al. Metagenome Sequencing of the Hadza Hunter-Gatherer Gut Microbiota. *Curr Biol*. 2015;25(13):1682-1693. doi:10.1016/j.cub.2015.04.055

12. Cordain L, Miller JB, Eaton SB, Mann N. Macronutrient estimations in hunter-gatherer diets. *Am J Clin Nutr*. 2000;72(6):1589-1590. doi:10.1093/ajcn/72.6.1589

13. Miller JB, Mann N, Cordain L, Selinger A, Green A. Paleolithic nutrition: what did our ancestors eat? In: *Genes to Galaxies: The Lecture Series of the 35th Professor Harry Messel International Science School : 12-25 July 2009*. Science Foundation for Physics within the University of Sydney; 2009:29-42.

14. Bang HO, Dyerberg J, Sinclair HM. The composition of the Eskimo food in north western Greenland. *Am J Clin Nutr*. 1980;33(12):2657-2661. doi:10.1093/ajcn/33.12.2657

15. Cordain L, Eaton SB, Sebastian A, et al. Origins and evolution of the Western diet: health implications for the 21st century. *Am J Clin Nutr*. 2005;81(2):341-354. doi:10.1093/ajcn.81.2.341

16. Broussard JL, Devkota S. The changing microbial landscape of Western society: Diet, dwellings and discordance. *Mol Metab*. 2016;5(9):737-742. doi:10.1016/j.molmet.2016.07.007

17. Naja F, Hwalla N, Itani L, Karam S, Mehio Sibai A, Nasreddine L. A Western dietary pattern is associated with overweight and obesity in a national sample of Lebanese adolescents (13–19 years): a cross-sectional study. *Br J Nutr*. 2015;114(11):1909-1919. doi:10.1017/S0007114515003657

18. Mirmiran P, Bahadoran Z, Vakili AZ, Azizi F. Western dietary pattern increases risk of cardiovascular disease in Iranian adults: a prospective population-based study. *Appl Physiol Nutr Metab*. 2017;42(3):326-332. doi:10.1139/apnm-2016-0508

19. Heidemann Christin, Schulze Matthias B., Franco Oscar H., van Dam Rob M., Mantzoros Christos S., Hu Frank B. Dietary Patterns and Risk of Mortality From Cardiovascular Disease, Cancer, and All Causes in a Prospective Cohort of Women. *Circulation*. 2008;118(3):230-237. doi:10.1161/CIRCULATIONAHA.108.771881

20. Shu L, Shen X-M, Li C, Zhang X-Y, Zheng P-F. Dietary patterns are associated with type 2 diabetes mellitus among middle-aged adults in Zhejiang Province, China. *Nutr J*. 2017;16. doi:10.1186/s12937-017-0303-0

21. Esmaillzadeh A, Kimiagar M, Mehrabi Y, Azadbakht L, Hu FB, Willett WC. Dietary patterns, insulin resistance, and prevalence of the metabolic syndrome in women. *Am J Clin Nutr*. 2007;85(3):910-918. doi:10.1093/ajcn/85.3.910

22. Mehta RS, Song M, Nishihara R, et al. Dietary Patterns and Risk of Colorectal Cancer: Analysis by Tumor Location and Molecular Subtypes. *Gastroenterology*. 2017;152(8):1944-1953.e1. doi:10.1053/j.gastro.2017.02.015

23. Strate LL, Keeley BR, Cao Y, Wu K, Giovannucci EL, Chan AT. Western Dietary Pattern Increases, and Prudent Dietary Pattern Decreases, Risk of Incident Diverticulitis in a Prospective Cohort Study. *Gastroenterology*. 2017;152(5):1023-1030.e2. doi:10.1053/j.gastro.2016.12.038

24. Rezapour M, Ali S, Stollman N. Diverticular Disease: An Update on Pathogenesis and Management. *Gut Liver*. 2018;12(2):125-132. doi:10.5009/gnl16552

25. Oddy WH, Herbison CE, Jacoby P, et al. The Western dietary pattern is prospectively associated with nonalcoholic fatty liver disease in adolescence. *Am J Gastroenterol*. 2013;108(5):778-785. doi:10.1038/ajg.2013.95

26. Khadge S, Sharp JG, Thiele GM, et al. Dietary omega-3 and omega-6 polyunsaturated fatty acids modulate hepatic pathology. *The Journal of Nutritional Biochemistry*. 2018;52:92-102. doi:10.1016/j.jnutbio.2017.09.017

27. Hou JK, Abraham B, El-Serag H. Dietary intake and risk of developing inflammatory bowel disease: a systematic review of the literature. *Am J Gastroenterol*. 2011;106(4):563-573. doi:10.1038/ajg.2011.44

28. Ananthakrishnan AN, Khalili H, Song M, et al. High School Diet and Risk of Crohn's Disease and Ulcerative Colitis. *Inflamm Bowel Dis*. 2015;21(10):2311-2319. doi:10.1097/MIB.0000000000000501

29. Buscail C, Sabate J-M, Bouchoucha M, et al. Western Dietary Pattern Is Associated with Irritable Bowel Syndrome in the French NutriNet Cohort. *Nutrients*. 2017;9(9). doi:10.3390/nu9090986

30. Khayyatzadeh SS, Esmaillzadeh A, Saneei P, Keshteli AH, Adibi P. Dietary patterns and prevalence of irritable bowel syndrome in Iranian adults. *Neurogastroenterol Motil*. 2016;28(12):1921-1933. doi:10.1111/nmo.12895

31. Bortolin RC, Vargas AR, Gasparotto J, et al. A new animal diet based on human Western diet is a robust diet-induced obesity model: comparison to high-fat and cafeteria diets in term of metabolic and gut microbiota disruption. *Int J Obes (Lond)*. 2018;42(3):525-534. doi:10.1038/ijo.2017.225

32. O'Neill AM, Burrington CM, Gillaspie EA, Lynch DT, Horsman MJ, Greene MW. High-fat Western diet-induced obesity contributes to increased tumor growth in mouse models of human colon cancer. *Nutr Res*. 2016;36(12):1325-1334. doi:10.1016/j.nutres.2016.10.005

33. Nimri L, Saadi J, Peri I, Yehuda-Shnaidman E, Schwartz B. Mechanisms linking obesity to altered metabolism in mice colon carcinogenesis. *Oncotarget*. 2015;6(35):38195-38209. doi:10.18632/oncotarget.5561

34. Burke SJ, Batdorf HM, Burk DH, et al. db/db Mice Exhibit Features of Human Type 2 Diabetes That Are Not Present in Weight-Matched C57BL/6J Mice Fed a Western Diet. *J Diabetes Res*. 2017;2017:8503754. doi:10.1155/2017/8503754

35. Jeyapal S, Kona SR, Mullapudi SV, Putcha UK, Gurumurthy P, Ibrahim A. Substitution of linoleic acid with α-linolenic acid or long chain n-3 polyunsaturated fatty acid prevents Western diet induced nonalcoholic steatohepatitis. *Sci Rep*. 2018;8(1):1-14. doi:10.1038/s41598-018-29222-y

36. Clevers HC, Bevins CL. Paneth cells: maestros of the small intestinal crypts. *Annu Rev Physiol*. 2013;75:289-311. doi:10.1146/annurev-physiol-030212-183744

37. Wilson CL. Regulation of Intestinal -Defensin Activation by the Metalloproteinase Matrilysin in Innate Host Defense. *Science*. 1999;286(5437):113-117. doi:10.1126/science.286.5437.113

38. Vaishnava S, Behrendt CL, Ismail AS, Eckmann L, Hooper LV. Paneth cells directly sense gut commensals and maintain homeostasis at the intestinal host-microbial interface. *Proc Natl Acad Sci USA*. 2008;105(52):20858-20863. doi:10.1073/pnas.0808723105

39. Kobayashi KS, Chamaillard M, Ogura Y, et al. Nod2-dependent regulation of innate and adaptive immunity in the intestinal tract. *Science*. 2005;307(5710):731-734. doi:10.1126/science.1104911

40. Salzman NH, Hung K, Haribhai D, et al. Enteric defensins are essential regulators of intestinal microbial ecology. *Nat Immunol*. 2010;11(1):76-83. doi:10.1038/ni.1825

41. Johansson MEV, Hansson GC. Is the intestinal goblet cell a major immune cell? *Cell Host Microbe*. 2014;15(3):251-252. doi:10.1016/j.chom.2014.02.014

42. Birchenough GMH, Johansson MEV, Gustafsson JK, Bergström JH, Hansson GC. New developments in goblet cell mucus secretion and function. *Mucosal Immunol*. 2015;8(4):712-719. doi:10.1038/mi.2015.32

43. Hooper LV, Macpherson AJ. Immune adaptations that maintain homeostasis with the intestinal microbiota. *Nat Rev Immunol*. 2010;10(3):159-169. doi:10.1038/nri2710

44. Johansson MEV, Gustafsson JK, Holmén-Larsson J, et al. Bacteria penetrate the normally impenetrable inner colon mucus layer in both murine colitis models and patients with ulcerative colitis. *Gut*. 2014;63(2):281-291. doi:10.1136/gutjnl-2012-303207

45. Sorini C, Cosorich I, Lo Conte M, et al. Loss of gut barrier integrity triggers activation of islet-reactive T cells and autoimmune diabetes. *Proc Natl Acad Sci USA*. 2019;116(30):15140-15149. doi:10.1073/pnas.1814558116

46. Van der Sluis M, De Koning BAE, De Bruijn ACJM, et al. Muc2-deficient mice spontaneously develop colitis, indicating that MUC2 is critical for colonic protection. *Gastroenterology*. 2006;131(1):117-129. doi:10.1053/j.gastro.2006.04.020

47. Gum JR, Hicks JW, Toribara NW, Siddiki B, Kim YS. Molecular cloning of human intestinal mucin (MUC2) cDNA. Identification of the amino terminus and overall sequence similarity to prepro-von Willebrand factor. *J Biol Chem*. 1994;269(4):2440-2446.

48. Schneider H, Pelaseyed T, Svensson F, Johansson MEV. Study of mucin turnover in the small intestine by in vivo labeling. *Sci Rep*. 2018;8(1):1-11. doi:10.1038/s41598-018-24148-x

49. Johansson MEV, Hansson GC. Keeping Bacteria at a Distance. *Science*. 2011;334(6053):182-183. doi:10.1126/science.1213909

50. Bel S, Pendse M, Wang Y, et al. Paneth cells secrete lysozyme via secretory autophagy during bacterial infection of the intestine. *Science*. 2017;357(6355):1047-1052. doi:10.1126/science.aal4677

51. Vaishnava S, Yamamoto M, Severson KM, et al. The Antibacterial Lectin RegIIIγ Promotes the Spatial Segregation of Microbiota and Host in the Intestine. *Science*. 2011;334(6053):255-258. doi:10.1126/science.1209791

52. Johansson MEV. Fast renewal of the distal colonic mucus layers by the surface goblet cells as measured by in vivo labeling of mucin glycoproteins. *PLoS ONE*. 2012;7(7):e41009. doi:10.1371/journal.pone.0041009

53. Johansson MEV, Phillipson M, Petersson J, Velcich A, Holm L, Hansson GC. The inner of the two Muc2 mucin-dependent mucus layers in colon is devoid of bacteria. *Proc Natl Acad Sci USA*. 2008;105(39):15064-15069. doi:10.1073/pnas.0803124105

54. Antoni L, Nuding S, Weller D, et al. Human colonic mucus is a reservoir for antimicrobial peptides. *J Crohns Colitis*. 2013;7(12):e652-e664. doi:10.1016/j.crohns.2013.05.006

55. Tollin M, Bergman P, Svenberg T, Jörnvall H, Gudmundsson GH, Agerberth B. Antimicrobial peptides in the first line defence of human colon mucosa. *Peptides*. 2003;24(4):523-530. doi:10.1016/s0196-9781(03)00114-1

56. Yoshimura T, McLean MH, Dzutsev AK, et al. The Antimicrobial Peptide CRAMP Is Essential for Colon Homeostasis by Maintaining Microbiota Balance. *The Journal of Immunology*. February 2018:ji1602073. doi:10.4049/jimmunol.1602073

57. Iimura M, Gallo RL, Hase K, Miyamoto Y, Eckmann L, Kagnoff MF. Cathelicidin Mediates Innate Intestinal Defense against Colonization with Epithelial Adherent Bacterial Pathogens. *The Journal of Immunology*. 2005;174(8):4901-4907. doi:10.4049/jimmunol.174.8.4901

58. Johansson MEV, Jakobsson HE, Holmén-Larsson J, et al. Normalization of host intestinal mucus layers requires long-term microbial colonization. *Cell Host Microbe*. 2015;18(5):582-592. doi:10.1016/j.chom.2015.10.007

59. Kennedy EA, King KY, Baldridge MT. Mouse Microbiota Models: Comparing Germ-Free Mice and Antibiotics Treatment as Tools for Modifying Gut Bacteria. *Front Physiol*. 2018;9. doi:10.3389/fphys.2018.01534

60. Jakobsson HE, Rodríguez-Piñeiro AM, Schütte A, et al. The composition of the gut microbiota shapes the colon mucus barrier. *EMBO Rep*. 2015;16(2):164-177. doi:10.15252/embr.201439263

61. Rodríguez-Piñeiro AM, Johansson MEV. The colonic mucus protection depends on the microbiota. *Gut Microbes*. 2015;6(5):326-330. doi:10.1080/19490976.2015.1086057

62. Bergstrom KSB, Kissoon-Singh V, Gibson DL, et al. Muc2 Protects against Lethal Infectious Colitis by Disassociating Pathogenic and Commensal Bacteria from the Colonic Mucosa. *PLOS Pathogens*. 2010;6(5):e1000902. doi:10.1371/journal.ppat.1000902

63. Peterson DA, McNulty NP, Guruge JL, Gordon JI. IgA response to symbiotic bacteria as a mediator of gut homeostasis. *Cell Host Microbe*. 2007;2(5):328-339. doi:10.1016/j.chom.2007.09.013

64. Sansonetti PJ, Arondel J, Cantey JR, Prévost MC, Huerre M. Infection of rabbit Peyer's patches by Shigella flexneri: effect of adhesive or invasive bacterial phenotypes on follicle-associated epithelium. *Infect Immun*. 1996;64(7):2752-2764.

65. Boullier S, Tanguy M, Kadaoui KA, et al. Secretory IgA-mediated neutralization of Shigella flexneri prevents intestinal tissue destruction by down-regulating inflammatory circuits. *J Immunol*. 2009;183(9):5879-5885. doi:10.4049/jimmunol.0901838

66. Perrier C, Sprenger N, Corthésy B. Glycans on secretory component participate in innate protection against mucosal pathogens. *J Biol Chem*. 2006;281(20):14280-14287. doi:10.1074/jbc.M512958200

67. Moor K, Diard M, Sellin ME, et al. High-avidity IgA protects the intestine by enchaining growing bacteria. *Nature*. 2017;544(7651):498-502. doi:10.1038/nature22058

68. Vaerman JP, Derijck-Langendries A, Rits M, Delacroix D. Neutralization of cholera toxin by rat bile secretory IgA antibodies. *Immunology*. 1985;54(3):601-603.

69. Kurohane K, Nagano K, Nakanishi K, Iwata K, Miyake M, Imai Y. Shiga toxin-induced apoptosis is more efficiently inhibited by dimeric recombinant hybrid-IgG/IgA immunoglobulins than by the parental IgG monoclonal antibodies. *Virulence*. 2014;5(8):819-824. doi:10.4161/21505594.2014.973804

70. Cario E, Gerken G, Podolsky DK. Toll-like receptor 2 enhances ZO-1-associated intestinal epithelial barrier integrity via protein kinase C. *Gastroenterology*. 2004;127(1):224-238. doi:10.1053/j.gastro.2004.04.015

71. Li X, Wang C, Nie J, Lv D, Wang T, Xu Y. Toll-like receptor 4 increases intestinal permeability through up-regulation of membrane PKC activity in alcoholic steatohepatitis. *Alcohol*. 2013;47(6):459-465. doi:10.1016/j.alcohol.2013.05.004

72. Lu P, Sodhi CP, Yamaguchi Y, et al. Intestinal epithelial Toll-like receptor 4 prevents metabolic syndrome by regulating interactions between microbes and intestinal epithelial cells in mice. *Mucosal Immunol*. 2018;11(3):727-740. doi:10.1038/mi.2017.114

73. Shi H, Kokoeva MV, Inouye K, Tzameli I, Yin H, Flier JS. TLR4 links innate immunity and fatty acid-induced insulin resistance. *J Clin Invest*. 2006;116(11):3015-3025. doi:10.1172/JCI28898

74. Saberi M, Woods N-B, de Luca C, et al. Hematopoietic cell-specific deletion of toll-like receptor 4 ameliorates hepatic and adipose tissue insulin resistance in high-fat-fed mice. *Cell Metab*. 2009;10(5):419-429. doi:10.1016/j.cmet.2009.09.006

75. Wlodarska M, Thaiss CA, Nowarski R, et al. NLRP6 inflammasome orchestrates the colonic host-microbial interface by regulating goblet cell mucus secretion. *Cell*. 2014;156(5):1045-1059. doi:10.1016/j.cell.2014.01.026

76. Schirbel A, Kessler S, Rieder F, et al. Pro-angiogenic activity of TLRs and NLRs: a novel link between gut microbiota and intestinal angiogenesis. *Gastroenterology*. 2013;144(3):613-623.e9. doi:10.1053/j.gastro.2012.11.005

77. Latorre E, Layunta E, Grasa L, et al. Intestinal Serotonin Transporter Inhibition by Toll-Like Receptor 2 Activation. A Feedback Modulation. Pizzo SV, ed. *PLoS ONE*. 2016;11(12):e0169303. doi:10.1371/journal.pone.0169303

78. Layunta E, Latorre E, Forcén R, et al. NOD2 Modulates Serotonin Transporter and Interacts with TLR2 and TLR4 in Intestinal Epithelial Cells. *Cell Physiol Biochem*. 2018;47(3):1217-1229. doi:10.1159/000490218

79. Tantisira K, Klimecki WT, Lazarus R, et al. Toll-like receptor 6 gene (TLR6): single-nucleotide polymorphism frequencies and preliminary association with the diagnosis of asthma. *Genes Immun*. 2004;5(5):343-346. doi:10.1038/sj.gene.6364096

80. Lazarus R, Raby BA, Lange C, et al. TOLL-like receptor 10 genetic variation is associated with asthma in two independent samples. *Am J Respir Crit Care Med*. 2004;170(6):594-600. doi:10.1164/rccm.200404-491OC

81. Weidinger S, Klopp N, Rummler L, et al. Association of NOD1 polymorphisms with atopic eczema and related phenotypes. *J Allergy Clin Immunol*. 2005;116(1):177-184. doi:10.1016/j.jaci.2005.02.034

82. Franchimont D, Vermeire S, El Housni H, et al. Deficient host-bacteria interactions in inflammatory bowel disease? The toll-like receptor (TLR)-4 Asp299gly polymorphism is associated with Crohn's disease and ulcerative colitis. *Gut*. 2004;53(7):987-992. doi:10.1136/gut.2003.030205

83. Browning BL, Huebner C, Petermann I, et al. Has toll-like receptor 4 been prematurely dismissed as an inflammatory bowel disease gene? Association study combined with meta-analysis shows strong evidence for association. *Am J Gastroenterol*. 2007;102(11):2504-2512. doi:10.1111/j.1572-0241.2007.01463.x

84. Cheng Y, Zhu Y, Huang X, Zhang W, Han Z, Liu S. Association between TLR2 and TLR4 Gene Polymorphisms and the Susceptibility to Inflammatory Bowel Disease: A Meta-Analysis. Boone DL, ed. *PLoS ONE*. 2015;10(5):e0126803. doi:10.1371/journal.pone.0126803

85. Ogura Y, Bonen DK, Inohara N, et al. A frameshift mutation in NOD2 associated with susceptibility to Crohn's disease. *Nature*. 2001;411(6837):603-606. doi:10.1038/35079114

86. Hugot JP, Chamaillard M, Zouali H, et al. Association of NOD2 leucine-rich repeat variants with susceptibility to Crohn's disease. *Nature*. 2001;411(6837):599-603. doi:10.1038/35079107

87. Castro FA, Försti A, Buch S, et al. TLR-3 polymorphism is an independent prognostic marker for stage II colorectal cancer. *Eur J Cancer*. 2011;47(8):1203-1210. doi:10.1016/j.ejca.2010.12.011

88. Klimosch SN, Försti A, Eckert J, et al. Functional TLR5 genetic variants affect human colorectal cancer survival. *Cancer Res*. 2013;73(24):7232-7242. doi:10.1158/0008-5472.CAN-13-1746

89. Wang H, Flannery SM, Dickhöfer S, et al. A coding IRAK2 protein variant compromises Toll-like receptor (TLR) signaling and is associated with colorectal cancer survival. *J Biol Chem*. 2014;289(33):23123-23131. doi:10.1074/jbc.M113.492934

90. Lu C-C, Kuo H-C, Wang F-S, Jou M-H, Lee K-C, Chuang J-H. Upregulation of TLRs and IL-6 as a marker in human colorectal cancer. *Int J Mol Sci*. 2014;16(1):159-177. doi:10.3390/ijms16010159

91. Huhn S, da Silva Filho MI, Sanmuganantham T, et al. Coding variants in NOD-like receptors: An association study on risk and survival of colorectal cancer. Ahmad A, ed. *PLoS ONE*. 2018;13(6):e0199350. doi:10.1371/journal.pone.0199350

92. Allen IC, TeKippe EM, Woodford R-MT, et al. The NLRP3 inflammasome functions as a negative regulator of tumorigenesis during colitis-associated cancer. *J Exp Med*. 2010;207(5):1045-1056. doi:10.1084/jem.20100050

93. Larsson E, Tremaroli V, Lee YS, et al. Analysis of gut microbial regulation of host gene expression along the length of the gut and regulation of gut microbial ecology through MyD88. *Gut*. 2012;61(8):1124-1131. doi:10.1136/gutjnl-2011-301104

94. Vijay-Kumar M, Aitken JD, Carvalho FA, et al. Metabolic syndrome and altered gut microbiota in mice lacking Toll-like receptor 5. *Science*. 2010;328(5975):228-231. doi:10.1126/science.1179721

95. Chassaing B, Ley RE, Gewirtz AT. Intestinal epithelial cell toll-like receptor 5 regulates the intestinal microbiota to prevent low-grade inflammation and metabolic syndrome in mice. *Gastroenterology*. 2014;147(6):1363-1377.e17. doi:10.1053/j.gastro.2014.08.033

96. Xiao L, Chen B, Feng D, Yang T, Li T, Chen J. TLR4 May Be Involved in the Regulation of Colonic Mucosal Microbiota by Vitamin A. *Front Microbiol*. 2019;10:268. doi:10.3389/fmicb.2019.00268

97. Kamdar K, Johnson AMF, Chac D, et al. Innate Recognition of the Microbiota by TLR1 Promotes Epithelial Homeostasis and Prevents Chronic Inflammation. *J Immunol*. 2018;201(1):230-242. doi:10.4049/jimmunol.1701216

98. Ubeda C, Lipuma L, Gobourne A, et al. Familial transmission rather than defective innate immunity shapes the distinct intestinal microbiota of TLR-deficient mice. *J Exp Med*. 2012;209(8):1445-1456. doi:10.1084/jem.20120504

99. Zhang W, Hartmann R, Tun HM, Elson CO, Khafipour E, Garvey WT. Deletion of the Toll-Like Receptor 5 Gene Per Se Does Not Determine the Gut Microbiome Profile That Induces Metabolic Syndrome: Environment Trumps Genotype. *PLoS ONE*. 2016;11(3):e0150943. doi:10.1371/journal.pone.0150943

100. Couturier-Maillard A, Secher T, Rehman A, et al. NOD2-mediated dysbiosis predisposes mice to transmissible colitis and colorectal cancer. *J Clin Invest*. 2013;123(2):700-711. doi:10.1172/JCI62236

101. Petnicki-Ocwieja T, Hrncir T, Liu Y-J, et al. Nod2 is required for the regulation of commensal microbiota in the intestine. *Proc Natl Acad Sci USA*. 2009;106(37):15813-15818. doi:10.1073/pnas.0907722106

102. Elinav E, Strowig T, Kau AL, et al. NLRP6 inflammasome regulates colonic microbial ecology and risk for colitis. *Cell*. 2011;145(5):745-757. doi:10.1016/j.cell.2011.04.022

103. Hu B, Elinav E, Huber S, et al. Microbiota-induced activation of epithelial IL-6 signaling links inflammasome-driven inflammation with transmissible cancer. *Proc Natl Acad Sci USA*. 2013;110(24):9862-9867. doi:10.1073/pnas.1307575110

104. Levy M, Thaiss CA, Zeevi D, et al. Microbiota-Modulated Metabolites Shape the Intestinal Microenvironment by Regulating NLRP6 Inflammasome Signaling. *Cell*. 2015;163(6):1428-1443. doi:10.1016/j.cell.2015.10.048

105. Wen L, Ley RE, Volchkov PY, et al. Innate immunity and intestinal microbiota in the development of Type 1 diabetes. *Nature*. 2008;455(7216):1109-1113. doi:10.1038/nature07336

106. Lemire P, Robertson SJ, Maughan H, et al. The NLR Protein NLRP6 Does Not Impact Gut Microbiota Composition. *Cell Reports*. 2017;21(13):3653-3661. doi:10.1016/j.celrep.2017.12.026

107. Robertson SJ, Zhou JY, Geddes K, et al. Nod1 and Nod2 signaling does not alter the composition of intestinal bacterial communities at homeostasis. *Gut Microbes*. 2013;4(3):222-231. doi:10.4161/gmic.24373

108. Ringel-Scaia VM, Qin Y, Thomas CA, et al. Maternal Influence and Murine Housing Confound Impact of NLRP1 Inflammasome on Microbiome Composition. *J Innate Immun*. 2019;11(5):416-431. doi:10.1159/000495850

109. Grice EA, Kong HH, Renaud G, et al. A diversity profile of the human skin microbiota. *Genome Res*. 2008;18(7):1043-1050. doi:10.1101/gr.075549.107

110. Gao Z, Tseng C, Pei Z, Blaser MJ. Molecular analysis of human forearm superficial skin bacterial biota. *Proc Natl Acad Sci USA*. 2007;104(8):2927-2932. doi:10.1073/pnas.0607077104

111. Quercia S, Candela M, Giuliani C, et al. From lifetime to evolution: timescales of human gut microbiota adaptation. *Front Microbiol*. 2014;5:587. doi:10.3389/fmicb.2014.00587

112. Ley RE, Peterson DA, Gordon JI. Ecological and evolutionary forces shaping microbial diversity in the human intestine. *Cell*. 2006;124(4):837-848. doi:10.1016/j.cell.2006.02.017

113. Yang X, Xie L, Li Y, Wei C. More than 9,000,000 unique genes in human gut bacterial community: estimating gene numbers inside a human body. *PLoS ONE*. 2009;4(6):e6074. doi:10.1371/journal.pone.0006074

114. Dominguez-Bello MG, Costello EK, Contreras M, et al. Delivery mode shapes the acquisition and structure of the initial microbiota across multiple body habitats in newborns. *Proc Natl Acad Sci USA*. 2010;107(26):11971-11975. doi:10.1073/pnas.1002601107

115. Hansen CHF, Nielsen DS, Kverka M, et al. Patterns of early gut colonization shape future immune responses of the host. *PLoS ONE*. 2012;7(3):e34043. doi:10.1371/journal.pone.0034043

116. Hanson LA, Ahlstedt S, Andersson B, et al. Protective factors in milk and the development of the immune system. *Pediatrics*. 1985;75(1 Pt 2):172-176.

117. Salazar N, Arboleya S, Valdés L, et al. The human intestinal microbiome at extreme ages of life. Dietary intervention as a way to counteract alterations. *Front Genet*. 2014;5:406. doi:10.3389/fgene.2014.00406

118. Solís G, de Los Reyes-Gavilan CG, Fernández N, Margolles A, Gueimonde M. Establishment and development of lactic acid bacteria and bifidobacteria microbiota in breast-milk and the infant gut. *Anaerobe*. 2010;16(3):307-310. doi:10.1016/j.anaerobe.2010.02.004

119. Fallani M, Young D, Scott J, et al. Intestinal microbiota of 6-week-old infants across Europe: geographic influence beyond delivery mode, breast-feeding, and antibiotics. *J Pediatr Gastroenterol Nutr*. 2010;51(1):77-84. doi:10.1097/MPG.0b013e3181d1b11e

120. Thum C, Cookson AL, Otter DE, et al. Can nutritional modulation of maternal intestinal microbiota influence the development of the infant gastrointestinal tract? *J Nutr*. 2012;142(11):1921-1928. doi:10.3945/jn.112.166231

121. Burcelin R. Regulation of metabolism: a cross talk between gut microbiota and its human host. *Physiology (Bethesda)*. 2012;27(5):300-307. doi:10.1152/physiol.00023.2012

122. Claesson MJ, Cusack S, O'Sullivan O, et al. Composition, variability, and temporal stability of the intestinal microbiota of the elderly. *Proc Natl Acad Sci USA*. 2011;108 Suppl 1:4586-4591. doi:10.1073/pnas.1000097107

123. Ley RE, Bäckhed F, Turnbaugh P, Lozupone CA, Knight RD, Gordon JI. Obesity alters gut microbial ecology. *Proc Natl Acad Sci USA*. 2005;102(31):11070-11075. doi:10.1073/pnas.0504978102

124. Candela M, Biagi E, Maccaferri S, Turroni S, Brigidi P. Intestinal microbiota is a plastic factor responding to environmental changes. *Trends Microbiol*. 2012;20(8):385-391. doi:10.1016/j.tim.2012.05.003

125. Ridaura VK, Faith JJ, Rey FE, et al. Gut microbiota from twins discordant for obesity modulate metabolism in mice. *Science*. 2013;341(6150):1241214. doi:10.1126/science.1241214

126. Moschen AR, Wieser V, Tilg H. Dietary Factors: Major Regulators of the Gut's Microbiota. *Gut Liver*. 2012;6(4):411-416. doi:10.5009/gnl.2012.6.4.411

127. Wu GD, Chen J, Hoffmann C, et al. Linking long-term dietary patterns with gut microbial enterotypes. *Science*. 2011;334(6052):105-108. doi:10.1126/science.1208344

128. Armougom F, Henry M, Vialettes B, Raccah D, Raoult D. Monitoring bacterial community of human gut microbiota reveals an increase in Lactobacillus in obese patients and Methanogens in anorexic patients. *PLoS ONE*. 2009;4(9):e7125. doi:10.1371/journal.pone.0007125

129. Million M, Maraninchi M, Henry M, et al. Obesity-associated gut microbiota is enriched in Lactobacillus reuteri and depleted in Bifidobacterium animalis and Methanobrevibacter smithii. *Int J Obes (Lond)*. 2012;36(6):817-825. doi:10.1038/ijo.2011.153

130. Goodrich JK, Waters JL, Poole AC, et al. Human genetics shape the gut microbiome. *Cell*. 2014;159(4):789-799. doi:10.1016/j.cell.2014.09.053

131. Davenport ER, Cusanovich DA, Michelini K, Barreiro LB, Ober C, Gilad Y. Genome-Wide Association Studies of the Human Gut Microbiota. *PLoS ONE*. 2015;10(11):e0140301. doi:10.1371/journal.pone.0140301

132. Benson AK, Kelly SA, Legge R, et al. Individuality in gut microbiota composition is a complex polygenic trait shaped by multiple environmental and host genetic factors. *Proc Natl Acad Sci USA*. 2010;107(44):18933-18938. doi:10.1073/pnas.1007028107

133. Nell S, Suerbaum S, Josenhans C. The impact of the microbiota on the pathogenesis of IBD: lessons from mouse infection models. *Nat Rev Microbiol*. 2010;8(8):564-577. doi:10.1038/nrmicro2403

134. Barnes D, Yeh AM. Bugs and Guts: Practical Applications of Probiotics for Gastrointestinal Disorders in Children. *Nutr Clin Pract*. 2015;30(6):747-759. doi:10.1177/0884533615610081

135. Cebra JJ. Influences of microbiota on intestinal immune system development. *Am J Clin Nutr*. 1999;69(5):1046S-1051S. doi:10.1093/ajcn/69.5.1046s

136. Stenman LK, Burcelin R, Lahtinen S. Establishing a causal link between gut microbes, body weight gain and glucose metabolism in humans - towards treatment with probiotics. *Benef Microbes*. 2016;7(1):11-22. doi:10.3920/BM2015.0069

137. FAO/WHO. Guidelines for the Evaluation of Probiotics in Food. 2002. https://www.who.int/foodsafety/fs_management/en/probiotic_guidelines.pdf.

138. Tareb R, Bernardeau M, Gueguen M, Vernoux J-P. In vitro characterization of aggregation and adhesion properties of viable and heat-killed forms of two probiotic Lactobacillus strains and interaction with foodborne zoonotic bacteria, especially Campylobacter jejuni. *Journal of Medical Microbiology*. 2013;62(Pt_4):637-649. doi:10.1099/jmm.0.049965-0

139. Xu H, Jeong HS, Lee HY, Ahn J. Assessment of cell surface properties and adhesion potential of selected probiotic strains. *Lett Appl Microbiol*. 2009;49(4):434-442. doi:10.1111/j.1472-765X.2009.02684.x

140. Yan F, Polk DB. Probiotic bacterium prevents cytokine-induced apoptosis in intestinal epithelial cells. *J Biol Chem*. 2002;277(52):50959-50965. doi:10.1074/jbc.M207050200

141. Cavaglieri CR, Nishiyama A, Fernandes LC, Curi R, Miles EA, Calder PC. Differential effects of short-chain fatty acids on proliferation and production of pro- and anti-inflammatory cytokines by cultured lymphocytes. *Life Sci*. 2003;73(13):1683-1690. doi:10.1016/s0024-3205(03)00490-9

142. Clavel T, Haller D. Bacteria- and host-derived mechanisms to control intestinal epithelial cell homeostasis: implications for chronic inflammation. *Inflamm Bowel Dis*. 2007;13(9):1153-1164. doi:10.1002/ibd.20174

143. Furusawa Y, Obata Y, Fukuda S, et al. Commensal microbe-derived butyrate induces the differentiation of colonic regulatory T cells. *Nature*. 2013;504(7480):446-450. doi:10.1038/nature12721

144. Cani PD, Amar J, Iglesias MA, et al. Metabolic endotoxemia initiates obesity and insulin resistance. *Diabetes*. 2007;56(7):1761-1772. doi:10.2337/db06-1491

145. Amar J, Chabo C, Waget A, et al. Intestinal mucosal adherence and translocation of commensal bacteria at the early onset of type 2 diabetes: molecular mechanisms and probiotic treatment. *EMBO Mol Med*. 2011;3(9):559-572. doi:10.1002/emmm.201100159

146. Andreasen AS, Larsen N, Pedersen-Skovsgaard T, et al. Effects of *Lactobacillus acidophilus* NCFM on insulin sensitivity and the systemic inflammatory response in human subjects. *Br J Nutr*. 2010;104(12):1831-1838. doi:10.1017/S0007114510002874

147. O'Mahony L, McCarthy J, Kelly P, et al. Lactobacillus and bifidobacterium in irritable bowel syndrome: symptom responses and relationship to cytokine profiles. *Gastroenterology*. 2005;128(3):541-551. doi:10.1053/j.gastro.2004.11.050

148. Whorwell PJ, Altringer L, Morel J, et al. Efficacy of an encapsulated probiotic Bifidobacterium infantis 35624 in women with irritable bowel syndrome. *Am J Gastroenterol*. 2006;101(7):1581-1590. doi:10.1111/j.1572-0241.2006.00734.x

149. Pathmakanthan S, Li CKF, Cowie J, Hawkey CJ. Lactobacillus plantarum 299: beneficial in vitro immunomodulation in cells extracted from inflamed human colon. *J Gastroenterol Hepatol*. 2004;19(2):166-173. doi:10.1111/j.1440-1746.2004.03181.x

150. Braat H, van den Brande J, van Tol E, Hommes D, Peppelenbosch M, van Deventer S. Lactobacillus rhamnosus induces peripheral hyporesponsiveness in stimulated CD4+ T cells via modulation of dendritic cell function. *Am J Clin Nutr*. 2004;80(6):1618-1625. doi:10.1093/ajcn/80.6.1618

151. Mihatsch WA, Braegger CP, Decsi T, et al. Critical systematic review of the level of evidence for routine use of probiotics for reduction of mortality and prevention of necrotizing enterocolitis and sepsis in preterm infants. *Clin Nutr*. 2012;31(1):6-15. doi:10.1016/j.clnu.2011.09.004

152. Ivey KL, Hodgson JM, Kerr DA, Lewis JR, Thompson PL, Prince RL. The effects of probiotic bacteria on glycaemic control in overweight men and women: a randomised controlled trial. *Eur J Clin Nutr*. 2014;68(4):447-452. doi:10.1038/ejcn.2013.294

153. Angelakis E, Bastelica D, Ben Amara A, et al. An evaluation of the effects of Lactobacillus ingluviei on body weight, the intestinal microbiome and metabolism in mice. *Microb Pathog*. 2012;52(1):61-68. doi:10.1016/j.micpath.2011.10.004

154. Meléndez-Illanes L, González-Díaz C, Chilet-Rosell E, Álvarez-Dardet C. Does the scientific evidence support the advertising claims made for products containing *Lactobacillus casei* and *Bifidobacterium lactis*? A systematic review. *J Public Health*. 2016;38(3):e375-e383. doi:10.1093/pubmed/fdv151

155. Korpela K, Flint HJ, Johnstone AM, et al. Gut microbiota signatures predict host and microbiota responses to dietary interventions in obese individuals. *PLoS ONE*. 2014;9(6):e90702. doi:10.1371/journal.pone.0090702

156. Senan S, Prajapati JB, Joshi CG, et al. Geriatric Respondents and Non-Respondents to Probiotic Intervention Can be Differentiated by Inherent Gut Microbiome Composition. *Front Microbiol*. 2015;6. doi:10.3389/fmicb.2015.00944

Chapter 2. Modifying Macronutrients is Superior to Microbial Transplants in Reversing the Progression of Non-Alcoholic Fatty Liver Disease

Adapted from:

Mitsinikos, F. T., **Chac, D.,** Shillingford, N. and R. William DePaolo. Modifying macronutrients is superior to microbial transplants in reversing the progression of non-alcoholic fatty liver disease.

2.1 Abstract

Non-alcoholic fatty liver disease (NAFLD) is the leading cause of chronic liver injury and one of the leading causes for liver transplantation in Western countries. The pathogenesis of NAFLD include overnutrition-associated metabolic syndrome or the improper consumption of dietary macro- and micro-nutrients that either support or prevent disease development. This altered nutrient landscape has been linked to shifts within the gut microbiota which can exacerbate liver pathology and the progression of NAFLD. Treatment goals for NAFLD target lifestyle changes and dietary modifications that restrict calories and adjust macronutrient content. It is not well understood how different macronutrients alter the microbiota and whether these diet-educated microbiota contribute to the resolution of liver pathology and inflammation. Using dietary interventions and microbiota transplantation, we found that despite very different compositional changes in the microbiota, intervention diets either high in polyunsaturated fat and fiber or low in fats and fiber but high in carbohydrates reversed the progression of NAFLD and dampened inflammation. In contrast, transplantation of cecal contents from the intervention diet-fed mice to mice on a NAFLD-inducing diet was unable to prevent disease progression and, in some cases, worsened disease. These data underscore the importance of dietary changes to treat NAFLD and caution against the use of fecal microbiota transplantation in the absence of dietary and lifestyle modifications.

2.2 Introduction

Nonalcoholic fatty liver disease (NAFLD) is the most common cause of liver disease in the Western world affecting 80-100 million adults and children in the United States and an estimated 1 billion people worldwide[1]. NAFLD refers to a spectrum of liver diseases that range from bland steatosis to nonalcoholic steatohepatitis (NASH). NASH is the progressive form of NAFLD and, if left untreated, can lead to cirrhosis and hepatocellular carcinoma. NAFLD typically occurs in the context of obesity or metabolic dysregulation. The pathophysiology of NAFLD is not entirely understood; however, it is thought to be the result of multiple factors including diet, environment, genetics and, more recently, the gut microbiome[2,3].

In the last few years, a significant role of intestinal microbiota in obesity and NAFLD development has been proposed. This is underscored by the findings that germ-free (GF) mice are resistant to diet-induced obesity[4] and colonization of GF mice with the microbiota from conventional raised donors leads to an increase in body fat and development of insulin resistance[5]. The current paradigm suggests that the increased consumption of foods enriched in fat and fructose may alter the gut microbiota. Production of potentially harmful molecules by this altered microbiota can be absorbed in the intestine and carried to the liver through the portal vein, causing a chronic low-grade inflammatory state and promote the progression of NAFLD[6]. However, the molecular mechanisms contributing to NAFLD by the gut microbiota is likely complex and multifactorial and may include the regulation of energy homeostasis[5,7], fermentation of carbohydrates to short chain fatty acids (SCFAs), synthesis of triglycerides[8,9], lipoprotein synthesis and hepatic lipid export[10], bile acid homeostasis[11,12], the generation of endogenous ethanol[13] and bacterial-derived toxins and virulence factors.

Currently, the most effective treatment to reverse NAFLD consists of modifying dietary intake of fat and sugar and increasing physical activity. Diet and dietary patterns also have a strong influence on the composition and function of the microbiota[14–17] and can modify the gut microbiota very rapidly[18]. While caloric restriction can reduce weight, it is generally acknowledged that the macro- and micro-nutrients of a given diet are crucial to treat NAFLD[19]. According to international guidelines limiting the intake of calories, fats (saturated fatty acids, trans fatty acids), and fructose, while increasing the intake of lean protein, fibers, and omega -3 (n-3) polyunsaturated fatty acid (PUFA) are the dietary modifications necessary to treat

NAFLD[20]. Altering the macronutrient composition (protein and fat content), the carbohydrate load or the presence of specific bioactive compounds (omega-3 fatty acids, fibers) have been shown to influence the diversity of the intestinal microbiota[21] and have important effects on gut microbiota structure, function and secretion of metabolites[22].

Using diets high in mono- and polyunsaturated fats and fiber, low in carbohydrates or low in fat and fiber, we evaluated their impact on the progression of NAFLD to NASH and the effects of these interventions on the microbiota. Further, we sought to dissociate the effects of the diet-educated microbiota from the dietary intervention using microbiota transfers (MT). Our results indicate that both intervention diets were able to prevent the progression of NAFLD, reverse steatosis and this was accompanied by distinct changes in the microbiota. However, the microbiota was unable to transfer this phenotype and actually accelerated fibrosis when given to mice receiving food high in cholesterol and fructose. These data suggest that diets modified in types of fats and fibers can be efficacious at reversing the progression of NAFLD, but cautions that manipulating the microbiota of patients with NAFLD or NASH may not be effective without continued dietary changes.

2.3 Results

Non-alcoholic fatty liver disease (NAFLD)-inducing diet in rodent model can mimic liver pathology

There are a number of animal models that recapitulate the various hallmarks of NAFLD using deficient diets such as the methionine- and choline-deficient diet and the high fructose diet[23]. These diets, however, have additional changes not related to the human counterpart including altered metabolic profile[24] and disparate fat accumulation in the liver[25]. In this study we developed a NAFLD-inducing diet (NAF) consisting of high fat, cholesterol and fructose.

To establish the modified diet's ability to induce steatosis and non-alcoholic steatohepatitis (NASH), C57bl/6 mice were fed either a control normal-chow diet (NC) or NAF for 12 weeks (Figure 2.1A). Mice on NAF gained significantly more weight than NC mice at week 9 through to week 12 (Figure 2.1B) and this correlated with an increase in daily consumption of kilocalories (Figure 2.1C). After 12 weeks, NAF mice had significantly heavier livers and white adipose tissue than NC mice (Figure 2.1D). Development of

A

%kcal	NC	NAF
Protein	25.0	11.5
Carbohydrates	62.0	38.0
Fat	13.0	50.5

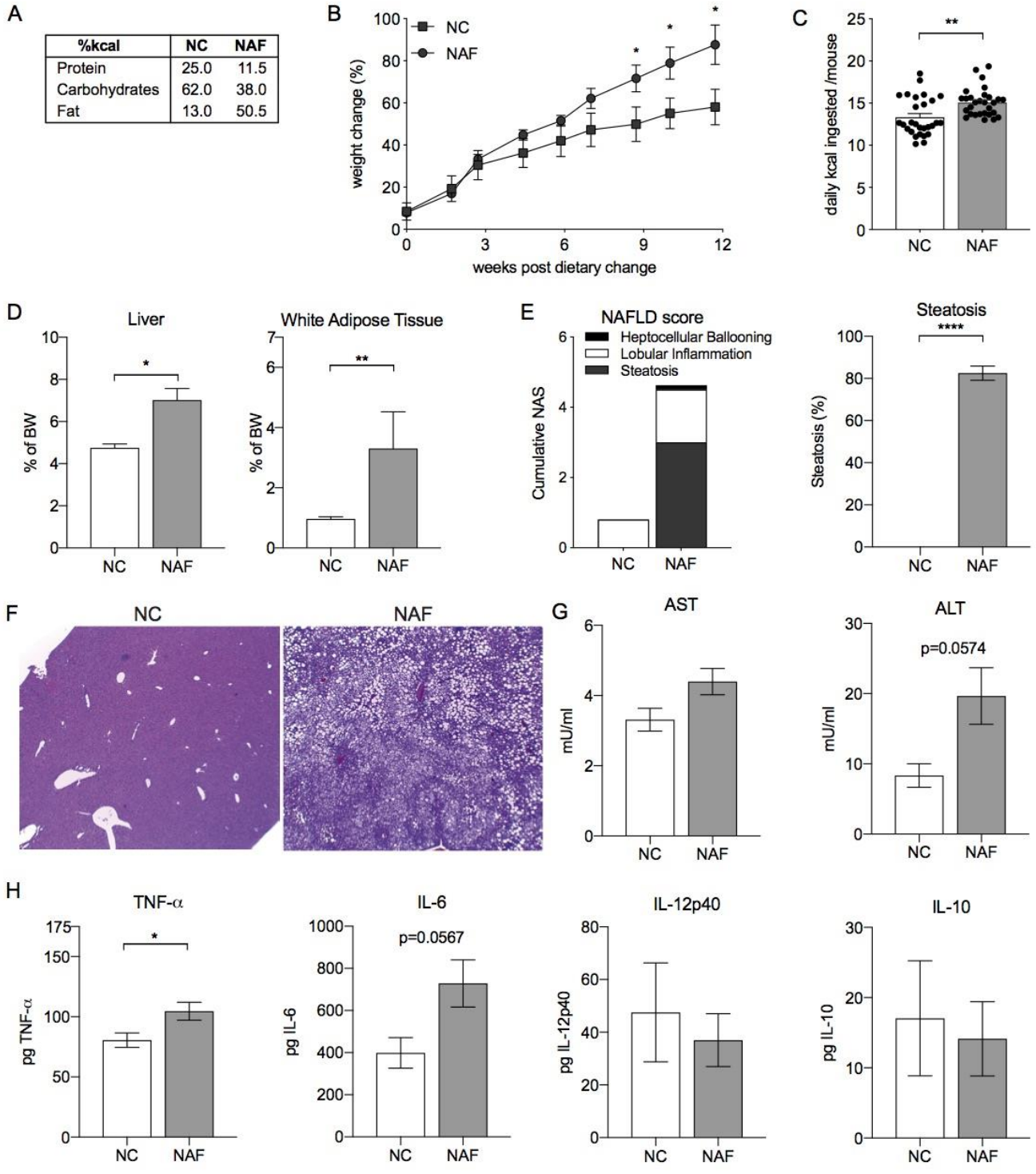

Figure 2.1: Liver inflammation and steatosis induced by a diet high in fructose, cholesterol and low in fiber

NAFLD was evaluated through liver histology. As expected, NAF mice had a high NAFLD Activity Score (NAS) with high scores for steatosis, lobular inflammation and presence of hepatocellular ballooning (Figure 2.1E). NAF mice also had significant levels of steatosis with 80% fatty liver accumulation. Staining NAF livers revealed both micro- and macrovesicular fat accumulation with greater steatosis and mild fibrosis (Figure 2.1F).

One hallmark of NAFLD progression to NASH is the presence of necroinflammatory foci and other inflammatory associated markers[26]. To assess inflammation, liver enzymes aspartate aminotransferase (AST) and alanine aminotransferase (ALT) were measured in serum and cytokines were measured in liver homogenates. Despite elevated levels of AST and ALT in NAF mice, they did not reach statistical significance (Figure 2.1G). NAF mice also had statistically elevated levels of liver TNF-α and near significant levels of IL-6 while there was no difference in IL-12p40 or IL-10 (Figure 2.1H). Taken together, these data indicate that the NAF diet could induce a disease similar to human NAFLD with increased steatosis, liver inflammation, AST and ALT levels.

Figure 2.1: Liver inflammation and steatosis induced by a diet high in fructose, cholesterol and low in fiber

C57bl/6 wildtype mice were treated with a non-alcoholic fatty liver disease diet (**NAF**) or normal control diet (**NC**) for 12 weeks ad libitum. (**A**) macronutrient breakdown of diets. (**B**) Percent weight change during diet. (**C**) Daily consumption of diet by kilocalories (kcal) per mouse per diet. (**D**) Liver and white adipose tissue weights by percent body weight at the end of the 12 weeks. (**E**) NAFLD-activity score (NAS) and percent steatosis of mice scored in a blinded fashion by a pediatric liver pathologist. (**F**) Representative images of hematoxylin & eosin (H&E) and trichrome stained liver sections. (**G**) Aspartate transaminase (AST) and alanine transaminase (ALT) levels measured in serum by ELISA. (**H**) Levels of TNF-a, IL-6, IL-12p40, and IL-10 cytokine in 50 mg homogenized liver tissue. Data is the mean ± SEM of 2 independent experiments, n=5 – 8 mice per group. Statistics for (B) is 2-way ANOVA, Sidak's multiple comparisons; (C-E, G-H) is Student's unpaired t-test. *, $p<0.05$; **, $p<0.01$; and ****, $p<0.001$.

Dietary intervention suppresses weight gain and reverses fat accumulation in the liver

The most optimal treatment for NAFLD is currently managing a healthy lifestyle through dietary modification which allow NAFLD patients are able to reduce weight, improve blood pressure and cholesterol levels, and potentially reduce liver steatosis[27]. In this study, we assessed the potential of preventing NAFLD using two different intervention diets. We developed these diets based on current NAFLD management recommendations[28]: one diet with high polyunsaturated and saturated fats and high fiber (HFF) and another with high carbohydrates with low fats and low fiber (LFF) (Figure 2.2A; Supplemental Table 2.1).

Mice were placed on the NAF diet for 6 weeks (NAF6) and then switched to one of the intervention diets or maintained on the NAF diet for an additional 6 weeks (Figure 2.2B). To investigate whether the intervention diets could reverse or halt NAFLD progression, mice on the dietary interventions were compared to mice on NAF for 6 weeks (NAF6). During the 6 weeks of intervention diet, mice on HFF and LFF gained significantly less weight than mice on NAF (Figure 2.2C). While both dietary interventions reduced the weight of the liver and adipose tissue (Figure 2.2D), the HFF diet had a more significant impact on liver weight, while the LFF diet promoted loss of white adipose tissue (Figure 2.2D). Following dietary intervention, NAFLD activity score (NAS) was assessed on liver pathology. Mice receiving intervention diets had NAS scores of less than 2 whereas NAF6 mice had an average cumulative score of 4.67 (Figure 2.2E). Mice receiving either the HFF or LFF diets had a significant reduction in lobular inflammation compared to the NAF6 mice. However, mice receiving the LFF-diet had a complete reversal of steatosis and hepatocyte ballooning, while HFF mice had hepatocyte ballooning, and some steatosis, albeit still significantly less than NAF mice at 6 weeks (NAF6) (Figure 2.2E). The presence of fibrosis was assessed with Masson trichrome staining and demonstrated only rare cases of stage I, focal subcapsular areas of steatosis, and instances of perisinusoidal fibrosis in both HFF and LFF groups (Figure 2.2F). Taken together, these data demonstrate that both intervention diets were able to improve liver histology and reverse steatosis.

A

% kcal	NAF	HFF	LFF
Protein	11.5	15.4	18.3
Carbohydrates	38.0	18.3	62.5
Fat	50.5	66.3	19.2
Fat (g/kg)			
Saturated	128.4	178.0	15.9
Unsaturated (total)	141.7	110.4	51.2
Monounsaturated	118.0	67.3	16.5
Polyunsaturated	23.7	43.1	34.7
Others			
Cholesterol mg/kg	12772.6	535.5	396.3
Fiber (NDF), g/kg	40.9	290.0	50.0
Sucrose, g/kg	200.0	116.9	168.5
Fructose, g/kg	100.0	0.0	0.0

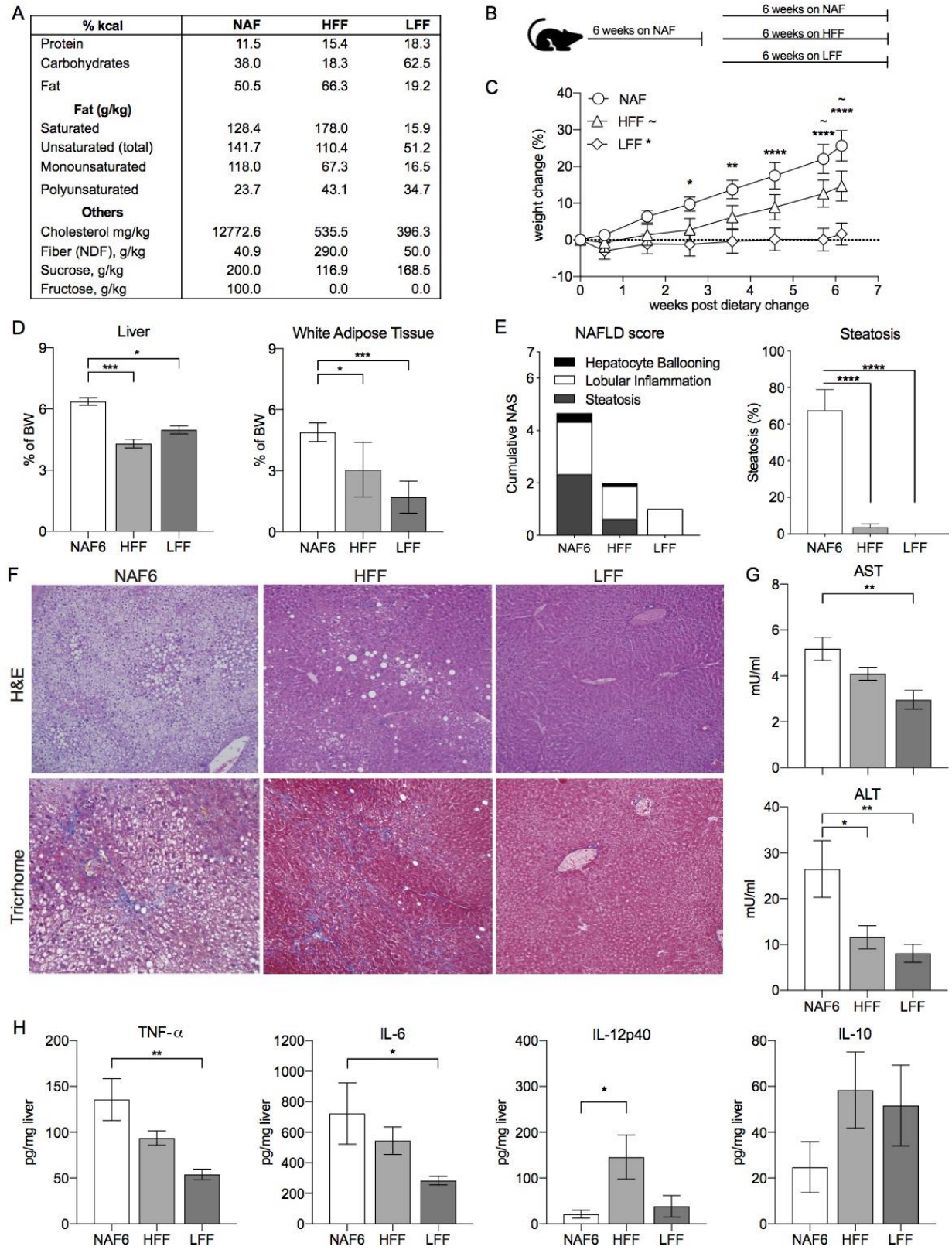

Figure 2.2: Both a high fat/high fiber and a low fat/low fiber diet can reverse the progression of NAFLD.

Figure 2.2: Both a high fat/high fiber and a low fat/low fiber diet can reverse the progression of NAFLD.

C57bl/6 wildtype mice were treated with NAF for 6 weeks ad libitum and then introduced to a dietary intervention of either a high-fat/high-fiber diet (**HFF**) or a low-fat/low-fiber diet (**LFF**) for 8 additional weeks. (**A**) Macronutrient breakdown of diets and (**B**) model of dietary intervention. (**C**) Percent weight change during dietary intervention using NAF at 6 weeks (NAF6) as a baseline. (**D**) Liver and white adipose tissue weights by percent body weight. (**E**) NAS and percent steatosis of mice scored by a pediatric liver pathologist blinded to the samples. (**F**) Representative image of H&E and trichrome stained liver section. (**G**) AST and ALT levels measured in serum by ELISA. (**H**) Levels of TNF-a, IL-6, IL-12p40, and IL-10 cytokine measurements in 50 mg homogenized liver tissue. Data is the mean ± SEM of 2 independent experiments, n=5-8mice/group. Statistics for (C) is 2way ANOVA, Dunnett's multiple comparisons; (C-E, G-H) is one-way ANOVA, Dunnett's multiple comparisons; *, $p<0.05$; **, $p<0.01$; ***, $p<0.005$; and ****, $p<0.001$.

Dietary intervention improves liver enzymes and cytokine levels

Inflammation levels were assessed in mice receiving dietary interventions using serum levels of ALT and AST which we had already seen elevated in NAF6 mice (Figure 2.2G). The HFF diet significantly reduced levels of ALT but had no significant impact on AST levels. In contrast, the LFF diet was able to significantly lower levels of both ALT and AST (Figure 2.2G). Analysis of cytokine levels using liver homogenates also revealed differences between the two intervention diets. Compared to NAF6 mice, mice receiving the LFF diet had significantly lower levels of TNF-α and IL-6 (Figure 2.2H). In contrast, the HFF diet had little impact on liver levels of TNF-α or IL-6, but caused significantly higher levels of proinflammatory cytokine, IL-12p40. Interestingly, levels of anti-inflammatory IL-10 trended higher in mice given either the LFF or HFF diet compared to mice receiving NAF diet for 6 weeks, but these levels did not reach statistical significance (Figure 2.2H). These data align with the histological improvements and suggest that implementing a dietary intervention can reverse hepatic steatosis and reduce inflammation in the liver.

Fecal microbial communities from dietary interventions shift to more organized and central microbiotas

Diet has a major influence in shaping the gut microbiome, therefore, it is not surprising that changes in the composition of the microbiota have been associated with NAFLD. Underscoring this association is the

finding that high-fat fed germ-free mice are resistant to obesity and steatosis[29]. In order to assess shifts in the microbiota accompanying the resolution of steatosis in mice fed the intervention diets we performed 16s rRNAsequencing on ileal and fecal samples. After being on NAF for 6 weeks, there was a shift from a Bacteroidetes-dominant to a Firmicutes-dominant microbiome, as seen in other studies using high-fat diets[14] (Figure 2.3A; Supplemental Figure 2.1). Mice on NAF maintained the Firmicutes-dominant microbiota composition through to week 12. Despite resolving steatosis and improving pathology, HFF-fed mice had a comparable phylum-level microbiota to mice maintained on the NAF diet. In contrast, mice receiving the LFF diet had a shift from the Firmicutes-dominant microbiota towards a more diverse community with significant increases in Actinobacteria and Bacteroidetes (Figure 2.3A). The change in microbiota community was also reflected in the ileum. Mice receiving the LFF diet had high levels of *Bifidobacteriaceae* present in the ileum as well as the fecal pellets (Supplemental Figure 2.2).

When comparing diversity using Inverse Simpson at the genus level, we found that the HFF-, LFF- and NAF-fed mice had more diversity than the NAF6 mice (Figure 2.3B). Despite a similar phylum-level composition, the HFF-fed mice also had an increase in diversity compared to the NAF6 mice, suggesting differences at the genus level within Firmicutes. This was confirmed using principal coordinate of analysis (PCoA) which showed an overlap in bacterial communities between the NAF6 and NAF that is significantly distinct from both HFF and LFF microbiotas via AMOVA analysis (Figure 2.3C)[30]. Whereas the HFF community had a wide spread on the PCoA, the LFF microbiota are tightly clustered with little overlap with NAF6 or NAF mice with statistical significance via HOMOVA analysis (Figure 2.3C). To identify the differences in the microbiota communities we visualized microbial families having greater than 1% abundance using a heatmap. Both NAF groups had high levels of *Erysipelotrichaceae* and *Verrucomicrobiaceae*, which made up over half of the microbiota composition (Figure 2.3D). mice receiving the HFF diet had comparable phylum-level abundance of Firmicutes to the NAF compositions also had high abundance of *Erysipelotrichaceae* (10.4%) but also had increases in the abundance of Firmicutes families *Peptostreptococcaceae* (10.3%), *Staphylococcaceae* (16.8%) and *Lactobacillaceae* (17.9%) and a decrease in *Verrucomicrobiaceae*. *Erysipelotrichaceae* (11.6%) was also abundant in the LFF-fed mice but was accompanied by increases in *Porphyromonadaceae* (12.7%), *Bifidobacteriaceae* (25.6%), and *Verrucomicrobiaceae* (50%). Interestingly, our data shows that the abundance of *Erysipelotrichaceae and*

Verrucomicrobiaceae have an inverse relationship (Figure 2.3E), which is especially significant when comparing the NAF6 and NAF slopes (Supplemental Table 2.2). *Erysipelotrichaceae* also had a significant positive correlation with weight gain regardless of diet, while *Verrucomicrobia* trended with less weight gain (Figure 2.3F). While the relationship with *Erysipelotrichaceae* did not depend on diet, there was a significant difference between slopes depending on diet with weight change and *Verrucomicrobiaceae*. *Bifidobacteriaceae*, on the other hand, had a significant negative relationship with weight change regardless of diet (Figure 2.3F, Supplemental Table 2.3). These data demonstrate a shift in the microbial composition of NAF6 mice fed either of the intervention diets and that resolution of steatosis occurred in the presence of these very different microbial compositions.

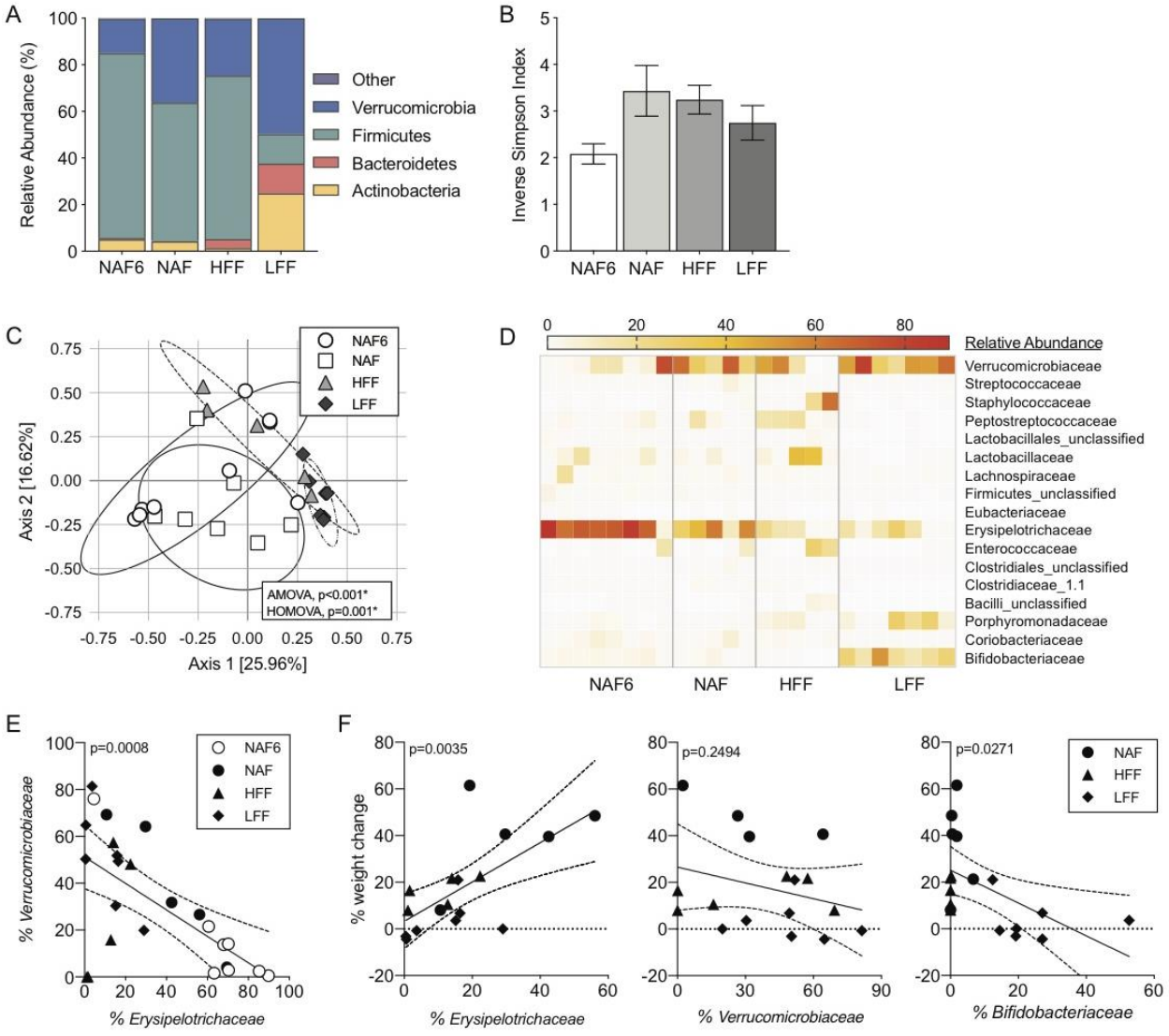

Figure 2.3: HFF and LFF diets cause distinct shifts in the composition of the microbiota following dietary intervention

Figure 2.3. HFF and LFF diets cause distinct shifts in the composition of the microbiota following dietary intervention

Microbiota sampling of fecal contents of mice in treatment groups NAF6, NAF, HFF and LFF. (**A**) Phylum-level abundance and (**B**) diversity measured using Inverse Simpson Index. (**C**) Principal Coordinate of Analysis (PCoA) of microbiota composition at the genus level. (**D**) Heatmap representation of family level abundance with families >1% abundance. (**E**) Relative abundance of *Erysipelotrichaceae* and *Verrucomicrobiaceae* by scatter plot. (**F**) Correlation between weight change and abundance of *Erysipelotrichaceae, Verrucomicrobiaceae* and *Bifidobacteriaceae.* Data is the mean ± SEM of 2 independent experiments, n=5-8mice/group. Statistics in (C) is analysis of molecular variance (AMOVA) and homogeneity of molecular variance (HOMOVA). (E-F) is Pearson Correlation Coefficient of all data points.

Microbiota transplantation fails to relieve NAFLD symptoms and liver inflammation

To understand whether the intervention diet-educated microbiota could reverse steatosis or inflammation independent of the intervention diet itself, we performed microbiota reconstitution experiments. Mice fed NAF for 6 weeks were placed on a cocktail of antibiotics in their drinking water for 10 days. At the end of this period the recipient mice were administered the cecal contents from mice that had previously undergone one of the dietary interventions or stayed on NAF. Post-reconstitution, the mice were maintained on NAF diet for an additional week. During microbiota depletion, there was little weight loss observed in any of the groups, in fact, none of the mice lost more than 10% of their weight (Figure 2.4A). After the microbiota was reconstituted by oral gavage, mice receiving the microbiota from either HFF (HFF MT) or LFF (LFF MT) donors had less weight gain compared to mice receiving the microbiota from NAF donors (NAF MT) or untreated NAF mice (Figure 2.4A). Liver (Figure 2.4B) and adipose tissue (Supplemental Figure 2.3) weights were measured and no significant changes were observed.

Assessment of the liver pathology from NAF-MT mice displayed histological characteristics of late stage NAFLD/early NASH (Figure 2.4C). In addition to the presence of both macro- and microsteatosis, necroinflammatory foci and fibrosis were revealed by trichrome staining (Figure 2.4D). Despite the decrease in weight observed in mice receiving cecal contents from either of the intervention diets, there were no histological improvements. Mice receiving cecal contents from either diet had histological lesions that resembled the pathology of the NAF-MT and NAF-fed mice with similar overall NAS scores and a similar percentage of steatosis (Figure 2.4C-D).

As expected from the amount of injury observed in the liver, AST and ALT levels in the serum of mice receiving cecal contents from mice fed either of the intervention diets was as high as mice receiving the NAF diet for 12 weeks (Figure 2.4E). In addition to the elevated AST and ALT, mice reconstituted with either intervention-diet educated microbiota also had TNF-α, IL-6 and IL-12p40 levels in the liver equal to the NAF-MT mice (Figure 2.4F). Interestingly, IL-10 was not detected in the livers of the LFF-MT or HFF-MT mice but was present in the NAF-MT mice (Figure 2.4F). These data suggest that the microbiota from mice receiving dietary interventions, and who showed complete reversal of NAFLD, was unable to resolve disease in the absence of the dietary factors that shaped the microbiota. To determine if the transferred gut microbiota was maintained following reconstitution and 1 week of NAF feeding 16S sequencing was performed on representative donor cecum samples and fecal samples post microbiota transplant. At the phylum level, no significant differences were found. Both HFF- MT and LFF-MT groups had similar levels of Firmicutes and Bacteroidetes compared to NAF and NAF MT mice (Figure 2.4G, Supplemental Figure 2.4). Whereas the LFF cecum contents contained 10% of Actinobacteria, no Actinobacteria was recovered in the fecal pellets of LFF-MT mice. Analysis at the family level revealed no significant changes between MT groups (Supplemental Figure 2.3). To further understand why the microbiota of the intervention diets was unable to transfer protection from NAFLD, we compared the predicted metabolic functions of dietary intervention and MT mice using Phylogenetic Investigation of Communities by Reconstruction of Unobserved States (PICRUSt)[31]. Overall, there are significant differences in PICRUSt metabolic functions among mice on NAF for 6 weeks, the two dietary interventions and the MTs (Figure 2.4H). To analyze specific changes between groups, each experimental group was compared to NAF6. While both LFF and the LFF FMT group had significant differences compared to NAF6, some of the metabolic features were significant in one but not the other (Figure 2.4H-I).

All in all, we show that administering a microbiota transplant during a disease course without altering the diet does not improve NAFLD and is far less superior than dietary intervention. Whereas the dietary intervention significantly altered the microbiota, the NAFLD-inducing diet prevents changes in the microbiota despite MT and these changes are separate from predicted metabolic functions.

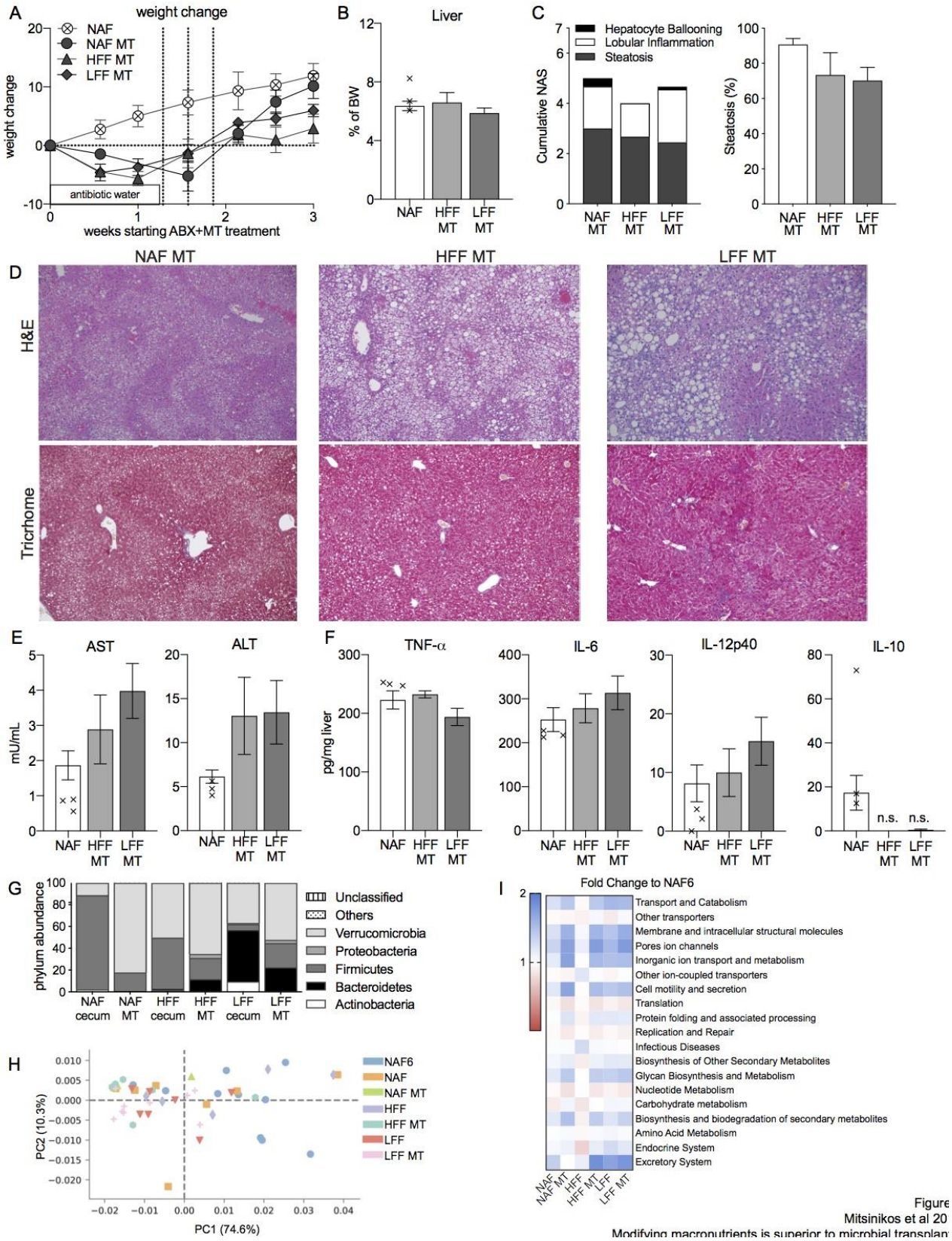

Figure 2.4: HFF or LFF diet-educated microbiota alone is not sufficient to reverse NAFLD.

Figure 2.4: HFF or LFF diet-educated microbiota alone is not sufficient to reverse NAFLD.
Mice on NAF for 6 weeks were given a cocktail of antibiotics (see Materials & Method) in their drinking water for 1-1.5 weeks and then given microbiota transplants (**MT**) using donor cecal contents from mice at the end of the diet intervention model. The recipient mice were maintained on the NAFLD diet for 2 weeks. (**A**) Percent weight change during MT using NAF at 6 weeks as baseline. (**B**) Liver weight as percent body weight. (**C**) NAS and percent steatosis of liver. (**D**) H&E and trichrome staining of liver histology. (**E**) AST and ALT measured in serum by ELISA. (**F**) TNF-a, IL-6, IL-12p40, and IL-10 cytokine measurements of homogenized liver tissue. (**G**) Phylum-level abundance of donor cecal and treated fecal microbiota. (**H**) Principal component analysis and (**I**) heatmap of fold change of Phylogenetic Investigation of Communities by Reconstruction of Unobserved States (PICRUSt) analysis. Data is the mean ± SEM of 2 independent experiments, n=3-9mice/group.

2.4 Discussion

In this study we demonstrate that altering specific macronutrients can be highly effective at reversing the progression of NAFLD in mice previously receiving a diet high in cholesterol, carbohydrates and fructose for 6 weeks. Nutritional interventions shifted the types of fat, altered the amount of carbohydrates and/or increased digestible and non-digestible fibers. These data demonstrate a reduction in steatosis, inflammation and liver enzyme levels following either of the dietary interventions. However, it is important to note that each diet had distinct effects on clinical characteristics and the microbiome. In contrast, microbiota transplants using cecal material from mice fed either of the intervention diets showed no clinical improvements and had liver pathology with inflammation and fibrosis. These results highlight the importance of diet in the treatment of NAFLD and further suggest that the use of microbiota transplants to treat NAFLD may not be efficacious in the absence of dietary and lifestyle changes.

It is widely accepted that diet exerts a strong influence on the microbiome and that high fat and Western-style diets are associated with a shift in the ratio of Bacteroidetes towards Firmicutes[14]. Using a modern Western diet, which is low in fiber and high in cholesterol and fructose with a carbohydrate to fat ratio at 1-1.5, we sought to determine whether diets with specific nutritional modifications in fats, fiber and carbohydrates could halt the progression of NAFLD. Both of the dietary interventions were able to reduce steatosis, lower AST and ALT and dampen inflammation, but differed in the extent of these reductions. While the LFF diet completely reversed steatosis and significantly decreased both AST and ALT, the HFF diet only partially resolved steatosis and only lowered AST.

We observed that mice on a diet supplemented with cholesterol and fructose for 6 weeks had a reduction in Bacteroidetes and an increase in Firmicutes, similar to reports in the literature using other high fat or Western-style diets[32]. We also observed an increase in Verrucomicrobia which correlated with the length of time the mice received the NAF diet and with less weight gain. The observed increase in Verrucomicrobia between the 6 week and 12 week NAF mice was also observed in mice fed the LFF diet and, to a lesser extent, mice fed the HFF diet. Verrucomicrobia, specifically *Akkermansia mucinaphilia*, has recently been shown to be decreased in mice fed high fat diets and has an inverse correlation with body weight in both mice and humans[33]. In this present study the increases in Verrucomicrobia do not correlate with loss of body weight of dietary intervention mice, nor does it seem to impact liver histology since mice fed NAF for 12 weeks had the second highest abundance of this phyla. These data may indicate that the abundance of a single species is not enough to reverse weight gain, but rather, it may be a combination of microbes that together produce a metabolic signature that can help reduce steatosis and reverse obesity. In addition to Verrucomicrobia, mice fed the LFF diet also had an increase in Actinobacteria, specifically *Bifidobacteriaceae*. Reports in the literature have shown that probiotic administration of *Bifidobacteria* increases the abundance of *Akkermansia*[34]. Therefore, it is possible that the dramatic effects in weight loss and the reversal of liver pathology in the LFF mice may be due to a symbiotic relationship between *Akkermansia*, *Bifidobacteria,* and the host. This may also explain why the LFF MT failed to provide protection because, despite finding an equal abundance of Verrucomicrobia, there was very low abundance of Actinobacteria in the mice that received the LFF MT. Overall these data suggest Verrucomicrobia alone is not enough to reverse or halt the progression of NAFLD, but may act in concert with other commensals to truly impact disease.

Switching mice to the HFF diet had little impact on the relative abundance at the phyla level, though we did observe shifts at the family level within Firmicutes. Prior to receiving either intervention diets at 6 weeks, the NAF mice were dominated by *Erysipelotrichaceae*. Mice that received an intervention with the HFF diet had increases in *Peptostreptococcaceae*, *Staphylococcaceae* and other families within the Bacilli class, while *Erysipelotrichaceae* was reduced. Unlike its HFF-fed counterparts, mice switched to the LFF diet had significant increases in Actinobacteria, Bacteroidetes and Verrucomicrobia with a significant decrease in Firmicutes. However, this also corresponded with a reduction in *Erysipelotrichaceae*. Taken together our

data associates steatosis with the presence of *Erysipelotrichaceae,* an observation also seen in patients with NAFLD[35]. Indeed, there is mounting evidence implicating a role for *Erysipelotrichaceae* in metabolic disorders and correlations between the levels of *Erysipelotrichaceae* and host cholesterol metabolites[36]. The relationship between *Erysipelotrichaceae* and cholesterol is intriguing, especially as cholesterol was supplemented in our NAFLD-inducing diet and low in both the HFF and LFF diets which had less *Erysipelotrichaceae*.

The fatty acid composition between the three diets was very different. Our NAFLD-inducing diet had an equal ratio of saturated fatty acid (SFA) and monounsaturated fatty acids (MUFA) but had a third less polyunsaturated fatty acids (PUFA) despite nearly 20 times more omega-6 than omega-3. The HFF diet had nearly 2.5 times more SFA than MUFA, however the sources of the saturated fats used for the diets were different (i.e. beef tallow and coconut oil versus anhydrous milkfat, lard and vegetable shortening). Unlike the NAFLD-inducing saturated fats that are comprised mostly of palmitic and stearic acid, the saturated fats in the HFF diet was enriched for lauric acid. Lauric acid has been shown to raise total cholesterol levels, but this is due to specifically raising high density lipoproteins (HDL) which has been shown to have health benefits[37]. The finding that our HFF diet. which is high in SFAs, was able to reverse steatosis and progression of NAFLD is not surprising in light of recent studies showing that diets high in fats, such as the Mediterranean diet[38], confer health benefits. Further, the high amount of lauric acid, which is a medium chain fatty acid (MCFA), has been shown to reduce steatosis and hepatic injury by upregulating fatty acid liver oxidation[39,40]. While it has been demonstrated that MCFAs can impact the composition of the gut microbiota by significantly decreasing the ratio of Firmicutes to Bacteroidetes leading to a reduction in steatosis, we did not observe any reduction in the abundance of Firmicutes or an expansion of Bacteroidetes in the HFF -fed mice. However, we did observe shifts in the OTUs within the Firmicutes phyla, though we cannot say whether those changes are due to the lauric acid and MCFAs found in the HFF diet. In contrast, the LFF diet had over 4 times less fat than both the NAFLD-inducing and the HFF diets and the fat present was mainly enriched in omega-3 PUFAs, approximately 2 times more than omega-6. A recent randomised clinical trial administering omega-3 to individuals saw increases in bifidobacterium[41] similar to what we observed in our mice fed the LFF diet.

Dietary modifications impact both the physiology of the host and the microbiota. In order to understand how dietary shifts in microbial composition impacted the progression of NAFLD we performed microbiota transplants. Instead of receiving a dietary intervention after 6 weeks on the NAF diet, mice were administered cecal contents from mice fed either of the intervention diets or from those that remained on the NAF diet throughout the experiment. Unlike the mice receiving either of the intervention diets, microbiota transplantation showed no improvement in steatosis, AST or ALT levels, or liver cytokines compared to mice receiving the NAF diet for 12 weeks. In fact, mice receiving microbiota from LFF mice had extensive pericellular fibrosis and necroinflammatory foci. Our data is in contrast to recent studies that have shown slight beneficial effect of FMT in treating metabolic disease in human and animal studies[42–44]. While several clinical reviews propose microbiota transplants, to our knowledge only one has tried FMTs in a NAFLD-induced diet mouse study. In this study by Zhou and colleagues, mice on a high-fat diet received FMT from healthy, untreated mice every day for 8 weeks. The mice receiving FMTs had marked improvements in the degree of hepatic steatosis, lobular inflammation and hepatocyte ballooning, as well as a reduction in body weight, epididymal fat and serum levels of ALT[44] (Zhou). In contrast, our study found FMTs for diet-induced NAFLD was not as effective. Obviously the frequency and the diets of the donor mice differ greatly between the two studies, our study only gave the mice 3 microbiota transplants over the course of 6 days and terminated the experiment 7 days following the last transplant. Additionally, our study did not evaluate the impact of microbiota transplants derived from donors on standard mouse chow. Instead, our study aimed to identify clinically relevant diets and their components that exacerbated or ameliorated NAFLD. Our results using diets with specific nutrient profiles that had positive outcomes exacerbated disease post microbiota transplant. While the study by Zhou and colleagues demonstrates the importance of restoring a 'physiological' gut microbiome, our current study shows that microbiota transplants may not be as advantageous as dietary modifications. These contrasting results highlight the critical need for clinical validation of FMTs.

Altogether, these data demonstrate that altering the diet composition at the macronutrient level can prevent steatosis and reverse NAFLD. Specifically, we found that a diet high in saturated fats derived from products that have high medium chain fatty acids, high in fiber and high in omega-3 PUFAs or a diet low in fats but high in omega-3 PUFA were both able to reverse the progression of NAFLD. However, microbiota

transplantation using cecal contents from mice fed these diets was unable to confer protection from NAFLD and, in some instances, lead to a more severe pathology. Our data suggests that microbial transplants to treat NAFLD may not be useful in the absence of continued dietary modifications and that more work must be done to understand the interaction between diet and the microbiome in the context of a given disease before they can be used to treat NAFLD.

2.5 Materials and Methods

Experimental Animals

Male C57BL/6 mice 5-6 weeks of age were purchased from Jackson Laboratory (Bar Harbor, Maine USA) and maintained at the University of Southern California (USC; Los Angeles, CA) animal facility under specific pathogen-free conditions. Mice were randomly separated into experimental and control groups. Mice were fed indicated diets for 6 weeks or 12-14 weeks and maintained on sterile, distilled non-chlorinated and non-acidified water ad libitum[5]. All animal experiments were performed following experimental review and approval by the Institutional Biosafety Committee and the Institutional Animal Care and Use Committee.

Rodent diets

Experimental mice were fed a NAFLD-inducing (NAF) diet that contains 50% of kcal from fat, 20% sucrose, 10% fructose, and 1.25% cholesterol (TD. 150235, Teklad Diet, Envigo, Madison, Wisconsin USA www.envigo.com). After 6 weeks, some mice were examined for liver pathology, steatosis and fibrosis, one group was switched to a dietary intervention, and an additional group was treated with antibiotic-water and given a fecal microbiota transplant. Mice undergoing dietary intervention were immediately switched to a high-fat, high fiber (HFF) diet containing 66% of kcal from fat (primarily beef tallow and coconut oil) and increased non-digestible fibers or a low-fat, low-fiber (LFF) diet containing 20% of kcal from fat (primarily beef tallow and coconut oil) for 8 weeks. Control mice were fed the NAF diet for a total of 12-14 weeks.

Microbiota transplant

Prior to microbiota transplant (MT), mice on the NAF diet for 6 weeks were placed on antibiotic water containing a cocktail of 1g/L ampicillin (Alfa Aesar), 1g/L gentamicin (Amresco), 1g/L neomycin (Sigma

Aldrich), 1g/L metronidazole (MP Biomedicals) and 0.5g/L vancomycin (Alfa Aesar) for 1.5 weeks. After switching to regular water, mice received three oral gavages every other day of cecal contents that were collected from mice that were on NAF for 6 weeks and subsequently placed on LFF or HFF or continued on NAF for 6-8 weeks. Cecal contents were resuspended in 1ml sterile PBS and mice were gavaged with 100uL of resuspended contents. Mice were maintained on NAF diet and euthanized 2 weeks following the first MT gavage.

Tissue collection

Stool was collected prior to dietary intervention (6 weeks on the NAF diet), and then 2 and 6 weeks following dietary intervention and at the end of the FMT. Samples were stored at -80°C. At the time of euthanization, tissue samples were collected. Blood was obtained via terminal cardiac puncture. Subcutaneous white adipose tissue from the right hind limb and the right sided epididymal white adipose tissue were obtained and weighed. All samples were flash frozen in liquid nitrogen and stored at -80°C. The liver was isolated from its vascular attachments and gallbladder, weighed, and divided into 4% paraformaldehyde for histology or frozen in liquid nitrogen and stored at -80° C.

Liver histology

Liver tissue fixed in 4% paraformaldehyde was transferred into 95% ethanol and processed at AML laboratories (Baltimore, Maryland). Formalin-fixed paraffin-embedded histologic sections were stained with hematoxylin and eosin (H&E) and Masson trichrome stains to assess and grade non-alcoholic fatty liver disease (NAFLD) and to determine the degree of fibrosis.

NAFLD activity score (NAS) and fibrosis

For each subject multiple H&E stained slides were evaluated for the percentage of hepatic steatosis, portal inflammation, lobular inflammation and hepatocyte ballooning. These slides were also assessed for the presence or absence of Mallory-Denk bodies, megamitochondria, lipogranuloma and glycogenated nuclei. The non-alcoholic fatty liver disease activity score (NAS) was derived using the extent of fatty change, degree of lobular activity and the presence or absence of ballooned hepatocytes[45,46]. The extent of steatosis was given a score between “0” and “3”, where a score of “0” was assigned to those liver sections in which

less than 5% of the surface area was involved by steatosis; a score of “1” for those with 5-33% involvement by steatosis, “2” for those with 33-66% and a score of “3” for those with more than 66% involvement by steatosis. Lobular activity was also scored between “0” and “3”. Those sections with no evidence of lobular necroinflammatory infiltrates were given a score of “0”; those with less than 2 foci of lobular necroinflammatory infiltrates per 200X field (20X objective) were given a score of “1”; those with 2-4 foci a score of “2” and those with more than 4 foci were assigned a score of “3”. The third component of the scoring system is hepatocyte ballooning. Where hepatocyte ballooning was absent a score of “0” was given. Sections in which ballooning was present but only occasionally were given a score of “1” and if many ballooned hepatocytes were present a score of “2” was issued. The score for these three components (steatosis, lobular activity and hepatocyte ballooning) were tallied to give the final NAS. The maximum attainable score is “8”. To assess the degree of fibrosis, histologic sections were stained with Masson trichrome stain. Fibrosis was scored from “0” to “4”. A score of “0” meant that there was no fibrosis to report. A score of “1” was given to biopsies with either perisinusoidal or periportal fibrosis. When perisinusoidal and portal/periportal fibrosis was present a score of “2” was assigned. If bridging fibrosis was detected a score of “3” would be assigned and frank cirrhosis would generate a fibrosis score of “4”.

Liver cytokine enzyme-linked immunosorbent assay (ELISA)

Liver tissue samples that were previously frozen at -80°C were thawed and homogenized using the Omni International Bead Ruptor 12. Briefly, approximately 100 mg of liver were placed into bead-beating tubes with 50 uL garnet beads and 1mL of phosphate-buffered saline supplemented with protease and phosphatase inhibitors (Pierce, Thermo Scientific). Samples were bead-beat at 1500 rpm for 15 seconds. Homogenized liver tissue was then analyzed for the following cytokines: tumor necrosis factor (TNF)-α, interleukin (IL)-10, IL-12p40, and IL-6 (BD Biosciences). TMB substrate (Dako, Carpinteria, CA) was used for detection and absorbance was read at optical density (OD) 450nm with 570nm correction.

Microbiota sequencing, sequence curation and analysis

Microbiota samples were processed and sequenced at Research and Testing Laboratory (RTL; Lubbock, TX) based upon RTL protocols using MiSeq Illumina platform. Universal bacterial primers 515F

'GTGCCAGCMGCCGCGGTAA' and 806R 'GGACTACHVGGGTWTCTAAT' were used to amplify the variable regions V3-V4 of the 16S rRNA genes. 16s rRNA gene sequences were curated using mothur v.1.36.1[47], following the MiSEQ SOP. Briefly, sequences were denoised using a flowgram denoising algorithm[48], aligned to Silva 16s rRNA sequence database[49] and pre-clustered to allow up to a 2-bp difference between sequences[50]. Chimeras were detected using UCHIME[51] and were culled along with chloroplast and mitochondrial sequences. Sequences were then classified using the Ribosomal Database Project version 14 with a confidence score greater than 80%[52] and phylotyped to the family level. Prior to any further data analysis, the number of sequences were normalized to 2000 reads per sample. Beta diversity was calculated using the Theta YC distance metric with the family-level data and visualized using principal coordinates analysis (PCoA).

Statistical analysis

Data are shown as the mean ± standard error of the mean (SEM). Student T-tests, one-way ANOVAs and two-way ANOVAs with post-hoc tests were used to determine statistical significance between the dietary treatments as indicated in each figure. Pearson Correlation Coefficient was used to analyze the correlation between weight and certain bacterial families. Graphpad Prism (San Diego, CA) was used for graphical and statistical analysis and $p < 0.05$ was considered statistically significant. 16S sequencing data was evaluated for statistical significance using analysis of molecular variance (AMOVA) and homogeneity of molecular variance (HOMOVA) tests of PCoAs on mothur v.1.36.1[30,47].

2.6 Supplemental Tables and Figures

Supplemental Table 2.1: Nutrient Breakdown of NAFLD and intervention Diets

g / kg	NAF	HFF	LFF
	TD.150235	**TD.150587**	**TD.150588**
Casein	160	130	130
L-Cystine	1.5	3	3
Mineral Mix, AIN-93M-MX	45	45	35
Vitamin Mix, AIN-93-VX	20	20	10
DL-Methionine, FG (99%)	-	2	2
Egg White Solids, spray-dried	-	36	36
Egg Yolk Powder	-	10	10
Fish Meal, menhaden	-	5	5
High Amylose Corn Starch	-	50	482
Sucrose	200	116.936	168.482
Fructose	100	-	-
Corn Starch	44.96	-	-
Maltodextrin	100	-	-
Anhydrous Milkfat	94	-	-
Vegetable Shortening, hydrogenated	105	-	-
Palm Oil	74	-	-
Coconut Oil	-	122	2
Beef Tallow	-	89	2
Fish Oil	-	32	25
Lard	-	10	2
Flaxseed Oil	-	33	33
Cholesterol	12.5	-	-
Cellulose	-	290	50
Choline Bitartrate	2	2	2
Biotin	-	0.004	0.004
TBHQ, antioxidate	0.04	0.06	0.14
Potassium Phosphate, dibasic	-	4	2.5

Supplemental Table 2.2: Relationship between Erysipelotrichaceae and Verrucomicrobiaceae

% Erysipelotrichaceae vs % Verrucomicrobiaceae				
Pearson r	p-value	0.0008	***	
	X vs. NAF6	**X vs. NAF**	**X vs. HFF**	**X vs. LFF**
Pearson r				
r	-0.9499	-0.961	0.8451	-0.7803
95% CI	-0.9911 to -0.7418	-0.9975 to -0.5177	-0.1463 to 0.9895	-0.9658 to -0.06604
R squared	0.9024	0.9236	0.7141	0.6089
P value				
P (two-tailed)	0.0003	0.0092	0.0715	0.0385
P value summary	***	**	ns	*
Significant? (alpha = 0.05)	Yes	Yes	No	Yes
Number of XY Pairs	8	5	5	7

Supplemental Table 2.3: Relationship among bacterial families and weight change

% *Erysipelotrichaceae* vs weight change			
Pearson r	p-value	0.0035	**
	X vs. NAF	**X vs. HFF**	**X vs. LFF**
r	-0.7709	0.6661	0.4061
95% confidence interval	-0.9839 to 0.3482	-0.5242 to 0.9752	-0.4998 to 0.8877
R squared	0.5943	0.4437	0.165
P value			
P (two-tailed)	0.127	0.2196	0.3659
P value summary	ns	ns	ns

% *Verrucomicrobiaceae* vs weight change			
Pearson r	p-value	0.2494	ns
	X vs. NAF	**X vs. HFF**	**X vs. LFF**
r	-0.839	0.8183	-0.1127
95% confidence interval	-0.9891 to 0.1666	-0.2302 to 0.9876	-0.7980 to 0.6997
R squared	0.7039	0.6695	0.01271
P value			
P (two-tailed)	0.0757	0.0904	0.8098
P value summary	ns	ns	ns

% *Bifidobactereaceae* vs weight change			
Pearson r	p-value	0.0271	*
	X vs. NAF	**X vs. HFF**	**X vs. LFF**
r	0.6264	0.6993	-0.1754
95% confidence interval	-0.5719 to 0.9717	-0.4777 to 0.9781	-0.8201 to 0.6656
R squared	0.3924	0.489	0.03077
P value			
P (two-tailed)	0.2582	0.1888	0.7068
P value summary	ns	ns	ns

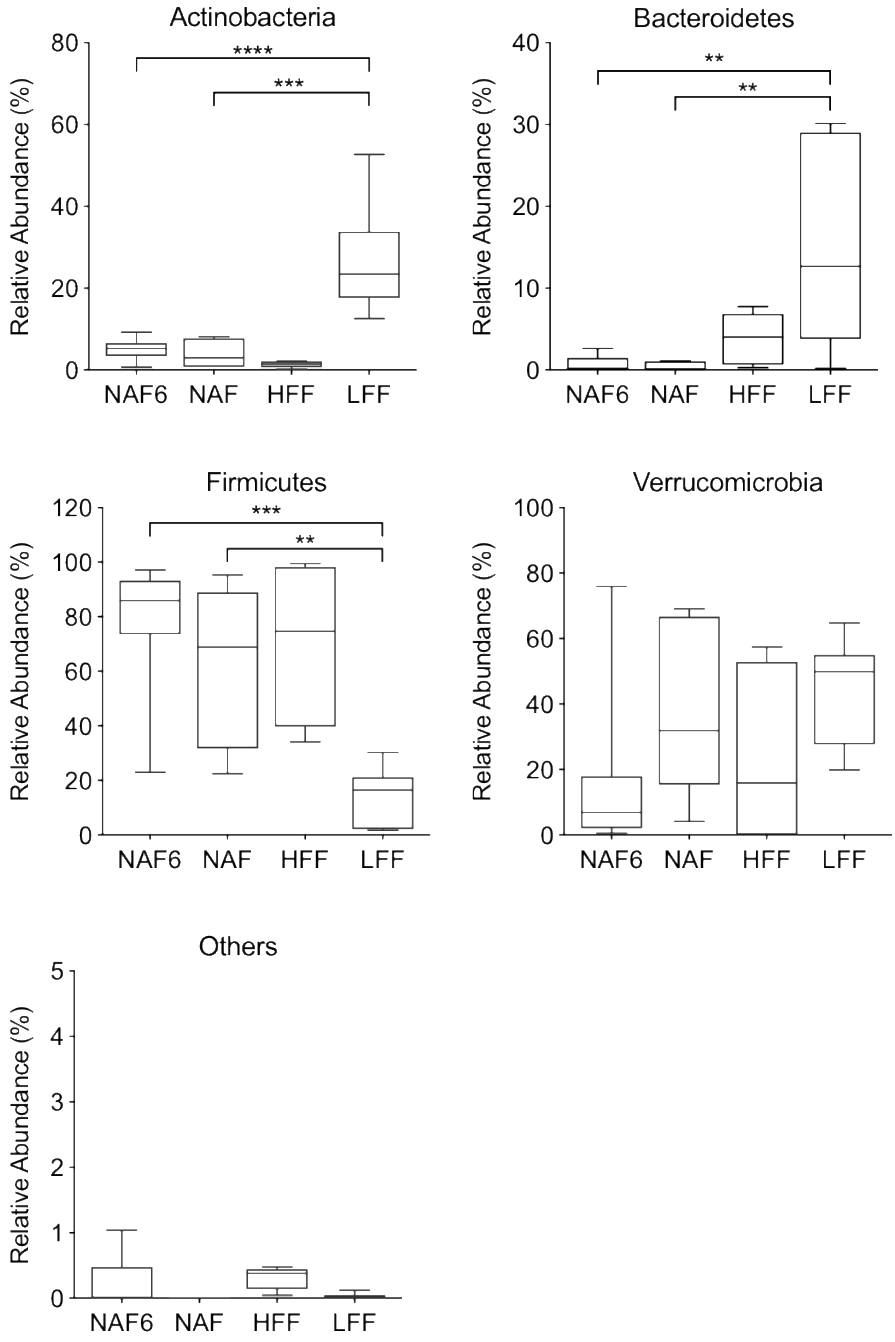

Supplemental Figure 2.1: Phylum abundance of NAFLD and intervention diet microbiota

Microbiota sampling of fecal contents of mice in treatment groups NAF6, NAF, HFF and LFF. Relative abundance of major phylum-level commensals. Data is the mean ± SEM of 2 independent experiments, n=5-9mice/group. One-way ANOVA, Dunnett's multiple comparisons; **, $p<0.01$; ***, $p<0.005$; and ****, $p<0.001$.

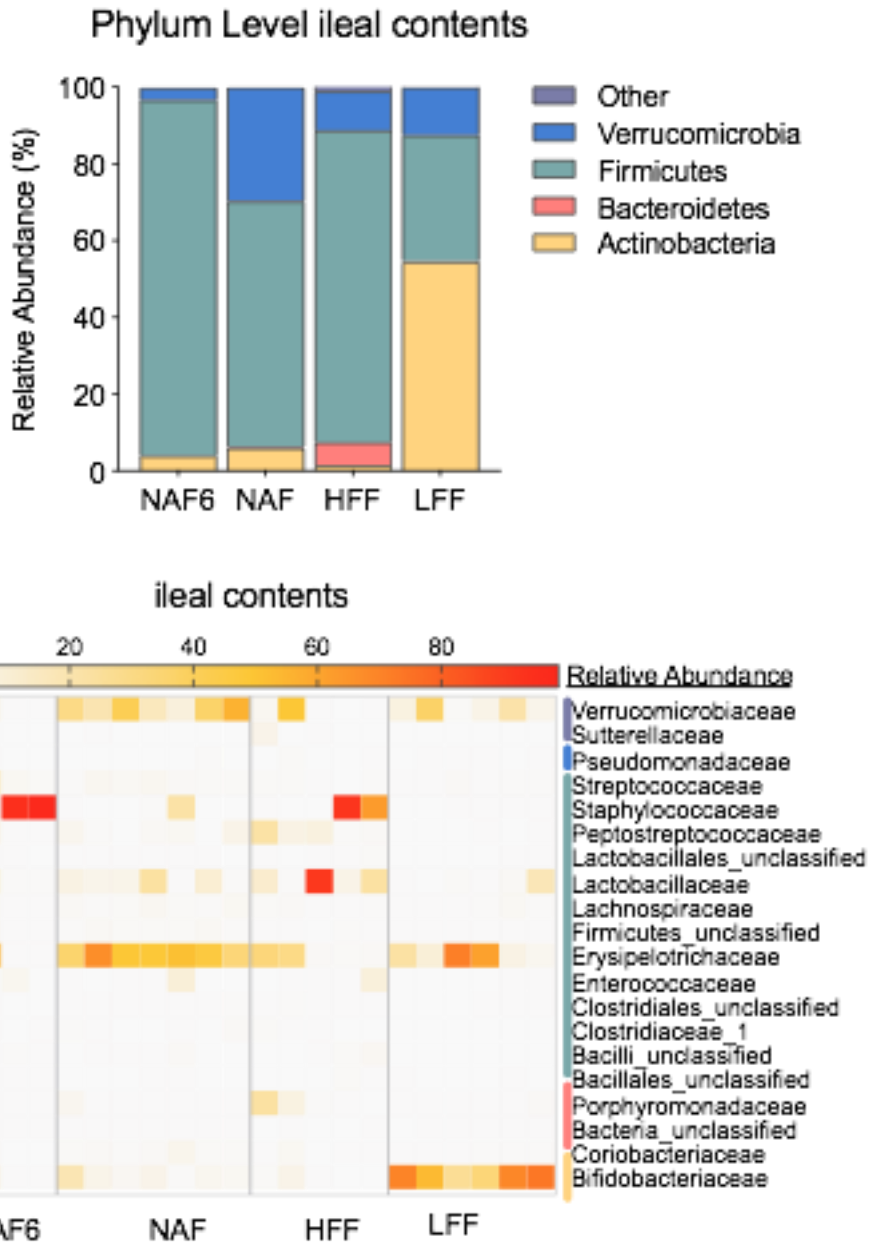

Supplemental Figure 2.2: Heat map of family abundance of ileal microbiota of NAFLD and intervention diet mice

Microbiota sampling of ileal contents of mice in treatment groups NAF6, NAF, HFF and LFF. (A) Phylum-level abundance and Heatmap of family-level abundance with families >1% abundance. Data is the mean ± SEM of 2 independent experiments, n=4-8mice/group.

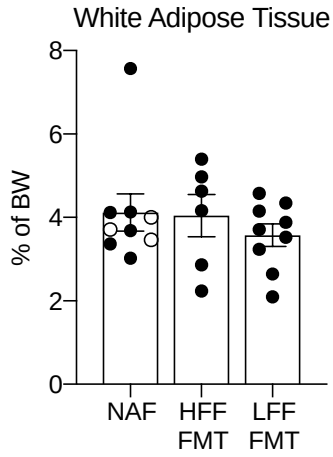

Supplemental Figure 2.3: Adipose tissue weight of mice following microbiota transplant

Weight of white adipose tissue as percentage of body weight of mice following microbiota transplant using cecal contents of donors previously on intervention diets. Data is the mean ± SEM of 2 independent experiments, n=3-9mice/group.

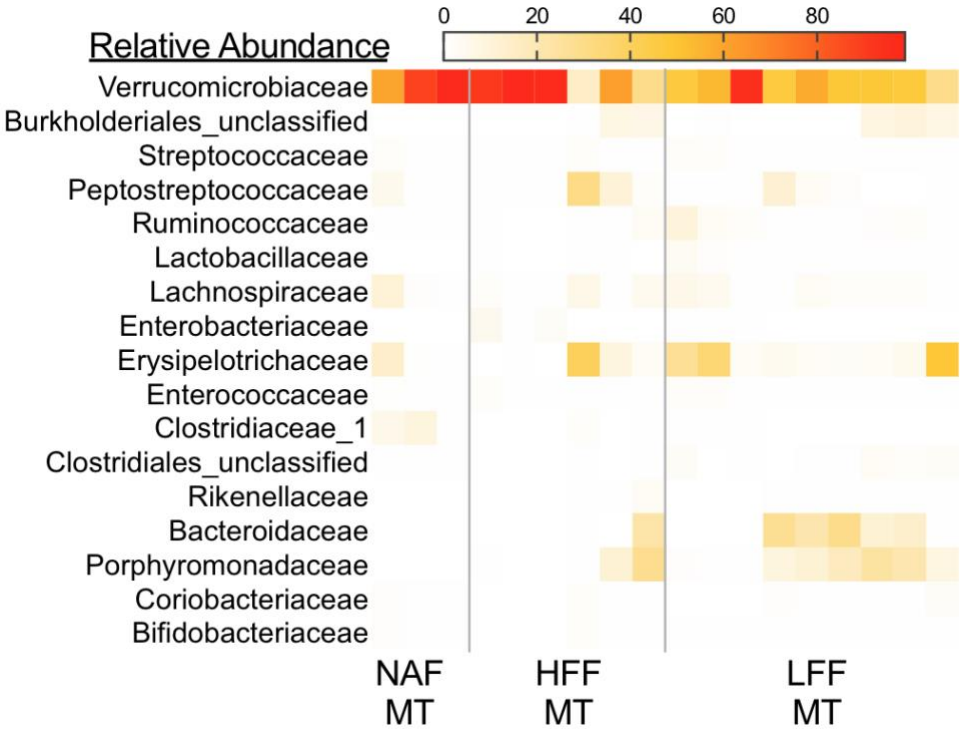

Supplemental Figure 2.4: Heat map of family abundance of fecal microbiota of microbiota transplant mice

Fecal microbiota of mice post microbiota transplant was sampled. Heatmap of family-level abundance with families >1% abundance. Data is from 2 independent experiments, n=3-9mice/group.

2.7 References

1. Schwimmer JB, Deutsch R, Kahen T, et al. Prevalence of fatty liver in children and adolescents. Pediatrics 2006;118:1388-1393.

2. Neuschwander-Tetri BA. Non-alcoholic fatty liver disease. BMC Med 2017;15:45.

3. Buzzetti E, Pinzani M, Tsochatzis EA. The multiple-hit pathogenesis of non-alcoholic fatty liver disease (NAFLD). Metabolism 2016;65:1038-1048.

4. Bäckhed F, Manchester JK, Semenkovich CF, et al. Mechanisms underlying the resistance to diet-induced obesity in germ-free mice. Proc Natl Acad Sci U S A 2007;104:979-984.

5. Bäckhed F, Ding H, Wang T, et al. The gut microbiota as an environmental factor that regulates fat storage. Proc Natl Acad Sci U S A 2004;101:15718-15723.

6. Vajro P, Paolella G, Fasano A. Microbiota and gut-liver axis: their influences on obesity and obesity-related liver disease. J Pediatr Gastroenterol Nutr 2013;56:461-468.

7. Jumpertz R, Le DS, Turnbaugh PJ, et al. Energy-balance studies reveal associations between gut microbes, caloric load, and nutrient absorption in humans. Am J Clin Nutr 2011;94:58-65.

8. Høverstad T, Midtvedt T. Short-chain fatty acids in germfree mice and rats. J Nutr 1986;116:1772-1776.

9. Wolin MJ. Fermentation in the rumen and human large intestine. Science 1981;213:1463-1468.

10. Krishnan S, Ding Y, Saedi N, et al. Gut Microbiota-Derived Tryptophan Metabolites Modulate Inflammatory Response in Hepatocytes and Macrophages. Cell Rep 2018;23:1099-1111.

11. Swann JR, Want EJ, Geier FM, et al. Systemic gut microbial modulation of bile acid metabolism in host tissue compartments. Proc Natl Acad Sci U S A 2011;108 Suppl 1:4523-4530.

12. Jiang C, Xie C, Li F, et al. Intestinal farnesoid X receptor signaling promotes nonalcoholic fatty liver disease. J Clin Invest 2015;125:386-402.

13. Cope K, Risby T, Diehl AM. Increased gastrointestinal ethanol production in obese mice: implications for fatty liver disease pathogenesis. Gastroenterology 2000;119:1340-1347.

14. Hildebrandt MA, Hoffmann C, Sherrill-Mix SA, et al. High-fat diet determines the composition of the murine gut microbiome independently of obesity. Gastroenterology 2009;137:1716-24.e1-2.

15. Turnbaugh PJ, Ridaura VK, Faith JJ, et al. The effect of diet on the human gut microbiome: a metagenomic analysis in humanized gnotobiotic mice. Sci Transl Med 2009;1:6ra14.

16. de Wit N, Derrien M, Bosch-Vermeulen H, et al. Saturated fat stimulates obesity and hepatic steatosis and affects gut microbiota composition by an enhanced overflow of dietary fat to the distal intestine. Am J Physiol Gastrointest Liver Physiol 2012;303:G589-99.

17. Duncan SH, Lobley GE, Holtrop G, et al. Human colonic microbiota associated with diet, obesity and weight loss. Int J Obes (Lond) 2008;32:1720-1724.

18. David LA, Maurice CF, Carmody RN, et al. Diet rapidly and reproducibly alters the human gut microbiome. Nature 2014;505:559-563.

19. Mouzaki M, Allard JP. The role of nutrients in the development, progression, and treatment of nonalcoholic fatty liver disease. J Clin Gastroenterol 2012;46:457-467.

20. Kesse-Guyot E, Ahluwalia N, Lassale C, et al. Adherence to Mediterranean diet reduces the risk of metabolic syndrome: a 6-year prospective study. Nutr Metab Cardiovasc Dis 2013;23:677-683.

21. Nadal I, Santacruz A, Marcos A, et al. Shifts in clostridia, bacteroides and immunoglobulin-coating fecal bacteria associated with weight loss in obese adolescents. Int J Obes (Lond) 2009;33:758-767.

22. Clemente JC, Ursell LK, Parfrey LW, et al. The impact of the gut microbiota on human health: an integrative view. Cell 2012;148:1258-1270.

23. Takahashi Y, Soejima Y, Fukusato T. Animal models of nonalcoholic fatty liver disease/nonalcoholic steatohepatitis. World J Gastroenterol 2012;18:2300-2308.

24. Rinella ME, Green RM. The methionine-choline deficient dietary model of steatohepatitis does not exhibit insulin resistance. J Hepatol 2004;40:47-51.

25. Kawasaki T, Igarashi K, Koeda T, et al. Rats fed fructose-enriched diets have characteristics of nonalcoholic hepatic steatosis. J Nutr 2009;139:2067-2071.

26. Arrese M, Cabrera D, Kalergis AM, et al. Innate Immunity and Inflammation in NAFLD/NASH. Dig Dis Sci 2016;61:1294-1303.

27. Barrera F, George J. The role of diet and nutritional intervention for the management of patients with NAFLD. Clin Liver Dis 2014;18:91-112.

28. Perumpail BJ, Cholankeril R, Yoo ER, et al. An Overview of Dietary Interventions and Strategies to Optimize the Management of Non-Alcoholic Fatty Liver Disease. Diseases 2017;5.

29. Kaden-Volynets V, Basic M, Neumann U, et al. Lack of liver steatosis in germ-free mice following hypercaloric diets. Eur J Nutr 2019;58:1933-1945.

30. Kozich JJ, Westcott SL, Baxter NT, et al. Development of a Dual-Index Sequencing Strategy and Curation Pipeline for Analyzing Amplicon Sequence Data on the MiSeq Illumina Sequencing Platform. Appl Environ Microbiol 2013;79:5112-5120.

31. Langille MG, Zaneveld J, Caporaso JG, et al. Predictive functional profiling of microbial communities using 16S rRNA marker gene sequences. Nat Biotechnol 2013;31:814-821.

32. Rabot S, Membrez M, Blancher F, et al. High fat diet drives obesity regardless the composition of gut microbiota in mice. Sci Rep 2016;6:32484.

33. Dao MC, Everard A, Aron-Wisnewsky J, et al. Akkermansia muciniphila and improved metabolic health during a dietary intervention in obesity: relationship with gut microbiome richness and ecology. Gut 2016;65:426-436.

34. Pedret A, Valls RM, Calderón-Pérez L, et al. Effects of daily consumption of the probiotic Bifidobacterium animalis subsp. lactis CECT 8145 on anthropometric adiposity biomarkers in abdominally obese subjects: a randomized controlled trial. Int J Obes (Lond) September 2018.

35. Shen F, Zheng RD, Sun XQ, et al. Gut microbiota dysbiosis in patients with non-alcoholic fatty liver disease. Hepatobiliary Pancreat Dis Int 2017;16:375-381.

36. Martínez I, Perdicaro DJ, Brown AW, et al. Diet-induced alterations of host cholesterol metabolism are likely to affect the gut microbiota composition in hamsters. Appl Environ Microbiol 2013;79:516-524.

37. Denke MA, Grundy SM. Comparison of effects of lauric acid and palmitic acid on plasma lipids and lipoproteins. Am J Clin Nutr 1992;56:895-898.

38. Abenavoli L, Greco M, Milic N, et al. Effect of Mediterranean Diet and Antioxidant Formulation in Non-Alcoholic Fatty Liver Disease: A Randomized Study. Nutrients 2017;9.

39. Ronis MJ, Baumgardner JN, Sharma N, et al. Medium chain triglycerides dose-dependently prevent liver pathology in a rat model of non-alcoholic fatty liver disease. Exp Biol Med (Maywood) 2013;238:151-162.

40. Wang ME, Singh BK, Hsu MC, et al. Increasing Dietary Medium-Chain Fatty Acid Ratio Mitigates High-fat Diet-Induced Non-Alcoholic Steatohepatitis by Regulating Autophagy. Sci Rep 2017;7:13999.

41. Watson H, Mitra S, Croden FC, et al. A randomised trial of the effect of omega-3 polyunsaturated fatty acid supplements on the human intestinal microbiota. Gut 2018;67:1974-1983.

42. Vrieze A, Van Nood E, Holleman F, et al. Transfer of intestinal microbiota from lean donors increases insulin sensitivity in individuals with metabolic syndrome. Gastroenterology 2012;143:913-6.e7.

43. Kootte RS, Levin E, Salojärvi J, et al. Improvement of Insulin Sensitivity after Lean Donor Feces in Metabolic Syndrome Is Driven by Baseline Intestinal Microbiota Composition. Cell Metab 2017;26:611-619.e6.

44. Zhou D, Pan Q, Shen F, et al. Total fecal microbiota transplantation alleviates high-fat diet-induced steatohepatitis in mice via beneficial regulation of gut microbiota. Sci Rep 2017;7:1529.

45. Kleiner DE, Brunt EM, Van Natta M, et al. Design and validation of a histological scoring system for nonalcoholic fatty liver disease. Hepatology 2005;41:1313-1321.

46. Santiago-Rolón A, Purcell D, Rosado K, et al. A Comparison of Brunt's Criteria, the Non-Alcoholic Fatty Liver Disease Activity Score (NAS), and a Proposed NAS Scoring that Includes Fibrosis in Non-Alcoholic Fatty Liver Disease Staging. P R Health Sci J 2015;34:189-194.

47. Schloss PD, Westcott SL, Ryabin T, et al. Introducing mothur: open-source, platform-independent, community-supported software for describing and comparing microbial communities. Appl Environ Microbiol 2009;75:7537-7541.

48. Quince C, Lanzen A, Davenport RJ, et al. Removing noise from pyrosequenced amplicons. BMC Bioinformatics 2011;12:38.

49. Pruesse E, Quast C, Knittel K, et al. SILVA: a comprehensive online resource for quality checked and aligned ribosomal RNA sequence data compatible with ARB. Nucleic Acids Res 2007;35:7188-7196.

50. Schloss PD, Gevers D, Westcott SL. Reducing the effects of PCR amplification and sequencing artifacts on 16S rRNA-based studies. PLoS One 2011;6:e27310.

51. Edgar RC, Haas BJ, Clemente JC, et al. UCHIME improves sensitivity and speed of chimera detection. Bioinformatics 2011;27:2194-2200.

52. Cole JR, Wang Q, Cardenas E, et al. The Ribosomal Database Project: improved alignments and new tools for rRNA analysis. Nucleic Acids Res 2009;37:D141-5.

Chapter 3. Detection of Physiological Changes from Environmental Conditions through Matrix-Assisted Laser Desorption/Ionization – Time of Flight (MALDI-TOF) Mass Spectrometry

Adapted from:

Denise Chac*, Melissa Kordahi*, Leandra Brettner, Arushi Verma, Paul McCleary, Cara Yee, and R. William DePaolo. Detection of Physiological Changes from Environmental Conditions through Matrix-Assisted Laser Desorption/Ionization – Time of Flight (MALDI-TOF) Mass Spectrometry.

3.1 Abstract

In the past decade, matrix-assisted laser desorption/ionization time-of-flight (MALDI-TOF) mass spectrometry (MS) has become a timely and cost-effective alternative to bacterial identification. The MALDI-TOF MS technique analyzes the total protein of culturable microorganisms at the species level and produces a mass spectra based on peptides which is compared to a database of identified profiles. Consequently, unique signatures of each microorganism is produced allowing species and strain level identification. Our present study proposes that the MALDI-TOF MS can be further used to screen functional and metabolic differences. While other studies applied the MALDI-TOF technique to identify subgroups within species, we investigated how various environmental factors could alter the unique bacterial signatures. We found that genetic and phenotypic differences between microorganisms belonging to the same species can be reflected in peptide-mass fingerprints generated by MALDI-TOF MS. These results suggest that MALDI-TOF MS can screen intra-species phenotypic differences of several microorganisms.

3.2 Introduction

The MALDI-TOF (matrix-assisted desorption/ionization time-of-flight) mass spectrometry (MS) technology offers a time- and cost-effective method of identifying microorganisms. Compared to previous time-consuming and expensive methods to identify microorganisms based on 16s rRNA or whole genome sequencing, the MALDI-TOF MS provides rapid, accurate and inexpensive identification within minutes via proteotyping[1]. While the MALDI-TOF is limited to culturable microorganisms and public databases, it has been quickly incorporated in the clinical setting and used for diagnosis. Studies have shown that MALDI-TOF MS can equally or even better identify sources of systemic infections[2,3], urinary tract infections[4–6], respiratory tract infections[7] and intestinal infections[8,9]. The MALDI-TOF MS technology allows for identification down to the strain level and has been shown to discriminate between strains of methicillin-resistant *Staphylococcus aureus*[10–13], shiga-toxigenic *Escherichia coli*[14], clinically relevant strains of Aspergillus species [15]and many others[1].

Although many existing methods allow rapid identification of microorganisms to the species level, identification to the more specific ‘‘strain’’ taxon tends to be more challenging, as strains within a single microbial species are often very genotypically and phenotypically similar, despite having different functions. Higher resolution approaches such as molecular genetics are thus commonly employed to identify and characterize strains within a microbial species [16]. These include pulsed field gel electrophoresis (PFGE)[17], multilocus sequence typing[18] (MLST), repetitive extragenic palindromic PCR[19] (rep-PCR), housekeeping gene (e.g., PheS) sequence analysis[20], and whole genome sequencing[21,22]. Each of these approaches has been shown to have adequately high resolution to distinguish microbial strains from one another; however, these approaches are labor- and time-intensive as well as costly techniques that might lack the required rapid high-throughput nature of MALDI TOF. A big advantage of the MALDI TOF MS strain typing application would be epidemiologic investigations that require rapid identification of a single strain within a single species to determine the origin and spread of an outbreak in order to mitigate risks to public safety posed by microbial food and water contamination or potential acts of bioterrorism [16,23].

The MALDI-TOF MS is an ionization process that became commercially available in the early 1990s. The ionization process involves the mixture of an analyte with a “matrix” solution and the co-crystallization of

both matrix and analyte (Diagram 3.1A-B). During ionization, a laser of a determined UV nm wavelength is fired at the mixture and causes its desorption into a gaseous phase. MALDI ion sources are combined with time of flight (ToF) tubes for ion separation[16]. A peptide mass fingerprint (PMF) is generated per sample and compared to a data base of known bacterial species PMFs (Diagram 3.1C). MALDI-TOF looks at whole cell differences as opposed to a methods that target a handful of molecules such as qPCR, protein blots, etc. which allows identification of species and strain differences that these would miss. While the technique lacks discriminatory power with some species such as *Enterococucs faecium* and *Staphylococcus aureus*[24], the MALDI-TOF MS can robustly identify bacterial species in various culturing conditions[25,26].

In contrast to studies that only look at the MALDI-TOF MS ability to identify bacterial species regardless of environmental conditions, we propose that the variation of MALDI-TOF MS-produced peaks due to culturing can detect environmental imprints. By comparing PMF peaks and observing the differences in dendrogram and principle component of analysis (PCA) format (Diagram 3.1D and E), we report that the MALDI-TOF can reliably differentiate between various conditions including oxygen presence, nutrient availability and temperature stress. The MALDI-TOF MS is also able to detect previous environmental conditions after culturing out of the initial environment. Our study shows that the MALDI-TOF can be applied to screening isolates from various environmental conditions to see potential functional differences within the same microorganism.

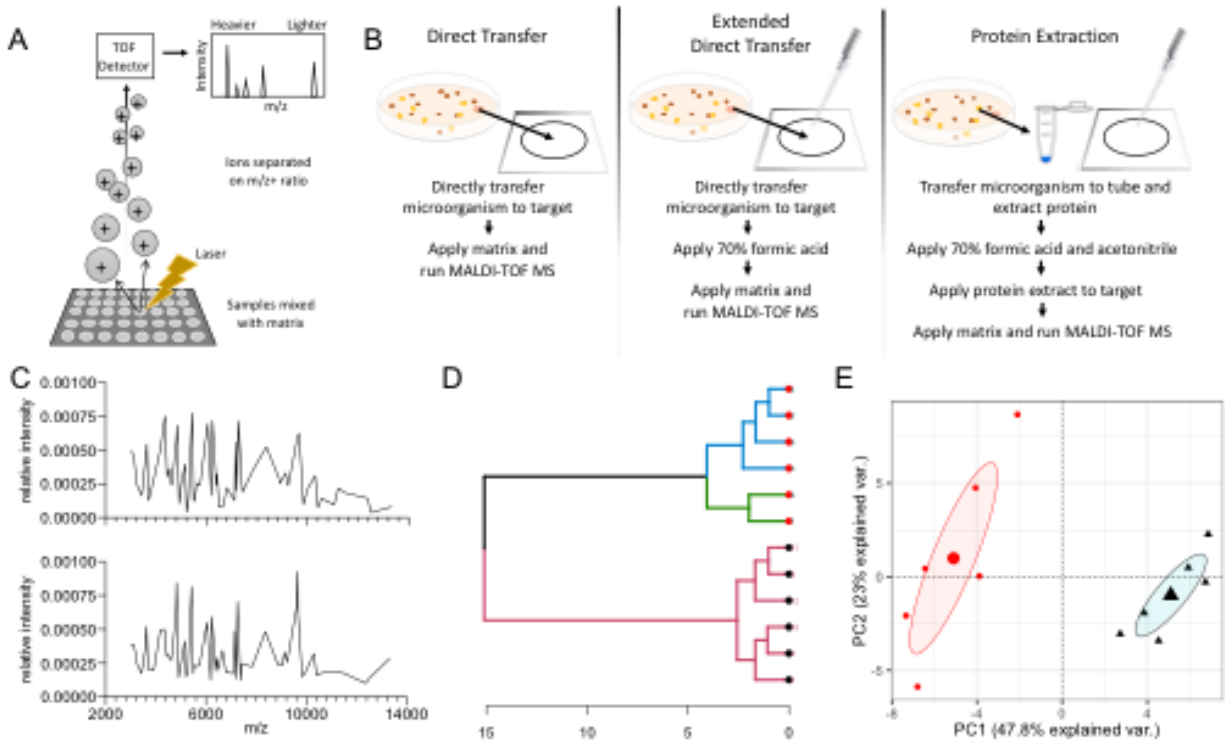

Diagram 3.1: MALDI-TOF MS methodology

A) Schematic of MALDI-TOF MS technology and B) methods of processing as described by manufacturer Bruker. Analysis of peptide-mass fingerprinting by C) spectra, D) dendrogram and E) principle component analysis (PCA).

3.3 Results & Discussion

Peptide mass fingerprints distinguish genetic differences within microbial species

MALDI TOF based bacterial profiling at the genus and species levels has provided results that are superior to and less expensive and time consuming than those obtained from more conventional approaches such as 16S rRNA sequencing. Such successes can be found across diverse areas of research and across many disciplines such as clinical microbiology, biodefense, food safety and environmental health. Although many studies have reported strain-specific peaks generated by MALDI TOF MS, identification of reliable peaks as strain-specific biomarkers has been hindered by poor profile reproducibility. Further, it appears that the limits of the taxonomic resolution of MALDI TOF MS profiling at the strain level has been determined so far

in large part by the nature of the particular bacterium profiled. The more genetically indistinguishable bacteria are, the more challenging their profiling has been[27].

In this study, we show that MALDI-TOF MS offers the possibility to discriminate between highly genetically similar genetic mutants or between different strains of the same bacterial species. To investigate the capabilities of MALDI-TOF to distinguish strain-level differences, we analyzed three different gram-negative bacteria.

Bacteroides fragilis is an Gram-negative, obligate anaerobic, rod-shaped bacterium. It is part of the normal microbiota of the human colon and is generally commensal but can cause infection if displaced into the bloodstream or surrounding tissue following surgery, disease, or trauma. Enterotoxigenic *B. fragilis* (ETBF) strains are strains of *B. fragilis* that secrete a 20-kDa heat-labile zinc-dependent metalloprotease toxin termed the *B. fragilis* toxin (BFT). ETBF strains are associated with inflammatory diarrheal disease in children older than 1 year of age and in adults as well as in inflammatory bowel disease flare-ups and colorectal cancer[28–31]. Here we show that MALDI TOF MS can discriminate between the enterotoxigenic *B. fragilis* strain and a genetic mutant for the *B. fragilis* toxin (Figure 3.1A).

Escherichia coli is another gram-negative, rod-shaped bacterium that is commonly found in the lower intestines. While most *E. coli* strains are harmless, pathogenic varieties can cause serious gastroenteritis, urinary tract infections, meningitis or septic shock in humans[32]. EPEC is a pathogenic strain of E. coli that uses a virulence factor known as intimin, an adhesin that binds host intestinal cells, causing watery diarrhea in those afflicted[33]. As we demonstrated with the *B. fragilis*, the MALDI-TOF can also differentiate lab strains of *E. coli* from the highly pathogenic EPEC (Figure 3.1B).

Another gram-negative bacteria associated with diarrheal disease is *Y. enterocolitica.* Unlike the previous bacteria, *Y. enterocolitica* is a common food-borne disease found in contaminated water and meat. *Y. enterocolitica* is a transient infection in immunocompetent adults but can be deadly to immunocompromised individuals especially young children under the age of 5[34,35]. Using the MALDI-TOF, we are able to see

three distinct clusters among a wild type *Y. enterocolitica* strain (Ye8081) and two mutants of the same strain that are lacking an adhesion gene, *YadA*, or a *Yersinia* translocation protein *(YscA)* (Figure 3.1C).

As the MALDI-TOF MS uses whole protein of bacterial samples to generate unique profiles, lack of phenotypic or metabolic differences between subgroups of species can complicate identification. Meanwhile, our results confirm the findings of other studies. The technique has proved to be highly performant and reproducible in distinguishing peaks within highly genetically similar species. Several known strains can then be used to create a reference library that affords identification of unidentified strains with potentially useful applications such as diagnosing pathogenic strains in certain disease states or rapidly identifying the origin of an outbreak.

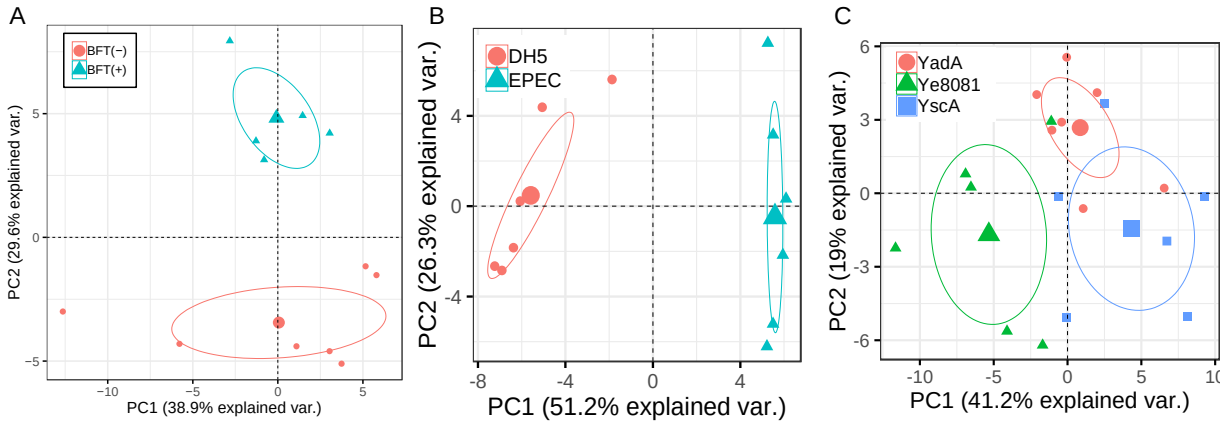

Figure 3.1:Differentiation of bacterial genetic mutants on MALDI-TOF MS
Principal component analysis based on peptide mass fingerprint profile of various bacterial strains and mutants. A) *Bacteroides fragilis* with and without the enterotoxigenic gene (BFT) is compared. B) Enteropathogenic *Eschericia coli* and DH5a strains are compared. C) *Yersinia enterocolitica strain 8081* WT (Ye8081) and mutants with genetic differences in genes *YadA* and *YscA* are compared. Data is mean +/- of two independent experiments with n=5-7. Each dot represents the average of 4 technical replicates.

Condition	Species	Reference
Media type	*E. coli*	This study
		Arnold et al. 1999[36]
		Valentine et al., 2005[26]
		Reich et al., 2013[37]
		Veenemans et al., 2016[38]
	Y. enterocolitica	Valentine et al., 2005[26]
	B. subtilis	Valentine et al., 2005[26]
	Mycobacteria	Balážová et al., 2015 [39]
	S. aureus	Reich et al., 2013[37]
	Lactobacillus spp.	Šedo et al., 2013[40]
	Acetic Acid bacteria	Wieme et al., 2013[41]
	Nocardia spp.	McTaggart et al., 2018[42]
Growth rate / Age	*E. coli*	Arnold et al. 1999[36]
		Wunschel et al., 2005[25]
		Reich et al., 2013[37]
		Veenemans et al., 2016[38]
	Mycobacteria	Balážová et al., 2015 [39]
	Beverage spoiling yeasts	Usbeck et al., 2013[43]
	S. aureus	Reich et al., 2013[37]
	LActobacillus	Šedo et al., 2013[40]
	Rhizobium	Mandal et al., 2007[44]
	Nocardia spp.	McTaggart et al., 2018[42]
Oxygen	*L. Rhamnosus GG*	This study
	Beverage spoiling yeasts	Usbeck et al., 2013[43]
Temperature	*E. coli*	This study
		Wunschel et al., 2005[25]
	Y. enterocolitica	This study
		Wunschel et al., 2005[25]
	Bacillus spp.	Shu and Yang 2017[45]
	LActobacillus	Šedo et al., 2013[40]
Broth vs agar	*Beverage spoiling yeasts*	Usbeck et al., 2013[43]
	E. coli	Reich et al., 2013[37]
	S. aureus	Reich et al., 2013[37]
pH	*E. coli*	Wunschel et al., 2005[25]

Table 3.1: Environmental influences on MALDI-TOF MS analyses

PMFs distinguish phenotypic differences within genetically identical strains

The reproducibility of the mass spectra generated in MALDI TOF MS analysis of proteins from bacterial extracts can be impacted by several experimental factors. Other researchers have discovered that differences in incubation and culturing conditions can alter peak intensities[38] and identification rates[46] (Table 3.1). We sought to determine if the effects of environmental factors can reproducibly identified.

In this work, we have identified factors related to the environmental conditions in which one same microorganism is grown before the sample preparation and how these factors affect the peptide mass fingerprint signature of the microorganism at hand. The first environmental factor tested was presence or absence of oxygen. Using the facultative anaerobe gut bacteria *Lactobacillus reuteri*, we investigated if the MALDI-TOF could detect differences in PMF after incubation in aerobic and anaerobic environments. *Lactobacillus spp.* are facultative anaerobes and several genes are modified with the presence of oxygen[47]. In our experiment we find that despite using the same starting culture, aerobic or anaerobic conditions has significantly different PMFs (Figure 3.2A).

As others have noted, culturing on various media does not alter species identification. For our study we cultured *E. coli* on four different nutrient-rich media. Whereas *E. coli* grown on MacConkey (MC) and eosin methylene blue (EMB) agar had overlapping PMFs and clustered together, there were clearly different clusters for TSA and TSA blood *E. coli* (Figure 3.2B). The overlapping of MC and EMB-grown *E. coli* is likely due lactose fermentation on the two agars. Whereas the differences between MC and EMB agars did not separate *E. coli*, the presence of 5% blood in the TSA was enough to significantly distinguish between TSA and TSA blood.

Another environmental condition that strongly affects PMF clustering is temperature. The gut pathogen *Y. enterocolitica* is well adapted for survival and proliferation at room temperature (RT) and induces its virulence factors when consumed or introduced to host temperatures of 37°C[48]. These metabolic adaptations are clearly captured when we analyze *Y. enterocolitica* grown at these two temperatures on the MALDI-TOF with *Y. enterocolitica* grown at RT clustering away from the 37°C treated group (Figure 3.2C). Previous studies using MALDI-TOF on *Y. enterocolitica* point out that temperature and media both

play a role in PMF intensities with inference that temperature may play a bigger role[25,26]. Whereas Wunschel and collegues[25] identified that *Y. enterocolitica* grown at 37°C has similar PMFs despite the media, we demonstrate that the MALDI-TOF can reliably distinguish the temperature conditions.

Temperature also affected the PMF clustering of *E. coli*. When *E. coli* is introduced to temperatures greater than 42°C, the bacteria starts to produce heat shock proteins[49]. Not only do we see differential clustering due to the temperature treatment, we also see increasing differentiation with the incubation time (Figure 3.2D).

All together these results with bacteria grown in different oxygen, nutrient and temperature demonstrate how the MALDI-TOF is capable of reproducibly discriminate between metabolic states through PMFs. Other studies have investigated whether these environmental and culture conditions can impact the MALDI-TOF identification of bacteria. Our experiments took it one step further and demonstrate that the MALDI-TOF can easily differentiate the direct effects of environmental conditions on the bacteria, allowing identification of biological environmental influences as it affects the proteomic profile of microorganisms.

To further understand the extent of the MALDI-TOF technique on discerning environmental influences on bacteria, we tested if previous environmental stressors can be impact PMF clustering. For this experiment, DH5a was grown in liquid culture at 37°C and 50°C for 2 hour and then plated on TSA for 24 hours. Whereas our previous experiment measured the direct environmental impact of temperature on DH5a (Figure 3.2D), this experiment examined if the MALDI-TOF could pick up the same temperature effects after the bacteria was removed from the conditions and plated. Sure enough, the PMFs of DH5a grown in the two different cultures has distinct clusters (Figure 3.2E-F). While there were some overlaps in clusters, this data demonstrates that the MALDI-TOF can pick up environmental conditioning effects despite the removal of the immediate conditions. These results have major implications in the lab setting where microorganisms are often studied outside of its natural environment. Our ability to detect environmental conditionings even when the bacteria is removed from the initial stresses further highlight the advantage of proteotyping using the MALDI-TOF.

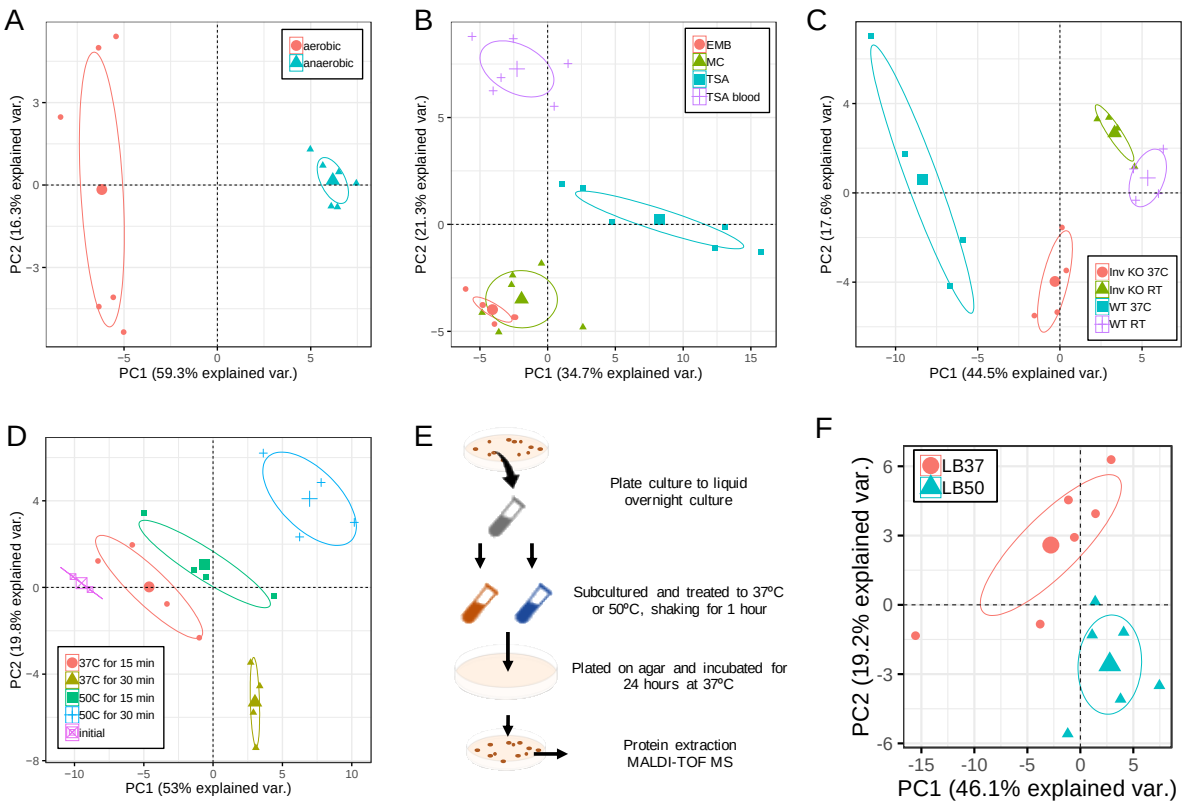

Figure 3.2: Differentiation of bacterial biological environments on MALDI-TOF MS
Principal component analysis based on peptide mass fingerprint profile of various bacterial species cultured in different growth conditions. A) *Lactobacillus reuteri* plated on Tryptic Soy agar and incubated overnight at 37°C in aerobic and anaerobic conditions is compared. B) DH5a *Escherichia coli* strain grown on 4 different types of Media: Tryptic soy agar (TSA), Tryptic soy agar with 5% defibrinated sheep blood (TSA blood), McConkey agar (MC), and Eosin Methylene Blue agar (EMB) is compared. C) *Y. enterocolitica* and strain InvKO grown at room temperature or 37°C for 2 days on TSA. D) DH5a grown in liquid culture at 37°C and 50°C for 15 and 30min while shaking. E) Diagram and F) PCA of DH5a grown in liquid culture at 37°C and 50°C and then plated to observe residual effects of different environmental conditions. Data is representative of two independent experiments with n=4-7. Each dot represents the average of 4 technical replicates.

PMFs identify metabolic states of *Y. enterocolitica* during in vitro adhesion and invasion assay

MALDI-TOF analysis of *Y. enterocolitica* at the various temperatures demonstrated that PMF can potentially distinguish between virulent states. Other than temperature, *Y. enterocolitica* has different metabolic states during infection and various genes that are modified during the course of infection[50]. The stages of *Y. enterocolitica* infection were investigated using human intestinal cells, SW620s. PMFs of untreated *Y. enterocolitica*, *Y. enterocolitica* applied to SW620s for 1 hour, or applied to SW620s for 1 hour and treated with gentamicin to remove extracellular bacteria were compared (Figure 3.3A). After samples were collected, *Y. enterocolitica* was plated on TSA and incubated at room temperature for 48 hours.

As we previously demonstrated with liquid cultures of DH5a plated on TSA, we found that *Y. enterocolitica* clustered depending on treatment group (Figure 3.3B-C). Cultures of intracellular *Y. enterocolitica* recovered following gentamicin had greater similarity whereas the *Y. enterocolitica* recovered after 1 hour has more variable PMFs. More divergent PMFs within a population could be due to natural heterogeneity within a clonal population[51] or differences in transcriptional or virulent states.

Our data using *DH5a E. coli* and *Y. enterocolitica* demonstrate that the MALDI-TOF can detect differences in metabolic and virulence states, respectively, even after those environmental influences are removed. This is especially important for trying to assess phenotypic differences of clinical isolates or samples that cannot be readily grown in its natural environments. These methods could be applied to situations in which metabolic or phenotypic difference of experimental groups can be compared against known culturing conditions. It can be used as a method of screening of known bacterial phenotypes.

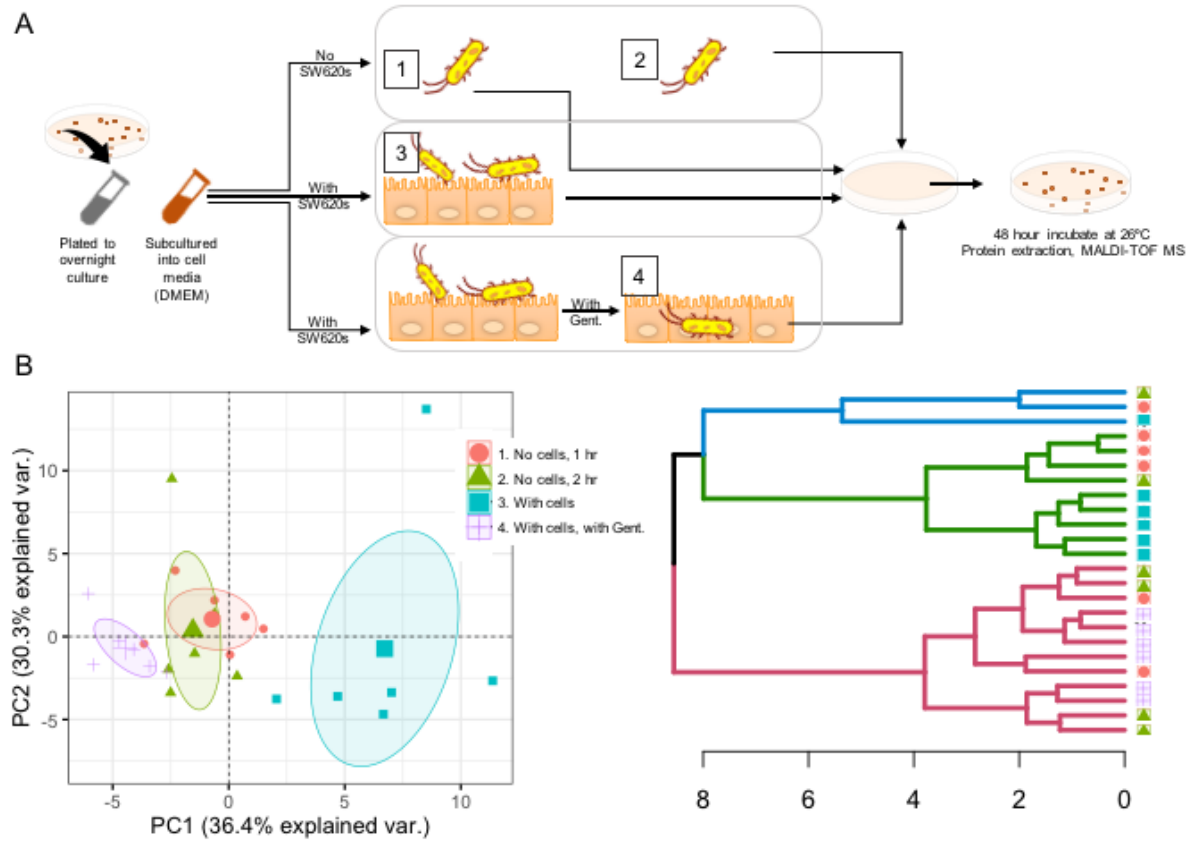

Figure 3.3: PMF Analysis of Y. enterocolitica virulence states
A) Schematic of protocol. B) PCA and dendrogram of *Y. enterocolitica* cultured 48 hours at room temperature on TSA following adhesion/invasion assay with SW620 cells.

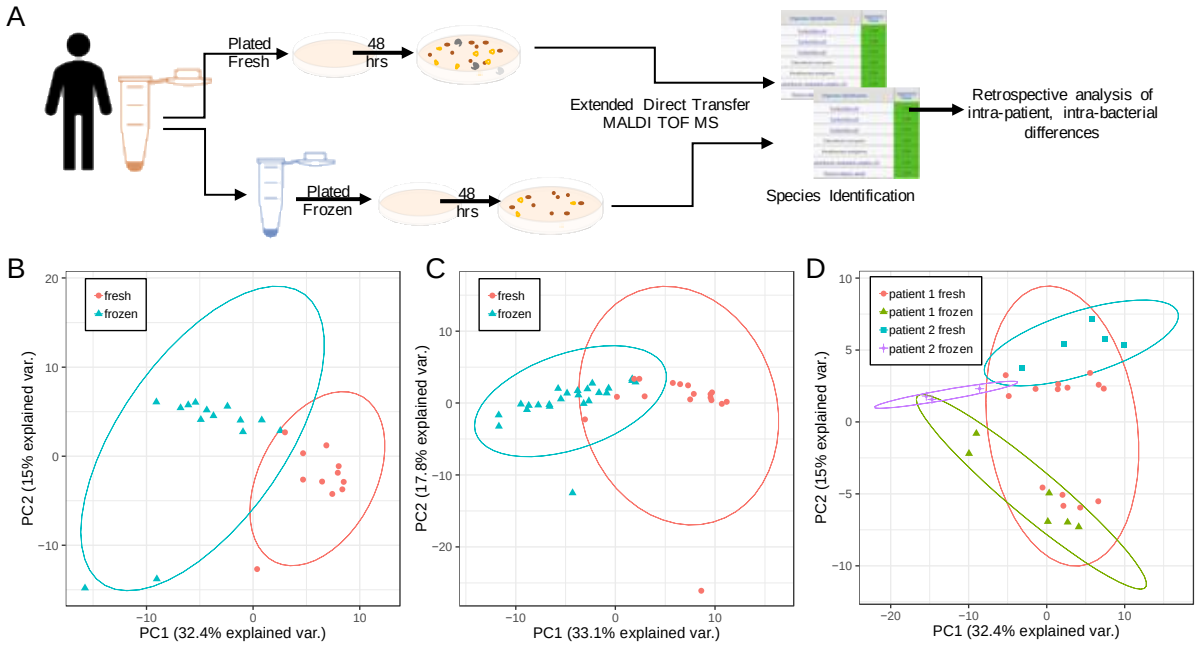

Figure 3.4: PMF analysis of fresh and frozen clinical isolates
A) Schematic of clinical sample analysis. PCA of fresh and frozen PMFs from B) *C. sedlakii*, C) *E. coli* and D) *B. ovatus* isolates identified on aerobic TSA with 5% sheep blood. Each dot resembles a biological replicate.

PMFs distinguish between fresh and frozen clinical isolates of the same species

While our experiments show that the MALDI-TOF has a lot to offer during well controlled environment, examining the PMFs for phenotypic differences in clinical samples can be challenging. In a clinical setting, using the protein extraction method is time consuming and not all samples are processed immediately. Additionally, freezing samples prior to culturing can reduce the number of bacteria recovered, skew the diversity of bacteria, and alter community composition[52,53].

Using fresh human fecal samples, we tested whether culturing fresh or frozen microbiota samples altered the phenotype of clinical isolates (Figure 3.4A). In these experiments, fecal samples were plated aerobically on TSA blood plates for 48 hours. Single CFUs were then processed using the extended direct colony method. Bacteria identified as the same species were then compiled and examined.

Within our clinical samples, the MALDI-TOF identified *Citrobacter sedlakii*, *E. coli* and *Bacteroides ovatus* from both fresh and frozen cultures. *C. sedlakii* and *E. coli* both gram-negative bacteria in the family Enterobacteriaceae. Isolates of *C. sedlakii* and *E. coli* within one patient clustered separately depending on fresh or frozen PMF but were not statistically significant (Figure 3.4B-C). Whereas *C. sedlakii* isolates appear to have little overlap, the *E. coli* isolates had more similarities.

In comparison, MALDI TOF analysis of fresh and frozen *B. ovatus* from two patients clustered by patient (Figure 3.4D). While fresh or frozen status has less impact on clustering of *B. ovatus* from patient 2, patient 1 had high variability of PMFs within fresh and frozen groups. These data indicate that proteomic differences between fresh and frozen isolates may alter the phenotypic PMF by MALDI-TOF.

Our results using clinical isolates derived from a mixed microbiota sample reveal that fresh versus frozen culturing techniques may alter the proteotyping of microorganisms. Further study is needed to analyze the freezing effects. This clinical experiment was limited by MALDI-TOF processing, lack of technical replicates, and difference in MALDI-TOF sampling days. These results exemplify a need for rigorous sample preparation and analysis. Given our ability to proteotype bacteria by various environmental factors, there is huge potential in analyzing phenotypic differences amongst clinical samples. There are numerous applications should this methodology be adapted in the clinic such as distinguishing proteotypes from inflammatory, nutrient-rich or -depleted, or competitive microenvironments.

3.4 Conclusion

The emergence of MALDI-TOF MS has reinvigorated microbial identification over the past decade. By creating proteomic signatures through PMFs of microorganisms, species and subspecies identification is possible via proteotyping. Routine use of MALDI-TOF MS as a diagnostic tool is favorable due to its ease of use, time and cost efficiency, and robust sensitivity. Our current study demonstrates a new function by exploiting the unique proteomic signatures and comparative analysis afforded by the MALDI-TOF MS bioinformatic packages. While proteotyping of different physiological and metabolic states of microorganisms through MALDI-TOF has been previously suggested by others[54,55] and variations in culturing conditions have been extensively tested for impact on species identification (Table 1), we test the

ability to distinguish between multiple environmental conditions within the same microorganism. Environmental effects of oxygen, temperature and nutrients can all be easily distinguished. As a proof-of-principle, we also demonstrate that PMF signatures can differentiate by stressors even when microorganisms are removed from the initial environment. We further exemplify how the MALDI-TOF MS technique can separate different virulent states of *Y. enterocolitica* with the SW620 adhesion assay.

One limitation of proteotyping of metabolic and functional states include lack of PMF peak to protein identification. There still remains a need to develop a database of peak information that can be readily incorporated with MALDI-TOF MS data. Another limitation is addressed with our clinical data in which rigorous protein extraction and technical replicates may not be easily incorporated in a clinical setting. While our data inconclusively delineate fresh versus frozen isolates, these experiments need to be repeated with a wide variety of microorganisms.

Altogether, we demonstrate the potential of MALDI-TOF MS to screen for physiological changes from direct and indirect environmental conditions. In conjunction with transcriptomic data and validation through PCR or LC/MS, this technique could provide a rapid and efficient way to screen for metabolic functions and physiological states of microorganisms. This methodology can be especially useful for analyzing phenotypic changes of bacteria cultured from previously unique environments such as an inflamed gastrointestinal tract or progression through virulence. In addition to the original function of species identification, the MALDI-TOF MS provides a plethora of data that has yet to be fully explored and exploited.

3.5 Materials and Methods

Bacterial strains and growth conditions:

DH5a *Escherichia coli* and enteropathogenic *E. coli* were grown on tryptic soy agar (TSA) plates and incubated at 37°C for 24 hours. *Yersinia enterocolitica* 8081 and *Y. enterocolitica INV, YadA, and YscA* knock-out strains were grown on TSA and incubated at room temperature for 48 hours. Enterotoxigenic *Bacteroides fragilis* (ETBF) and Non-enterotoxigenic *B. fragilis* (NTBF) were grown on TSA with 5% defibrinated sheep blood (TSBA) from skim milk stocks and incubated at 37°C anaerobically for 5 days.

Lactobacillus rhamnosus GG was grown on TSA and incubated at 37°C for 24 hours aerobically and anaerobically.

For testing of various growth agar, DH5a was plated on TSA, TSBA, McConkey and Eosin Methylene Blue. The plates were then incubated aerobically at 37°C for 24 hours. For testing of temperature stress environment, overnight cultures of DH5a in Lysogeny broth (LB) were diluted and incubated at 37°C or 50°C for 15 and 30 minutes. For testing of residual effects of environment, overnight cultures of DH5a in tryptic soy broth (TSB) were subcultured in various media and then plated on TSA. Briefly, DH5a overnight culture in TSB was centrifuged at 3,000 x g for 5 minutes and washed in sterile PBS twice. The pellet was then resuspended in PBS and cultured with TSB or LB at 37°C or 50°C for 1 hour, shaking. Samples were then plated on TSA plates and incubated at 37°C for 24 hours.

Isolation and growth of clinical samples:

Stool samples were collected from pre diabetic adolescents aged 13-19 years as part of an ongoing study after institutional IRB approval. Participants were given a sterile stool collection kit (stool collection container [Precision (Covidien, Fisher Scientific)]), stool collector hat and sterile gloves to self-collect stool at home and mail to the University of Washington laboratory within 24-48 hours of collection at room temperature. When received, the sample was immediately aliquoted and one tube was used for the analysis of 'Fresh' sample on the same day it was received. The other aliquots were stored at -80°C for 2-3 months until analyzed. For analysis of the 'Frozen sample', the sample was thawed on ice for 30 mins and then room temperature for 30 mins. 40-80 mg of each sample suspended in 1ml PBS and then centrifuged at 300 rpm for 2 mins. Serial dilutions were made and plated on TSA and TSA blood and incubated in aerobic and anaerobic conditions at 37°C for 48 hours. Both 'Fresh' and 'Frozen' samples were analyzed using the direct protein method.

Direct Protein Method

Bacterial colonies on agar were picked and placed directly on a target plate for identification. Samples were then overlaid with 1 uL of 70% formic acid and alpha-cyano-4-hydroxycinnamic acid matrix solution (Bruker Daltonics, Bremen, Germany). Target plate was placed in the MALDI TOF Biotyper for microbial identification (Bruker, Germany).

Cellular adhesion and invasion assays with *Y. enterocolitica*

SW620s (ATCC; CCL-227) human intestinal epithelial adenoma cells were used. SW620s were maintained in DMEM supplemented with 10% fetal bovine serum and 200uM L-glutamine. Prior to cellular assays, SW620s were seeded into 24-well plates and grown to a nearly confluent monolayer over 3-4 days. SW620s were rinsed with PBS and infected with *Y. enterocolitica* at an MOI of 10:1 with each starting dose plated on TSA to enumerate CFUs. Briefly, overnight Y*. enterocolitica* cultures were diluted 1:10 in TSB. Subcultures were then incubated for 2 hours at 37°C while shaking at 150 rpm. Cultures were then centrifuged, rinsed in PBS and diluted to the appropriate infection dose in cell media. The *Y. enterocolitica* samples were introduced to the cells and infection initiated by centrifuging the plates for 5 minutes at 500 x g. For adhesion, Y*. enterocolitica* was co-cultured with SW620s for 1 hour at 37°C in a 5% CO_2 incubator. For intracellular invasion, *Y. enterocolitica* was co-cultured with SW620s for 1 hour, washed with PBS and then treated with 100 ug/ml gentamicin (Corning, Corning, NY). To elute the *Y. enterocolitica* and lyse the SW620s, each well was washed three times with warm PBS and then treated with 500ul PBS with 1% Triton X-100 (AMRESCO, VWR, Randor PA) for 5 minutes. Samples were then plated on TSA in serial dilutions to enumerate *Y. enterocolitica* colonization. In parallel, wells containing media only were infected with an equal amount of bacteria. Percentage of colonization was calculated by dividing the number of *Y. enterocolitica* CFU recovered from co-cultures by the number of *Y. enterocolitica* CFU initially applied to the wells.

Protein extraction method

Colonies grown on agar plates were picked and added to 300 ul of HPLC-grade water in a 1.5 ml Eppendorf tube and then mixed thoroughly with 900 ul of 100% Ethanol. After centrifugation at 13000 rpm for 2 min twice, pellets were dried at room temperature for 5 minutes then they were directly mixed with equal volumes of 70% formic acid and acetonitrile (20-40 ul, depending on pellet size). After centrifugation at 13000 rpm for 2 minutes, 1 ul of protein extract was spotted on a 96-target polished steel plate (Bruker Daltonics, Bremen, Germany) in four replicates, air-dried, and overlaid with 1 ul of matrix solution (Bruker Daltonics, Bremen, Germany). Target plate was placed in the MALDI TOF Biotyper for microbial identification (Bruker, Germany).

Methods Data analysis

Raw spectra text files were analyzed using the R package, MALDIquant [https://www.ncbi.nlm.nih.gov/pubmed/22796955]. The raw data were trimmed to a spectra range of 3,000 to 15,000 m/z. The spectra intensities were then square-root transformed and smoothed using the Savitzky-Golay algorithm. Baseline noise was removed using the statistics-sensitive non-linear iterative peak clipping (or SNIP) algorithm with 100 iterations. The data were then normalized using total ion current (or TIC) calibration, which sets the total intensity to 1. Multiple spectra within the same analysis were aligned to the same x-axis using the Lowess warping method, a signal-to-noise ratio of 3, and a tolerance of 0.001. Peaks were detected from the average of at least 4 technical replicates using median absolute deviation. Principal components analyses and hierarchical clustering were also performed in R using the base stats package. Hierarchical clustering was performed on a calculated Euclidean distance matrix using Ward's method.

3.5 References

1. Singhal N, Kumar M, Kanaujia PK, et al. MALDI-TOF mass spectrometry: an emerging technology for microbial identification and diagnosis. Front Microbiol 2015;6.

2. Bhavsar SM, Dingle TC, Hamula CL. The impact of blood culture identification by MALDI-TOF MS on the antimicrobial management of pediatric patients. Diagnostic Microbiology and Infectious Disease 2018;92:220-225.

3. Khan S, Dunn D, Patel G, et al. MALDI-TOF MS in Adult Inpatients with Bloodstream Infections: Pre- and Post-intervention Study. Open Forum Infectious Diseases 2017;4:S626-S626.

4. Haiko J, Savolainen LE, Hilla R, et al. Identification of urinary tract pathogens after 3-hours urine culture by MALDI-TOF mass spectrometry. Journal of Microbiological Methods 2016;129:81-84.

5. Ferreira L, Sanchez-Juanes F, Gonzalez-Avila M, et al. Direct Identification of Urinary Tract Pathogens from Urine Samples by Matrix-Assisted Laser Desorption Ionization-Time of Flight Mass Spectrometry. Journal of Clinical Microbiology 2010;48:2110-2115.

6. Íñigo M, Coello A, Fernández-Rivas G, et al. Direct Identification of Urinary Tract Pathogens from Urine Samples, Combining Urine Screening Methods and Matrix-Assisted Laser Desorption Ionization–Time of Flight Mass Spectrometry. Munson E, ed. J Clin Microbiol 2016;54:988-993.

7. Svarrer CW, Uldum SA. The occurrence of Legionella species other than Legionella pneumophila in clinical and environmental samples in Denmark identified by mip gene sequencing and matrix-assisted laser desorption ionization time-of-flight mass spectrometry. Clinical Microbiology and Infection 2012;18:1004-1009.

8. Samb-Ba B, Mazenot C, Gassama-Sow A, et al. MALDI-TOF Identification of the Human Gut Microbiome in People with and without Diarrhea in Senegal. Chakravortty D, ed. PLoS ONE 2014;9:e87419.

9. Rizzardi K, Åkerlund T. High Molecular Weight Typing with MALDI-TOF MS - A Novel Method for Rapid Typing of Clostridium difficile. Popoff MR, ed. PLoS ONE 2015;10:e0122457.

10. Wang H-Y, Lee T-Y, Tseng Y-J, et al. A new scheme for strain typing of methicillin-resistant Staphylococcus aureus on the basis of matrix-assisted laser desorption ionization time-of-flight mass spectrometry by using machine learning approach. Becker K, ed. PLoS ONE 2018;13:e0194289.

11. Wolters M, Rohde H, Maier T, et al. MALDI-TOF MS fingerprinting allows for discrimination of major methicillin-resistant Staphylococcus aureus lineages. International Journal of Medical Microbiology 2011;301:64-68.

12. Manukumar HM, Umesha S. MALDI-TOF-MS based identification and molecular characterization of food associated methicillin-resistant Staphylococcus aureus. Sci Rep 2017;7:11414.

13. Nisa S, Bercker C, Midwinter AC, et al. Combining MALDI-TOF and genomics in the study of methicillin resistant and multidrug resistant Staphylococcus pseudintermedius in New Zealand. Sci Rep 2019;9:1271.

14. Christner M, Trusch M, Rohde H, et al. Rapid MALDI-TOF Mass Spectrometry Strain Typing during a Large Outbreak of Shiga-Toxigenic Escherichia coli. Greub G, ed. PLoS ONE 2014;9:e101924.

15. Alanio A, Beretti J -L., Dauphin B, et al. Matrix-assisted laser desorption ionization time-of-flight mass spectrometry for fast and accurate identification of clinically relevant Aspergillus species. Clinical Microbiology and Infection 2011;17:750-755.

16. Tenover FC, Arbeit RD, Goering RV. How to select and interpret molecular strain typing methods for epidemiological studies of bacterial infections: a review for healthcare epidemiologists. Molecular Typing Working Group of the Society for Healthcare Epidemiology of America. Infect Control Hosp Epidemiol 1997;18:426-439.

17. Parizad EG, Parizad EG, Valizadeh A. The Application of Pulsed Field Gel Electrophoresis in Clinical Studies. J Clin Diagn Res 2016;10:DE01-DE04.

18. Killgore G, Thompson A, Johnson S, et al. Comparison of seven techniques for typing international epidemic strains of Clostridium difficile: restriction endonuclease analysis, pulsed-field gel electrophoresis, PCR-ribotyping, multilocus sequence typing, multilocus variable-number tandem-repeat analysis, amplified fragment length polymorphism, and surface layer protein A gene sequence typing. J Clin Microbiol 2008;46:431-437.

19. de Bruijn FJ. Use of repetitive (repetitive extragenic palindromic and enterobacterial repetitive intergeneric consensus) sequences and the polymerase chain reaction to fingerprint the genomes of Rhizobium meliloti isolates and other soil bacteria. Appl Environ Microbiol 1992;58:2180-2187.

20. Parolo CCF, Do T, Henssge U, et al. Genetic diversity of Lactobacillus paracasei isolated from in situ human oral biofilms. J Appl Microbiol 2011;111:105-113.

21. Balloux F, Brønstad Brynildsrud O, van Dorp L, et al. From Theory to Practice: Translating Whole-Genome Sequencing (WGS) into the Clinic. Trends Microbiol 2018;26:1035-1048.

22. Schürch AC, Arredondo-Alonso S, Willems RJL, et al. Whole genome sequencing options for bacterial strain typing and epidemiologic analysis based on single nucleotide polymorphism versus gene-by-gene–based approaches. Clinical Microbiology and Infection 2018;24:350-354.

23. Murray PR. Matrix-assisted laser desorption ionization time-of-flight mass spectrometry: usefulness for taxonomy and epidemiology. Clin Microbiol Infect 2010;16:1626-1630.

24. Lasch P, Fleige C, Stämmler M, et al. Insufficient discriminatory power of MALDI-TOF mass spectrometry for typing of Enterococcus faecium and Staphylococcus aureus isolates. Journal of Microbiological Methods 2014;100:58-69.

25. Wunschel DS, Hill EA, McLean JS, et al. Effects of varied pH, growth rate and temperature using controlled fermentation and batch culture on Matrix Assisted Laser Desorption/Ionization whole cell protein fingerprints. Journal of Microbiological Methods 2005;62:259-271.

26. Valentine N, Wunschel S, Wunschel D, et al. Effect of Culture Conditions on Microorganism Identification by Matrix-Assisted Laser Desorption Ionization Mass Spectrometry. Applied and Environmental Microbiology 2005;71:58-64.

27. Ghyselinck J, Van Hoorde K, Hoste B, et al. Evaluation of MALDI-TOF MS as a tool for high-throughput dereplication. Journal of Microbiological Methods 2011;86:327-336.

28. Rashidan M, Azimirad M, Alebouyeh M, et al. Detection of B. fragilis group and diversity of bft enterotoxin and antibiotic resistance markers cepA , cfiA and nim among intestinal Bacteroides fragilis strains in patients with inflammatory bowel disease. Anaerobe 2018;50:93-100.

29. Zamani S, Hesam Shariati S, Zali MR, et al. Detection of enterotoxigenic Bacteroides fragilis in patients with ulcerative colitis. Gut Pathog 2017;9:53.

30. Purcell RV, Pearson J, Aitchison A, et al. Colonization with enterotoxigenic Bacteroides fragilis is associated with early-stage colorectal neoplasia. Brim H, ed. PLoS ONE 2017;12:e0171602.

31. Goodwin AC, Shields CED, Wu S, et al. Polyamine catabolism contributes to enterotoxigenic Bacteroides fragilis-induced colon tumorigenesis. Proceedings of the National Academy of Sciences 2011;108:15354-15359.

32. Chart H, Smith HR, La Ragione RM, et al. An investigation into the pathogenic properties of Escherichia coli strains BLR, BL21, DH5alpha and EQ1. J Appl Microbiol 2000;89:1048-1058.

33. Clarke SC, Haigh RD, Freestone PPE, et al. Virulence of Enteropathogenic Escherichia coli, a Global Pathogen. Clinical Microbiology Reviews 2003;16:365-378.

34. Lee LA, Taylor J, Carter GP, et al. Yersinia Enterocolitica O:3: An Emerging Cause of Pediatric Gastroenteritis in the United States. Journal of Infectious Diseases 1991;163:660-663.

35. Ray SM, Ahuja SD, Blake PA, et al. Population-Based Surveillance for *Yersinia enterocolitica* Infections in FoodNet Sites, 1996–1999: Higher Risk of Disease in Infants and Minority Populations. CLIN INFECT DIS 2004;38:S181-S189.

36. Arnold RJ, Karty JA, Ellington AD, et al. Monitoring the Growth of a Bacteria Culture by MALDI-MS of Whole Cells. Anal Chem 1999;71:1990-1996.

37. Reich M. Species Identification of Bacteria and Fungi from Solid and Liquid Culture Media by MALDI-TOF Mass Spectrometry. J Bacteriol Parasitol 2013;01.

38. Veenemans J, Welker M, van Belkum A, et al. Comparison of MALDI-TOF MS and AFLP for strain typing of ESBL-producing Escherichia coli. Eur J Clin Microbiol Infect Dis 2016;35:829-838.

39. Balážová T, Makovcová J, Šedo O, et al. The influence of culture conditions on the identification of *Mycobacterium* species by MALDI-TOF MS profiling. FEMS Microbiol Lett 2014;353:77-84.

40. Šedo O, Vávrová A, Vad'urová M, et al. The influence of growth conditions on strain differentiation within the *Lactobacillus acidophilus* group using matrix-assisted laser desorption/ionization time-of-flight mass spectrometry profiling: Growth conditions influence strain differentiation using MALDI-TOF MS. Rapid Commun Mass Spectrom 2013;27:2729-2736.

41. Wieme AD, Spitaels F, Aerts M, et al. Effects of Growth Medium on Matrix-Assisted Laser Desorption–Ionization Time of Flight Mass Spectra: a Case Study of Acetic Acid Bacteria. Appl Environ Microbiol 2014;80:1528-1538.

42. McTaggart LR, Chen Y, Poopalarajah R, et al. Incubation time and culture media impact success of identification of Nocardia spp. by MALDI-ToF mass spectrometry. Diagnostic Microbiology and Infectious Disease 2018;92:270-274.

43. Usbeck JC, Kern CC, Vogel RF, et al. Optimization of experimental and modelling parameters for the differentiation of beverage spoiling yeasts by Matrix-Assisted-Laser-Desorption/Ionization–Time-of-Flight Mass Spectrometry (MALDI–TOF MS) in response to varying growth conditions. Food Microbiology 2013;36:379-387.

44. Mandal SM, Pati BR, Ghosh AK, et al. Letter: Influence of Experimental Parameters on Identification of Whole Cell *Rhizobium* by Matrix-Assisted Laser Desorption/Ionization Time-of-Flight Mass Spectrometry. Eur J Mass Spectrom (Chichester) 2007;13:165-171.

45. Shu L-J, Yang Y-L. Bacillus Classification Based on Matrix-Assisted Laser Desorption Ionization Time-of-Flight Mass Spectrometry—Effects of Culture Conditions. Sci Rep 2017;7:15546.

46. Vithanage NR, Bhongir J, Jadhav SR, et al. Species-Level Discrimination of Psychrotrophic Pathogenic and Spoilage Gram-Negative Raw Milk Isolates Using a Combined MALDI-TOF MS Proteomics–Bioinformatics-based Approach. J Proteome Res 2017;16:2188-2203.

47. Zotta T, Parente E, Ricciardi A. Aerobic metabolism in the genus *Lactobacillus* : impact on stress response and potential applications in the food industry. J Appl Microbiol 2017;122:857-869.

48. Straley SC, Perry RD. Environmental modulation of gene expression and pathogenesis in Yersinia. Trends Microbiol 1995;3:310-317.

49. Tomoyasu T, Gamer J, Bukau B, et al. Escherichia coli FtsH is a membrane-bound, ATP-dependent protease which degrades the heat-shock transcription factor sigma 32. EMBO J 1995;14:2551-2560.

50. Bent ZW, Poorey K, Brazel DM, et al. Transcriptomic Analysis of Yersinia enterocolitica Biovar 1B Infecting Murine Macrophages Reveals New Mechanisms of Extracellular and Intracellular Survival. McCormick BA, ed. Infect Immun 2015;83:2672-2685.

51. Ackermann M. A functional perspective on phenotypic heterogeneity in microorganisms. Nat Rev Microbiol 2015;13:497-508.

52. Lau JT, Whelan FJ, Herath I, et al. Capturing the diversity of the human gut microbiota through culture-enriched molecular profiling. Genome Med 2016;8:72.

53. Wu W-K, Chen C-C, Panyod S, et al. Optimization of fecal sample processing for microbiome study — The journey from bathroom to bench. Journal of the Formosan Medical Association 2019;118:545-555.

54. Grenga L, Pible O, Armengaud J. Pathogen proteotyping: A rapidly developing application of mass spectrometry to address clinical concerns. Clinical Mass Spectrometry April 2019:S2376999818300503.

55. Karlsson R, Gonzales-Siles L, Boulund F, et al. Proteotyping: Proteomic characterization, classification and identification of microorganisms – A prospectus. Systematic and Applied Microbiology 2015;38:246-257.

Chapter 4. Polyunsaturated fatty acid arachidonic acid increases the virulence of gut pathogen, *Yersinia enterocolitica*

Adapted from:

Denise Chac, Kelly Crebs, Cara Yee and R. William DePaolo. Polyunsaturated fatty acid arachidonic acid increases the virulence of gut pathogen, *Yersinia enterocolitica*.

4.1 Abstract

Food-borne illnesses are a major health concern, as 1 in 6 individuals are infected yearly in the US alone, yet there is little research into what dietary factors can alter the risk of infection. Despite epidemiological evidence suggesting a correlation between obesity and enteric infection, the few reported studies focus on the role of dietary factors and the impact on host tissues. However, the impact of dietary constituents on the virulence of a pathogen has largely been ignored. Here, we show that the pro-inflammatory polyunsaturated fatty acid, arachidonic acid, can directly alter the pathogenicity of gram-negative Proteobacteria, *Yersinia enterocolitica.* Using *in vitro* cellular adherence assays, proteomic peptide mass fingerprint profiles and *in vivo* mouse models, we show that arachidonic acid can alter the pathogenesis of *Y. enterocolitica* by increasing proliferation and intracellular invasion. These findings have major implications in not just food safety, but also potentially revealing how diet-related illnesses might increase the virulence of food borne pathogens.

4.2 Introduction

Polyunsaturated fatty acids (PUFAs) play a vital role in human development and health. As essential fatty acids, PUFAs cannot be synthesized by humans and must be acquired through diet in a balanced manner. While deficiencies in PUFAs can lead to skin and neurological impairment, excessive PUFAs can cause inflammation[1,2]. The omega-6 fatty acid arachidonic acid is especially of interest as it has become highly available with foods in plant-derivatives such as corn oil and is linked to inflammatory diseases such as obesity[3,4] and diabetes[2,5]. Whereas studies of arachidonic acid in mice models have been inconsistent in regards to colonic inflammation[6–9], insulin resistance[10,11] and obesity[10–12], human studies have found excessive levels of arachidonic acid among patients with obesity[3,4], metabolic dysregulation[13,14], and ulcerative colitis[15–18].

Arachidonic acid and its derivatives such as eicosanoids are also important for antibacterial functions. Arachidonic acid is highly bactericidal against gram-positive species including *Neisseria*, *Pseudomonas* and members of *Enterobacteriaceae*[19] and reduces growth and adherence of gram-positive probiotic *Lactobacillus* species [20]. In a recent study, serum arachidonic acid levels increased following *Streptococcus pneumoniae* infection and *in vitro* assays demonstrated its antimicrobial activity on the pneumococcal membrane[21] (Eijkelkamp 2018). On the other hand, the effect of arachidonic acid on gram-negative pathogens is variable. Whereas arachidonic acid is less potent on *Eschericia coli*[19], arachidonic acid can be incorporated into the bacterial membrane of *Acinetobacter baumannii* and reduce bacterial fitness and membrane integrity[22].

Unfortunately, several food-borne pathogens are gram-negative including *E. coli*, *Listeria*, *Salmonella*, and *Yersinia enterocolitica*. According to the CDC, food-borne illnesses affect 48 million individuals and have caused 128,000 hospitalizations and 3,000 deaths each year[23] (CDC). In less developed countries, food- and water-borne diarrheal diseases have killed approximately 1.9 million people[24]. One such food-borne pathogen is gamma-proteobacteria *Y. enterocolitica*. While *Y. enterocolitica* causes self-limiting gastroenteritis and mesenteric lymphadenitis in healthy individuals, it can be lethal in immunocompromised patients or young children[25]. There is also a disproportionate incidence of *Y. enterocolitica* infection found among children less than 1 year of age[26].

Y. enterocolitica is naturally exposed to arachidonic acid in meats[27] and may also encounter fatty acids in the gut lumen[28–30]. The effect of arachidonic acid on *Y. enterocolitica* has not yet been established. One study using saturated fatty acids found lauric acid to inhibit *Y. enterocolitica* growth but not myristic and palmitic acid[31]. Another study found oregano and nutmeg essential oils ineffective against bacterial colonization of chicken[32]. There is a lack of studies investigating foodborne bacterial pathogens in the presence of polyunsaturated fatty acids, both dietary and host derived.

We found that PUFAs differentially affect the growth of food-borne pathogen *Y. enterocolitica*. Exposure to arachidonic acid increases the proliferation of *Y. enterocolitica* and alters the disease pathogenesis. Under normal conditions *Y. enterocolitica* exhibits different virulent states depending on mammalian cell presence, but when arachidonic acid is added *Y. enterocolitica* becomes hyper-virulent. These results highlight the necessity to investigate how dietary fats can impact the virulence of food-borne pathogens.

4.3 Results

Polyunsaturated fatty acids differentially affect proliferation of *Yersinia enterocolitica*

Recent studies involving polyunsaturated fatty acids (PUFAs) have shown both beneficial and detrimental effects on bacterial pathogens[33,34]. There are currently no studies investigating the effect of omega-6 and omega-3 PUFAs on gut pathogen *Yersinia enterocolitica* (Ye). In this study, we supplemented bacterial growth media with PUFAs and monitored growth at room temperature (26°C) by measuring the optical density (OD).

Supplementation of the PUFAs into the growth media increased the growth of Ye following 4 hours with the highest concentration of 500uM (Figure 4.1A). Whereas linoleic acid (LA), alpha-linolenic acid (ALA) and eicosapentanoic acid (EPA) had significant growth, AA altered growth in a dose-dependent manner. After 180 and 240 minutes, Ye treated 250 uM and 500 uM AA had significant growth compared to vehicle-treated Ye (Figure 4.1A). To analyze the effect across all the PUFAs, the experiment was repeated at 500uM. Again, the omega-6 PUFA AA significantly increased the growth of Ye over the course of 4 hours (Figure 4.1B). The other PUFAs did not significantly affect growth of Ye. Ye treated with PUFAs was also

grown at 37°C to activate the Ye virulence plasmid (pYV) which encodes the type 3 secretion needle and other factors necessary for adherence to epithelial cells[35].

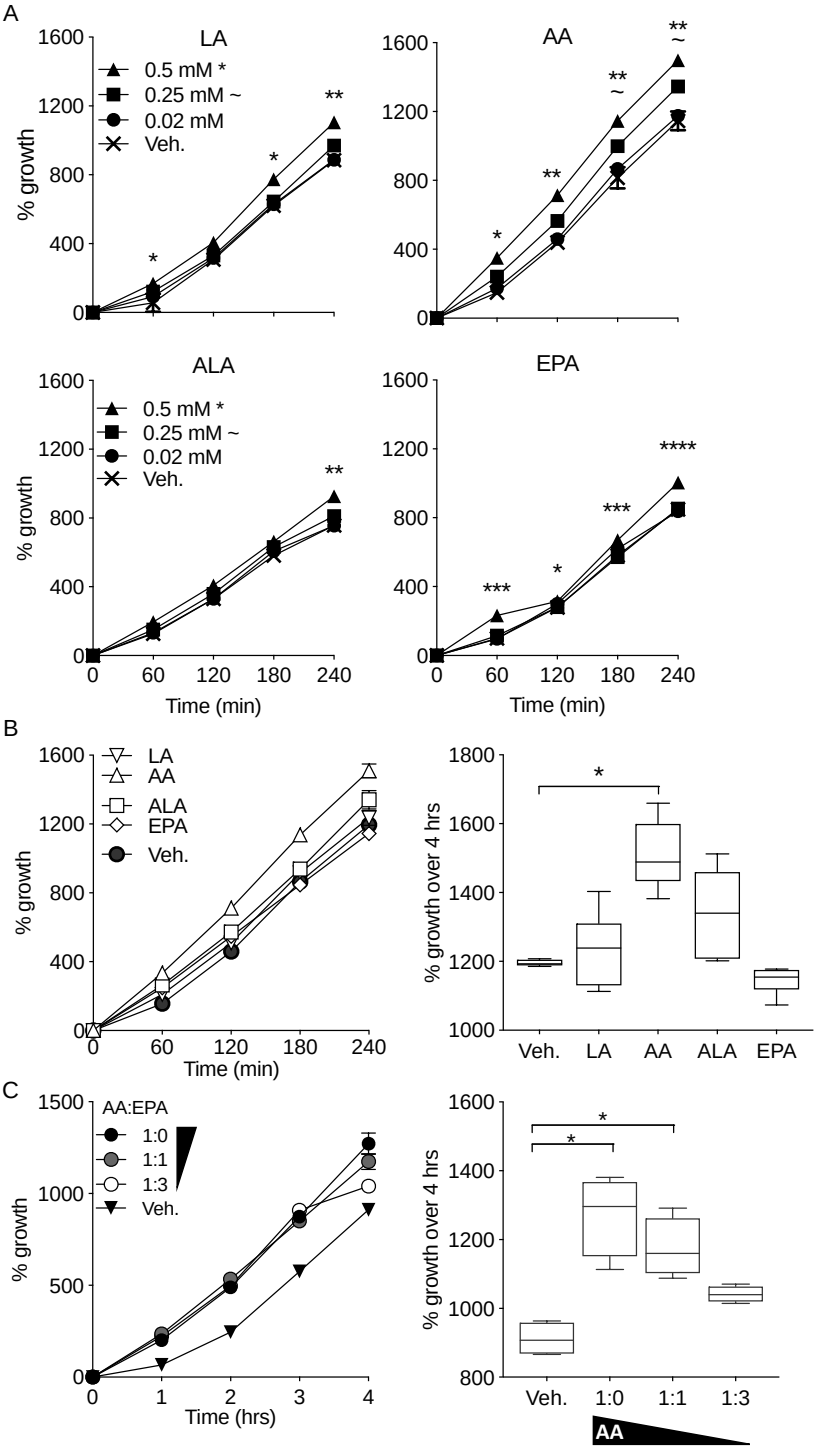

Figure 4.1:Arachidonic acid increases proliferation and intracellular invasion of Y. enterocolitica

A) Growth curve of Ye grown with addition of 20-500uM of linoleic acid (LA), arachidonic acid (AA), alpha-linolenic acid (ALA), and eicosapentaenoic acid (EPA). (B) Growth curve and overall percent growth of Ye over 4 hours following addition of 500uM of PUFAs. (C) Growth curve and overall percent growth of Ye with ratios of AA to EPA: 500uM AA (1:0 ratio), 250uM AA to 250uM EPA (1:1 ratio), and 125uM AA to 375uM EPA (1:3 ratio). (A) Two-way ANOVA, multiple comparisons. Data is mean ± SEM from 3 independent studies with duplicates. * = 0.5mM, ~ = 0.25mM. $p<0.05$, *; $p<0.01$ **; $p<0.005$, ***; $p<0.001$, ****. (B, C) Kruskal-Wallis Test with Dunn's multiple comparisons test. Data is shown as mean ± SEM from 3 independent studies with duplicates. $p<0.05$, *.

Ye treated with PUFAs had significantly increased growth compared to control regardless of PUFA type (Supplemental Figure 4.1). Next, we tested the growth of Ye in the presence of two PUFAs. As the recommended dietary intake of omega-6 to -3 fatty acid ratio is 1:1 to 3:1[36,37], we tested whether the ratio of AA to EPA could alter the growth of Ye. Interestingly, EPA dampens the increased proliferation of Ye in a dose-dependent manner (Figure 4.1C).

Arachidonic acid increases intracellular invasion of *Yersinia enterocolitica* in vitro

To test the effect of AA on Ye virulence, bacteria was grown with AA for two hours at 37°C, washed in PBS and introduced to human epithelial cells SW620s (Figure 4.2A). Bacteria were recovered after 1 hour to analyze the percentage of Ye adhered to cells or treated with gentamicin and recovered an hour later to analyze intracellular Ye. Ye treated with AA trended towards higher adherence compared to the untreated Ye (Figure 4.2B). Analysis of intracellular Ye revealed significant increases of Ye invasion when treated with AA compared to untreated and vehicle control (Figure 4.2B). As we saw variable growth with increasing decreasing ratios of AA to EPA (Figure 4.1C), we evaluated whether the ratios could also affect bacterial invasion. We found no significant differences in invasion in Ye treated with either only AA or AA and EPA (Supplemental Figure 4.2). Together with the proliferation data, these data point to an altered virulence state when Ye is exposed to AA.

Arachidonic acid alters the peptide mass fingerprint of *Yersinia enterocolitica*

Following the cellular adhesion and invasion assay, Ye was plated on TSA to enumerate the amount colonized. These same bacteria were also analyzed for changes in peptide mass fingerprints (PMFs). The bacteria from naïve Ye, extracellular Ye, or intracellular Ye were analyzed using matrix-assisted laser desorption/ionization – time of flight (MALDI-TOF) mass spectrometry (MS). MALDI-TOF has been useful for bacterial identification and has recently been validated in identifying strain-level and functional differences[38]. Using the MALDI-TOF MS, we compared the PMFs of the three Ye groups.

Treatment with vehicle control in the three groups have three distinct clusters depending on virulence state (Figure 4.2C-D, Supplemental Figure 4.3A). On the other hand, there are no distinct clustering of Ye when treated with AA (Figure 4.2C-D, Supplemental Figure 4.3B). All three AA-treated Ye groups clustered

together and appear to overlap with the intracellular Ye treated with vehicle control (Figure 4.2C). To further assess virulence state and protein production, these bacteria was examined by Coomassie Blue staining.

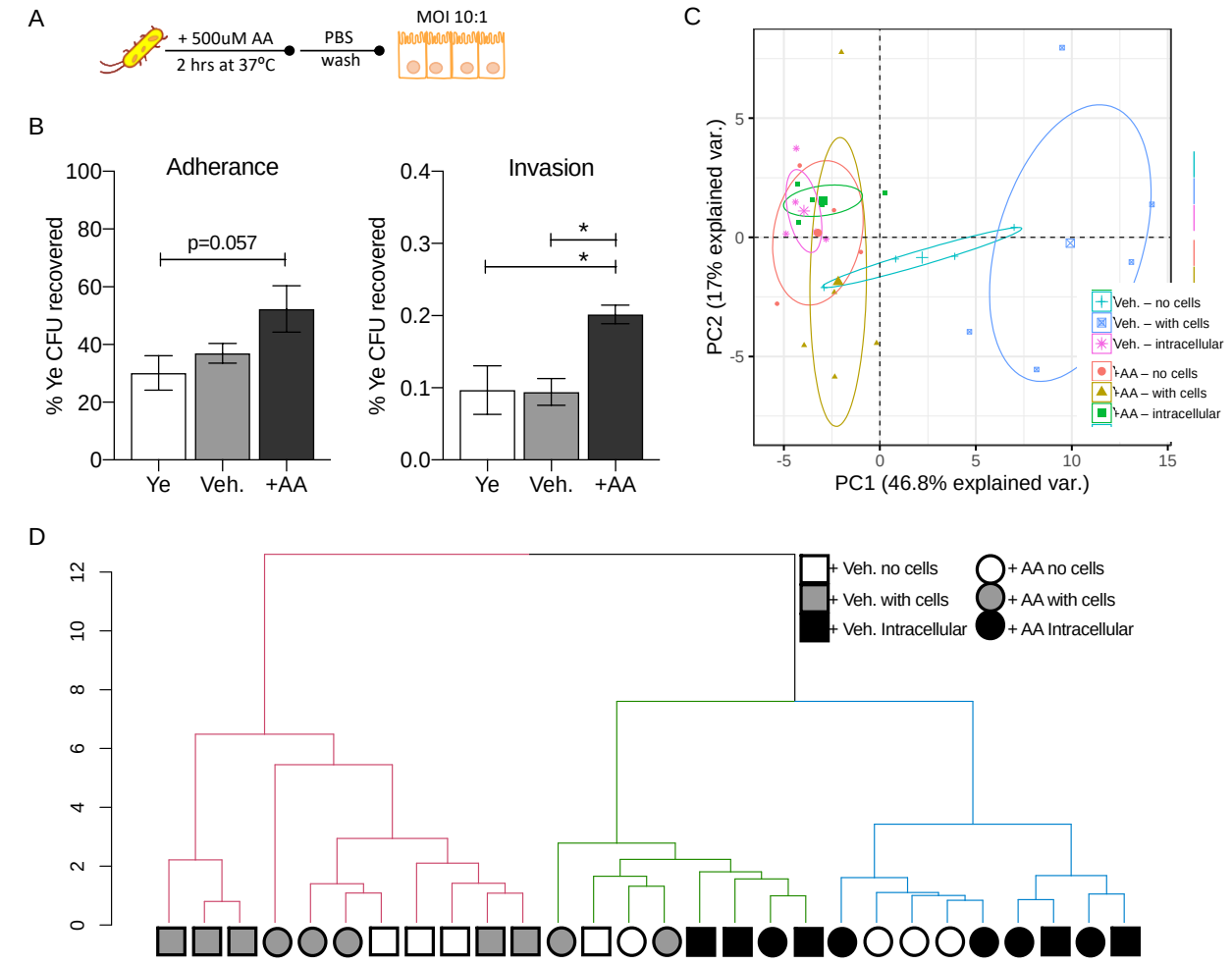

Figure 4.2: Exposure to AA alters invasion and PMF of Y. enterocolitica
(A) Diagram of *in vitro* assay using *Y. enterocolitica* exposed to 500uM AA and then introduced to human colonic epithelial cells SW620s. (B) (left) Percentage of Ye CFUs recovered after 60 minutes of incubation and (right) percentage of Ye CFU recovered after 60 minutes of incubation then treatment of 100ug/ml gentamicin for 60 minutes. One-way ANOVA with Tukey's multiple comparisons test, $p<0.05$, *. Data is mean ± SEM from a representative from 2 independent studies with duplicates. (C) Principal component analysis (PCA) and (D) dendrogram of peptide mass fingerprint profiles of *Y. enterocolitica* of various treatment groups with ellipses drawn on average mean of each group.

Arachidonic acid induces a virulent state in *Yersinia enterocolitica*

The virulence plasmid in *Y. enterocolitica* is temperature dependent. When Ye is at room temperature, the virulence plasmid is dormant and the bacteria express proliferation and motility genes[39,40]. At host

temperatures of 37°C, Ye induces the virulence plasmid and begins to produce and secrete Yersinia outer proteins and Yersinia secreted proteins[39,40]. To evaluate these presence of these proteins, Ye treated with AA was grown at room temperature and assessed by SDS-PAGE and Coomassie blue staining. In both bacterial lysates and supernatant, there is staining in the virulent Ye grown at 37°C compared to the non-virulent Ye grown at room temperature (Figure 4.3). For the Ye supplemented with AA, there is staining in the lysates and some in the supernatant despite being grown at room temperature (Figure 4.3). Altogether, these data point to a hyper-proliferative and virulent state when *Y. enterocolitica* is in the presence of arachidonic acid.

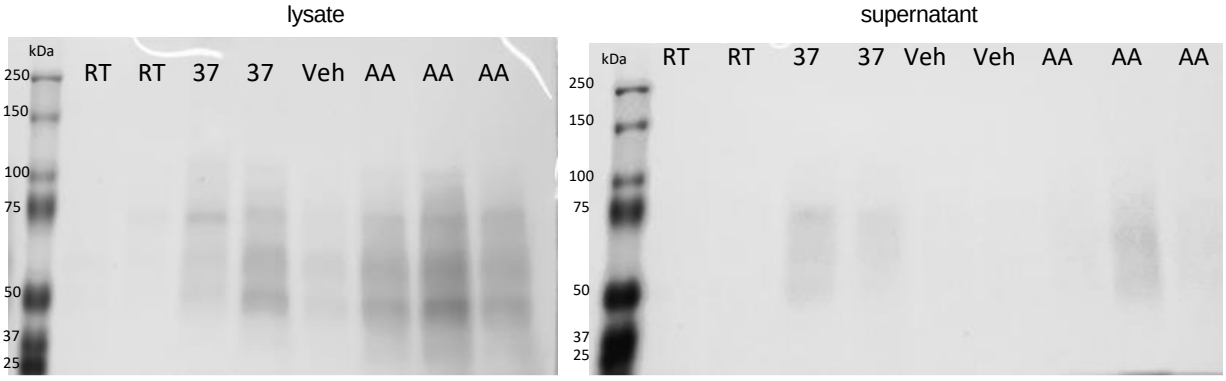

Figure 4.3: AA alters the virulence state of Y. enterocolitica
Coomassie blue staining of *Y. enterocolitica* lysates and supernatant grown at room temperature (RT), 37°C, or exposed to 500uM AA or vehicle at RT.

Y. enterocolitica becomes more virulent *in vivo* after exposure to arachidonic acid

To determine if the AA-induced virulent state in Ye found *in vitro* could be replicated in the host, we tested AA-treated Ye in a mouse model of infection. As before, Ye is pretreated with AA for 2 hours at 37°C and washed prior to infection (Figure 4.4A). Mice were given an oral infection of $1x10_7$ CFU of either vehicle-treated or AA-treated Ye. During the infection, mice infected with vehicle control did not lose any weight while mice with the AA-treated Ye lost significant weight (Figure 4.4B). These mice exhibited visible discomfort with an average of 10% weight loss. Due to the rapid decline in health, the mice were euthanized at day 3 post infection and *Y. enterocolitica* colonization was assessed. Mice with untreated Ye typically lose weight around day 4 post infection with bacteria colonization of the spleen at day 6 post infection (unpublished observations).

At day 3 post infection, Ye colonization was assessed. Of the mice infected with vehicle-treated Ye, only half had colonization in the ileum and Peyer's patches (Figure 4.4C, Supplemental Figure 4.4). On the other hand, all mice infected with the AA-treated Ye had ileal colonization with more bacterial CFU recovered. To evaluate systemic infection, bacteria in the spleen of infected mice was also enumerated. While no vehicle-treated Ye infected mice had bacteria in the spleen at day 3, mice with the AA-treated Ye had high levels of colonization in the spleen (Figure 4.4C).

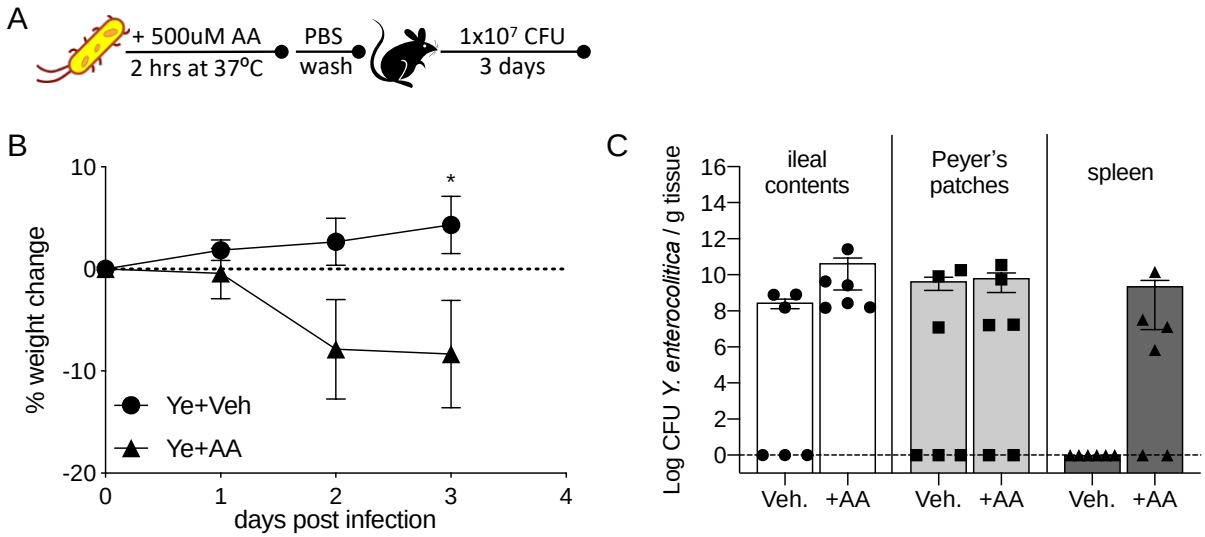

Figure 4.4: Exposure to AA increases virulence of Y. enterocolitica in vivo
A) Diagram of mouse model with *Y. enterocolitica* pre-treated with 500uM AA. B) Percent weight change post infection. C) Bacterial burden post infection at day 3 in the ileum, Peyer's patches (pp) and spleen. Statistical tests- B) Two-Way ANOVA with Bonferroni's multiple comparisons test for. Data is mean ± SEM from two independent experiments, n=6/6. $p<0.05$, *.

4.4 Discussion

Polyunsaturated fatty acids (PUFAs) are a vital component of our diet. As dietary recommendations are constantly changing, it is important to analyze the effects of dietary fats on potential bacterial food pathogens. In this study, we analyze the effect of omega-6 polyunsaturated fatty acid arachidonic acid on *Y. enterocolitica*. We found that arachidonic acid significantly increases the growth of *Y. enterocolitica* and co-supplementation with eicosapentaenoic acid can suppress this growth in a dose-dependent manner. Supplementation with arachidonic acid also induced protein production much like the *Y. enterocolitica* grown in virulence-inducing conditions. Indeed, our invasion assays demonstrate that *Y. enterocolitica*

treated with arachidonic acid have more intracellular colonization and the MALDI-TOF analysis revealed PMF signatures similar to intracellular bacteria regardless if co-cultured with mammalian cells or not. Furthermore, when we moved our model system into the murine host, we discovered that arachidonic acid-treated *Y. enterocolitica* has a more severe pathogenesis. While mice infected with *Y. enterocolitica* typically lose weight around day 4 and succumb to the infection with colonization of spleen at day 6, mice in this study experienced rapid weight loss and surprising amounts of *Y. enterocolitica* colonization in the spleen at day 3. To our knowledge, this is the first study to show that a pathogen can have increased virulence in a host with altered pathogenesis after exposure to arachidonic acid.

There is a pronounced disconnect between dietary recommendations and the literature regarding the consumption of omega-6 (n-6) polyunsaturated fatty acids. According to the 2015-2020 Dietary Guidelines for Americans provided by the U.S. Department of Health and Human Services, the recommended consumption of dietary oils should be 27 g per day for a 2,000-calorie diet[41]. These guidelines do not distinguish between n-6 and n-3 PUFAs in the daily recommendations despite several studies finding that the excessive consumption of n-6 PUFAs in the American diet can be associated with inflammatory diseases. While n-6 PUFAs are essential fatty acids necessary for proper development and growth, arachidonic acid has been positively correlated with heart disease[42], obesity and diabetes[43]. In rodent studies, diets high in omega-6 fatty acids cause systemic low-grade inflammation and metabolic endotoxemia[44] and increase the abundance of gut microbes associated with inflammation[45].

More recently, diets high in n-6 PUFAs has also been associated with infections. Studies using in vitro cell assays and mouse models have found that n-6 PUFAs may worsen inflammation when challenged with viral and bacterial pathogens[46–48]. Whereas these studies use dietary models, our study introduces the bacterial pathogen to physiologically relevant levels of PUFAs prior to infection. Not only do we find the bacterial pathogen altered by arachidonic acid, the pathogenesis within a mouse host is also severely worsened. Collectively, our study and others highlight the need to further investigate how pathogens interact with dietary components and how the consumption of excessive fat diets may increase susceptibility to infections.

The literature reports that excessive dietary n-6 PUFAs is detrimental due to the increasing ratio of n-6 to n-3 PUFAs. As both n-6 and n-3 PUFAs rely on the same enzymes to breakdown into their respective metabolites, a healthy n-6:3 ratio is between 1:1 and 3:1 based on ancestral diets[36,49]. Following the advent of the agricultural revolution, there has been an incline of n-6 PUFA consumption without a paralleling incline of n-3 consumption, leading to the Western diet having a PUFA ratio ranging from 10:1 to 20:1[37,50]. Indeed, several human studies have shown that decreasing n-6:3 ratios can lower levels of inflammation associated with metabolic syndrome[51], obesity[52], non-alcoholic fatty liver disease[53], rheumatoid arthritis[54], and inflammatory bowel disease[55]. With regards to infections, however, few studies examine how the n-6:3 ratio can affect bacterial pathogen susceptibility and none of those examine how the n-6:3 ratio can impact the pathogen. In our study we briefly investigate this when we expose *Y. enterocolitica* to various ratios of n-6:3 and find that increasing n-3 PUFA eicosapentaenoic acid can suppress proliferation to normal levels. Future studies are necessary to examine these effects on bacterial pathogens such as *Y. enterocolitica* and viral infections.

While excessive dietary arachidonic acid is associated with increased inflammation, studies have shown that it may also act as an antimicrobial agent. One study found that n-6, n-7, and n-9 fatty acids including arachidonic acid can inhibit the growth of oral bacteria[34]. Another study demonstrated that macrophages release arachidonic acid after exposure to gram-negative pathogen Salmonella typhimurium but not after exposure to Y. enterocolitica[56]. Interestingly, Golubeva and colleagues recently discovered that host intestinal free long-chain fatty acids may also serve as a metabolic cue for *S. enterica* to start intestinal colonization[57]. The data presented in this study show that exogenous arachidonic acid does not have an antimicrobial effect on *Y. enterocolitica*. Instead, arachidonic acid increases *Y. enterocolitica* proliferation and alters its virulence in vitro and in vivo. Typically, *Y. enterocolitica* is considered an extracellular pathogen that interacts with the host cell surface but recent studies have found and analyzed intracellular *Y. enterocolitica* populations[58,59]. As with the study by Golubeva et al[57], arachidonic acid may act as an indicator to invade as we see increased intracellular invasion in vitro and which may also cause the quickening of disease in vivo. More studies involving host and dietary PUFAs with *Y. enterocolitica* will provide insight into how this gram-negative pathogen can alter its pathogenesis.

To conclude, the present work demonstrates that PUFAs can differentially modulate *Y. enterocolitica* and affect its virulence. Our study exposed *Y. enterocolitica* to arachidonic acid for a short period of time and found it to be nearly lethal in wild-type mice after 3 days. These types of studies provide valuable insight not only to the pathogen itself, but also how dietary factors may compromise the host.

4.5 Materials and Methods

Bacterial strains and growth conditions

The strain used for this study is Yersinia enterocolitica 8081, biotype 1B serotype O:8. *Y. enterocolitica* was grown on tryptic soy agar (TSA) plates and in tryptic soy broth (TSB) for liquid cultures. For regular culturing, frozen stocks were plated on TSA and incubated at room temperature for 48 hours. After 48 hours, one colony forming unit was cultured in TSB and incubated overnight, shaking at room temperature. Subcultures were created by diluting overnight cultures 1:10 in TSB.

Polyunsaturated fatty acid (PUFA) treatments and growth curves

Subcultures of *Y. enterocolitica* were treated with PBS, vehicle control, or 500uM of the following polyunsaturated fatty acids: linoleic acid (LA), arachidonic acid (AA), alpha-linolenic acid (ALA) and eicosapentaenoic acid (EPA) (Cayman Chemicals, Ann Arbor, MI). PUFAs were diluted in 200 proof ethanol (VWR, Randor, PA) and were not used more than 3 times to limit the amount of oxidation. *Y. enterocolitica* cultures were incubated at room temperature with vigorous shaking and OD600 was measured every hour for 4 hours on a Genesys 30 Visible Spectrophotometer (ThermoFisher, Waltham, MA).

Cellular adhesion and invasion assays

SW620s (ATCC; CCL-227) human intestinal epithelial adenoma cells were used. SW620s were maintained in DMEM supplemented with 10% fetal bovine serum and 200uM L-glutamine. Prior to cellular assays, SW620s were seeded into 24-well plates and grown to a nearly confluent monolayer over 3-4 days. SW620s were rinsed with PBS and infected with *Y. enterocolitica* at an MOI of 10:1 with each starting dose plated on TSA to enumerate CFUs. Briefly, overnight Y. enterocolitica cultures were diluted 1:10 in TSB and supplemented with either 500uM AA, equal volume ethanol as vehicle control, or PBS. Subcultures were then incubated for 2 hours at 37°C while shaking at 150 rpm. Cultures were then centrifuged, rinsed

in PBS and diluted to the appropriate infection dose in cell media. The *Y. enterocolitica* samples were introduced to the cells and infection initiated by centrifuging the plates for 5 minutes at 500 x g. For adhesion, Y. enterocolitica was co-cultured with SW620s for 1 hour at 37°C in a 5% CO_2 incubator. For intracellular invasion, *Y. enterocolitica* was co-cultured with SW620s for 1 hour, washed with PBS and then treated with 100 ug/ml gentamicin (Corning, Corning, NY). To elute the *Y. enterocolitica* and lyse the SW620s, each well was washed three times with warm PBS and then treated with 500ul PBS with 1% Triton X-100 (AMRESCO, VWR, Randor PA) for 5 minutes. Samples were then plated on TSA in serial dilutions to enumerate *Y. enterocolitica* colonization. In parallel, wells containing media only were infected with an equal amount of bacteria. Percentage of colonization was calculated by dividing the number of *Y. enterocolitica* CFU recovered from co-cultures by the number of *Y. enterocolitica* CFU initially applied to the wells.

MALDI-TOF peptide-mass fingerprint analysis

Y. enterocolitica plated on TSA following the cellular and invasion assays were analyzed using matrix-assisted laser desorption/ionization – time of flight (MALDI-TOF) on Bruker's Microflex LT/SH (Bruker, Billerica, MA) Protein was extracted per manufacturer's protein extraction method. Briefly, CFUs were picked into sterile H2O and 100% ethanol. After centrifuging and air-drying the protein pellets, the pellets were resuspended in 70% formic acid and acetonitrile. The protein extracts were centrifuged and 1ul was plated on stainless-steel target in triplicates. Samples were then overlaid with 1ul of alpha-Cyano-r-hydroxycinnamic acid (HCCA) Matrix and analyzed using the Microflex. For MALDI-TOF standard, Bruker's bacterial test standard (BTS) was used.

Raw spectra text files were analyzed using the R package, MALDIquant [https://www.ncbi.nlm.nih.gov/pubmed/22796955]. The raw data were trimmed to a spectrum range of 3,000 to 15,000 m/z. The spectra intensities were then square-root transformed and smoothed using the Savitzky-Golay algorithm. Baseline noise was removed using the statistics-sensitive non-linear iterative peak clipping (or SNIP) algorithm with 100 iterations. The data were then normalized using total ion current (or TIC) calibration, which sets the total intensity to 1. Multiple spectra within the same analysis were aligned to the same x-axis using the Lowess warping method, a signal-to-noise ratio of 3, and a tolerance of 0.001.

Peaks were detected from the average of at least 4 technical replicates using median absolute deviation. Principal components analyses and hierarchical clustering were also performed in R using the base stats package. Hierarchical clustering was performed on a calculated Euclidean distance matrix using Ward's method.

SDS-PAGE and Coomassie Blue stain

Y. enterocolitica subcultures were supplemented with vehicle controls or PUFAs and incubated at room temperature or 37°C shaking. After incubation for 2 hours, bacterial cells were separated by centrifugation. Supernatant was collected and bacterial pellets were washed in PBS and resuspended in 100ul of 10% SDS in PBS. Proteins from the supernatant and bacterial lysates were extracted by trichloroacetic acid (TCA) precipitation. Briefly, TCA was added to samples at a final concentration of 5% and incubated on ice for 2 hours. Protein was recovered by centrifuging at 13,000 x g for 10 minutes at 4°C and washed twice in ice-cold acetone. Samples were then resuspended in sample buffer and run on a 10% polyacrylamide pre-cast gel (Bio-Rad, Hercules, CA) for sodium dodecyl sulfate-polyacrylamide gel electrophoresis (SDS-PAGE). The gel was then stained with Coomassie blue stain containing 40% (v/v) methanol, 10% (v/v) glacial acetic acid, and 0.1% (w/v) Coomassie Brilliant Blue R-250 (ThermoFisher, Waltham MA), de-stained until desired background was reached and imaged.

Oral mouse infections

C57Bl/6 wild type male mice 4-5 weeks of age were used for in vivo infections. *Y. enterocolitica* treated with either vehicle control or 500uM arachidonic acid was washed and resuspended in PBS. Mice were given oral infection of 100ul of $1x10_8$ CFU/ml using a sterile blunt-ended needle and infection was carried out for 3 days. Mice weight and fecal consistency was monitored daily. After 3 days, mice were euthanized and tissue was collected. Ileal contents, Peyer's patches and spleens were sterile extracted and plated in dilutes on *Y. enterocolitica* selective plates (Fisher, Waltham MA) or TSA. *Y. enterocolitica* CFUs were enumerated after 48 hours. All animal experiments were performed at the University of Washington, Seattle following experimental review and approval by the Institutional Biosafety Committee and the Institutional Animal Care and Use Committee.

Statistical analysis

All statistics were performed on GraphPad Prism v7 (GraphPad Software, San Diego, CA, www.graphpad.com) except for the MALDI-TOF data which is described above. Either one-way or two-way ANOVA tests were used to determine the significance of the experiments as indicated in each figure legend. Data is shown as mean with error bars showing standard error of the mean.

4.6 Supplemental Material

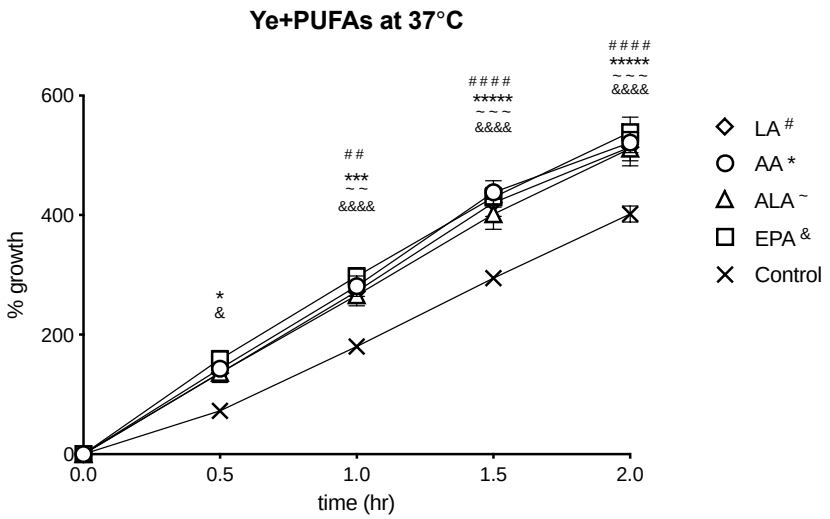

Supplemental Figure 4.1: Growth of Y. enterocolitica with PUFAs at 37C

Growth curve of Y. enterocolitica over 2 hours following addition of 500uM of linoleic acid (LA), arachidonic acid (AA), alpha-linolenic acid (ALA), and eicosapentaenoic acid (EPA). Two-way ANOVA with Sidak's multiple comparisons test; each sample is compared to control with significant symbols: LA, #; AA, *; ALA, ~; and EPA, &. Data is mean ± SEM from 2 independent studies with duplicates. $p<0.05$, *; $p<0.01$, **; $p<0.005$,***; $p<0.001$,****.

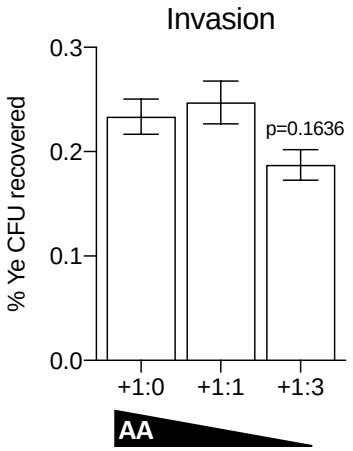

Supplemental Figure 4.2: Invasion of* Y. enterocolitica *with altered ratios of AA and EPA

Percentage of *Y. enterocolitica* CFU recovered after 60 minutes of incubation of SW620s with *Y. enterocolitica* then treatment of 100ug/ml gentamicin for 60 minutes for bacterial invasion. *Y. enterocolitica* was pretreated with 500uM AA (1:0 ratio), 250uM AA to 250uM EPA (1:1 ratio), and 125uM AA to 375uM EPA (1:3 ratio).

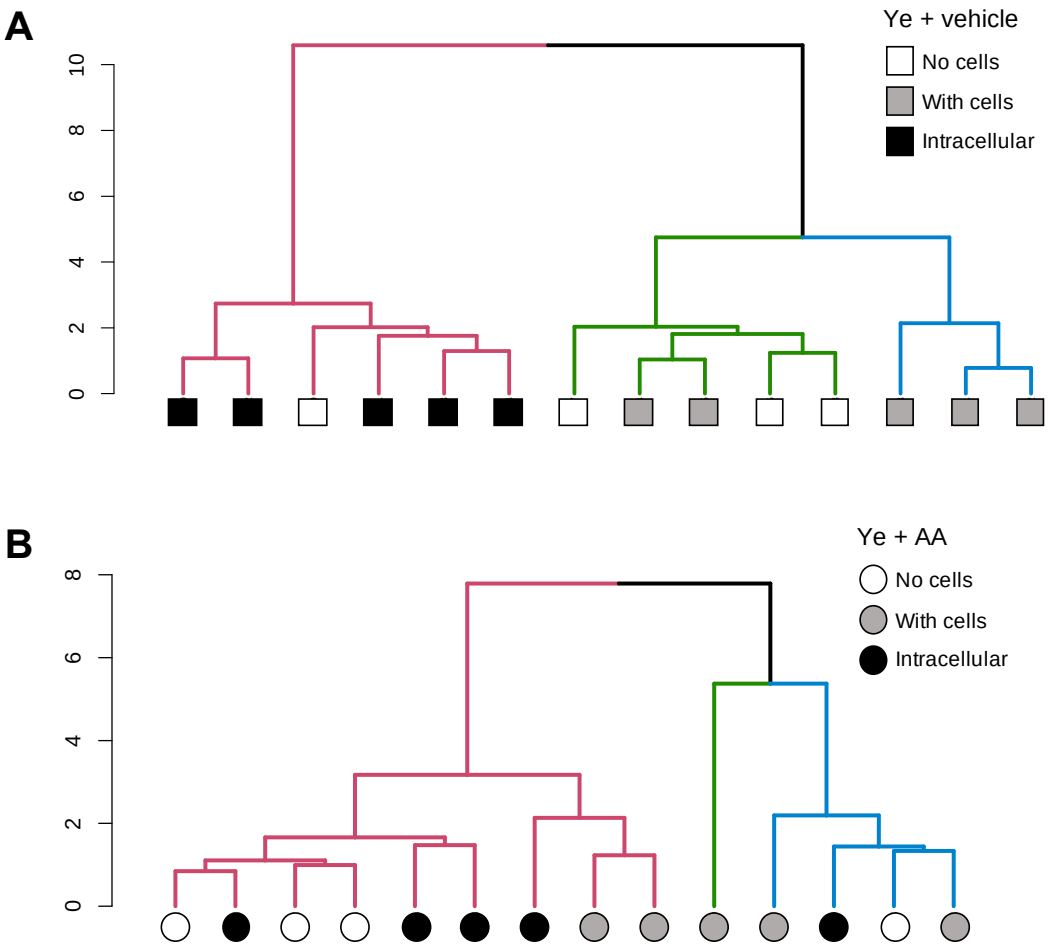

Supplemental Figure 4.3: Dendrogram of* Y. enterocolitica *PMF with cellular assay

Dendrogram of peptide mass fingerprint of *Y. enterocolitica* with vehicle (A) or AA treatment (B) and introduced to intestinal epithelial cells.

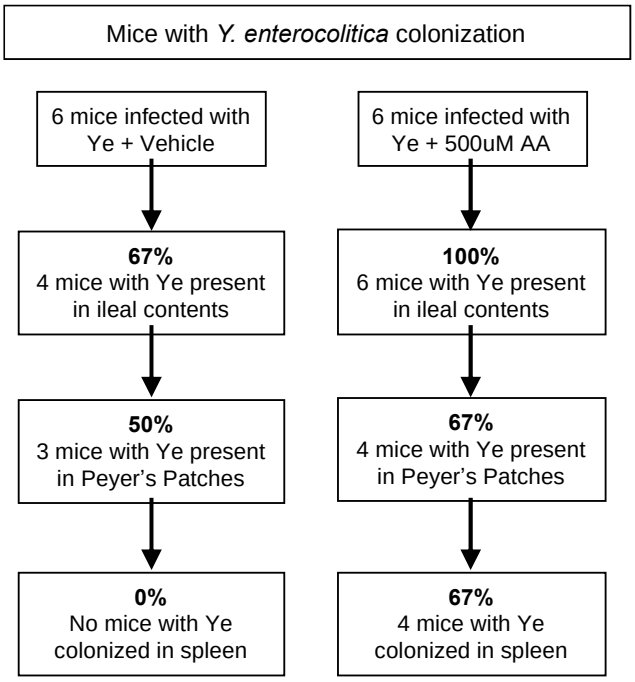

Supplemental Figure 4.4: Flow diagram of percentage and number of mice with* Y. enterocolitica *colonization

4.7 References

1. Patterson E, Wall R, Fitzgerald GF, Ross RP, Stanton C. Health Implications of High Dietary Omega-6 Polyunsaturated Fatty Acids. *Journal of Nutrition and Metabolism*. 2012;2012:1-16. doi:10.1155/2012/539426

2. Raphael W, Sordillo LM. Dietary polyunsaturated fatty acids and inflammation: the role of phospholipid biosynthesis. *Int J Mol Sci*. 2013;14(10):21167-21188. doi:10.3390/ijms141021167

3. Pickens CA, Sordillo LM, Zhang C, Fenton JI. Obesity is positively associated with arachidonic acid-derived 5- and 11-hydroxyeicosatetraenoic acid (HETE). *Metab Clin Exp*. 2017;70:177-191. doi:10.1016/j.metabol.2017.01.034

4. Savva SC, Chadjigeorgiou C, Hatzis C, et al. Association of adipose tissue arachidonic acid content with BMI and overweight status in children from Cyprus and Crete. *Br J Nutr*. 2004;91(4):643-649. doi:10.1079/BJN20031084

5. Calder PC. n−3 Polyunsaturated fatty acids, inflammation, and inflammatory diseases. *Am J Clin Nutr*. 2006;83(6):1505S-1519S. doi:10.1093/ajcn/83.6.1505S

6. Petrik MBH, McEntee MF, Chiu C-H, Whelan J. Antagonism of Arachidonic Acid Is Linked to the Antitumorigenic Effect of Dietary Eicosapentaenoic Acid in ApcMin/+ Mice. *J Nutr*. 2000;130(5):1153-1158. doi:10.1093/jn/130.5.1153

7. Whelan J, Hansen Petrik MB, McEntee MF, Obukowicz MG. Dietary Epa Reduces Tumor Load in ApcMin/+Mice by Altering Arachidonic Acid Metabolism, But Conjugated Linoleic Acid, Gamma- And Alpha-Linolenic Acids Have No Effect. In: Honn KV, Marnett LJ, Nigam S, Dennis E, Serhan C, eds. *Eicosanoids and Other Bioactive Lipids in Cancer, Inflammation, and Radiation Injury, 5*. Advances in Experimental Medicine and Biology. Boston, MA: Springer US; 2002:579-584. doi:10.1007/978-1-4615-0193-0_88

8. Ramakers JD, Mensink RP, Verstege MI, te Velde AA, Plat J. An arachidonic acid-enriched diet does not result in more colonic inflammation as compared with fish oil- or oleic acid-enriched diets in mice with experimental colitis. *Br J Nutr*. 2008;100(2):347-354. doi:10.1017/S0007114507901257

9. Monk JM, Turk HF, Fan Y-Y, et al. Antagonizing arachidonic acid-derived eicosanoids reduces inflammatory Th17 and Th1 cell-mediated inflammation and colitis severity. *Mediators Inflamm*. 2014;2014:917149. doi:10.1155/2014/917149

10. Zhuang P, Shou Q, Lu Y, et al. Arachidonic acid sex-dependently affects obesity through linking gut microbiota-driven inflammation to hypothalamus-adipose-liver axis. *Biochim Biophys Acta Mol Basis Dis*. 2017;1863(11):2715-2726. doi:10.1016/j.bbadis.2017.07.003

11. Lazic M, Inzaugarat ME, Povero D, et al. Reduced dietary omega-6 to omega-3 fatty acid ratio and 12/15-lipoxygenase deficiency are protective against chronic high fat diet-induced steatohepatitis. *PLoS ONE*. 2014;9(9):e107658. doi:10.1371/journal.pone.0107658

12. Juman S, Hashimoto M, Katakura M, et al. Effects of long-term oral administration of arachidonic acid and docosahexaenoic acid on the immune functions of young rats. *Nutrients*. 2013;5(6):1949-1961. doi:10.3390/nu5061949

13. Williams ES, Baylin A, Campos H. Adipose Tissue Arachidonic Acid and the Metabolic Syndrome in Costa Rican Adults. *Clin Nutr*. 2007;26(4):474-482. doi:10.1016/j.clnu.2007.03.004

14. Sergeant S, Hugenschmidt CE, Rudock ME, et al. Differences in arachidonic acid levels and fatty acid desaturase (FADS) gene variants in African Americans and European Americans with diabetes or the metabolic syndrome. *Br J Nutr*. 2012;107(4):547-555. doi:10.1017/S0007114511003230

15. de Silva PSA, Olsen A, Christensen J, et al. An association between dietary arachidonic acid, measured in adipose tissue, and ulcerative colitis. *Gastroenterology*. 2010;139(6):1912-1917. doi:10.1053/j.gastro.2010.07.065

16. de Silva PSA, Luben R, Shrestha SS, Khaw KT, Hart AR. Dietary arachidonic and oleic acid intake in ulcerative colitis etiology: a prospective cohort study using 7-day food diaries. *Eur J Gastroenterol Hepatol*. 2014;26(1):11-18. doi:10.1097/MEG.0b013e328365c372

17. Nishida T, Miwa H, Shigematsu A, Yamamoto M, Iida M, Fujishima M. Increased arachidonic acid composition of phospholipids in colonic mucosa from patients with active ulcerative colitis. *Gut*. 1987;28(8):1002-1007. doi:10.1136/gut.28.8.1002

18. Pearl DS, Masoodi M, Eiden M, et al. Altered colonic mucosal availability of n-3 and n-6 polyunsaturated fatty acids in ulcerative colitis and the relationship to disease activity. *J Crohns Colitis*. 2014;8(1):70-79. doi:10.1016/j.crohns.2013.03.013

19. Knapp HR, Melly MA. Bactericidal effects of polyunsaturated fatty acids. *J Infect Dis*. 1986;154(1):84-94. doi:10.1093/infdis/154.1.84

20. Kankaanpää PE, Salminen SJ, Isolauri E, Lee YK. The influence of polyunsaturated fatty acids on probiotic growth and adhesion. *FEMS Microbiology Letters*. 2001;194(2):149-153. doi:10.1111/j.1574-6968.2001.tb09460.x

21. Eijkelkamp BA, Begg SL, Pederick VG, et al. Arachidonic Acid Stress Impacts Pneumococcal Fatty Acid Homeostasis. *Front Microbiol*. 2018;9. doi:10.3389/fmicb.2018.00813

22. Jiang J-H, Hassan KA, Begg SL, et al. Identification of Novel Acinetobacter baumannii Host Fatty Acid Stress Adaptation Strategies. *mBio*. 2019;10(1):e02056-18. doi:10.1128/mBio.02056-18

23. Scallan E, Hoekstra RM, Angulo FJ, et al. Foodborne Illness Acquired in the United States—Major Pathogens. *Emerg Infect Dis*. 2011;17(1):7-15. doi:10.3201/eid1701.P11101

24. Beaglehole R, Irwin A, Prentice T. *The World Health Report 2003: Shaping the Future*. (Barbara C, ed.). Geneva; 2003.

25. Cover TL, Aber RC. Yersinia enterocolitica. *N Engl J Med*. 1989;321(1):16-24. doi:10.1056/NEJM198907063210104

26. Koehler KM, Lasky T, Fein SB, et al. Population-Based Incidence of Infection With Selected Bacterial Enteric Pathogens in Children Younger Than Five Years of Age, 1996???1998: *The Pediatric Infectious Disease Journal*. 2006;25(2):129-134. doi:10.1097/01.inf.0000199289.62733.d5

27. Li D, Ng A, Mann NJ, Sinclair AJ. Contribution of meat fat to dietary arachidonic acid. *Lipids*. 1998;33(4):437-440. doi:10.1007/s11745-998-0225-7

28. Chow SL, Hollander D. Arachidonic acid intestinal absorption: mechanism of transport and influence of luminal factors of absorption in vitro. *Lipids*. 1978;13(11):768-776. doi:10.1007/bf02533474

29. Nilsson A, Melin T. Absorption and metabolism of orally fed arachidonic and linoleic acid in the rat. *Am J Physiol*. 1988;255(5 Pt 1):G612-618. doi:10.1152/ajpgi.1988.255.5.G612

30. Kawajiri H, Hsi LC, Kamitani H, et al. Arachidonic and linoleic acid metabolism in mouse intestinal tissue: evidence for novel lipoxygenase activity. *Arch Biochem Biophys*. 2002;398(1):51-60. doi:10.1006/abbi.2001.2685

31. Altieri C, Bevilacqua A, Cardillo D, Sinigaglia M. Effectiveness of fatty acids and their monoglycerides against gram-negative pathogens. *International Journal of Food Science & Technology*. 2009;44(2):359-366. doi:10.1111/j.1365-2621.2008.01744.x

32. Firouzi R, Shekarforoush SS, Nazer AHK, Borumand Z, Jooyandeh AR. Effects of essential oils of oregano and nutmeg on growth and survival of Yersinia enterocolitica and Listeria monocytogenes in barbecued chicken. *J Food Prot*. 2007;70(11):2626-2630. doi:10.4315/0362-028x-70.11.2626

33. Eder AE, Munir SA, Hobby CR, et al. Exogenous polyunsaturated fatty acids (PUFAs) alter phospholipid composition, membrane permeability, biofilm formation and motility in Acinetobacter baumannii. *Microbiology*. 2017;163(11):1626-1636. doi:10.1099/mic.0.000556

34. Huang CB, George B, Ebersole JL. Antimicrobial activity of n-6, n-7 and n-9 fatty acids and their esters for oral microorganisms. *Arch Oral Biol*. 2010;55(8):555-560. doi:10.1016/j.archoralbio.2010.05.009

35. Straley SC, Perry RD. Environmental modulation of gene expression and pathogenesis in Yersinia. *Trends Microbiol*. 1995;3(8):310-317.

36. Simopoulos AP. Evolutionary aspects of diet and essential fatty acids. *World Rev Nutr Diet*. 2001;88:18-27.

37. Simopoulos AP. An Increase in the Omega-6/Omega-3 Fatty Acid Ratio Increases the Risk for Obesity. *Nutrients*. 2016;8(3):128. doi:10.3390/nu8030128

38. Vrioni G, Tsiamis C, Oikonomidis G, Theodoridou K, Kapsimali V, Tsakris A. MALDI-TOF mass spectrometry technology for detecting biomarkers of antimicrobial resistance: current achievements and future perspectives. *Ann Transl Med*. 2018;6(12):240-240. doi:10.21037/atm.2018.06.28

39. Lambert de Rouvroit C, Sluiters C, Cornelis GR. Role of the transcriptional activator, VirF, and temperature in the expression of the pYV plasmid genes of Yersinia enterocolitica. *Mol Microbiol*. 1992;6(3):395-409.

40. Rohde JR, Luan X, Rohde H, Fox JM, Minnich SA. The Yersinia enterocolitica pYV Virulence Plasmid Contains Multiple Intrinsic DNA Bends Which Melt at 37°C. *J Bacteriol*. 1999;181(14):4198-4204.

41. U.S. Department of Health and Human Services and U.S. Department of Agriculture. *2015-2020 Dietary Guidelines for Americans.* 8th Edition.; 2015.

42. Hjelte LE, Nilsson Å. Arachidonic Acid and Ischemic Heart Disease. *The Journal of Nutrition*. 2005;135(9):2271-2273. doi:10.1093/jn/135.9.2271

43. Sonnweber T, Pizzini A, Nairz M, Weiss G, Tancevski I. Arachidonic Acid Metabolites in Cardiovascular and Metabolic Diseases. *Int J Mol Sci*. 2018;19(11). doi:10.3390/ijms19113285

44. Kaliannan K, Wang B, Li X-Y, Kim K-J, Kang JX. A host-microbiome interaction mediates the opposing effects of omega-6 and omega-3 fatty acids on metabolic endotoxemia. *Sci Rep*. 2015;5(1):11276. doi:10.1038/srep11276

45. Ghosh S, DeCoffe D, Brown K, et al. Fish Oil Attenuates Omega-6 Polyunsaturated Fatty Acid-Induced Dysbiosis and Infectious Colitis but Impairs LPS Dephosphorylation Activity Causing Sepsis. Fuss IJ, ed. *PLoS ONE*. 2013;8(2):e55468. doi:10.1371/journal.pone.0055468

46. Rutting S, Zakarya R, Bozier J, et al. Dietary Fatty Acids Amplify Inflammatory Responses to Infection through p38 MAPK Signaling. *Am J Respir Cell Mol Biol*. 2019;60(5):554-568. doi:10.1165/rcmb.2018-0215OC

47. Jordao L, Lengeling A, Bordat Y, et al. Effects of omega-3 and -6 fatty acids on Mycobacterium tuberculosis in macrophages and in mice. *Microbes and Infection*. 2008;10(12-13):1379-1386. doi:10.1016/j.micinf.2008.08.004

48. Pierre M, Husson M-O, Le Berre R, et al. Omega-3 polyunsaturated fatty acids improve host response in chronic Pseudomonas aeruginosa lung infection in mice. *Am J Physiol Lung Cell Mol Physiol*. 2007;292(6):L1422-1431. doi:10.1152/ajplung.00337.2006

49. Kuipers RS, Luxwolda MF, Janneke Dijck-Brouwer DA, et al. Estimated macronutrient and fatty acid intakes from an East African Paleolithic diet. *Br J Nutr*. 2010;104(11):1666-1687. doi:10.1017/S0007114510002679

50. Eaton SB. The ancestral human diet: what was it and should it be a paradigm for contemporary nutrition? *Proc Nutr Soc*. 2006;65(1):1-6. doi:10.1079/pns2005471

51. Tulk HMF, Robinson LE. Modifying the n-6/n-3 polyunsaturated fatty acid ratio of a high–saturated fat challenge does not acutely attenuate postprandial changes in inflammatory markers in men with metabolic syndrome. *Metabolism*. 2009;58(12):1709-1716. doi:10.1016/j.metabol.2009.05.031

52. Nelson T. Acute changes in dietary omega-3 fatty acid intake lowers soluble interleukin-6 receptor in healthy adult normal weight and overweight males. *Cytokine*. 2004;26(5):195-201. doi:10.1016/j.cyto.2004.02.010

53. Larter CZ, Yeh MM, Cheng J, et al. Activation of peroxisome proliferator-activated receptor alpha by dietary fish oil attenuates steatosis, but does not prevent experimental steatohepatitis because of hepatic lipoperoxide accumulation. *J Gastroenterol Hepatol*. 2008;23(2):267-275. doi:10.1111/j.1440-1746.2007.05157.x

54. Adam O, Beringer C, Kless T, et al. Anti-inflammatory effects of a low arachidonic acid diet and fish oil in patients with rheumatoid arthritis. *Rheumatol Int*. 2003;23(1):27-36. doi:10.1007/s00296-002-0234-7

55. Shimizu T, Fujii T, Suzuki R, et al. Effects of highly purified eicosapentaenoic acid on erythrocyte fatty acid composition and leukocyte and colonic mucosa leukotriene B4 production in children with ulcerative colitis. *J Pediatr Gastroenterol Nutr*. 2003;37(5):581-585. doi:10.1097/00005176-200311000-00015

56. Sheppe AEF, Kummari E, Walker A, et al. PGE2 Augments Inflammasome Activation and M1 Polarization in Macrophages Infected With Salmonella Typhimurium and Yersinia enterocolitica. *Front Microbiol*. 2018;9:2447. doi:10.3389/fmicb.2018.02447

57. Golubeva YA, Ellermeier JR, Cott Chubiz JE, Slauch JM. Intestinal Long-Chain Fatty Acids Act as a Direct Signal To Modulate Expression of the *Salmonella* Pathogenicity Island 1 Type III Secretion System. *mBio*. 2016;7(1):e02170-15, /mbio/7/1/e02170-15.atom. doi:10.1128/mBio.02170-15

58. Sansonetti P. Host-pathogen interactions: the seduction of molecular cross talk. *Gut*. 2002;50 Suppl 3:III2-8. doi:10.1136/gut.50.suppl_3.iii2

59. Bent ZW, Poorey K, Brazel DM, et al. Transcriptomic Analysis of Yersinia enterocolitica Biovar 1B Infecting Murine Macrophages Reveals New Mechanisms of Extracellular and Intracellular Survival. McCormick BA, ed. *Infect Immun*. 2015;83(7):2672-2685. doi:10.1128/IAI.02922-14

Chapter 5. Innate Recognition of the Microbiota by TLR1 Promotes Epithelial Homeostasis and Prevents Chronic Inflammation

Adapted from:

Karishma Kamdar, Andrew M. F. Johnson, **Denise Chac**, Kalisa Myers, Vrishika Kulur, Kyle Truevillian and R. William DePaolo. Innate Recognition of the Microbiota by TLR1 Promotes Epithelial Homeostasis and Prevents Chronic Inflammation. J Immunol 2018; 201:230-242; Prepublished online 23 May 2018; doi: 10.4049/jimmunol.1701216

5.1 Abstract

There is cross-talk between the intestinal epithelium and the microbiota that functions to maintain a tightly regulated microenvironment and prevent chronic inflammation. This communication is partly mediated through the recognition of bacterial proteins by host-encoded innate receptors, such as TLRs. However, studies examining the role of TLR signaling on colonic homeostasis have given variable and conflicting results. Despite its critical role in mediating immunity during enteric infection of the small intestine, TLR1-mediated recognition of microbiota-derived ligands and their influence on colonic homeostasis has not been well studied. In this study, we demonstrate that defective TLR1 recognition of the microbiome by epithelial cells results in disruption of crypt homeostasis specifically within the secretory cell compartment, including a defect in the mucus layer, ectopic Paneth cells in the colon, and an increase in the number of rapidly dividing cells at the base of the crypt. As a consequence of the perturbed epithelial barrier, we found an increase in mucosal-associated and translocated commensal bacteria and chronic low-grade inflammation characterized by an increase in lineage-negative Sca1+Thy1hi innate lymphoid-like cells that exacerbate inflammation and worsen outcomes in a model of colonic injury and repair. Our findings demonstrate that sensing of the microbiota by TLR1 may provide key signals that regulate the colonic epithelium, thereby limiting inflammation through the prevention of bacterial attachment to the mucosa and exposure to the underlying immune system.

5.2 Introduction

The intestinal epithelium is the major interface between the 100 trillion commensal bacteria that comprise our gut microbiome and the immune cells found within the lamina propria (LP). The interactions between the gut microbiota and the epithelium shape important biological processes such as metabolism, development of the mucosal-associated tissues, and immunity against invading pathogens[1–4]. Despite the extraordinary microbial burden within the intestine, translocation across the epithelium is a rare event because of the highly specialized cells that form this barrier. Tightly regulated communication via the direct sensing of the microbiome by innate immune receptors encoded within the epithelium is important for the homeostasis of the intestine. This process is mediated by the recognition of commensal ligands by host receptors, such as the TLRs[5–7]and the Nod-like receptors (NLRs)[8–10], and the presence of gut bacteria has been shown to impact the rate of proliferation within the stem cell compartment of the intestinal crypt[5,8,11–16]. Genetic and environmental factors, such as infection, can also influence the dialogue between the microbiota and epithelium, leading to alterations in proliferation, generation of inflammation, and bacterial translocation[15,17,18] traits shared with the two types of inflammatory bowel disease (IBD), Crohn's disease and ulcerative colitis[16,19,20].

TLRs and NLRs are expressed throughout the intestine and have been identified on crypt and intestinal stem cells[17,19,21–24]. TLR signaling mediates a number of cellular responses[1,22] and can be classified into two groups based upon the intracellular signaling adaptor. TLR1, 2, 5, 6, and 10 signal through the myeloid differentiation primary response gene-88 (MyD88), whereas TLR3, 4, and 9 signal through the TIR-domain–containing adapter-inducing IFN-β (TRIF)-dependent pathways[1,19,22–24]. Studies disrupting innate signaling in mice, either through deletion of a specific TLR or through MyD88, have shown that sensing of the microbiota via these receptors is critical in mediating their own epithelial expression, regulating epithelial proliferation, and in the response to intestinal injury[23,25,26]. TLR2, which is expressed throughout the small intestine and colon [14,25,27], recognizes lipoproteins from gram-positive and gram-negative bacteria as well as zymosans from yeast. TLR2 achieves this heterogeneity in ligand recognition by dimerizing with other TLRs, such as TLR1, 6, and 10. Major functions attributed to TLR2 in the maintenance of intestinal epithelial integrity is through the regulation of tight junctional proteins, proliferation/apoptosis signals[23,26], antimicrobial peptide expression [25,27], and goblet cell activation[28–30]. Although these studies have shed light

on the role of TLR2, they have not delineated whether TLR2 signaling alone is sufficient to drive these processes or if other binding partners may be contributing to its effect. Recently, our group has shown that TLR1 is important in coordinating cellular immunity against infection of the small intestine by *Yersinia enterocolitica*[15,17,18]. Despite elimination of *Y. enterocolitica*, TLR1 deficiency promotes dysbiosis of the microbiota and the development of chronic anticommensal immune sequela[18]. Therefore, disrupted innate immunity against an enteric pathogen may have long-term consequences and may promote the development of chronic inflammatory disease.

In this study, we show that disruption of TLR1 signaling compromises the colonic epithelium, leading to innate immune activation and chronic inflammation. Upon colonic injury, the chronic inflammatory state prevents healing and promotes more severe disease, suggesting that endogenous sensing of the microbiota through TLR1 contributes to colon homeostasis and prevents epithelial and immune dysfunction.

5.3 Results

TLR1-deficiency is associated with mucosal-associated bacteria, gut permeability, and systemic bacteria

Our previous work had shown a critical role for TLR1 signaling in the epithelium of the small intestine during pathogenic *Y. enterocolitica* infection[18,22,31]. However, analysis of mRNA transcripts for *Tlr1* in naive WT mice revealed that the ileum had significantly less expression of *Tlr1* than the proximal colon or distal colon (data not shown). We sought to determine whether the expression of TLR1 may influence colonic homeostasis by assessing the location of the microbiota within the colonic compartment of TLR1-deficient (1KO) and littermate control mice (a mixture of heterozygotes and homozygotes for TLR1, WT) using fluorescent in situ hybridization to visualize bacteria with a probe directed against eubacterial 16S rRNA. Although we observed a clear separation between cells of the epithelium and the 16S rRNA probe in WT colons, this spatial separation was not observed in the 1KO mice (Figure 5.1A). Instead, we observed a diverse spectrum of 16S rRNA expression, including areas where the probe was in intimate contact with epithelial cells (Figure 5.1A). The increase in epithelial adjacent bacteria in the 1KO mice corresponded with 15-fold more 16S DNA associated with the mucosa than in the WT mice despite equivalent luminal levels (Figure 5.1B).

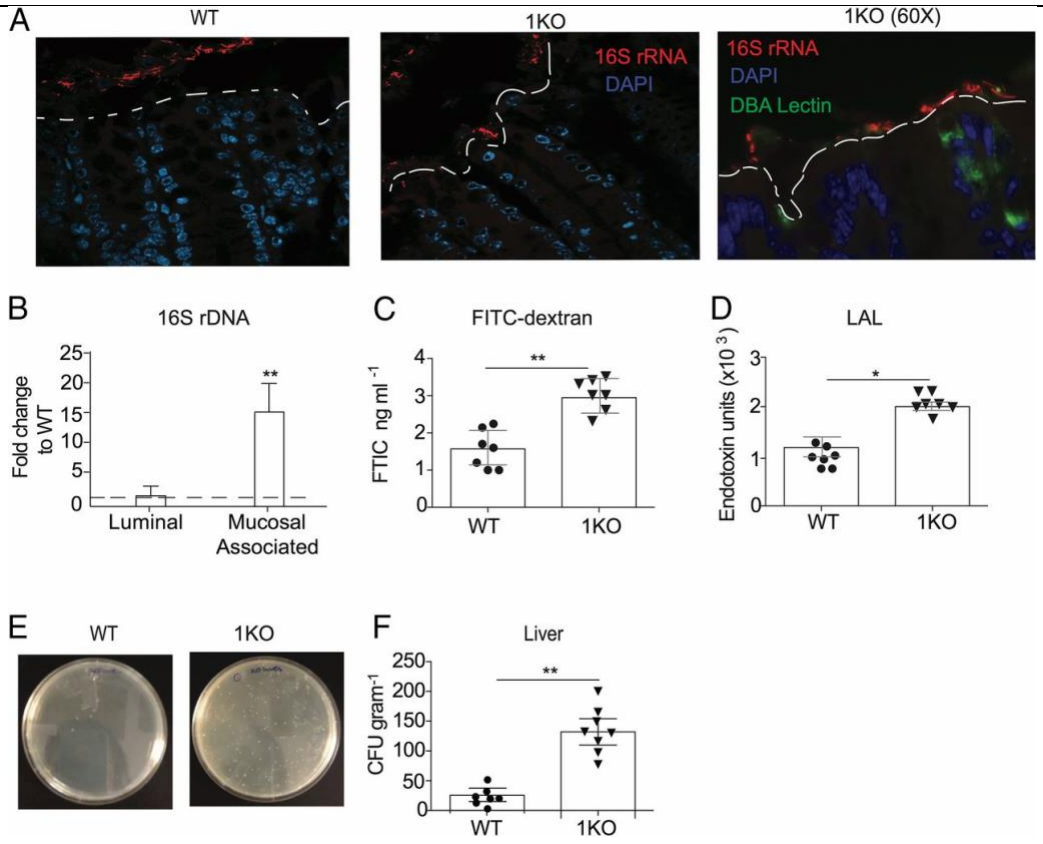

Figure 5.1: Expression of TLR1 prevents mucosal-associated bacteria and their translocation to the periphery

Colons from naive 1KO mice were compared with naive WT colons. (A) Representative original magnification 340 confocal images from Carnoy's fixed sections of the distal colon of WT and 1KO mice hybridized with a probe against eubacterial 16S rRNA (red) and counter-stained with DAPI (blue). Image on the far right is a fluorescent microscope image of 1KO using the 16S fluorescent in situ hybridization probe (red), DAPI (blue), and Dolichos biflorus agglutinin (DBA) lectin (green). The white dotted line indicates the apical edge of the epithelium. (B) Fold change of 16S DNA expression from 1KO luminal colonic contents or colonic mucosal scrapings normalized to WT. (C) Relative fluorescent units in the serum of WT and 1KO mice 1 h postintrarectal administration of FITC-Dextran. Each dot represents an individual mouse. (D) Endotoxin units from serum of WT and 1KO mice as determined using the Limulus amebocyte lysate (LAL) test. Each dot represents an individual mouse. (E) Representative bacterial plates from livers of 1KO and WT mice. (F) CFU per gram of liver cultured anaerobically on TSA plates. Each dot represents an individual mouse. Data are represented as the mean ± SEM from two to three independent experiments. (A), n = 3 mice per group; (B–F), n = 7–10 mice per group. *p <0.05, **p <0.01, Student unpaired t test.

To assess whether there was also altered colonic permeability, FITC-labeled dextran was measured in the peripheral blood of WT and 1KO mice 1 h after intrarectal administration. Indeed, there was a significant increase in the amount of FITC in the blood of the 1KO mice, indicating leakage from the colon into the periphery (Figure 5.1C) as well as elevated endotoxin levels, suggesting translocated commensal bacteria or their products (Figure 5.1D). To determine the extent of bacterial translocation in 1KO mice, the spleen,

liver, and blood were plated anaerobically on TSA plates. The liver (Figure 5.1E-F), spleen, and blood from 1KO mice all had significantly elevated amounts of bacteria compared with littermates (data not shown). Furthermore, the transfer of TLR1-deficient bone marrow to reconstitute an irradiated WT mouse was not sufficient to cause an increase in bacterial colonies in liver (data not shown), indicating that the elevated levels of systemic bacteria in the naive 1KO mice are not due to an ineffectual immune response against mouse pathogens that may be resident in SPF facilities. Gut permeability may result from defects in the regulation of tight junctional proteins, and previous studies have implicated TLR2 in this regulation[10,21]. However, using qPCR, we were unable to find any difference in the expression of *Cldn3* (claudin-3), *Cldn10* (claudin-10), *Ocln*(occludin), and *Tjp1* (ZO-1) transcripts (data not shown). We also quantified claudin-2 and claudin-3 by Western blot and assessed occludin-1 expression by immunofluorescence and observed no differences between 1KO and WT mice (Supplemental Figure 5.1). Altogether, these data demonstrate an inability to maintain normal geographical and spatial localization of commensal bacteria in the absence of TLR1 independent of barrier defects.

Elevated innate immune responses in TLR1-deficient mice

Mucosal-associated and translocated commensals are often associated with inflammation because of increased exposure to, and subsequent recognition by, the immune system. As the 1KO mice have inherent bacterial translocation, we evaluated cytokine levels in homogenates of whole colon by ELISA (Figure 5.2A). Of the 10 cytokines we evaluated, only IL-1β and IL-23 and the cytokines they play a role in regulating, IL-22 and IL-17[27,32,33], were significantly increased in the colons of the 1KO (Figure 5.2A).

There are three IL-23–responsive cells that produce IL-22 and IL-17 within the colonic mucosa. These include γδ T cells[33–35], IL-17–producing CD4 T cells (T_H17/T_H22)[19], and type 3 innate lymphoid cells (ILC3)[36]. We sought to identify the frequency of these cell populations in naive mice and found no difference in the frequency or numbers of γδ T cells (Figure 5.2B) and T_H17 cells (Figure 5.2C) between 1KO and WT controls (Figure 5.2B). However, the frequency (Figure 5.2D) and absolute cell number (Figure 5.2E) of lin-Sca1+Thy1^{hi}cells in the colons of the 1KO mice were significantly elevated compared with naive WT controls (Figure 5.2D-E). Lin-negative, Sca1-positive, and Thy1-positive cells have been identified as IL-22– and IL-17–producing ILC3[16]. Molecular analysis of the mRNA transcripts from sorted

lin-Sca1+Thy1hi cells revealed prototypic molecular signatures of ILC3, such as *Rorc* (Figure 5.2F), *Il22* (Figure 5.2G), *Il17*, and *Il23r* (data not shown), to be increased in 1KO compared with WT cells, whereas *Ifng* expression was not changed (Figure 5.2G).

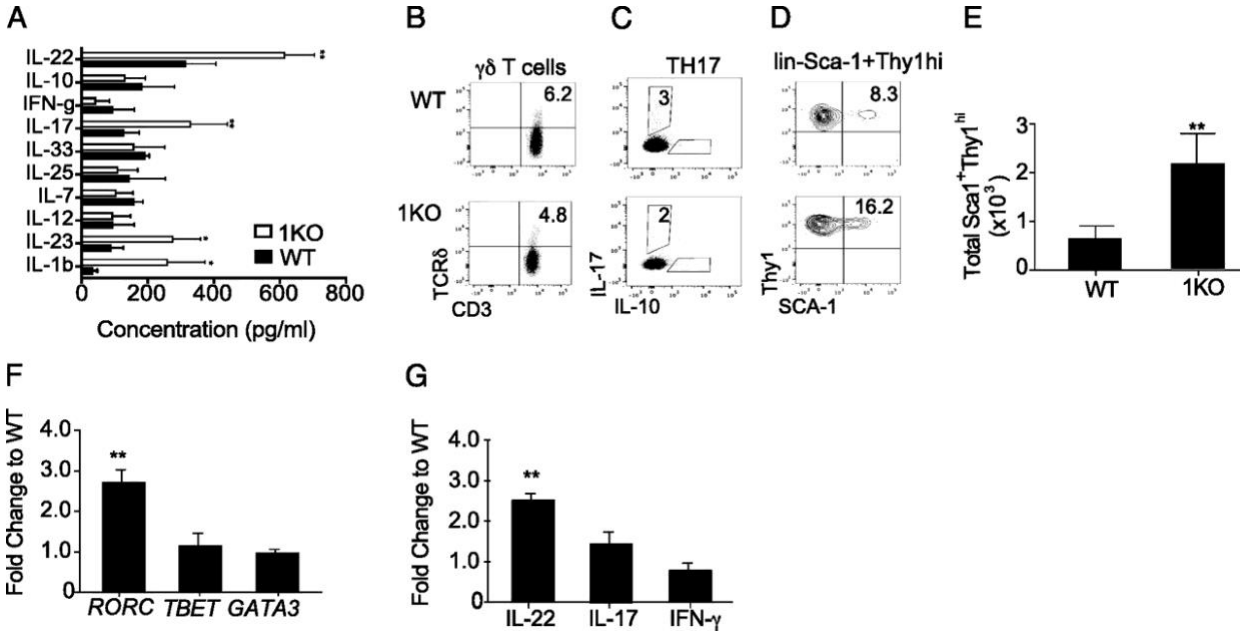

Figure 5.2:TLR1 deficiency is associated with disturbed immune homeostasis in the colonic LP. (A) Cytokine levels in whole colonic lysate were measured and normalized to the weight of the tissue of naive 1KO and WT. Representative FACS plots of naive WT and 1KO LP cells. Dead cells were excluded, and all live cells were gated on forward scatter and side scatter, (B) CD3+ and TCR d+ T cells, (C) CD3+ CD4+ and intracellular IL-17 and IL-10, (D) lin2 (CD11b2, CD11c2, NKp442, F4802, B2202, CD192, CD32), and Sca1+ and Thy1hi cells. Relative expression of mRNA transcripts for indicated (E) absolute cell number of lin2Sca1+ Thy1hi cells in the colonic LP from mice. The lin2Sca1+ Thy1hi cells were sorted from the colonic LP, and quantitative RT-PCR was performed to obtain relative expression levels of (F) transcription factors and (G) cytokines using GAPDH as a reference housekeeping gene, and showing fold changed to WT using 22DDct. Data are pooled from two independent experiments; (A and E–G) are expressed as mean±SEM. (A–E) n = 5–6 mice per group. (F–G) Cells were isolated by pooling isolated and sorted lin2Sca1+ Thy1hi from two mice from each genotype, and the experiment was repeated twice. (A) One-way ANOVA; (E–G) Student unpaired t test. *p< 0.05, **p <0.01.

TLR1-sensing of the microbiota by nonhematopoietic cells restrains innate immune responses

Despite the proximity of commensal bacteria to colonic tissue in healthy individuals, there are conflicting reports regarding the role of the microbiota in the development of members of the innate lymphoid cell family. To determine whether the microbiota were necessary for innate immune activation in the 1KO mice, we employed a rigorous ABX treatment regimen to deplete the microbiota. Pregnant dams from a heterozygous cross were administered a mixture of five ABX (amoxicillin, vancomycin, neomycin, metronidazole, and gentamicin) the last week of their pregnancy and were maintained on the ABX water until the pups were weaned. The newly weaned mice continued to receive the ABX water for an additional 7 d, at which time their colons were analyzed for levels of IL-23 and $Sca1^{+}Thy1^{hi}$ cells. This ABX approach generally yields a 5–8-fold reduction in the endogenous commensals (R.W. DePaolo and R. Rankin, unpublished observations). Although the ABX treatment had little effect on the basal level of $Sca1^{+}Thy1^{hi}$ cells in WT mice, it significantly reduced the number of these cells (Figure 5.3A) along with colonic level of IL-1β and IL-23 (Figure 5.3B) in the 1KO mice. As the microbiota was necessary for the elevated innate immune response, we asked whether the specific composition of the microbiota of 1KO mice would be sufficient to transfer this phenotype to ABX-treated WT mice via fecal microbiota transplantation (FMT). WT mice receiving an FMT with stool from a 1KO mouse showed no change in either the $lin^{-}Sca1^{+}Thy1^{hi}$ population (Figure 5.3C) or levels of IL-1β and IL-23 (Figure 5.3D). In contrast, WT stool given to an ABX-treated 1KO recipient restored both the $lin^{-}Sca1^{+}Thy1^{hi}$ population (Figure 5.3C) and IL-1β and IL-23 (Figure 5.3D).

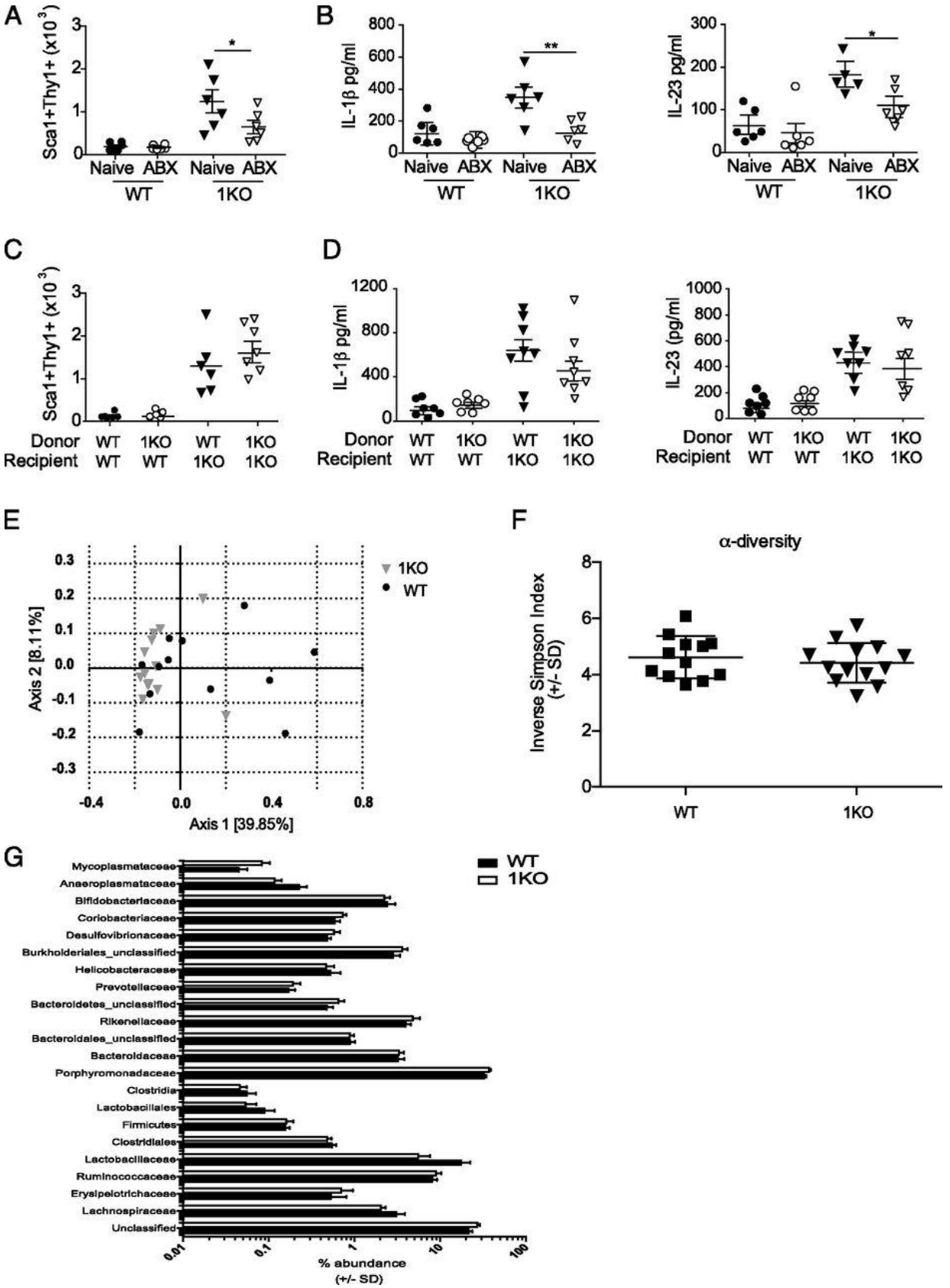

Figure 5.3: The microbiota of the TLR1KO mice are required for homeostatic immune regulation.

Figure 5.3: The microbiota of the TLR1KO mice are required for homeostatic immune regulation. (A and B) 1KO and WT mice born from ABX-treated pregnant dams were maintained on ABX-treated water 1–2 wk after weaning and were analyzed for (A) absolute number of lin2Sca1+ Thy1hi cells in ABXtreated WT and 1KO mice compared with naive (untreated) mice determined by flow cytometry and (B) the concentration of IL-1b and IL-23 detected in colonic homogenates as measured by ELISA. (C and D) A different set of ABX-treated WT and 1KO mice were given an FMT from the indicated donors and allowed to reconstitute for 2 wk before quantification of (C) absolute cell number of lin2Sca1+ Thy1hi cells and (D) concentration of IL-1b and IL-23 detected in the colonic LP of FMT-treated WT and 1KO mice. Data are expressed as individual mice pooled from two to three independent experiments with (A and B) n = 5–6 mice per group and (C and D) n = 5–9 mice per group. (E) PCoA analysis based on genus-level identification of 16s rDNA sequences from 1KO (n = 13) or WT (n = 12) mouse cecal contents. (F) Inverse Simpson measurement of a diversity in 1KO and WT mice. (G) Family relative abundance in 1KO and WT cecal contents. Student t test with false discovery rate correction showed no significant difference in relative abundance of different families between 1KO and WT mice. *p< 0.05, **p< 0.01, one-way ANOVA.

These data suggest that although bacteria are necessary for the colonic inflammation observed in the 1KO mice, the lack of signaling through TLR1 does not alter the microbiota to cause inflammation when transferred to a WT setting. This was further supported by comparing the 16s rRNA sequencing analysis of cecal contents between 1KO and WT mice. Principal coordinate analysis (PCoA) (Figure 5.3E) and Inverse Simpson index (Figure 5.3F) indicated considerable overlap in community structure and no difference in community α diversity between naive WT and 1KO mice, respectively. Differences in the relative abundances of bacterial families in the cecum of 1KO and WT mice were evaluated by Student *t* tests corrected for multiple testing using the Benjamini–Hochberg false discovery rate (set at 5%). Consistent with the α diversity and PCoA, there were no significant differences in bacterial families between 1KO and WT mice (Figure 5.3G). To confirm the results obtained using cecal contents and to evaluate specific biogeographical changes in the bacterial community of the colon, we performed compositional analysis on mucosal-associated tissue from the proximal and distal colon in a subset of 1KO and of WT mice. PCoA of the 16S rDNA data again revealed no significant differences in these mucosal-associated communities between 1KO and WT mice (Supplemental Figure 5.2). Thus, it is unlikely that the aberrant immune response observed in the 1KO mice is due to a compositional shift in the microbial communities within the colon.

The finding that 1KO mice had elevated innate cytokines and increased lin$^-$Sca1$^+$Thy1^{hi} cells after receiving WT stool and the lack of a compositional change in the microbiota of 1KO mice suggests that the

dysregulation of the innate immune response may be due to a more general defect in the mucosal response to commensal bacteria. Previously, we have shown that TLR1 can signal in both the intestinal epithelium and in mucosal dendritic cells to induce protective immunity against enteric infections[22,31]. To discern which cellular compartment may be mediating the elevated innate immune activation, we created bone marrow chimeras. Two months after reconstitution, IL-1β and IL-23 concentration in the colonic LP and the bacterial burden in the liver were quantified. The transfer of 1KO bone marrow to WT mice had no effect on colonic LP levels of IL-1β or IL-23 (Figure 5.4A), and no increase in bacterial burden was observed (Figure 5.4B). In contrast, IL-1β and IL-23 (Figure 5.4A) were elevated in the LP, and there was an increase in bacterial counts (Figure 5.4B) when 1KO recipients were reconstituted with WT bone marrow. These data suggest that nonhematopoietic cellular expression of TLR1 prevents commensal-mediated inflammation and bacterial translocation. Together, the FMT and bone marrow chimera studies establish that defective TLR1–sensing of the microbiome by nonhematopoietic cells, and not a compositional dysbiosis, is responsible for the innate inflammatory phenotype observed in the 1KO mice.

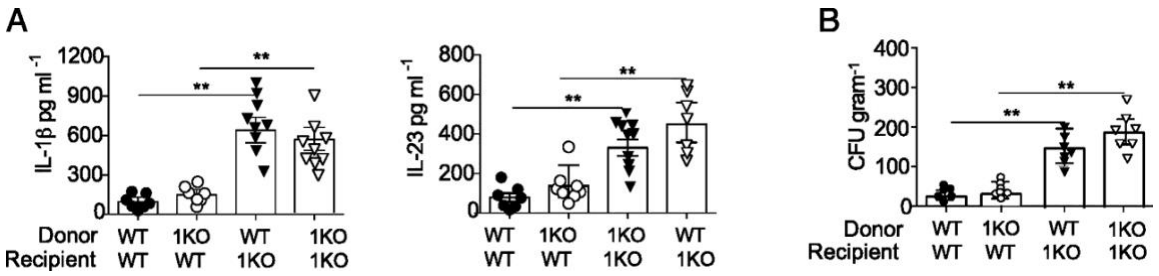

Figure 5.4: Aberrant immune activation is due to loss of TLR1 signaling in the epithelium
Bone marrow chimeras were generated using WT and 1KO recipients and WT and 1KO mice as donors. Six weeks after reconstitution, (A) IL-1b and IL-23 levels from the colonic LP were measured and (B) the number of bacteria in the liver was evaluated by qPCR for 16S. (A and B) Data are represented as the mean±SEM from two independent experiments with n = 7–9 mice per group. **p , 0.01, one-way ANOVA.

TLR1 signaling contributes to homeostasis of the colonic epithelium

The intestinal epithelium is composed of a single layer of cells that form a physical barrier between us and our microbiota. The epithelium is composed of specialized IEC. The four types of IEC are derived from a single crypt progenitor but have distinct developmental pathways. Using immunohistochemistry and gene expression, we evaluated key markers and products of differentiated IEC. Goblet cells are one of the four types of IEC and function to produce a physical mucus barrier. WT colonic sections stained for Muc2, the

main peptide component of intestinal mucins, revealed a visible mucus layer and characteristic goblet cell staining (Figure 5.5A). In contrast, 1KO mice had large areas completely devoid of MUC2, and there was a lack of intensity in the positively stained goblet cells (Figure 5.5A). Further analysis using AB and mucicarmine staining revealed a reduction in acidic mucins in the colons of 1KO mice, whereas PAS staining of neutral mucins appeared more similar between 1KO and WT (Figure 5.5A). The reduction in acidic mucins was not due to an exocytosis of the whole endocytic granule, as we were unable to find PAS-, PAS/AB, or AB-positive cells in the lumen, a phenotype recently observed in NLRP6$^{-/-}$ mice[37]. However, using confocal microscopy, we did observe a strong reduction in the expression of GOB5, which is found on the outer surface of mucus-containing granules (Figure 5.5A). The thickness of the mucus layer was measured at multiple points around distal colonic sections stained with AB to quantify any differences between 1KO and WT mice (Figure 5.5B). Quantification revealed a significant reduction in the average thickness of the mucus layer in 1KO compared with WT mice (Figure 5.5C). Changes in the mucus layer may be due to either a defect in the production or the secretion of mucus by cells within the crypt. Quantification of the number of AB-positive vesicles per crypt indicated an accumulation of mucus within the epithelial cells of 1KO mice (Figure 5.5D). Recently, it has been shown that mucus secretion by sentinel goblet cells in the colon can be induced by TLR1/2 agonism via a mechanism dependent on ROS[29]. Consistent with this pathway, we found significantly reduced levels of ROS in the colonic mucosa of the 1KO mice relative to WT counterparts (Figure 5.5E).

Figure 5.5: Reduced mucus secretion and an increase in antibacterial peptides occur in the colonic crypt in the absence of TLR1 signaling. Methacarn-fixed sections from the colons of WT and 1KO mice were stained by immunohistochemistry for the indicated markers. (A) Original magnification 340 fluorescent microscopy images of colon tissue stained with MUC2 (peptide sequence of mucin), AB (acidic mucins), mucicarmine (acidic mucins), and PAS/AB (neutral/acidic mucins). Scale bar, 50 mm. Confocal images of GOB5 (mCLCA3) staining of the distal colon. (B) AB-stained distal colonic sections from WT and 1KO mice were used for quantification of (C) mucus layer thickness and (D) AB-positive vesicles per crypt. (E) Relative ROS activity in mucosa and colonic contents. (F) Original magnification 310 and 340 fluorescent microscope images of distal colon stained with Abs against Lyz and DEFA-1 and 103image of isotype control. Scale bar, 50 mm. (A, B, and F) Representative images taken from three to five mice per group; (C and D) individual measurements of mucus thickness along the distal colon taken from three mice per group; (E) each point is an individual mouse from two different experiments. (C and D) Mann–Whitney U test; (F) Student t test corrected for multiple comparisons (Holm–Sidak). *p = 0.02, ****p <0.0001.

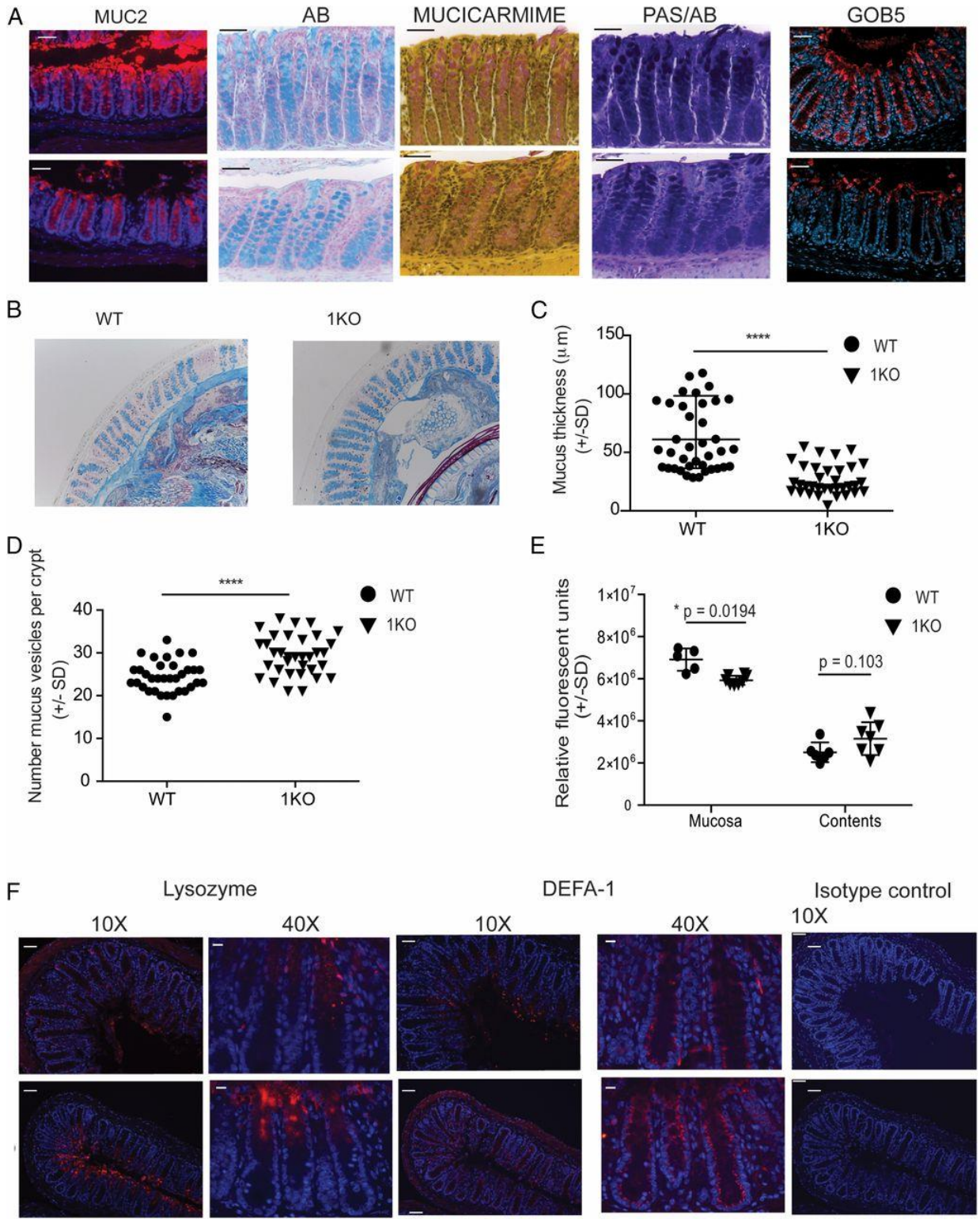

Figure 5.5: Reduced mucus secretion and an increase in antibacterial peptides occur in the colonic crypt in the absence of TLR1 signaling

Under chronic stress or inflammatory conditions, the colon, which is normally devoid of Paneth cells, will express Paneth cell products, and these cells are referred to as ectopic Paneth cells[38–41]. To determine whether the chronic inflammation observed in the 1KO mice was causing a reprogramming of the colonic crypt, we compared the expression of two products normally secreted by small intestinal Paneth cells, Lyz and DEFA-1. As expected, Lyz expression in the colon of healthy, naive WT mice was very low (Figure 5.5F), whereas exposure-matched images of colons from 1KO mice demonstrated high expression of Lyz at the top of the crypts (Figure 5.5F). WT mice expressed a gradient of DEFA-1 that increased basolaterally (Figure 5.5F) and was absent in the 1KO mice (Figure 5.5F). Instead, the whole crypt stained uniformly positive for DEFA-1 (Figure 5.5F). Taken all together, the absence of TLR1 signaling is associated with alterations in the production and function of factors associated with secretory cells of the epithelium.

TLR1 signaling restrains microbiota-induced epithelial cell proliferation

IEC differentiation is a tightly regulated process involving many important factors that control cellular proliferation as well as differentiation. We began by examining the proliferation of the epithelial cells in naive WT and 1KO mice. Ki67 is a marker used to identify cells that are currently, or have recently, undergone proliferation by labeling cells in S, G_1, and G_2 phases of the cell cycle. Histological analysis of colonic tissue sections of naive mice revealed an increase in Ki67-positive cells within the colonic epithelium of 1KO mice when compared with WT mice (Figure 5.6A). In the colon, rapidly cycling stem cells at the base of the colonic crypt control proliferation and renewal of the epithelium. Aberrant regulation of these crypts may lead to altered IEC differentiation and disrupt epithelial barrier integrity. We used in vivo injections of BrdU to label newly synthesized DNA in actively replicating cells during synthesis phase for 2.5 h. Analysis of BrdU-positive cells by immunohistochemistry confirmed the presence of three to four BrdU-positive cells per WT crypt (Figure 5.6B-C). In contrast, mice deficient for TLR1 had twice the number of BrdU-positive cells per crypt (Figure 5.6B-C). Cyclin D1 is a factor downstream in the Wnt signaling cascade involved in cell cycle regulation[5]. As expected based upon the Ki67 and BrdU data, transcripts for *Ccnd1* (cyclin D1) were elevated in the colonic tissue of 1KO mice (Figure 5.6D).

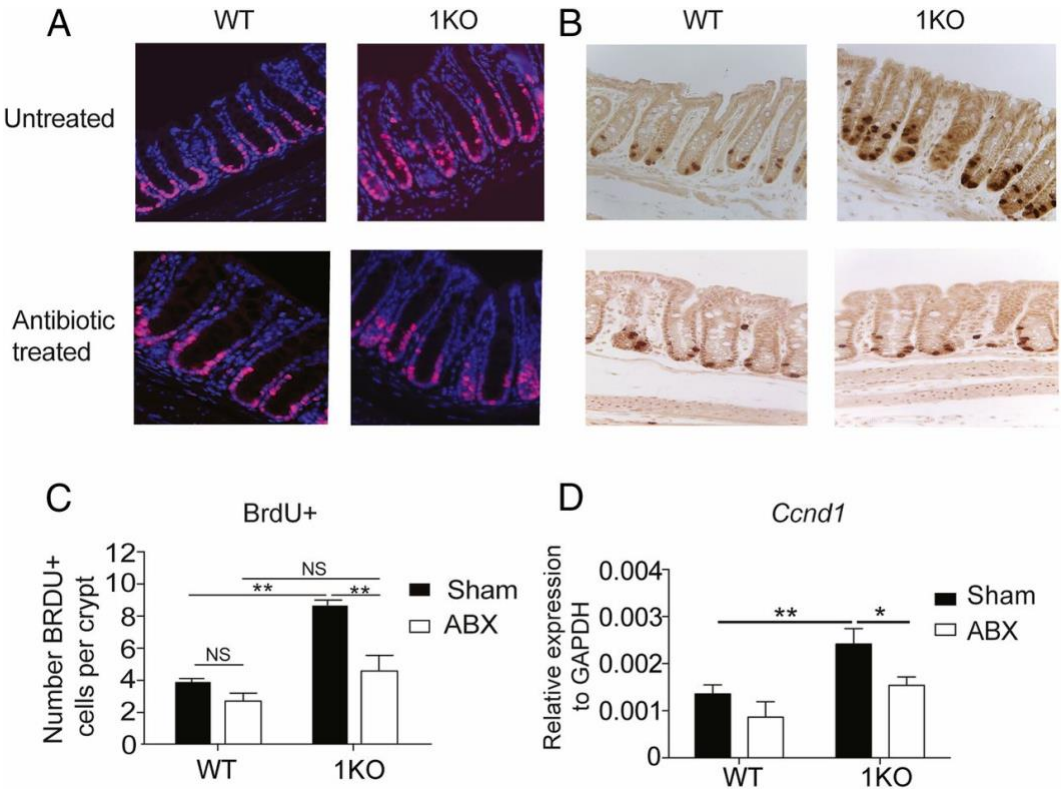

Figure 5.6: Endogenous TLR1 signaling regulates colonic crypt proliferation.

(A–C) Histological sections of the colon from 1KO and WT mice under normal SPF conditions or 1KO and WT mice born from a dam receiving ABX-treated water and then maintained on ABX for another 2 wk postweaning. (A) Original magnification 340 of colon stained with Ki67. (B) Original magnification 340 images of colons from mice injected with BrdU 2.5 h prior to euthanasia. (C) Quantification of total BrdU+ cells per crypt. (D) Relative transcript expression of Ccnd1 in colonic crypts isolated from control and ABX-treated WT and 1KO mice. (A and B) Representative original magnification 340 images taken from five mice. (C) Data are expressed as the mean ± SEM of counts performed independently by two individuals, each counted 30 crypts from five mice. (D) Data are expressed as mean ± SEM from three independent experiments. (D) n = 5–6 mice per group. (C) Student unpaired t test; (D) two-way ANOVA. *p <0.05, **p <0.01.

ABX depletion was used to assess whether the proliferation in the colonic crypt of the 1KO mice was dependent upon the microbiota. Reducing the bacterial load caused a significant reduction in overall Ki67 (Figure 6.6A), BrdU staining (Figure 5.6B-C), and *Ccnd1* expression (Figure 5.6D) in the colons of the 1KO mice. These data suggest that TLR1 expression may antagonize or inhibit other innate signals that promote proliferation, or TLR1 regulates the stem cell niche. To test for the latter, we analyzed expression of canonical stem cell genes (*Lgr5*, *Bmi1*) and Notch signaling genes that regulate cell differentiation along absorptive and secretory pathways (*Notch1*, *Hes1*, *Atoh1*) and found no differences between 1KO and WT mice (Supplemental Figure 5.3).

TLR1 deficiency exacerbates tissue injury and prevents epithelial healing

Basal changes in mucosal and epithelial homeostasis may set the stage for sustained inflammation and chronic intestinal disease following intestinal injury. We sought to determine whether the absence of TLR1 during injury caused by 2.5% DSS may induce a more chronic, long-term inflammatory response. 1KO and WT mice were given 2.5% DSS in their drinking water for 7 d followed by a 7-d recovery period in which normal drinking water was restored. The WT littermate controls followed the typical disease course known for DSS with a transient, mild weight loss (Figure 5.7A), very high survival (Figure 5.7B), and a shortening of the colon observed on day 7 that returned to normal length by day 14 (Figure 5.7C). In contrast, 1KO mice began losing weight earlier than WT controls, lost more weight (Figure 5.7A), and only 30% of mice survived treatment (Figure 5.7B). The 1KO mice also had shorter colons on both day 7 and day 14 (Figure 5.7C) and had higher levels of blood in their stool, which persisted throughout the 14 d (Figure 5.7D).

Histological scoring was performed blinded by gastroenterologist on H&E-stained colonic tissue after injury (day 7) and after repair (day 14). Despite a greater weight loss and less overall survival, the histological score was strikingly similar between the 1KO and WT mice on day 7 (Figure 5.7E, data not shown). On day 14, after the mice had been returned to normal drinking water, the histological score of WT mice was improved compared with day 7, indicating effective mucosal repair and resolution (Figure 5.7F). In contrast, the colons of 1KO mice showed little resolution on day 14 and, in fact, scored significantly worse than on day 7 (Figure 5.7E), with large areas of denuded epithelium, inflammatory cell infiltrate, and loss of goblet cells (Figure 5.7F).

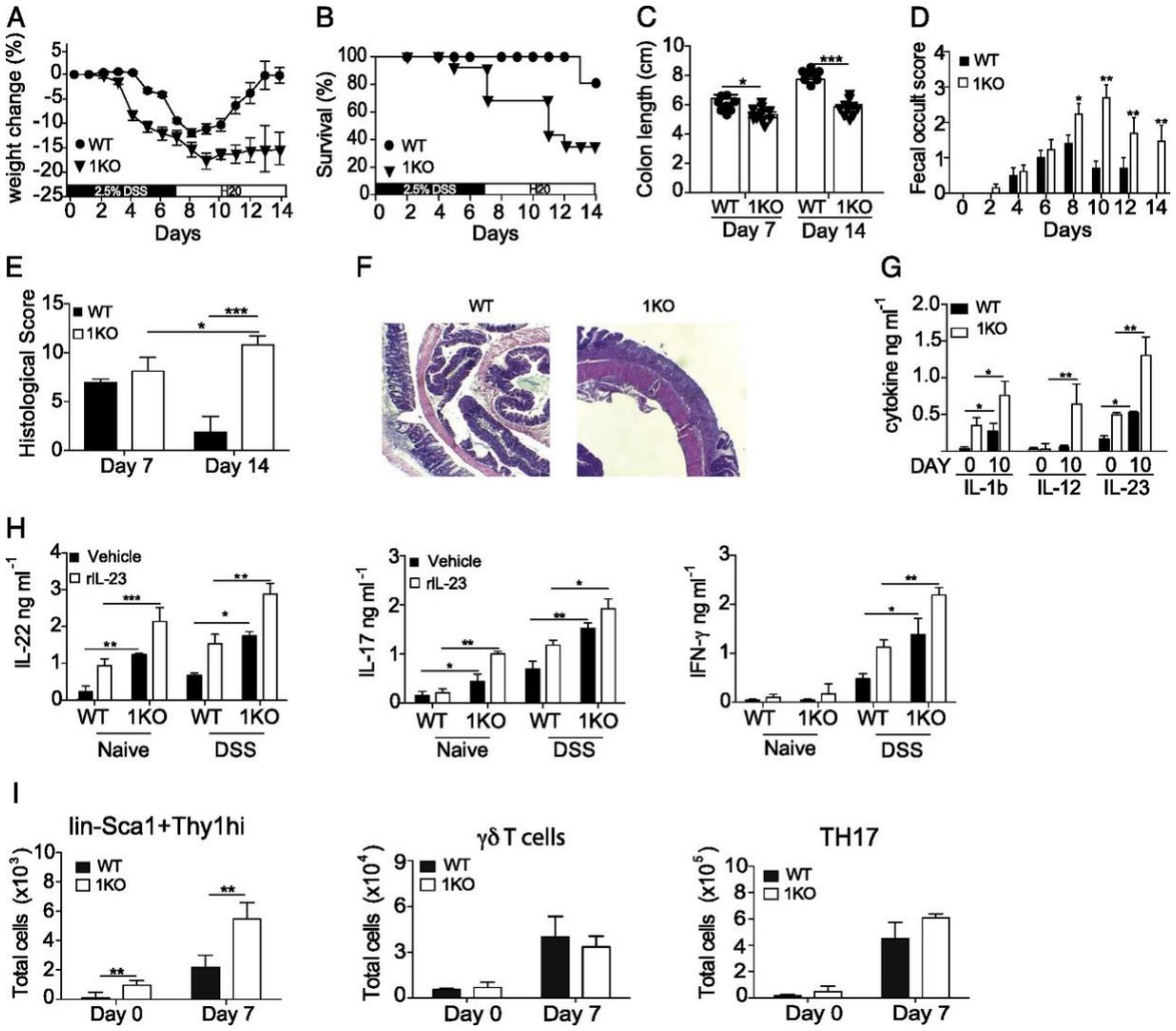

Figure 5.7: Loss of TLR1 exacerbates DSS-induced cytokine production and prevents colonic repair.

WT and 1KO littermates were administered drinking water containing 2.5% DSS for 7 d to induce epithelial injury followed by a 7-d recovery period in which they were returned to normal drinking water. (A) Percent change in weight, (B) survival, (C) colon length on days 7 and 14, and (D), fecal occult score. On days 7 and 14, colons were fixed and stained with (E) H&E, and (F) histological score was given after analysis by a gastroenterologist. (G) Concentration of IL-1b and IL-23 found in whole colon homogenates. (H) IL-17, IL-22, and IFN-g levels from the supernatants of colonic explant cultures derived from naive mice or mice treated with DSS for 10 d. (I) Mean number of cells in the colonic LP determined by flow cytometry for indicated cell type gated as described in Fig. 5.1 legend. (A–D) Data are expressed as mean ± SEM from three independent experiments, n = 8–10 mice per group. (E) The mean of histological scores from two independent experiments, n = 3 mice per group. (F) Representative microscopy images of three mice per group. (G–I) Data are expressed as mean ± SEM from two independent experiments, n = 6–8 mice per group. (A) Wilcoxon log-rank test; (B) Kaplan Meyer; (C, E, and G–I) Student t test; (D) two-way ANOVA. *p< 0.05, **p< 0.01, ***p < 0.001.

Whole colonic tissue was collected on days 0 and 10 for analysis of IL-1β, IL-23, and IL-12. Consistent with our earlier data, colonic tissue from naive 1KO mice had higher levels of IL-1β and IL-23, but not IL-12p70 (Figure 5.7G). After receiving DSS for 7 d and normal drinking water for 3 d, there was an increase in the amount of IL-1β and IL-23 in both WT and 1KO mice, with significantly higher levels found in the 1KO (Figure 5.7G). Interestingly, IL-12p70 was only detected on day 10 in the colonic homogenate of 1KO mice (Figure 5.7G). To assess the IL-23–dependent production of IL-22 and IL-17, colonic explants were performed on tissues harvested at the same time points and restimulated in vitro with recombinant IL-23. Colons from naive WT mice produced detectable IL-22 only in the presence of rIL-23 but failed to produce IL-17 (Figure 5.7H). In contrast, the unstimulated colon explants from naive 1KO produced detectable IL-22 and IL-17 that was further increased by the addition of rIL-23 (Figure 5.7H). Seven days after initial DSS exposure and 3 d into the repair cycle, IL-22 and IL-17 were elevated in the 1KO explants stimulated with the vehicle control, and the addition of rIL-23 significantly increased these levels (Figure 5.7H). Interestingly, IFN-γ levels were not detected in the colons from naive WT and 1KO mice, yet after DSS exposure, IFN-γ production was significantly increased in the cultures containing colons from the 1KO mice (Figure 5.7G). Analysis of the major colonic IL-23R responsive cells in the mice on day 7 of DSS revealed elevated numbers of $Sca1^{+}Thy1^{hi}$ cells in both WT and 1KO mice, yet they were significantly higher in the 1KO mice, whereas the numbers of γδ T cells and T_H17 cells did not increase (Figure 5.7I).

To determine if the severe pathology and inability to recover from intestinal injury in the 1KO mice was due to elevated numbers of $Sca1^{+}Thy1^{hi}$ cells, these mice were bred onto a RAG2-deficient (Rag KO) background, allowing us to deplete $Sca1^{+}Thy1^{hi}$ cells using a polyclonal Ab against Thy1. Confirming our results in Figure 5.7, the absence of TLR1 in Rag KO mice resulted in a much more rapid and severe weight loss (Figure 5.8A), significantly less survival (Figure 5.8B), and a shorter colon length (Figure 5.8C) than TLR1-sufficient Rag KO mice. Administration of the anti-Thy1 Ab significantly improved the disease outcome in the DSS-treated Rag KO mice, with less weight loss (Figure 5.8A), less mortality (Figure 5.8B), and longer colon lengths (Figure 5.8C). TLR1-deficient Rag KO mice treated with anti-Thy1 also had significantly fewer IL-22 (Figure 5.8D), IL-17 (Figure 5.8E), and IFN-γ (Figure 5.8F) than control Ab-treated TLR1-deficient Rag KO mice. Interestingly, the depletion of the $Sca1^{+}Thy1^{hi}$ cells in the TLR1-deficient Rag KO mice had no effect on IL-23 or IL-12 (Figure 5.8G).

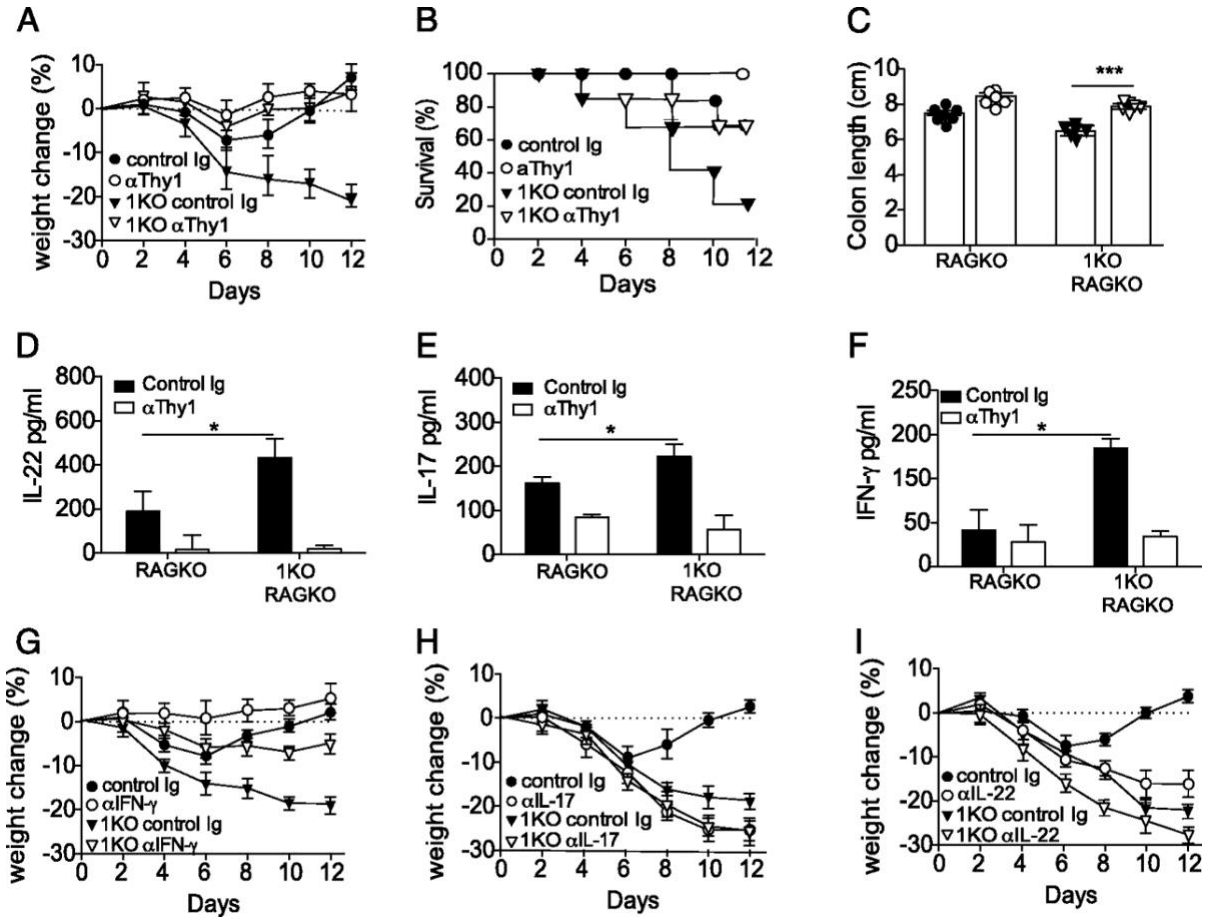

Figure 5.8: IFN-γ contributes to the mortality observed in the context of TLR1 deficiency.
RAG2 KO (RAG KO and 1KOxRAG2 KO (1KO–RAG KO) were treated with anti-Thy1–depleting Ab every other day beginning on the day of DSS administration through day 12. (A) Percent change in weight, (B) percent survival, and (C) colon length on day 12 were assessed. Colonic tissue explants were incubated overnight, and the concentration of (D) IL-22 was measured in the supernatant. Levels of (E) IL-17 and (F) IFN-γ were determined from whole mucosal scrapings. All data are expressed as the mean ± SEM pooled from two to three independent experiments. RAG KO and 1KO–RAG KO were treated with polyclonal Abs against (G) IFN-γ, (H) IL-17, or (I) IL-22 throughout the course of both DSS and recovery, and percent change in weight was observed. (A) n = 7–12 mice per group; (B–F, and I) n = 5–7 mice per group. *p <0.05, ***p <0.001, Student t test.

To determine if any single cytokine was driving the heightened inflammation and the inability to heal in the 1KO mice, we administered either neutralizing Abs to IFN-γ, IL-17, or IL-22 every other day for the 7-d course of DSS, and weight loss and survival were measured. In line with other studies, there was moderate but significantly less weight loss in Rag KO mice given DSS and treated with anti–IFN-γ[41] (Figure 5.8G). In contrast, treatment with anti–IL-17 or anti–IL-22 resulted in much more weight loss (Figure 5.8H, 5.8I, respectively) and a more severe histological disease in WT mice given DSS (data not shown). In the TLR1-

deficient Rag KO mice, anti–IFN-γ treatment resulted in a complete reversal of the observed weight loss, whereas anti–IL-17 and anti–IL-22 treatment had little effect on weight loss (Figure 5.8H, 5.8I, respectively). Altogether, these data suggest that in the absence of TLR1 and under chronic inflammation, the $Sca1^{+}Thy1^{hi}$ cell shift produces IFN-γ, which is responsible for the worse pathology and severe disease observed following DSS.

5.4 Discussion

In this study, we show that endogenous TLR1 signaling is necessary to regulate homeostasis of the colon. In the absence of these TLR1 signals, there is a disruption of colonic crypt microarchitecture, mucosal-associated and translocated commensal bacteria, and low-level inflammation. The low-level inflammation was characterized by elevated IL-1β and IL-23 production and an increase in IL-22–producing $lin^{-}Sca1^{+}Thy1^{hi}RORC^{+}$ ILC3. Despite significantly more translocated bacteria, a leaky gut, and heightened colonic inflammation, TLR1-deficient mice do not exhibit any overt phenotype. However, upon intestinal injury induced by DSS, TLR1-deficient mice decline rapidly and are unable to heal after DSS withdrawal. Using neutralizing Abs, we show that an increase in $Sca1^{+}Thy1^{hi}$ ILC3 and a concomitant rise in tissue levels of IFN-γ contribute to this phenotype.

One key question is whether the altered colonic epithelial phenotype of the 1KO is due to a primary impact of TLR1-deficiency, secondary to an altered microbiota, and/or a response to chronic inflammation. 1KO mice had no major alterations in their cecal microbial community, and fecal microbiota transfer between 1KO and WT mice was not sufficient to induce inflammation, arguing against a secondary effect due to a microbial dysbiosis. This is consistent with the work of Ubeda et al.[42], who found only minor differences in microbial community when comparing littermates from TLR-deficient mouse strains. Bone marrow chimera studies determined that barrier function was mediated by TLR1 signaling in the nonhematopoietic cell compartment, further suggesting that a defect of TLR1 in the epithelium is primary in this model. Whether epithelial derangement precedes the chronic inflammatory response or is a symptom of dysregulated immune activation is challenging to determine, and these processes likely develop in concert in vivo.

The intestinal epithelium is in a state of constant renewal, being replaced roughly every 5 d[13,32,43], and this renewal is mediated via the coordinated signals of factors that are involved in proliferation and differentiation. In addition to the observation that TLR1-deficiency was associated with an increase in proliferation of the colonic crypt, we also found these mice had spatial and functional differences of the specialized epithelial cell. One intriguing finding was the presence of Lyz- and DEFA-1–expressing cells. These antimicrobial agents are typically restricted to the small intestine where they are coexpressed in Paneth cells. Ectopic expression of Paneth cell markers have been reported in a number of studies[2,6,10,34,39,44–46], particularly those examining WNT and Notch signaling because of their roles in proliferation[11,43] and differentiation[47], respectively. However, we were unable to find any difference in *Notch1* and its downstream target genes (R.W. DePaolo and A.M.F. Johnson, unpublished observations).

There is increasing evidence that innate sensing of the microbiota plays an important role in regulating epithelial cell proliferation. Studies using germ-free or ABX-treated mice have shown a reduction in the proliferation of IEC respective to controls[12,48–50]. More recently, a comparison of ABX that favor either the depletion of gram-positive or gram-negative bacteria found a reduction in proliferation when only the gram-positive bacteria were depleted[11]. However, the data concerning the role of MyD88 in this process are conflicting. Using MyD88 KO mice, Rakoff-Nahoum et al.[7] reported that commensal TLR signaling was required for homeostasis and, in particular, found an increase in the number of $BrdU^+$cells in the colons of MyD88 KO mice, suggesting an inhibitory role of TLRs on proliferation, yet subsequent reports have demonstrated that TLR and MyD88 signaling promote epithelial proliferation[5,11,14]. Our data align with the studies by Rakoff-Nahoum et al., as we identified a significant increase in $BrdU^+$ and $Ki67^+$ cells within the colonic epithelium of naive TLR1-deficient mice. An intriguing possibility is that engagement of commensal-derived TLR1 ligands may induce a genetic program that regulates or coordinates signaling of growth and/or differentiation factors in the colon, leading to regulation of proliferation. However, analysis of *Notch1*, *Wnt5a*, *Wnt3*, *Jagged1*, and the downstream Notch1-responsive transcription factor *Hes1*revealed no difference in expression between the colons of WT and 1KO mice (Supplemental Figure 5.2, R.W. DePaolo and A.M.F. Johnson, unpublished observations). The Notch and WNT families contain many members and are both regulated by a variety of different factors. Thus, a much more

comprehensive screen looking at the role of TLR1 in the direct regulation of WNT and Notch family members and their inhibitors is currently underway in our laboratory.

In this study, using ABX to deplete the commensal microbiota, we provide evidence that the microbiota is necessary for the increased proliferation observed in the TLR1-deficient mice, yet the composition and the function of the microbiota from TLR1-deficient mice were not sufficient to induce this proliferative response when transferred to ABX-treated WT recipients. These data do not exclude a role for TLR1 in directly regulating the growth and differentiation signals in the crypt, as it is possible that through other innate immune receptors the microbiome drives proliferation, and TLR1 drives regulatory factors that counter this commensal-driven activation.

To our knowledge, our study is also the first to identify a role of TLR1 in regulation of the epithelium and the first to support a regulatory role for this molecule in proliferation. Our data are in sharp contrast to studies using TLR2 agonists[25,26] and TLR2 KO mice[5,11,14], which show increased and decreased proliferation, respectively. TLR1 forms a heterodimer with TLR2 to recognize triacylated lipoproteins[11,12,28]. Our group, and others, have shown that TLR2/1 signaling induces proinflammatory innate immune responses through activation of MyD88 and NF-κB or Pi3K/Akt and mTOR[3,22,23,31,35,51,52] in immune cells, but its downstream signaling pathways may be different in epithelial cells because of the expression of different coreceptors. The promiscuity in binding by TLR2 allows it to form complexes with coreceptors TLR6, TLR10, Dectin-1, TLR4, CD14, and CD36. Analysis of mRNA transcripts for *Tlr1* by our group has revealed increasing expression as you move distally from the ileum to the rectum. In porcine small intestinal tissue, *Tlr1* gene expression is low at the base of the crypt and increases as you move toward the villous tip[53]. *Tlr1* expression has also been observed in the colons of naive mice, yet unlike expression of *Tlr2* and *Tlr6*, which increases during DSS administration, *Tlr1* expression remains unchanged[54]. Additionally, it is not known whether TLR1, TLR6, and TLR10 compete with each other for binding with TLR2, as no studies to date have analyzed TLR2/6 and TLR2/10 expression in 1KO mice or in individuals with the polymorphisms that disrupt cellular surface expression, such as the TLR1 I602S polymorphism. It is a distinct possibility that shifting recognition of commensal ligands to TLR2/6 or, in humans, TLR2/10, may promote proliferation. Interestingly, analysis of TLR6-deficient crypts revealed no change in the

number of BrdU^{+} cells (R.W. DePaolo and R. Rankin, unpublished observations), further demonstrating the differential effects mediated by TLR1 and TLR6.

We observed a shift in the expression of cytokines and transcription factors in the lin^{-}Sca1^{+}Thy1^{hi} ILC3 in the TLR1-deficient mice. In naive WT and 1KO controls, these cells expressed higher levels of *Il22*, but the latter also expressed transcripts for *Il17*. Upon tissue injury induced by DSS, the lin^{-}Sca1^{+}Thy1^{hi} cells from WT mice had an increase in *Il22* transcripts as well as *Il17*. In contrast, after DSS-induced injury in the 1KO, there was an increase in *Tbet* and *Ifng* expression in the lin^{-}Sca1^{+}Thy1^{hi} cells (data not shown) that correlated with an elevation of IFN-γ protein in the tissue. This phenotype, along with our observed increase in IL-12, is reminiscent of IL-22^{+}Rorγt^{+} ILC3, which acquire *Tbet* in the presence of IL-12 and have been termed “exILC3” in both mice and humans[8,55]. It is well established that IFN-γ negatively regulates the epithelial barrier and antagonizes proliferation[15,56,57], and thus its presence during DSS in the 1KO mice would block the beneficial effects of IL-22, thereby preventing epithelial proliferation and exacerbating the damage. Indeed, depletion of the Thy1^{+} cells in the TLR1-deficient Rag KO mice and neutralization of IFN-γ both ameliorated the severity of DSS administration. Other studies have shown that chronic inflammation of the intestine leads to IL-12 production and the expansion of IFN-γ^{+} cells[45,46,58] or the reprogramming of IL-17–expressing cells[33].

Our results provide new insight into the regulation of the colonic crypt and suggest an unexpected role for TLR1 sensing of endogenous ligands in this process. Understanding how the microbiome may contribute to epithelial homeostasis and the consequence of disrupted signaling through host genes or changes in the gut microbiome has broad implications. These data provide biological evidence for the observations of an increased frequency of patients expressing mutations in the TLR1 locus with IBD, and that IBD patients expressing defective TLR1 genes are more likely to have anticommensal Abs[18,51]. These studies also provide a biological framework for the development of TLR1 agonists that could be used to promote a healthy intestinal barrier and suggest that persons expressing variant *TLR1* alleles may be at a higher risk for developing systemic inflammation, leaky gut, and long-term chronic intestinal disease.

5.5 Materials and Methods

Mice

TLR1 knockout (1KO), TLR1 heterozygote, and TLR1 wild type (WT) mice were generated through the breeding of 1KO males with WT or heterozygous females. Litters were mixed upon separation, and genotypes were cohoused together in cages through the duration of all experiments unless stated otherwise in the figure legends or Materials and Methods. Mice were maintained at the University of Southern California and the University of Washington, and experiments were performed following protocol review and approval by the institutional biosafety committee and the institutional animal care and use committee. Mice were housed in specific pathogen-free (SPF) conditions, administered sterile, nonchlorinated, nonacidified water, and fed a normal mouse chow (AIN-76) ad libitum. The mice in this colony are Helicobacter hepaticus–free and clear of other pathogens, such as murine norovirus or Pasteurella. Rag2 knockout (Rag2KO) mice [B6(Cg)-Rag2tm1.1Cgn/J] were purchased from Jackson Laboratory (Bar Harbor, ME) and mated with 1KO mice for at least 10 generations prior to use.

Dextran sulfate sodium treatment

Five- to seven-week-old female mice received 2.5% w/v dextran sulfate sodium (DSS) (m.w. 35,000–50,000 kDa; Affymetrix, Santa Clara, CA) in drinking water for 7 d followed by 7 d of regular drinking water.

Immunohistochemistry and Immunofluorescence

Murine colons were rolled using the Swiss roll technique and fixed in 10% neutral buffer formalin (VWR International, Visalia, CA) or methacarn fixative (VWR International) overnight. For preservation of the mucus layer, colon pieces with contents were placed in methacarn fixative (60% dry methanol, 30% chloroform, 10% glacial acetic acid) overnight. Methacarn pieces were washed twice in 100% methanol, once in 100% ethanol, and twice in xylene prior to paraffin embedding. Paraffin-embedded (without formalin) tissues were cut 5 μm thick. H&E, Alcian blue (AB), mucicarmine, and periodic acid–Schiff (PAS) staining was performed by AML Laboratories (Saint Augustine, FL) or in-house using AB pH 2.5 according to the manufacturer's instructions (Abcam, Cambridge, MA). Quantification of mucus layer thickness and mucin vesicles were conducted by an individual blinded to the experiment groups. Muc2 (1:200, ab76774; Abcam), BrdU, Ki67 (1:500, MKI67; Novus Biologicals), Gob5 (1:50, M-53; Santa Cruz), lysozyme (Lyz)

(1:200, catalog no. ab108508; Abcam), α-defensin-1 (DEFA-1) (1:2000, a kind gift from A. Ouellette), rabbit polyclonal IgG, (1:200, ab27472; Abcam), and rabbit monoclonal IgG (1:200, ab172730; Abcam).

For Ag retrieval, slides were placed into tubes containing sodium citrate buffer (pH 6) (Sigma-Aldrich, St. Louis, MO) and heated at 99°C in water bath. The slides were washed and blocked before staining with primary Ab. The slides with primary Ab were incubated overnight at 4°C in a humid chamber and the following day were washed and incubated with secondary Ab at 37°C for 1 h. The slides were mounted with DAPI, and confocal images were acquired using a Nikon Eclipse C1 Laser Scanning Microscope (Nikon, PA) fitted with a 60 Nikon objective (PL APO, 1.4NA) and Nikon image software.

H&E-stained colonic tissue sections were scored by a blinded gastroenterologist using the following measures: crypt architecture (normal, 0; severe crypt distortion with loss of entire crypts, 3), degree of inflammatory cell infiltration (normal, 0; dense inflammatory infiltrate, 3), muscle thickening (base of crypt sits on the muscularis mucosae, 0; marked muscle thickening present, 3), goblet cell depletion (absent, 0; present, 1), and crypt abscess (absent, 0; present, 1). The histological damage score is the sum of each individual score.

Colonic epithelial cell and LP isolation

The colon was removed, flushed with ice-cold PBS and 1 mM DTT (Sigma-Aldrich), and shaken at 37°C in HBSS containing 2 mM EDTA (Sigma-Aldrich,) and 2 mM DTT (Sigma-Aldrich) for 10 min, and the supernatants were collected. This was repeated, and supernatants were pooled together and constitute the epithelial fraction. The remaining tissue was digested with Collagenase Type IV (Sigma-Aldrich) in RPMI 1640 with 20% FBS (GE Healthcare, Logan, UT) for 20 min. The supernatants were collected, passed through 70-μM mesh filters (BD Biosciences, San Jose, CA), and washed in ice-cold PBS.

Detection of bacterial 16S rDNA by using RT-PCR and by plating

16S rDNA was analyzed as previously described (9, 31). Briefly, the DNA from colonic mucosa, stool, or colonic lumen was extracted using the QIAamp DNA stool kit (Qiagen, Germantown, MD) and 2 μl of bacterial DNA was used as a template. The gene copy number per microliter of DNA was determined using plasmids expressing the target of the 16S primers (31). For enumeration of bacteria using standard plating

techniques, the spleen and liver were aseptically removed and homogenized in 1 ml sterile prereduced oxygen-free tryptic soy agar (TSA) (Anaerobe, Morgan Hill, CA). Samples were serially diluted and plated in duplicate and placed in anaerobic jars (Sigma-Aldrich). Forty-eight hours later, the colonies were enumerated and compared with plates grown in the presence of oxygen.

Bone marrow chimeras

Mice were irradiated with 1000 cGy. The mice were immediately reconstituted i.v. with $10 \times 10_6$ cells isolated from indicated donor bone marrow. The mice recovered for 6 wk prior to use.

Fecal microbiota transplants

Mice were treated with a mixture of five antibiotics (ABX): neomycin (1 g/l; Sigma), amoxicillin (1 g/l; VWR International), gentamicin (1 g/l), vancomycin (0.5 g/l; VWR International), and metronidazole (1 g/l; VWR International) in their drinking water for 2 wk and received 150 µl of stool contents from indicated donor by oral gavage every other day for a total of three total gavages. The mice were left undisturbed for up to 4 wk before any procedures were performed.

Anti-Thy1, anti–IL-22, anti–IL-17, and anti–IFN-γ treatment

TLR1-sufficient and -deficient Rag2KO mice were administered 1 mg of anti-Thy1–depleting mAb (YTS 154.7.7.10) or rat isotype control (YKIX 337.217.1), 500 µg anti–IL-17A (rat IgG2a; MAB421; clone 50104; R&D, Minneapolis, MN), 500 µg anti–IL-22 (rat IgG2a; 16-7222-85; clone IL22JOP; eBioscience, San Diego, CA), or 500 µg anti–IFN-γ (rat IgG1; 505802; clone XMG1.2; BioLegend) i.p. the day of DSS administration and then every other day through day 8.

Intestinal permeability and endotoxin measurement

FITC-conjugated dextran (4000 MW) dissolved in water (Sigma-Aldrich) was administered rectally to anesthetized mice at 2 mg/10 g of body weight using a Foley catheter. Whole blood was collected using heparinized needles via cardiac puncture 1 h after FITC-dextran administration. Fluorescence intensity in sera was analyzed using a standard plate reader and determined by comparison with a FITC-dextran

standard curve. Bacterial endotoxin in the serum was assayed using an endpoint chromogenic Limulusamebocyte lysate assay (Lonza, Anaheim, CA) per manufacturer's instructions.

Quantitative real-time RT-PCR

RNA was extracted from mucosal scrapings, isolated LP, intestinal epithelial cells (IEC), or sorted lineage (lin)−Sca1+Thy1hi cells using ISOLATE II RNA Mini Kit (Bioline, Boston, MA). RNA was reverse-transcribed into cDNA with SensiFAST cDNA Synthesis Kit (Bioline). Quantitative PCR (qPCR) was performed on a CFX96 Touch Real-Time PCR Detection System (Bio-Rad Laboratories, Irvine, CA) using SensiFAST SYBR No-ROX Kit (Bioline). No reverse transcriptase and water controls were performed for each sample. Data were normalized to product and amplified using primers for a housekeeping gene, GAPDH.

Abs, flow cytometry, and cell sorting

The following conjugated Abs were used: Sca1 (D7), Thy1 (G7), and γδ TCR (GL3); our lin-negative panel contained: CD11c (HL3), Gr-1 (Rb8-6CF), CD11b (M1/70), NK1.1 (PK136), CD19 (1D3), CD8a (53-6.7), CD3e (2C11), CD4 (RM4-5), and B220 (RA3-6B2) from BD Pharmingen (San Jose, CA). Flow cytometry analysis was performed with a FACS Canto (BD Biosciences) and analyzed using FlowJo software (FlowJo, Ashland, OR). For sorting, the LP for five to eight mice were pooled and stained with allophycocyanin -conjugated lin markers, followed by labeling with anti-allophycocyanin beads and negative sorting on autoMacs (Miltenyi Biotec, San Diego, CA). Enriched cells were stained with Sca1 and Thy1.2 and sorted on a FACSAria (BD Biosciences).

Detection of cytokines by ELISA

After isolation of the LP, the pellet was homogenized in 2 ml of PBS, and protein was quantified using Quick Start Bradford Protein Assay (Bio-Rad Laboratories). Cytokine levels in 50 µg/ml of protein were determined using ELISA assays for IL-1β (BD), IL-23 (BD), IL-12p70 (BD), IL-17 (R&D), and IL-22 (eBioscience).

Measurement of reactive oxygen species

Fresh mucosal scrapings were collected into preweighed tubes and homogenized at 40 mg/ml in sterile PBS. Reactive oxygen species (ROS) were measured in supernatant using the OxiSelect ROS/RNS Assay Kit (Cell Biolabs, San Diego, CA) according to the manufacturer's instructions.

Microbiota composition analysis by 16s rDNA sequencing

Cecal contents from littermate 1KO and WT mice were snap-frozen on collection. Genomic DNA was extracted from samples using the Qiagen MagAttract PowerSoil DNA Isolation Kit Optimized for the KingFisher (Qiagen, Valencia, CA) following the manufacturer's protocol at RTL Genomics (Lubbock, TX). Samples were amplified for sequencing at RTL Genomics (Lubbock, TX) in a two-step process using primers 515F 5′-GTGCCAGCMGCCGCGGTAA-3′ and 806R 5′-GGACTACHVGGGTWTCTAAT-3′ [59] and were sequenced using the MiSeq platform (Illumina, San Diego, CA). Sequencing data were curated using mothur using the MiSeq standard operating procedure[60]. Sequences were then classified using the Ribosomal Database Project version 14 and phylotyped to the genus level. Sequence data were deposited in the Sequence Read Archive under accession number SRP143628 (https://www.ncbi.nlm.nih.gov/sra/SRP143628).

Statistics

All data are expressed as the mean ± SEM. Differences were considered significant at $p < 0.05$, using a Student t test (two-tailed), ANOVA test, or Wilcoxon log-rank test as appropriate, and were performed with the statistical analysis software Prism (GraphPad Software). Statistical tests and pvalues are specified in the figure legends.

Study approval

All mice were maintained at the University of Southern California or the University of Washington, and experiments were performed following protocol review and approval by the institutional biosafety committee and the institutional animal care and use committee.

5.7 Supplemental Materials

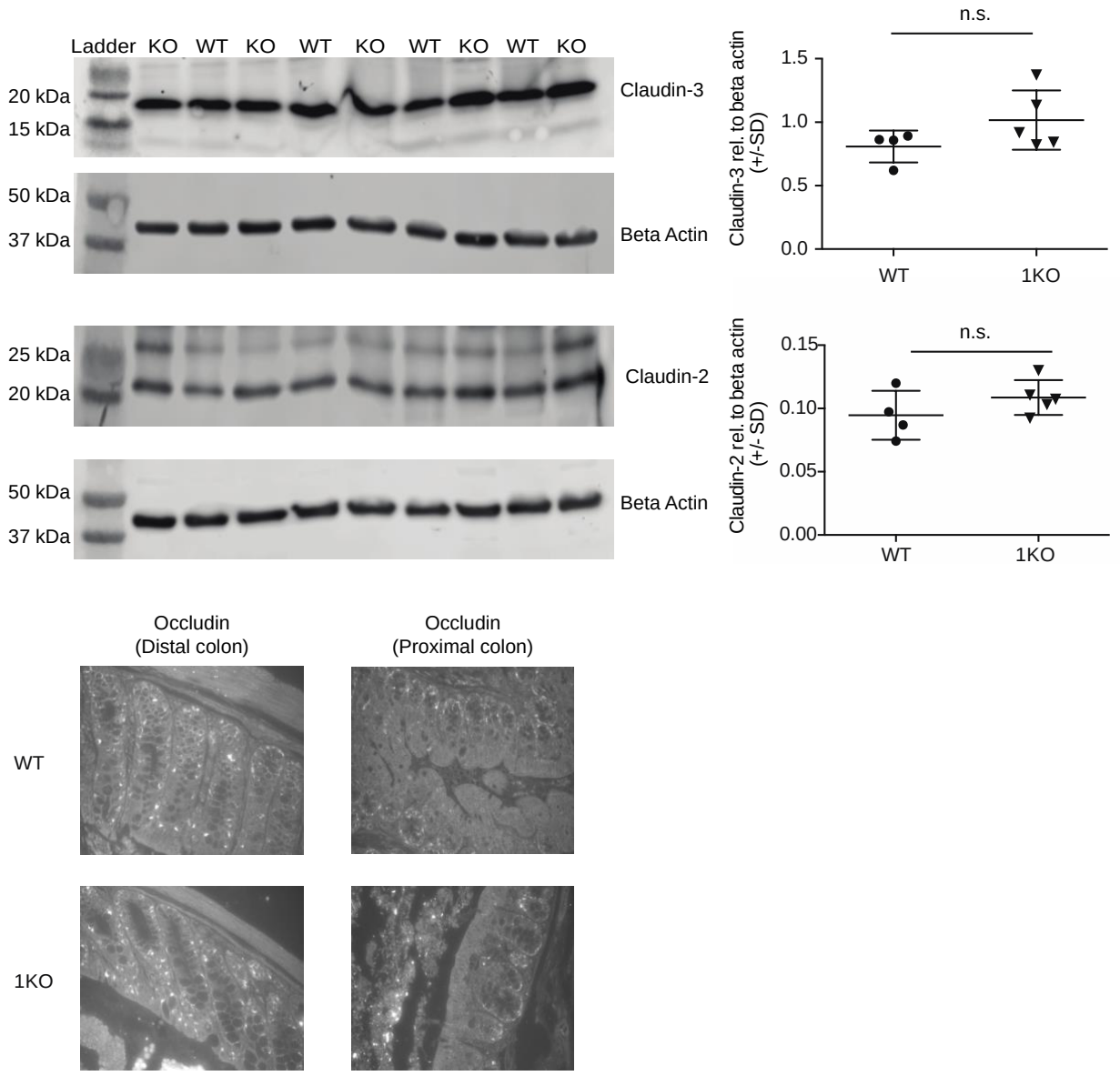

Supplemental Figure 5.1: Expression of claudin 2 and claudin 3 in colonic mucosal scrapings

Expression of Claudin 2 and Claudin 3 in WT and TLR1KO colon mucosal scrapings. Immune-fluorescnce staining of Occludin in Distal and Proximal colon of WT and 1KO colon.

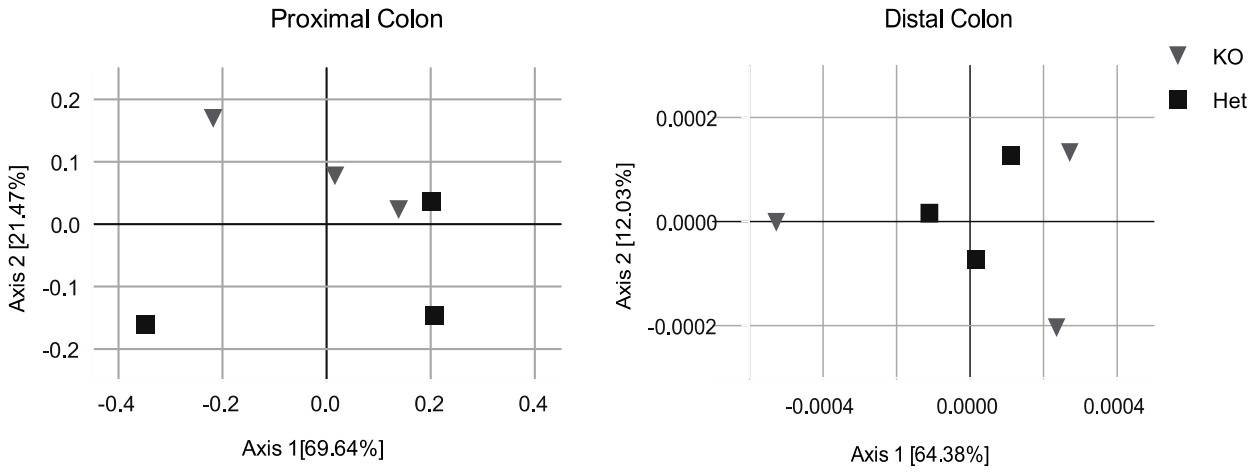

Supplemental Figure 5.2: PCoA of colon mucosal-associated bacteria communities

Principle Coordinate of Analysis (PCoA) of proximal and Distal colon mucosal-associated bacterial communities in TLR1KO (KO) and wild-type (Het) mice.

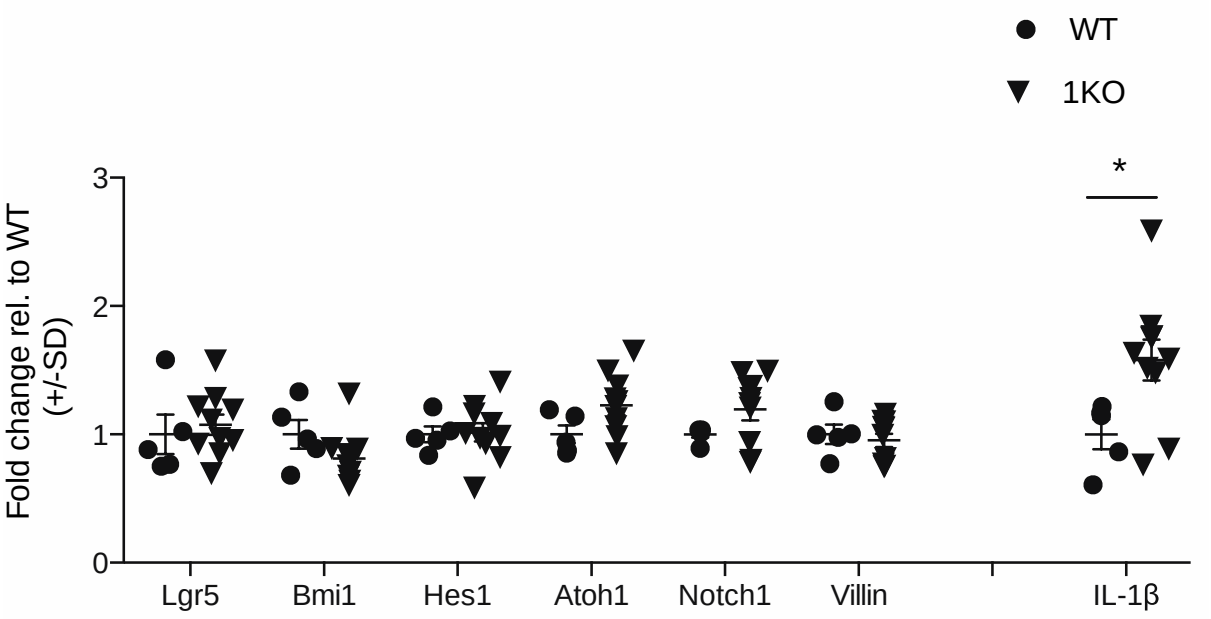

Supplemental Figure 5.3: Expression of stem-cell and notch-signaling genes of colonic mucosa

Expression of stem cell and notch-signaling genes in colonic mucosa of 1KO and WT mice

5.6 References

1. Abreu MT. Toll-like receptor signalling in the intestinal epithelium: how bacterial recognition shapes intestinal function. *Nat Rev Immunol*. 2010;10(2):131-144. doi:10.1038/nri2707

2. Andreu P, Colnot S, Godard C, et al. Crypt-restricted proliferation and commitment to the Paneth cell lineage following Apc loss in the mouse intestine. *Development*. 2005;132(6):1443-1451. doi:10.1242/dev.01700

3. Garrett WS, Gordon JI, Glimcher LH. Homeostasis and inflammation in the intestine. *Cell*. 2010;140(6):859-870. doi:10.1016/j.cell.2010.01.023

4. Tremaroli V, Bäckhed F. Functional interactions between the gut microbiota and host metabolism. *Nature*. 2012;489(7415):242-249. doi:10.1038/nature11552

5. Behrens J. Control of β-Catenin Signaling in Tumor Development. *Annals of the New York Academy of Sciences*. 2006;910(1):21-35. doi:10.1111/j.1749-6632.2000.tb06698.x

6. Andreu P, Peignon G, Slomianny C, et al. A genetic study of the role of the Wnt/beta-catenin signalling in Paneth cell differentiation. *Dev Biol*. 2008;324(2):288-296. doi:10.1016/j.ydbio.2008.09.027

7. Rakoff-Nahoum S, Paglino J, Eslami-Varzaneh F, Edberg S, Medzhitov R. Recognition of commensal microflora by toll-like receptors is required for intestinal homeostasis. *Cell*. 2004;118(2):229-241. doi:10.1016/j.cell.2004.07.002

8. Bernink JH, Peters CP, Munneke M, et al. Human type 1 innate lymphoid cells accumulate in inflamed mucosal tissues. *Nat Immunol*. 2013;14(3):221-229. doi:10.1038/ni.2534

9. Barman M, Unold D, Shifley K, et al. Enteric Salmonellosis Disrupts the Microbial Ecology of the Murine Gastrointestinal Tract. *Infection and Immunity*. 2008;76(3):907-915. doi:10.1128/IAI.01432-07

10. Kufer TA, Sansonetti PJ. NLR functions beyond pathogen recognition. *Nat Immunol*. 2011;12(2):121-128. doi:10.1038/ni.1985

11. Park J, Kotani T, Konno T, et al. Promotion of Intestinal Epithelial Cell Turnover by Commensal Bacteria: Role of Short-Chain Fatty Acids. *PLOS ONE*. 2016;11(5):e0156334. doi:10.1371/journal.pone.0156334

12. Reikvam DH, Erofeev A, Sandvik A, et al. Depletion of murine intestinal microbiota: effects on gut mucosa and epithelial gene expression. *PLoS ONE*. 2011;6(3):e17996. doi:10.1371/journal.pone.0017996

13. Khoury KA, Floch MH, Hersh T. Small Intestinal Mucosal Cell Proliferation and Bacterial Flora in the Conventionalization of the Germfree Mouse. *Journal of Experimental Medicine*. 1969;130(3):659-670. doi:10.1084/jem.130.3.659

14. Bogunovic M, Davé SH, Tilstra JS, et al. Enteroendocrine cells express functional Toll-like receptors. *Am J Physiol Gastrointest Liver Physiol*. 2007;292(6):G1770-1783. doi:10.1152/ajpgi.00249.2006

15. Bruewer M, Samarin S, Nusrat A. Inflammatory bowel disease and the apical junctional complex. *Ann N Y Acad Sci*. 2006;1072:242-252. doi:10.1196/annals.1326.017

16. Buonocore S, Ahern PP, Uhlig HH, et al. Innate lymphoid cells drive interleukin-23-dependent innate intestinal pathology. *Nature*. 2010;464(7293):1371-1375. doi:10.1038/nature08949

17. Cario E, Gerken G, Podolsky DK. Toll-like receptor 2 enhances ZO-1-associated intestinal epithelial barrier integrity via protein kinase C. *Gastroenterology*. 2004;127(1):224-238. doi:10.1053/j.gastro.2004.04.015

18. Kamdar K, Khakpour S, Chen J, et al. Genetic and Metabolic Signals during Acute Enteric Bacterial Infection Alter the Microbiota and Drive Progression to Chronic Inflammatory Disease. *Cell Host Microbe*. 2016;19(1):21-31. doi:10.1016/j.chom.2015.12.006

19. Cua DJ, Sherlock J, Chen Y, et al. Interleukin-23 rather than interleukin-12 is the critical cytokine for autoimmune inflammation of the brain. *Nature*. 2003;421(6924):744-748. doi:10.1038/nature01355

20. Gong J, Xu J, Zhu W, Gao X, Li N, Li J. Epithelial-specific blockade of MyD88-dependent pathway causes spontaneous small intestinal inflammation. *Clin Immunol*. 2010;136(2):245-256. doi:10.1016/j.clim.2010.04.001

21. Hisamatsu T, Suzuki M, Reinecker H-C, Nadeau WJ, McCormick BA, Podolsky DK. CARD15/NOD2 functions as an antibacterial factor in human intestinal epithelial cells. *Gastroenterology*. 2003;124(4):993-1000. doi:10.1053/gast.2003.50153

22. DePaolo RW, Kamdar K, Khakpour S, Sugiura Y, Wang W, Jabri B. A specific role for TLR1 in protective TH17 immunity during mucosal infection. *Journal of Experimental Medicine*. 2012;209(8):1437-1444. doi:10.1084/jem.20112339

23. Depaolo RW, Tang F, Kim I, et al. Toll-like receptor 6 drives differentiation of tolerogenic dendritic cells and contributes to LcrV-mediated plague pathogenesis. *Cell Host Microbe*. 2008;4(4):350-361. doi:10.1016/j.chom.2008.09.004

24. Yamamoto M, Sato S, Hemmi H, et al. Role of Adaptor TRIF in the MyD88-Independent Toll-Like Receptor Signaling Pathway. *Science*. 2003;301(5633):640-643. doi:10.1126/science.1087262

25. Dessein R, Gironella M, Vignal C, et al. Toll-like receptor 2 is critical for induction of Reg3β expression and intestinal clearance of Yersinia pseudotuberculosis. *Gut*. 2009;58(6):771-776. doi:10.1136/gut.2008.168443

26. Hörmann N, Brandão I, Jäckel S, et al. Gut microbial colonization orchestrates TLR2 expression, signaling and epithelial proliferation in the small intestinal mucosa. *PLoS ONE*. 2014;9(11):e113080. doi:10.1371/journal.pone.0113080

27. Eberl G. Development and evolution of RORγt+ cells in a microbe's world. *Immunol Rev*. 2012;245(1):177-188. doi:10.1111/j.1600-065X.2011.01071.x

28. Farhat K, Riekenberg S, Heine H, et al. Heterodimerization of TLR2 with TLR1 or TLR6 expands the ligand spectrum but does not lead to differential signaling. *Journal of Leukocyte Biology*. 2008;83(3):692-701. doi:10.1189/jlb.0807586

29. Birchenough GMH, Nyström EEL, Johansson MEV, Hansson GC. A sentinel goblet cell guards the colonic crypt by triggering Nlrp6-dependent Muc2 secretion. *Science*. 2016;352(6293):1535-1542. doi:10.1126/science.aaf7419

30. Johansson MEV, Hansson GC. Immunological aspects of intestinal mucus and mucins. *Nat Rev Immunol*. 2016;16(10):639-649. doi:10.1038/nri.2016.88

31. Sugiura Y, Kamdar K, Khakpour S, Young G, Karpus WJ, DePaolo RW. TLR1-induced chemokine production is critical for mucosal immunity against Yersinia enterocolitica. *Mucosal Immunol*. 2013;6(6):1101-1109. doi:10.1038/mi.2013.5

32. Guo X, Qiu J, Tu T, et al. Induction of innate lymphoid cell-derived interleukin-22 by the transcription factor STAT3 mediates protection against intestinal infection. *Immunity*. 2014;40(1):25-39. doi:10.1016/j.immuni.2013.10.021

33. Harbour SN, Maynard CL, Zindl CL, Schoeb TR, Weaver CT. Th17 cells give rise to Th1 cells that are required for the pathogenesis of colitis. *PNAS*. 2015;112(22):7061-7066. doi:10.1073/pnas.1415675112

34. Hirata A, Utikal J, Yamashita S, et al. Dose-dependent roles for canonical Wnt signalling in de novo crypt formation and cell cycle properties of the colonic epithelium. *Development*. 2013;140(1):66-75. doi:10.1242/dev.084103

35. Petermann F, Rothhammer V, Claussen MC, et al. γδ T cells enhance autoimmunity by restraining regulatory T cell responses via an interleukin-23-dependent mechanism. *Immunity*. 2010;33(3):351-363. doi:10.1016/j.immuni.2010.08.013

36. Takatori H, Kanno Y, Watford WT, et al. Lymphoid tissue inducer–like cells are an innate source of IL-17 and IL-22. *Journal of Experimental Medicine*. 2009;206(1):35-41. doi:10.1084/jem.20072713

37. Wlodarska M, Thaiss CA, Nowarski R, et al. NLRP6 inflammasome orchestrates the colonic host-microbial interface by regulating goblet cell mucus secretion. *Cell*. 2014;156(5):1045-1059. doi:10.1016/j.cell.2014.01.026

38. Keshav S. Paneth cells: leukocyte-like mediators of innate immunity in the intestine. *Journal of Leukocyte Biology*. 2006;80(3):500-508. doi:10.1189/jlb.1005556

39. Ouellette AJ. Paneth cells and innate mucosal immunity. *Curr Opin Gastroenterol*. 2010;26(6):547-553. doi:10.1097/MOG.0b013e32833dccde

40. Steenwinckel V, Louahed J, Lemaire MM, et al. IL-9 Promotes IL-13-Dependent Paneth Cell Hyperplasia and Up-Regulation of Innate Immunity Mediators in Intestinal Mucosa. *The Journal of Immunology*. 2009;182(8):4737-4743. doi:10.4049/jimmunol.0801941

41. Ito R, Shin-Ya M, Kishida T, et al. Interferon-gamma is causatively involved in experimental inflammatory bowel disease in mice. *Clin Exp Immunol*. 2006;146(2):330-338. doi:10.1111/j.1365-2249.2006.03214.x

42. Ubeda C, Lipuma L, Gobourne A, et al. Familial transmission rather than defective innate immunity shapes the distinct intestinal microbiota of TLR-deficient mice. *J Exp Med*. 2012;209(8):1445-1456. doi:10.1084/jem.20120504

43. Krausova M, Korinek V. Wnt signaling in adult intestinal stem cells and cancer. *Cell Signal*. 2014;26(3):570-579. doi:10.1016/j.cellsig.2013.11.032

44. Feng Y, Sentani K, Wiese A, et al. Sox9 induction, ectopic Paneth cells, and mitotic spindle axis defects in mouse colon adenomatous epithelium arising from conditional biallelic Apc inactivation. *Am J Pathol*. 2013;183(2):493-503. doi:10.1016/j.ajpath.2013.04.013

45. Matsuoka K, Inoue N, Sato T, et al. T-bet upregulation and subsequent interleukin 12 stimulation are essential for induction of Th1 mediated immunopathology in Crohn's disease. *Gut*. 2004;53(9):1303-1308. doi:10.1136/gut.2003.024190

46. Neurath MF, Weigmann B, Finotto S, et al. The Transcription Factor T-bet Regulates Mucosal T Cell Activation in Experimental Colitis and Crohn's Disease. *Journal of Experimental Medicine*. 2002;195(9):1129-1143. doi:10.1084/jem.20011956

47. VanDussen KL, Carulli AJ, Keeley TM, et al. Notch signaling modulates proliferation and differentiation of intestinal crypt base columnar stem cells. *Development*. 2012;139(3):488-497. doi:10.1242/dev.070763

48. Scoville DH, Sato T, He XC, Li L. Current view: intestinal stem cells and signaling. *Gastroenterology*. 2008;134(3):849-864. doi:10.1053/j.gastro.2008.01.079

49. Smith K, McCoy KD, Macpherson AJ. Use of axenic animals in studying the adaptation of mammals to their commensal intestinal microbiota. *Semin Immunol*. 2007;19(2):59-69. doi:10.1016/j.smim.2006.10.002

50. Pull SL, Doherty JM, Mills JC, Gordon JI, Stappenbeck TS. Activated macrophages are an adaptive element of the colonic epithelial progenitor niche necessary for regenerative responses to injury. *PNAS*. 2005;102(1):99-104. doi:10.1073/pnas.0405979102

51. Pierik M, Joossens S, Van Steen K, et al. Toll-like receptor-1, -2, and -6 polymorphisms influence disease extension in inflammatory bowel diseases. *Inflamm Bowel Dis*. 2006;12(1):1-8. doi:10.1097/01.mib.0000195389.11645.ab

52. Santos-Sierra S, Deshmukh SD, Kalnitski J, et al. Mal connects TLR2 to PI3Kinase activation and phagocyte polarization. *The EMBO Journal*. 2009;28(14):2018-2027. doi:10.1038/emboj.2009.158

53. Gourbeyre P, Berri M, Lippi Y, et al. Pattern recognition receptors in the gut: analysis of their expression along the intestinal tract and the crypt/villus axis. *Physiological Reports*. 2015;3(2):e12225. doi:10.14814/phy2.12225

54. Zheng B, Morgan ME, van de Kant HJG, Garssen J, Folkerts G, Kraneveld AD. Transcriptional modulation of pattern recognition receptors in acute colitis in mice. *Biochimica et Biophysica Acta (BBA) - Molecular Basis of Disease*. 2013;1832(12):2162-2172. doi:10.1016/j.bbadis.2013.07.004

55. Vonarbourg C, Mortha A, Bui VL, et al. Regulated expression of nuclear receptor RORγt confers distinct functional fates to NK cell receptor-expressing RORγt(+) innate lymphocytes. *Immunity*. 2010;33(5):736-751. doi:10.1016/j.immuni.2010.10.017

56. Kaiser GC, Polk DB. Tumor necrosis factor alpha regulates proliferation in a mouse intestinal cell line. *Gastroenterology*. 1997;112(4):1231-1240. doi:10.1016/s0016-5085(97)70135-5

57. Ruemmele FM, Gurbindo C, Mansour AM, Marchand R, Levy E, Seidman EG. Effects of interferon gamma on growth, apoptosis, and MHC class II expression of immature rat intestinal crypt (IEC-6) cells. *J Cell Physiol*. 1998;176(1):120-126. doi:10.1002/(SICI)1097-4652(199807)176:1<120::AID-JCP14>3.0.CO;2-B

58. Fuss IJ, Becker C, Yang Z, et al. Both IL-12p70 and IL-23 are synthesized during active Crohn's disease and are down-regulated by treatment with anti-IL-12 p40 monoclonal antibody. *Inflamm Bowel Dis*. 2006;12(1):9-15. doi:10.1097/01.mib.0000194183.92671.b6

59. Caporaso JG, Lauber CL, Walters WA, et al. Global patterns of 16S rRNA diversity at a depth of millions of sequences per sample. *PNAS*. 2011;108(Supplement 1):4516-4522. doi:10.1073/pnas.1000080107

60. Kozich JJ, Westcott SL, Baxter NT, Highlander SK, Schloss PD. Development of a Dual-Index Sequencing Strategy and Curation Pipeline for Analyzing Amplicon Sequence Data on the MiSeq Illumina Sequencing Platform. *Appl Environ Microbiol*. 2013;79(17):5112-5120. doi:10.1128/AEM.01043-13

Chapter 6. TLR6 Signaling Prevents Inflammation and Impacts Composition of the Microbiota During Inflammation-Induced Colorectal Cancer

Adapted from:

Jee-Hyun Kim, Melissa Kordahi, **Denise Chac**, and R. William DePaolo. *TLR6 signaling prevents inflammation and impacts composition of the microbiota during inflammation-induced colorectal cancer.* Cancer Prevention Research, *2019. doi: 10.1158/1940-6207.CAPR-19-0286*

6.1 Abstract

Tightly regulated immune responses must occur in the intestine in order to avoid unwanted inflammation, which may cause chronic sequela and leading to diseases such as colorectal cancer. Toll-like receptors play an important role in preventing aberrant immune responses in the intestine by sensing endogenous commensal microbiota and delivering important regulatory signals to the tissue. However, the role that specific innate receptors may play in the development of chronic inflammation and their impact on the composition of the colonic microbiota is not well understood. Using a model of inflammation induced colorectal cancer, we found that Lactobacillus species are lost more quickly in WT mice than TLR6-deficient mice resulting in overall differences in bacterial compositions. Despite the longer retention of Lactobacillus, the TLR6-deficient mice presented with more tumors and a worse overall outcome. Restoration of the lost Lactobacillus species suppressed inflammation, reduced tumor number and prevented change in the abundance of Proteobacteria only when given to WT mice, indicating the effect of these Lactobacillus are TLR6-dependent. We found that the TLR6-dependent effects of Lactobacillus could be dissociated from one another via the involvement of IL-10, which was necessary to dampen the inflammatory microenvironment, but had no effect on bacterial composition. Altogether, these data suggest that innate immune signals can shape the composition of the microbiota under chronic inflammatory conditions, bias the cytokine milieu of the tissue microenvironment, and influence the response to microbiota-associated therapies.

6.2 Introduction

Colorectal cancer (CRC) is the third most common form of cancer and the second leading cause of cancer-related deaths in the United States[1]. A majority of CRC cases are due to sporadic tumorigenesis, while only 10% are associated with a genetic predisposition[2,3]. The increased risk of developing CRC in people with metabolic syndrome, type 2 diabetes and inflammatory bowel disease[4] highlights a strong role for chronic inflammation in the etiology of inflammation-associated or colitis-associated CRC[5,6]. Other common features shared between these patient populations include changes within the composition of the intestinal microbiota and the development of immune reactivity against these intestinal microbes[7,8].

The intestine is home to a large microbial ecosystem that provides protective, structural and metabolic functions[9]. The importance of the microbiota in CRC has been illustrated in both animal models and in studies of patients with CRC[10–12]. In models of inducible and sporadic CRC, the composition of conventionally raised mice changes over the course of tumorigenesis[13]. Shifts in the composition of the microbiota have also been observed in human studies, which have not only found changes in the abundance of certain bacterial taxa but have identified a number of microbes thought to be drivers in the progression to malignancy. These include *Fusobacterium nucleatum*[14,15], *Bacteroides fragilis*[16,17] and *Escherichia coli*[18]. The importance of the microbiota in CRC has also been demonstrated using germ-free mice which develop less inflammation and fewer tumors than conventionally housed animals[19,20]. Despite these findings, the molecular mechanism contributing to the selection of certain bacterial families over another for an intestinal niche has not been established for CRC.

Due to the proximity of the microbiota to the intestinal epithelium and underlying immune cells, tightly regulated communication must occur to prevent abnormal tissue responses that could lead to chronic inflammation and malignancy. Coordination of intestinal responses are initiated through the recognition of both microbial-derived and host-derived ligands by innate immune receptors, such as Nod-like receptors (NLR) and the Toll-like receptors (TLR)[21]. TLRs comprise a set of receptors that recognize conserved microbial motifs (e.g. LPS, flagellin), as well as endogenous danger signals (e.g. heat shock proteins)[22]. These receptors represent a line of defense against invading enteric pathogens[23], but also sense and respond to our own commensal bacteria in order to promote epithelial cell integrity[24], localized immune responses and even colonization of the host[25]. Disruption of these signals can lead to uncontrolled

inflammation and changes within the microbiota, which have significant roles in intestinal disease[26], tumorigenesis and tumor progression[10,27]. Toll-like Receptror-2 (TLR2) recognizes di- and tri-acylated bacterial lipoproteins when heterodimerized with TLR6[28] or TLR1[29], respectively. In a model of inflammation-associated CRC, mice deficient for TLR2 have shown an increase in size and number of colonic tumors, dysregulation of cytokine production and epithelial responses[30]. Since both TLR1 and TLR6 require TLR2 to signal[21], deletion of TLR2 also results in the disruption of their signaling, making it difficult to delineate the role that these receptors may play in sensing and responding to microbial ligands in CRC. Using a model of inflammation-associated CRC we sought to understand how TLR6 signaling would affect a disease associated with alterations of the microbiota in a highly inflamed environment. We found that TLR6 deficiency was associated with the development of more tumors and worse survival when housed with other TLR6KO mice or when cohoused with WT mice. Interestingly, cohousing provided protection against tumors in the WT mice due to the presence if Lactobacillus which induced IL-10 in a TLR6-dependent manner Overall these studies suggest that innate sensing of the microbiota during inflammation can influence the local cytokine milieu, the composition of the commensals and the response to microbiome based immune therapies.

6.3 Results

TLR6 deficiency exacerbates inflammation-associated CRC, while co-housing protects WT mice

TLR6-deficient (TLR6KO) and littermates (WT) were weaned from their mothers and separately housed by genotype (SH) or co-housed (CH) together, two weeks later the mice were treated with the mutagen azoxymethane (AOM) followed by three rounds of dextran sodium sulfate (DSS) over 66 days (Figure 6.1A). Despite little difference in weight loss (Figure 6.1B) TLR6-deficient mice had an overall worse survival outcome compared to the SH-WT mice regardless of whether they were co-housed or housed with only other TLR6KO's (Figure 6.1C). Both SH- and CH-TLR6KO mice showed an increase in the size and number of tumors (Figure 6.1D-E) compared to both the SH- and CH-WT mice. To our surprise, WT mice co-housed with TLR6KO mice exhibited smaller and less tumors than their CH-TLR6KO cage mates and compared to SH-WT mice (Figure 6.1F-G). Analysis of H&E sections of the colons from these mice indicated CH-WT

mice had less pathological changes in the colon, less inflammation and a reduction in overall pathology score than both their CH-TLR6KO cage mates and SH-WT mice (Figure 6.1F-G).

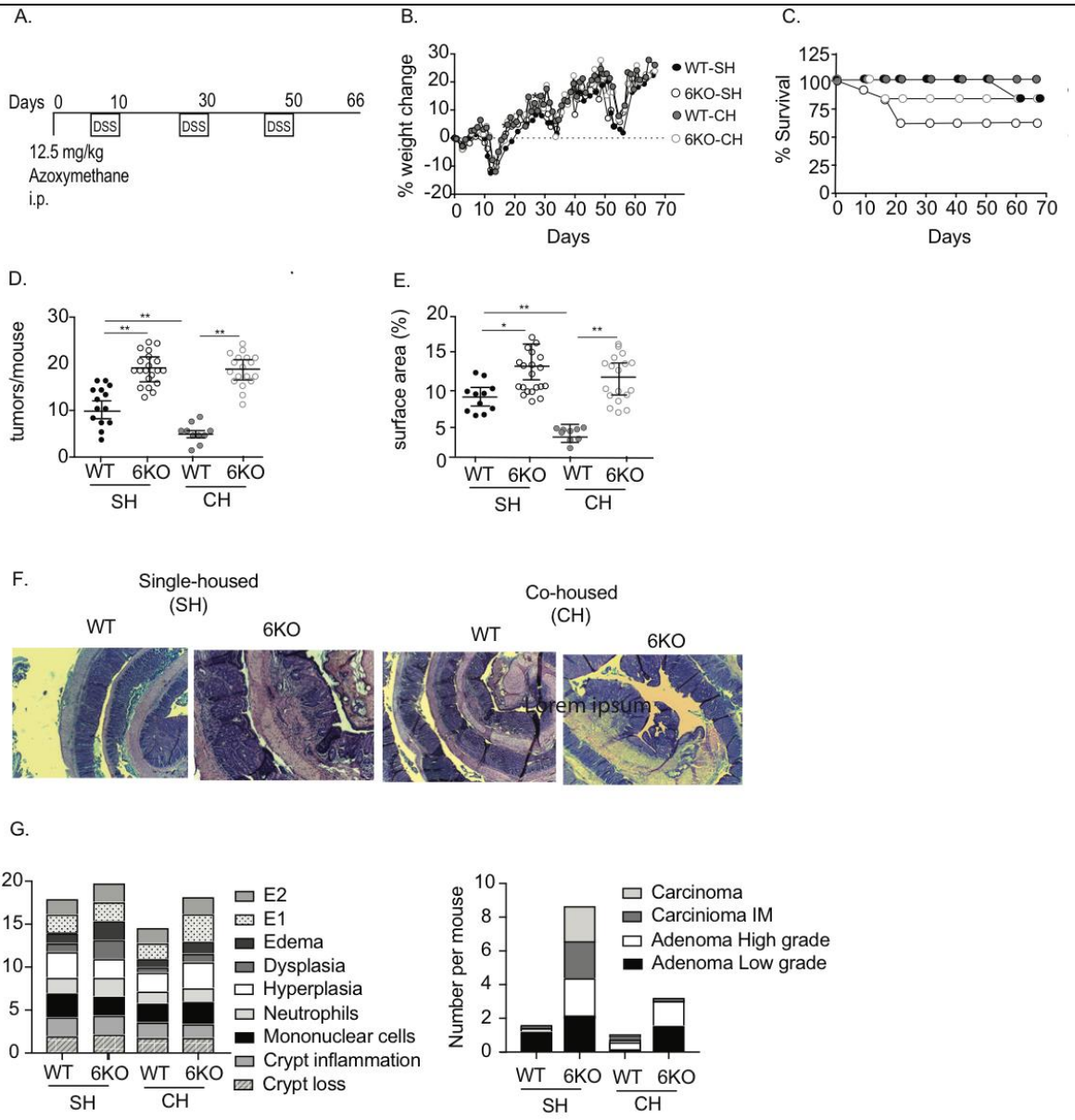

Figure 6.1: TLR6 signaling reduces the severity of inflammation-associated colorectal cancer
(A) Induction procedure for AOM/DSS model. (B) Percent change in weight of TLR6-deficient (TLR6KO) and littermates (WT) when co-housed (CH) or separately housed (SH) by genotype. (C) Percent survival over the course of AOM/DSS treatment, (D) Number of tumors and (E) the total surface area of tumors quantified using image j software. (F) Representative images of Hematoxylin and Eosin stained colons of mice collected on day 66. (G) Pathology scores of colonic tissues assessing inflammation and grade of lesion (see Methods for detailed criteria used to make these assessments). B-E, Data is pooled from 11-20 mice over 4 independent experiments and expressed as the mean ± s.e.m (B-C) or as individual points (D- E). F-G, data is pooled from 4-6 mice per group. *, $p < 0.05$. **, $p < 0.01$ (B, C) Wilcoxon Log-rank test, (D, E) Two-way ANOVA with Bonferroni post-hoc tests, (G) Unpaired Mann-Whitney t-test comparing; WT CH vs WT SH; KO-SH vs WT-SH; KO-CH vs WT-CH; KO-SH vs KO-CH).

Consistent with their increased tumor number and mortality, the TLR6KO mice had significantly worse dysplasia (p=0.02) and epithelial hyperplasia (p=0.03) compared to SH-WT mice (Figure 6.1G). Despite no significant differences in inflammatory parameters, hyperplasia, dysplasia or adenomas, the SH-TLR6KO mice had more crypt loss, high-grade adenocarcinomas and carcinomas than SH-WT mice (Figure 6.1F-G). Compared to SH-WT mice, co-housing significantly reduced epithelial hyperplasia (p=0.050) and dysplasia (p = 0.02) in WT mice. In contrast the CH-TLR6KO mice had significantly more hyperplasia, dysplasia, a greater extent of disease and more adenomas than the CH-WT mice (Figure 6.1F-G).

Our group and others have demonstrated a role for TLR6 and its binding partner, TLR2, in modulating inflammation via the induction of IL-10. Analysis of the lamina propria of the colon of AOM/DSS treated mice showed that TLR6KO mice, regardless of whether they were co- or single housed, had significantly higher levels of IL-17, IFN-γ and corresponding transcription factors *Rorc* and *Tbet*, compared to WT mice housed similarly (Figure 6.2A-B). Interestingly, only the CH-WT mice, which develop less tumors, had significantly elevated levels of IL-10 and higher expression of the transcription factors Gata3 and Foxp3 compared to SH-WT mice, and their co-housed TLR6KO counterparts (Figure 6.2A-B). Taken together, these data indicate that loss of TLR6 signaling causes an increase in tumor number and worsens survival, while co-housing protects WT mice from inflammation and developing tumors.

The exacerbated inflammatory response following AOM/DSS observed in the TLR6KO mice could be a result of deficient immune-modulatory mechanisms or mediated by a hyper-inflammatory microbiota associated with the TLR6KO mice. To begin to address both of these questions we measured IL-10 and IL-12p40 production from naive WT and TLR6KO bone-marrow derived dendritic cells (BMDCs) after stimulation with colonic contents harvested from cohoused and separately housed mice at day 66 of AOM/DSS treatment, or naïve age-matched controls. IL-10 production was significantly higher in WT BMDCs cultured with colonic contents from either naïve or AOM/DSS-treated cohoused mice compared to TLR6KO BMDCs stimulated with the same contents (Figure 6.2C). In contrast, separately housed WT and TLR6KO contents elicited much more IL-12p40 and very little IL-10 (Figure 6.2C). When the BMDCs were derived from TLR6KO mice, we observed a poor IL-10 response and elevated IL-12p40 levels from all samples except naïve WT and TLR6KO colonic contents (Figure 6.2C). Taken together these data indicate

that the colonic contents of co-housed TLR6KO and WT mice seemed to induce an IL-10 dominant response and dampen the levels of IL-12p40, while the colonic contents of both separately housed WT and TLR6KO promoted a more inflammatory response with high IL-12p40 and low IL-10. These data also suggest that in the context of TLR6 deficiency, colonic contents normally associated with high IL-10 instead induce a robust IL-12p40 response.

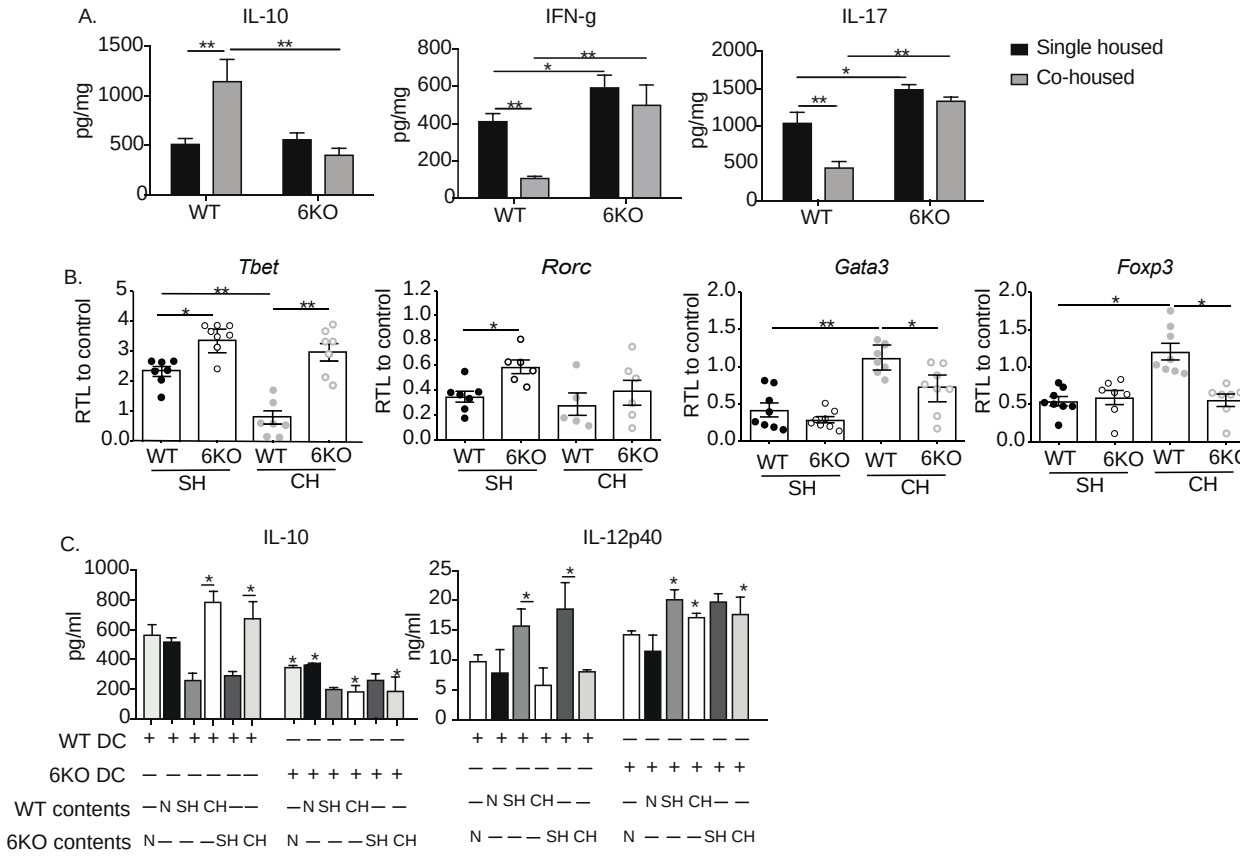

Figure 6.2: Colonic lysates from co-housed mice are less inflammatory and induce IL-10 in a TLR6-dependent manner.

(A) Levels of indicated cytokines from colonic lysates measured by ELISA. (B) Relative mRNA transcript levels of indicated transcription factors from colonic lysates were assessed by quantitative RT-PCR using naïve WT and TLR6KO mice as controls. (C) IL-10 (left) and IL-12p40 (right) protein production from BMDC generated from indicated naïve mouse (WT or TLR6KO) and stimulated with colonic lysates from indicated donors for 24 hours (N, naïve; SH, single-genotype housed; CH, cohoused; +, present; -, absent). A-C, data is expressed as mean + s.e.m of 6-8 mice from 2 independent experiments. *, $p < 0.05$. **, $p < 0.01$ Two-way ANOVA with Bonferroni post-hoc test.

Both genotype and housing influence dysbiosis associated with AOM/DSS

We hypothesized that both genotype and housing would contribute to alterations in the composition of the microbiota after AOM/DSS treatment. 16S rRNA sequencing was performed by scraping the colon with glass slides to capture both luminal and mucosal associated microbiota in naïve age-matched mice and day 66 AOM/DSS-treated mice. Analysis of the OTU's at the Phylum level revealed that co-housing significantly affected the composition of WT and TLR6KO mice, both naively and after AOM/DSS treatment (Figure 6.3A). Prior to AOM/DSS treatment, the colonic contents of SH-WT and SH-TLR6KO mice were dominated by taxa within Firmicutes, while co-housing WT and TLR6KO mice together lead to a dominance of Bacteroidetes (Figure 6.3A). Following AOM/DSS treatment there were major shifts in the Phylum level, regardless of genotype or housing (Figure 6.3A). Despite the absence of TLR6, co-housed mice shared a similar microbiome, dominated by the families Lactobacillaceae, Clostridiaceae and Erysipelotrichaceae (Figure 6.3B). In contrast, genotype seemed to impact the composition of the separately housed mice after AOM/DSS treatment in which we observed a significant increase in Helicobacteraceae and a small increase in Porphyromonadaceae in SH-WT mice (Figure 6.3B). This compositional phenotype was reversed in SH-TLR6KO mice who had much a higher abundance of Porphyromonadaceae and only a slight increase in Helicobacteraceae (Figure 6.3B).

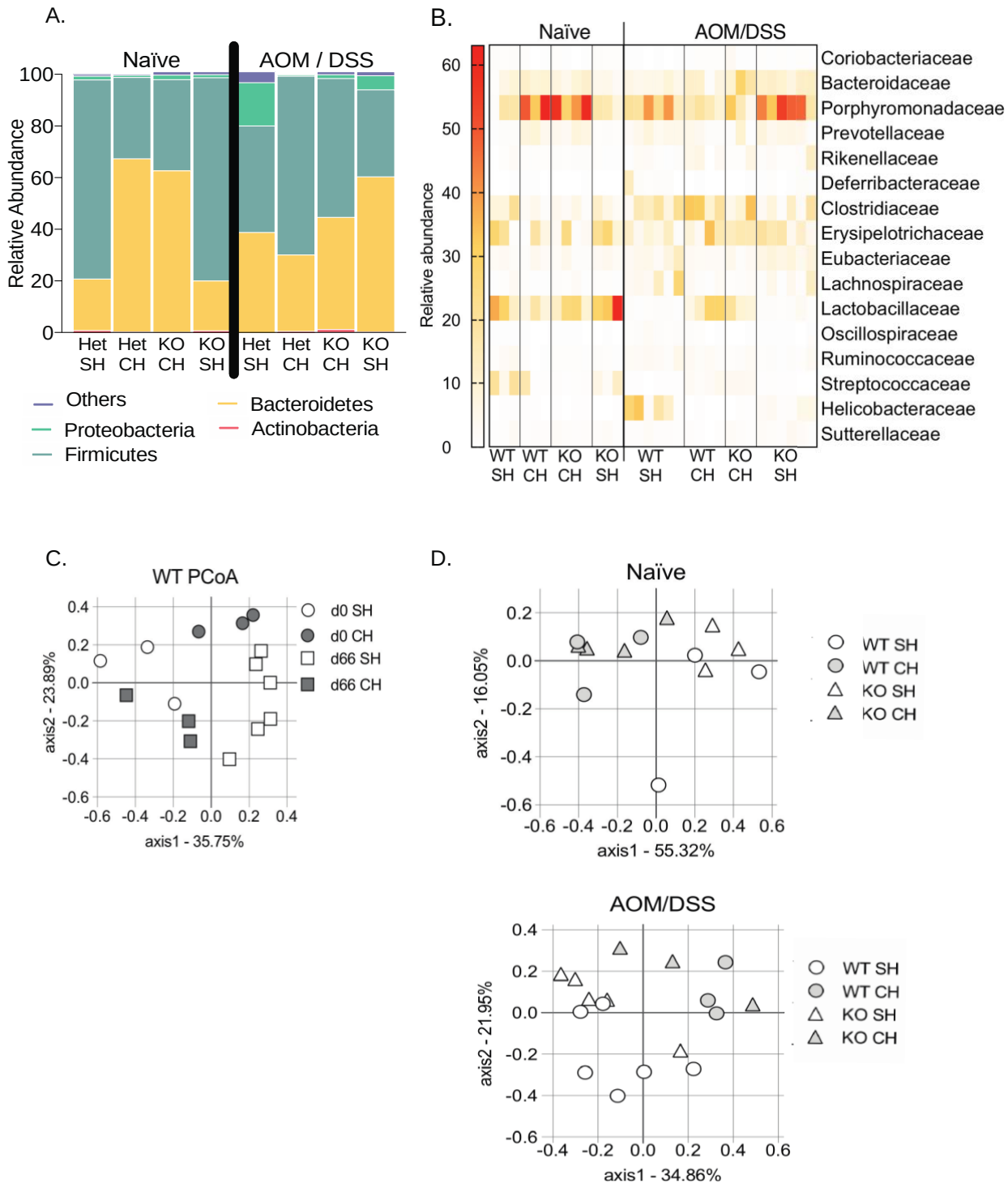

Figure 6.3: Compositional changes within the microbiota are influenced by TLR6 expression and housing status.

Figure 6.3: Compositional changes within the microbiota are influenced by TLR6 expression and housing status.

(A) Relative abundance of Phylum level microbiota from colons of naïve mice and mice treated with AOM/DSS under different housing conditions assessed by 16S rRNA sequencing. (B) Heatmap of family level abundance of colonic microbiota from colons of naïve and AOM/DSS treated mice under different housing conditions assessed by 16s rRNA sequencing. Bacterial families with less than 1% were not depicted. (C) Principal coordinates analysis (PCoA) of colonic microbiota samples of naïve (d0) and AOM/DSS treated (d66) WT mice. (D) Principal coordinates analysis (PCoA) of colonic microbiota samples of naïve and AOM/DSS treated WT and TLR6KO mice under different housing conditions. A-D. Data is pooled from two independent experiments with a total of 3-6 mice per group. A-D data is presented as mean + s.e.m. B-D individual points for each mouse are shown. C-D, $p < 0.001$, AMOVA.

Principal coordinate of analysis (PCoA) of naïve and SH-WT mice revealed that the colonic contents cluster distinctly depending on whether they were taken pre- or post-AOM/DSS treatment, whereas CH-WT mice have a microbiota more similar to naïve mice regardless of AOM/DSS treatment (Figure 6.3C). PCoA revealed a higher degree of likeness pre-AOM/DSS treatment in co-housed WT and TLR6KO mice than to their respective single house counterparts, suggesting that housing exerted a strong influence over composition in a steady state (Figure 6.3D). This influence was maintained under inflammatory conditions as the co-housed WT and TLR6KO mice clustered separately from both SH-WT and SH-TLR6KO following AOM/DSS treatment (p=0.006, AOM/DSS SH-WT vs CH-WT) (Figure 6.3D). However, the compositional changes that occurred in the SH-WT and SH-TLR6KO during AOM/DSS treatment were highly influenced by genotype as they showed distinct clusters in the PCoA (Figure 6.3D). Genotype and housing influence the kinetics and composition of the gut microbiota during AOM/DSS. The genus-level bacteria that were significantly affected by the interaction of housing and genotype by 3-way ANOVA, included *Porphyromonas* (p<0.0001), *Tannerella* (p<0.0001), *Prevotella* (p=0.0003), *Lactobacillus* (p<0.0001) and *Clostridium* (p=0.0122) (Supplementary Figure 6.1A). In order to more fully understand the changes in the composition, we collected colonic samples over the course of AOM/DSS treatment and performed PCR using primers that bind within conserved areas of 16S rDNA to identify bacterial families[31]. We found that the housing status had a significant impact on levels of bacterial DNA in the colon (Supplementary Figure 6.1B). In naïve co-housed mice roughly 50% of the total 16S rDNA was identified as Porphorymonadaceae, compared to only 15% in naïve single-housed mice of both genotypes (Supplementary Figure 6.1B). During AOM/DSS treatment, the levels of Porphorymonadaceae decreased in the co-housed mice regardless of genotype, increased in the SH-TLR6KO and stayed relatively the same in SH-WT mice (Supplementary

Figure 6.1B). In all untreated mice 30-40% of the total 16S DNA belonged to Lactobacillaceae. Upon AOM/DSS treatment we found that the SH-TLR6KO mice were able to maintain levels of Lactobacillaceae DNA until the second round of DSS, while these levels dropped significantly after the first round of DSS in SH-WT mice (Supplementary Figure 6.1B). In the co-housed mice we found that housing status had a positive effect on the amount of Lactobacillaceae DNA, as neither CH-WT nor CH-TLR6KO mice exhibited a reduction after the first or second rounds of DSS, and both genotypes maintained relatively consistent levels of Lactobacillaceae DNA throughout the experiment (Supplementary Figure 6.1B). After the first round of DSS, when the levels of Lactobacillaceae DNA dropped in the SH-WT mice, we found that Helicobacteraceae DNA increased from 1% to 15% (Supplementary Figure 6.1B). Unlike the SH-WT, we saw no increase in Helicobacteraceae in the co-housed mice or the SH-TLR6KO mice (Supplementary Figure 6.1B). Taken together, these data demonstrate the absence of TLR6 signaling affects the compositional changes during AOM/DSS and that co-housing allows a maintenance of probiotic Lactobacillaceae, suggesting that both genotype and housing influence the kinetics and composition of the gut microbiota during AOM/DSS.

Restoring commensals ameliorates disease and reduces inflammatory cytokines in WT mice via a TLR6-dependent mechanism.

Many Lactobacillus exist within our GI tract and confer health benefits, thus the overall reduction in the abundance of Lactobacillus observed in SH-WT and SH-TLR6KO during inflammation-associated CRC led us to hypothesize that a re-colonization strategy using Lactobacillus could be efficacious in treating disease. To accomplish this, mice were administered a mixture of two taxa that were the most reduced as determined by OTUs in our tumor model (*L. johnsonii* and *L. reuteri*) or a species that was not found either naïvely or post-AOM/DSS (*L. rhamnosus GG*). These OTUs were confirmed via 16S sequencing and through the bacterial isolation and culture of colonic contents from mice pre- or post-AOM/DSS (data not shown). To ensure that any effect on tumor development was not due to the metabolism of AOM by the *Lactobacillus*, the re-colonization was performed 5 days post-AOM injection, beginning simultaneously with DSS administration, and given every other day for a total of 4 feedings. This regimen was repeated for each round of DSS (Figure 6.4A).

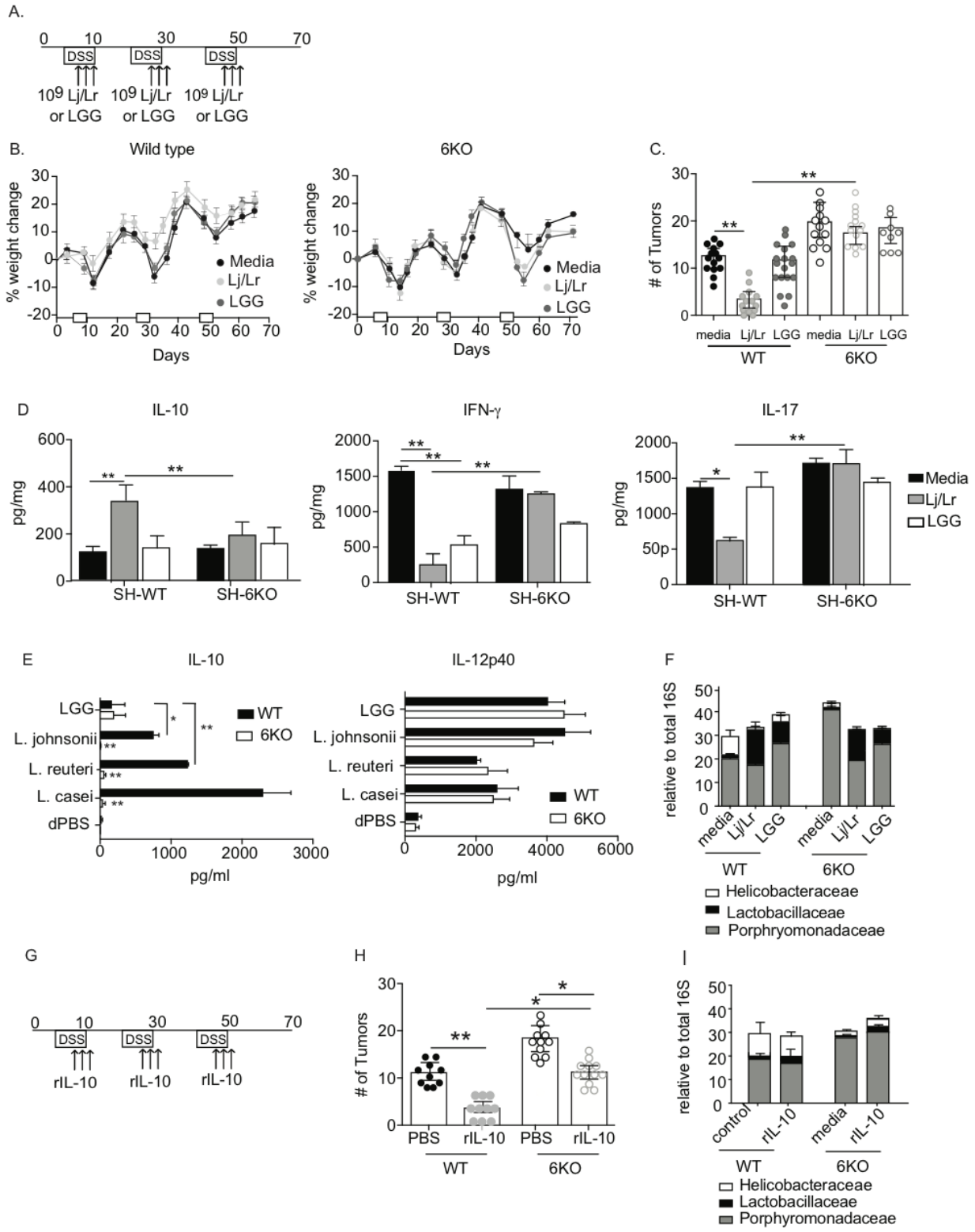

Figure 6.4: Restoration of* Lactobacillus *reduces tumor burden and suppresses inflammation in a TLR-6 dependent and independent manner.

Figure 6.4: Restoration of Lactobacillus reduces tumor burden and suppresses inflammation in a TLR-6 dependent and independent manner. (A) Methods for Figure 5 showing mice received an oral inoculation of sham (media) (n=9), *L. johnsonii* and *L. reuteri* (Lj/Lr) (n=11) or LGG (n=6) at the time-points indicated in the text and Materials and Methods. (B) % weight change and (C) number of macroscopic tumors from mice. (D) Levels of indicated cytokines from colonic lysates as measured by ELISA. (E) Concentration of IL-10 and IL-12p40 produced from WT or TLR6KO BMDC stimulated for 24 hours with 106 cfu indicated *Lactobacillus* species. (F) Relative DNA levels of indicated bacterial families to total 16S rDNA from colon taken at day 66. (G) Same method as in (A, above) except WT mice were given an i.p. injection of rIL-10 instead of Lactobacillus and (H) the number of tumors and (I) the relative DNA levels of indicated bacterial families to total 16S rDNA from colon at day 66. A-I, Data is the mean + s.e.m of 7-12 mice pooled from 3 independent experiments. *, $p< 0.05$; **, $p<0.01$, C-F, Student's t-test; H-I Two-way ANOVA with Bonferroni post-hoc tests.

Physical observations after administration of *L. johnsonni/L. reuteri* (Lj/Lr) revealed no effect on weight (Figure 6.4B), however the SH-WT mice treated with Lj/Lr had significantly fewer tumors than the media control treated SH-WT mice (Figure 6.4C). Further, the reduction in tumor number seemed to be dependent upon TLR6 expression as Lj/Lr treatment failed to reduce tumor number or size in the SH-TLR6KO mice (Figure 6.4C). In contrast, treating SH-WT mice with *L. rhamnosus GG* (LGG) failed to suppress both tumor number and size (Figure 6.4C).

Analysis of the mucosal cytokines associated with Lactobacillus treatment revealed distinct cytokine patterns. SH-WT mice treated with Lj/Lr had a significant increase in anti-inflammatory IL-10 and subsequent suppression of inflammatory cytokines, IFN-γ and IL-17, compared to control media treated WT mice (Figure 6.4D). The observed cytokine effects were also mediated by TLR6 as Lj/Lr treated SH-TLR6KO mice were unable to induce IL-10 or suppress IFN-γ or IL-17 (Figure 6.4D). In contrast, treatment with LGG had no effect on cytokine production and seemed to be independent of TLR6 signaling as WT and TLR6KO mice had similar cytokine patterns (Figure 6.4D).

In addition to their ability to secrete anti-microbial peptides[32] and shift the pH of the colonic environment to kill pathogenic bacteria[33], *Lactobacillus* are also well known for their anti-inflammatory properties[34]. Our group and others have shown that TLR6 signaling in antigen presenting cells promotes IL-10 production[35] and polarize anti-inflammatory T cells[36]. As we observed IL-10 production in SH-WT mice treated with Lj/Lr, but not by LGG, we wanted to assess the ability of a panel of lactic acid-producing bacteria to induce IL-10 and IL-12p40 and determine their dependency on TLR6 by using bone-marrow derived dendritic cells

(BMDC) from naive WT and TLR6KO mice. *L. johnsonii*, *L. reuteri* and *L. casei* induced IL-10 and IL-12p40 from WT BMDCs, but only IL-10 was dependent upon the expression of TLR6 (Figure 6.4E). LGG stimulated BMDC were able to produce IL-10 regardless of TLR6 expression and had a robust TLR6-independent IL-12p40 response (Figure 6.4E). These data suggest that LGG induces low amounts of IL-10 through a TLR6-independent mechanism and could explain its inability to protect WT mice.

We next wanted to determine if the Lj/Lr treatment had any effect on the microbiota by screening the colonic contents of mice at the end of the AOM/DSS treatment by qPCR using the same primers used in Figure 4. Confirming our 16S and qPCR data, we detected high amounts of Helicobacteraceae DNA in colons from SH-WT mice, while SH-TLR6KO mice had higher amounts of Porphyromonadaceae DNA and only a small amount of DNA from Helicobacteraceae (Figure 6.4F). Treatment with Lj/Lr was able to reduce the levels of Helicobacteraceae and Porphyromonadaceae in both the SH-WT and SH-TLR6KO mice, respectively (Figure 6.4F). Despite the lack of any anti-tumor activity in our model, we found that LGG treatment was also able to reduce the amount of Helicobacteraceae and Porphyromonadaceae DNA recovered from the colons of both SH-WT and SH-TLR6KO mice. Interestingly, treatment by either Lj/Lr or LGG resulted in an increase in Lactobacillaceae DNA in both WT and TLR6KO mice (Figure 6.4F).

IL-10 is responsible for the partial reduction in tumor number but is dispensable for changes in the microbiota

The molecular pathobiology of CRC has implicated inflammation in the promotion of tumor progression, invasion, and metastasis[37]. A clear example of this is the finding that patients with inflammatory bowel disease are at higher risk of CRC[38]. One mechanism that could account for the reduction in tumor number observed in SH-WT mice given Lj/Lr may be the ability to limit inflammation via the production of IL-10. To evaluate whether IL-10 alone was sufficient to suppress tumor number and limit colonization by Helicobacteraceae, we substituted Lj/Lr treatments with direct intraperitoneal (i.p.) administration of recombinant IL-10 (rIL-10) (Figure 6.4G). This protocol allowed us to determine if IL-10 could mediate any of the phenotype observed in Lj/Lr treated WT mice. Further, it would allow us to determine the requirement for TLR6, as administration of rIL-10 to TLR6KO mice would bypass the need for TLR6 signaling, and these mice should behave more similarly to the WT mice treated with AOM/DSS. Similar to treatment with Lj/Lr,

rIL-10 provided a partial reduction in tumor number in SH-WT mice (Figure 6.4H), but it failed to reduce the amount of Helicobacteraceae DNA (Figure 6.4H-I). As expected, the TLR6KO mice treated with rIL-10 treatment also had a significant reduction in the number and size of tumors compared to control treated TLR6KO mice given AOM/DSS (Figure 4.4H). However, the number of tumors was still significantly higher in the TLR6KO mice treated with rIL-10 than WT mice given rIL-10 (Figure 6.4H) suggesting that there may be other molecular pathways contributing to the development of tumors in the TLR6KO mice. Similar to WT mice, we found no effect on the level of Helicobacteraceae or Porphyromonadaceae DNA in the colons of the rIL-10-treated TLR6KO mice.

The requirement for *Lactobacillus*-induced IL-10 was also further determined by co-administering a neutralizing antibody against IL-10 beginning one day prior to treatment with Lj/Lr and continuing for two days post-treatment (Figure 6.5A). Co-administration of an IL-10-neutralizing antibody with Lj/Lr had little effect on the weight of SH-WT or SH- TLR6KO mice (Figure 6.5B). Neutralizing IL-10 in the absence of Lj/Lr had no effect on the number of tumors observed in WT or TLR6KO mice (Figure 6.5C). Co-administration of anti-IL-10 with Lj/Lr only partially reversed the reduction in tumor number and had no effect on the levels Helicobacteraceae DNA in WT mice (Figure 6.5C-D). As expected, neutralizing IL-10 during Lj/Lr treatment in TLR6KO mice had little effect, likely due to the inability of TLR6KO mice to produce IL-10 during treatment (Figure 6.5B-D). Analysis of the mucosal cytokines demonstrated that neutralizing IL-10 was able to reverse the reduction in the levels of IFN-γ and IL-17 observed in Lj/Lr treated SH-WT mice (Figure 6.5E). Taken together, these results demonstrate that IL-10 production by Lj/Lr can partially explain the reduction in tumor size and number. While IL-10 did play a partial role in the reduction of tumors, it had no impact on the amount of Helicobacteraceae, Porphyromonadaceae or Lactobacillaceae DNA. These data thereby dissociate the anti-inflammatory effects of IL-10 from the regulation of the microbiota in inflammation-associated CRC.

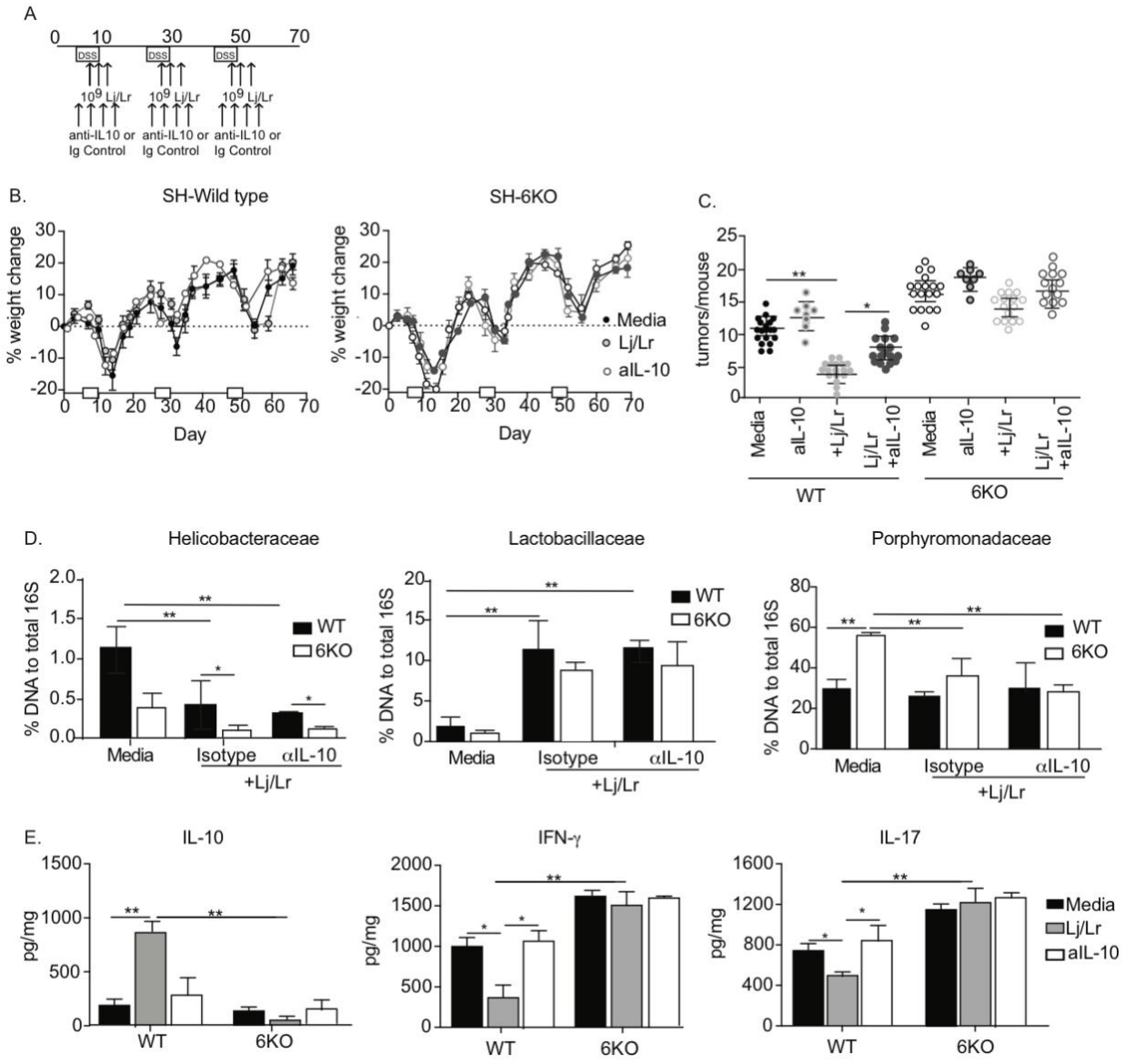

Figure 6.5: Requirement for IL-10 dissociates Lactobacillus effects on inflammation and composition.

(A) Methods. Mice were treated as described in Figure 5A and Materials and Methods but instead a monoclonal antibody against IL-10 was administered i.p. at indicated time points during Lj/Lr treatments. (B) % weight change and (C) number of tumors from mice receiving Lactobacillus plus anti-IL-10 or control immunoglobulin (isotype). (D) Relative DNA levels of indicated bacterial families to total 16S rDNA from colon taken at day 66. (E) Levels of cytokines detected from colonic lysates of mice at day 66 by ELISA. B-E, Data is represented as the mean ± s.e.m of 8-12 mice pooled from 3 independent experiments. C-E, *, $p < 0.05$. **, $p < 0.01$. Two-way ANOVA with Bonferroni post-hoc test.

Impaired apoptosis during AOM/DSS in TLR6-deficient mice

While the data above provide evidence as to how co-housing would lead to reduced tumors in the WT mice, it does not address why both single and co-housed TLR6KO mice have more tumors than the SH-WT mice. We hypothesized that in the absence of TLR6 an important cellular regulatory pathway may be altered leading to an environment more sensitive to mutagenesis. We also hypothesized that this effect would be independent of a specific microbiota signature, as the CH-TLR6KO and SH-TLR6KO have distinct colonic microbial compositions.

One of the early steps in CRC progression is the increase in epithelial cell proliferation and/or an inhibition of apoptosis. To assess the proliferation of enterocytes, we performed immunohistochemical staining on colon sections of AOM/DSS treated WT and TLR6KO mice for Ki67 and bromodeoxyuridine (5-bromo-2'-deoxyuridine, BrdU). Ki67 is a commonly used marker that identifies cells that have recently undergone proliferation by labelling S, G1, and G2 phases of the cell cycle, while BrDU incorporates into newly synthesized DNA in actively replicating cells during S phase. There was an increase in the number of Ki67+ cells found in both the co-housed and single genotype housed TLR6KO mice compared to WT mice (Figure 6.6A). Two hours following injection of BrdU into AOM/DSS treated mice the colons were removed and stained for actively proliferating cells. In contrast to the Ki67 staining, we identified on average 3-4 BrdU+ cells per crypt, regardless of housing or genotype (Figure 6.6A). These data indicate that the disruption of TLR6 signaling or the housing status was not impacting the turnover of intestinal stem cells. In order to assess whether the TLR6KO mice may have defects in apoptosis[39], we performed immunohistochemistry on AOM/DSS colons looking for the anti-apoptotic factor Bcl-2. Analysis of the stained tissue revealed many Bcl-2+ cells within the epithelium, as well as in the lamina propria of SH-TLR6KO and CH-TLR6KO mice compared to WT mice (Figure 6.6B). TLR2 signaling has been shown to signal through the PI3K/Akt pathway[40]. Pi3K/Akt has been shown to phosphorylate Stat3 which has been shown to influence apoptosis and proliferation signals in enterocytes[39,40]. We performed Western blot analysis on the colonic enterocytes at day 28 during AOM/DSS to assess if signaling pathways upstream and downstream of Bcl-2 were disturbed in the TLR6KO mice, thereby driving less apoptosis and making these mice more sensitive to AOM/DSS. Both SH- and CH-TLR6KO mice had lower levels of cleaved caspase-3 compared to WT mice (Figure 6.6C). Despite the reduction in cleaved caspase-3 and the increase in Bcl-2, the TLR6KO mice had

and similar levels of phosphorylated Akt and phosphorylated Stat3 (Figure 6.6C). Taken together these data suggest that the deficiency in TLR6 may lead to an anti-apoptotic response that is Stat3- and Akt-independent but involves Bcl-2 and cleaved caspase-3.

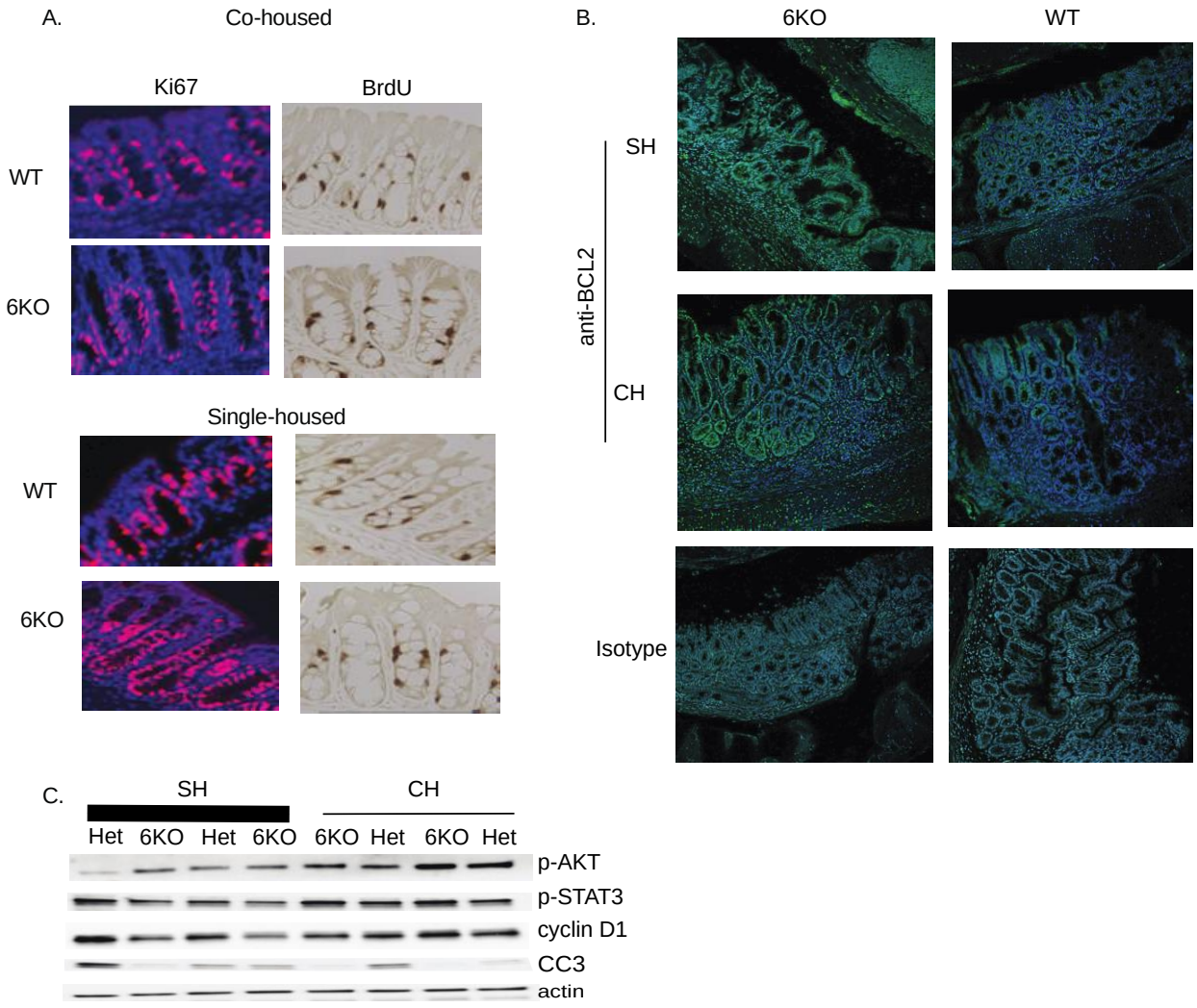

Figure 6.6: Proliferation and apoptosis of colonocytes are altered in TLR6KO mice.
(A) Colons from mice at day 28 post-AOM/DSS stained with Ki67 or from mice injected with BrdU 2 hours before the end of the experiment. Representative image from one of 3-5 mice per group (B) Histological sections of the colon from mice at day 28 stained with anti-Bcl-2 antibody or isotype control. Representative image from one of 3-6 mice per group (C) Western blot of whole colon from individual mice at day 28 post-AOM/DSS blotted for phosphorylated Akt, phosphorylated Stat3, and Cleaved caspase-3.

6.4 Discussion

In the present study, we established a potential treatment for CRC using a microbiome-associated therapy that restores commensal species lost during inflammatory disease. Compositional data generated by 16S rRNA sequencing of colons from AOM/DSS treated WT mice revealed a distinct microbiota from their naïve counterparts. Most noticeably, was an increase in the abundance of cancer-promoting Helicobacteraceae, and a loss of beneficial Lactobacillaceae. Restoring *Lactobacillus* dampened inflammation and reduced tumor number. These data underscore the need for a more personalized approach in using probiotics to treat or ameliorate disease. The rationale "not all probiotics are created equal" has been used to explain the failure of probiotics in clinical trials, focusing on differences between bacterial species, strain or dose. However, data from this study and others[41,42] suggest that the personal relationship established between the innate immune system, intestinal cells and the resident commensals determine whether a given probiotic will be effective. Our study also demonstrates that the effects on inflammation-associated CRC by *L. johnsonii* and *L. reuteri* (Lj/Lr) are mediated by multiple mechanisms that can be dissociated from each other by the involvement of IL-10. While Lactobacillus has been shown to treat disease via IL-10-dependent[43,44] and IL-10-independent[45–48] mechanisms, our study demonstrates that the most efficient anti-tumor effects were associated with inhibiting inflammation and restoring microbial ecology by reducing the abundance of Proteobacteria.

Genetics play an important part in disease susceptibility and response to treatment, yet their impact on the microbiota is still not understood. Here, genetic ablation of Tlr6 in mice was associated with an increased incidence of tumors, and an insensitivity to Lj/Lr therapy. Our data suggests that expression of TLR6 is critical for the production of IL-10 during treatment with Lj/Lr, confirming our previous studies linking TLR6 signaling with IL-10[49] and further implicating the role of TLR6 in the sensing of endogenous microbial signals. TLR6 signaling did have an effect on the kinetics associated with the loss of *Lactobacillus*, with a more gradual decrease observed in the TLR6KO mice. The prolonged presence of the *Lactobacillus* had no beneficial effect on tumor number in TLR6KO mice, likely due to their inability to sense immune-modulatory ligands through TLR6 and induce IL-10. However, the prolonged presence of *Lactobacillus* in AOM/DSS-treated TLR6KO mice had a protective effect on WT mice when co-housed together. It may be that the WT mice were able to maintain Lactobacillus levels due to ingestion/exposure of *Lactobacillus* in

TLR6KO stool through coprophagy and this helped prevent tumors in these mice. Indeed, our data shows that restoring *Lactobacillus* species during DSS exposures was able to reduce the tumor burden in SH-WT mice in part through production of IL-10.

Compositional analysis of the colonic microbiota by 16S sequencing and qPCR revealed that SH-WT mice had an increase in Helicobacteraceae, while the TLR6KO mice had an increase in Porphyromonadaceae. Each of these increases occurred when Lactobacillaceae was lowest after the first or second round of DSS in the WT and TLR6KO mice, respectively. It is plausible that Helicobacteraceae has only a small window of opportunity when a comfortable niche is created by the absence of Lactobacillus. If this window is missed than other commensals, such as Porphyromonadaceae, may fill that niche. Our data would suggest that innate immune sensing of the endogenous microbiome impacts dysbiosis through altering the kinetics in which bacterial species are reduced and by contributing to the inflammatory milieu of the local tissue microenvironment. These data imply that the genetics of the host are linked to dysbiosis through expression of such receptors and could possibly explain why many of the polymorphisms associated with IBD involve innate immune sensing.

The contribution of innate signaling to the cytokine milieu of the local tissue microenvironment must also not be overlooked. Here, IL-10 production by the *Lactobacillus* was almost completely dependent on TLR6 as BMDCs deficient in TLR6 failed to produce IL-10 after stimulation by these bacteria, but also by the finding that the beneficial effects of *Lactobacillus* are lost in TLR6KO mice. Importantly, we observed that after treatment with *Lactobacillus*, decreases in Helicobacteraceae and Porphyromonadaceae were both IL-10 and TLR6-independent. While this study did not identify the mechanism by which Lj/Lr modulates the microbiota, treatment with rIL-10 or neutralization of IL-10 during Lj/Lr administration had little effect on the levels of Helicobacteraceae and Porphyromonadaceae, thus ruling out a role of IL-10 in dysbiosis and indicating an IL-10-independent role for Lactobacillus in maintaining microbial ecology.

Regardless of housing, TLR6KO mice had higher tumor numbers and higher mortality compared to the WT mice. This increased tumor number is likely independent of the microbiota as single and cohoused TLR6KO mice had very different microbiomes at both the induction of the AOM/DSS and after the 66 days. We found

that TLR6KO mice have higher levels of Ki67+ cells in the intestinal epithelium during AOM/DSS. Further molecular analysis revealed an increase in the anti-apoptotic molecule Bcl-2 in the TLR6KO mice regardless of housing status. In line with the increase in Bcl-2, we also observed diminished cleaved caspase-3. TLR2 signaling has been shown to activate PI3K/Akt[39] and can regulate Bcl-2 via phosphorylation of Stat3[41–43]. However, we found that Akt, and Stat3 were not phosphorylated in the TLR6KO mice at day 28 of AOM/DSS were unchanged and may not be involved in the TLR6 signaling cascade leading to Bcl-2 activation.

Altogether, our findings highlight several important concepts and introduce novel paradigms in the relationship between chronic inflammation and its effects on the microbiota. First, microbiota-associated therapies can protect against tumorigenesis if they are specific and personal. Here, this effect was mediated through a TLR6-dependent induction of anti-inflammatory IL-10 and by altering the abundance of cancer-promoting commensals. Second, the genotype of an individual shapes the composition of the microbiota under chronic inflammatory conditions, biases the cytokine milieu of the tissue microenvironment and influences the response to microbiota-associated therapies. Lastly, our study establishes TLR6 as an important molecule involved in modulating the microbiota and immune response during inflammation-associated CRC. We originally examined TLR6 because of its profound requirement for IL-10 induction by *Lactobacillus* but discovered that TLR6 signaling influences the kinetics of compositional changes within the microbiota during inflammation. The strong influence of genetics and environment on the microbiota and the response to microbiota-associated therapy suggest that a personalized approach to understanding the microbiota during disease will be critical to the development of new microbiota-associated therapies.

6.5 Materials and Methods

Animals

TLR6KO and littermate control mice were bred in-house and maintained in a specific pathogen free facility at the University of Southern California. All mice used in these experiments were generated from 5-7 different founder cages where all female mice were wild type for TLR6. At the time of weaning pups from different litters but of the same sex were mixed together for group housing to reduce founder and cage effects on the microbiome. Mice were fed a standard rodent diet AIN-78 (Lab diets, St. Louis, MO) and

given non-chlorinated, non-acidified, distilled water ad libitum. All animal experiments were performed in accordance with institutional guidelines following experimental protocol review and approval by the Institutional Biosafety Committee and the Institutional Animal Care and Use Committee. Induction of inflammation-associated colorectal cancer 6- to 8-week-old female mice were injected intraperitoneally with 10 mg/kg azoxymethane (AOM; Sigma-Aldrich Chemical Co, St. Louis, MO). After 5 days, mice received 2.5% (w/v) dextran sulfate sodium (DSS; Affymetrix, Santa Clara, CA, molecular weight 35,000–50,000 kDa) in drinking water for 5 days followed by 16 days of regular drinking water. Mice were subjected to two additional DSS cycles[50]. The clinical course of disease was monitored by measurement of body weight, observation of rectal bleeding, diarrhea, and bloody stool during DSS treatment. Mice were euthanized 66 days post-AOM injection using CO2 followed by cervical dislocation.

Pathology and Scoring

The gastrointestinal tract was removed and the colon separated from the cecum. Macroscopic assessment of colonic tumors was noted and images taken to determine tumor size using ImageJ software. The colon was placed into 10% neutral buffered formalin, prepared in a “Swiss roll” technique[51], routine-processed for paraffin embedding and stained with hematoxylin and eosin. Colons were scored by a veterinary pathologist blinded to experimental groups. Inflammation scores were based on the severity of mucosal loss, crypt inflammation, lamina propria mononuclear cells, neutrophils, epithelial hyperplasia mucosal epithelial hyperplasia, dysplasia presence and extent of pathology as modified from Suzuki et al[52] and Kennedy et al[53]. Proliferative lesions were graded according to Boivin et al[54] with invasive carcinoma defined as invasion into the lamina propria or into but not through the muscularis mucosa, sparing carcinoma.

Collection of luminal and mucosal associated microbiota samples

Colons were removed and placed onto a chilled glass plate on ice and opened longitudinally. Luminal contents were collected and placed in a 1.5 ml conical tube. The colon tissue was then rinsed with ice cold PBS and then washed by submerging tissues into clean sterile PBS and then vigorously shaken for 5 seconds. This was repeated 5 times and then the colon was placed back onto glass plate and glass slides were used to gently scrape the colon tissue removing the mucosa. This was then added to the luminal contents and used for sequencing.

454 Pyrosequencing, sequence curation and microbiome analysis

Microbiota samples were processed and sequenced at Research and Testing Laboratory (RTL; Lubbock, TX) based upon RTL protocols using a Roche FLX Titanium genome sequencer. Universal bacterial primers 28F 'GAGTTTGATCNTGGCTCAG' and 519R 'GTNTTACNGCGGCKGCTG' were used to amplify the variable regions V1-V3 of the 16S rRNA genes. 16s rRNA gene sequences were curated using mothur v.1.35.1[55]. Briefly, sequences were denoised using a flow gram denoising algorithm[56], aligned to Silva 16s rRNA sequence database[57], and pre-clustered to allow up to a 2-bp difference between sequences[58]. Chimeras were detected using UCHIME[59] and were culled along with chloroplast and mitochondrial sequences. Sequences were then classified using the Ribosomal Database Project version 14 with a confidence score greater than 80%[60] and phylotyped to the family level. Prior to any data analysis the number of sequences were normalized per sample to at least 2000 sequences. Beta diversity was calculated using the Theta YC distance metric with the family-level data and visualized using principal coordinates analysis (PCoA).

Bacterial quantitative-PCR

DNA was extracted from proximal colonic contents using an ISOLATE Fecal DNA kit (Bioline, Taunton, MA). qPCR was performed on a CFX96 TouchTM Real-Time PCR Detection System (Bio-Rad Laboratories, Irvine, CA) using a SensiFAST SYBR® No-ROX Kit (Bioline) with 20 ng of bacterial DNA and the following primers: Helicobacteraceae primers forward (5'-CCGCAAATTGCAGCAATACTT-3') and reverse (5'-TCGTCC AAAATGCACAGGTG-3'); Lactobacillaceae 16S primers LabF362(5'-AGCAGTAGGGAATCTTCCA-3') and LabR677 (5'-CACCGCTACACATGGAG-3'); Porphyromonadaceae primers forward (5′-GGTGTCGGCTTAAGTGCCAT-3′) and reverse (5′-CGGA(C/T)GTAAGGGCCGTGC-3′). 10-fold serial dilutions of plasmid-based *H. hepaticus*, *L. reuteri*/*L. johnsonii* or *Tannerella forsythia* genomic DNA was used to generate a standard curve. Relative abundance was calculated by a ratio of the organism- specific DNA to total bacterial DNA used for the amplification.

***Lactobacillus* treatments**

L. johnsonii, *L. reuteri,* and LGG (*L. rhamnosus GG*) were grown overnight at 37°C in *Lactobacilli* MRS broth (EMD Chemicals, Gibbstown, NJ). Cultures were diluted the next day in sterile PBS, and concentrated

to 10_{10} CFU/ml. On day 2 of each DSS round, mice were administered 100 µl by intragastric gavage every other day for 10 days (total of 5 gavages).

ELISA

Colonic lamina propria was isolated, pelleted and protein determination was performed by Bradford assay. ELISA was performed according to product instructions from BD OptEIA kits (IFN-γ and IL-10) and R&D Systems kits (IL-13 and IL-17).

Quantitative reverse transcription PCR (qRT-PCR)

Colons were flushed with PBS, opened longitudinally and segmented into two sections. One third of the entire length of the colon measured up from the anus was denoted as distal, while the remaining two thirds of the colon was identified as proximal. RNA was extracted from mucosal scrapings using ISOLATE II RNA Mini Kit (Bioline, Taunton, MA) and reverse transcribed into cDNA with SensiFAST cDNA Synthesis Kit (Bioline). qRT-PCR was performed on a CFX96 TouchTM Real-Time PCR Detection System (Bio-Rad Laboratories, Irvine, CA) using a SensiFAST SYBR® No-ROX Kit (Bioline) with the following primers: Tbet forward 5'-AGCAAGGACGGCGAAGTT-3'; Tbet reverse 5'-GGGTGGACATATAAGCGGTTC-3'; Gata3 forward 5'-CAACCTCTACCCCACTGTG-3'; GATA3 reverse 5'-GATGTCCCTGCTCTCCTTG-3'; Rorc forward 5'-GCCTACAATGCCAACAACCACACA-3'; Rorc reverse 5'-ATTGATGAGAACCAGGGCCGTGTA-3'; Foxp3 forward 5'-AGAGAGGTATTGAGGGTGGG-3'; Foxp3 reverse 5'-GCTGAGATGTGACTGTCTTCC-3'; 18S forward 5'-GTAACCCGTTGAACCCCATT-3'; and 18S reverse 5'- CCATCCAATCGGTAGTAGCG-3'. Gene expression levels for each individual sample were normalized to that of 18S. Fold changes in gene expression were relative to unstimulated controls and calculated using the ΔΔCt method.

Dendritic cell isolation and stimulation

To purify dendritic cells, MLNs were digested with 400 units per ml of collagenase type IV (Sigma-Aldrich). After filtering, the cells were re-suspended in 22.5% Optiprep (Sigma-Aldrich), overlaid with Hank's Balanced Salt Solution Saline (HBSS, Sigma-Aldrich) and centrifuged at 670g for 30 minutes. Dendritic cells were harvested from the interface of the HBSS and Optiprep, incubated with anti-CD11c (Miltenyi),

and positively selected for CD11c using Automacs (Miltenyi). After isolation, the cells were stimulated overnight with bacterial lysates at 37°C before performing the ELISAs.

rIL-10 and αIL-10 treatments

In some experiments, mice were treated with probiotic bacteria and/or, corresponding to the days of probiotic therapy, were administered 200 µg of anti-IL-10 or anti-IgG1 (Bio X Cell, West Lebanon, NH) intraperitoneally. In other experiments mice were administered 1 ng of rIL-10 (R&D) diluted in 500 µl sterile PBS given intraperitoneally 3 times during every DSS cycle: on day 2, day 4 and the day after discontinuation of the DSS.

Immune fluorescence

Murine colons were rolled using the Swiss roll technique and fixed in 10% neutral buffer formalin (VWR International, Visalia, CA) overnight. Paraffin-embedded (without formalin) tissues were cut 5 µm thick. Hematoxylin and eosin, was performed by AML labs (Saint Augustine, FL) or in-house. Rabbit polyclonal IgG, (Abcam, ab27472), rabbit monoclonal IgG (Abcam, ab172730), anti-bcl2 (clone 3F11). BrdU staining was performed as per manufacturer's instructions (Abcam). For antigen retrieval, slides were placed into tubes containing sodium citrate buffer (pH 6.0) (Sigma-Aldrich, St. Louis, MO) buffer and heated at 99°C in water bath. The slides were washed and blocked before staining with primary antibody. The slides with primary antibody were incubated overnight at 4°C in a humid chamber and the following day, washed and incubated with secondary at 37°C for 1 hour. The slides were mounted with DAPI and confocal images were acquired using a Nikon Eclipse C1 laser-scanning microscope (Nikon, PA) fitted with a 60 Nikon objective (PL APO, 1.4NA) and Nikon image software.

Western Blot

Colonic scrapings of the whole colon were placed in radio-immunoprecipitation assay (RIPA) buffer (VWR) containing protease and phosphatase inhibitors (Thermofisher). Samples were normalized for protein content using Bradford reagent (Bio-Rad, 500-0205). Protein was separated by size by SDS-PAGE using Mini-Protein tris-glycine gels (4-15%) (Bio-Rad, 456-1083) and transferred to PVDF membrane for blotting. Membranes were blocked with 3% dry nonfat milk in Tris-Buffered Saline (TBS) containing 0.05% tween-

20 and incubated with primary antibody overnight at 4°C ((anti-cleaved caspase 3 (clone 3F11, Abcam); anti-pAkt thr308 (clone 244F9, Abcam); anti-pStat3 Y705 (clone S727, Abcam)). Membranes were washed with TBS containing 0.05% tween-20 and incubated with goat anti-rabbit-HRP secondary antibody (Santa Cruz Biotechnology) for 2 hours at room temperature. Membranes were developed using SuperSignal West Femto Maximum Sensitivity kit (Thermo Scientific) according to manufacturer's instructions and imaged using a LiCOR Odyssey.

Statistics

Data are expressed either as the mean value + standard error of the mean (s.e.m.) or as individual values. Specific statistical tests used for each experiment are described in the figure legends and performed in Graphpad PRISM (Graphpad Software LLC, San Diego CA). $p < 0.05$ was considered significantly different.

6.6 Supplemental Materials

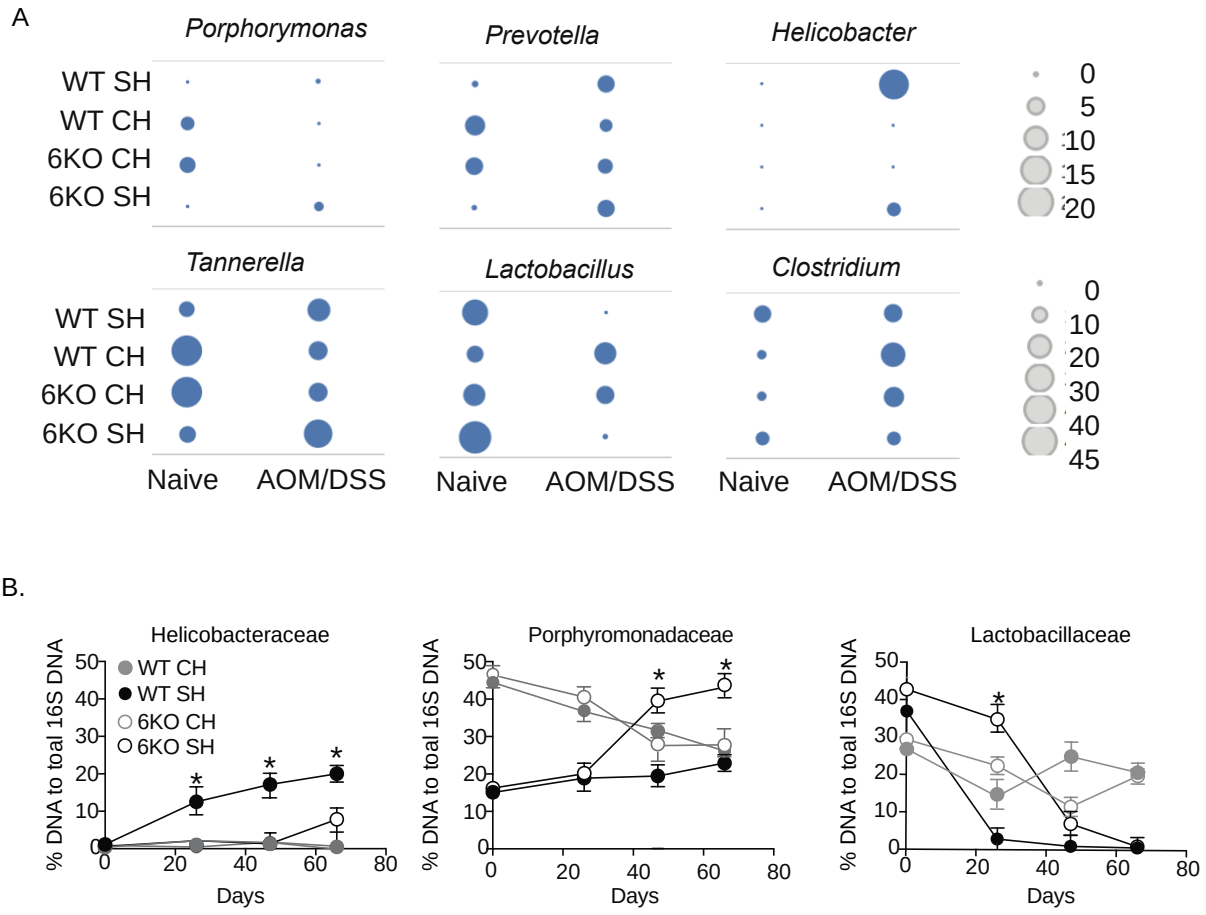

Supplemental Figure 6.1: TLR6 signaling impacts dysbiosis associated with AOM/DSS.

(**A**) Proportion of genus-level bacteria affected by the interaction of housing and genotype obtained by 16S rDNA sequencing. (**B**) Colonic contents were scraped from mice at the indicated time points. DNA was amplified using bacterial family specific primers for Helicobacteraceae, Porphyromonadaceae and Lactobacillaceae. Data is the mean ± s.e.m. of 5-7 mice pooled over two experiments. *, $p < 0.05$, **, $p < 0.01$, Two-way ANOVA with individual post-hoc tests (**A**) and Student's t-test (**B**).

6.7 References

1. Siegel RL, Miller KD, Fedewa SA, et al. Colorectal cancer statistics, 2017. *CA Cancer J Clin*. 2017;67(3):177-193. doi:10.3322/caac.21395

2. Lichtenstein P, Holm NV, Verkasalo PK, et al. Environmental and Heritable Factors in the Causation of Cancer — Analyses of Cohorts of Twins from Sweden, Denmark, and Finland. *N Engl J Med*. 2000;343(2):78-85. doi:10.1056/NEJM200007133430201

3. Grady WM. Genetic testing for high-risk colon cancer patients. *Gastroenterology*. 2003;124(6):1574-1594. doi:10.1016/s0016-5085(03)00376-7

4. Elinav E, Nowarski R, Thaiss CA, Hu B, Jin C, Flavell RA. Inflammation-induced cancer: crosstalk between tumours, immune cells and microorganisms. *Nat Rev Cancer*. 2013;13(11):759-771. doi:10.1038/nrc3611

5. Gupta RB, Harpaz N, Itzkowitz S, et al. Histologic inflammation is a risk factor for progression to colorectal neoplasia in ulcerative colitis: a cohort study. *Gastroenterology*. 2007;133(4):1099-1105; quiz 1340-1341. doi:10.1053/j.gastro.2007.08.001

6. Shalapour S, Karin M. Immunity, inflammation, and cancer: an eternal fight between good and evil. *J Clin Invest*. 2015;125(9):3347-3355. doi:10.1172/JCI80007

7. Manichanh C, Borruel N, Casellas F, Guarner F. The gut microbiota in IBD. *Nat Rev Gastroenterol Hepatol*. 2012;9(10):599-608. doi:10.1038/nrgastro.2012.152

8. Maynard CL, Elson CO, Hatton RD, Weaver CT. Reciprocal interactions of the intestinal microbiota and immune system. *Nature*. 2012;489(7415):231-241. doi:10.1038/nature11551

9. Bäckhed F, Ley RE, Sonnenburg JL, Peterson DA, Gordon JI. Host-bacterial mutualism in the human intestine. *Science*. 2005;307(5717):1915-1920. doi:10.1126/science.1104816

10. Arthur JC, Perez-Chanona E, Mühlbauer M, et al. Intestinal inflammation targets cancer-inducing activity of the microbiota. *Science*. 2012;338(6103):120-123. doi:10.1126/science.1224820

11. Shen XJ, Rawls JF, Randall T, et al. Molecular characterization of mucosal adherent bacteria and associations with colorectal adenomas. *Gut Microbes*. 2010;1(3):138-147. doi:10.4161/gmic.1.3.12360

12. Chen W, Liu F, Ling Z, Tong X, Xiang C. Human intestinal lumen and mucosa-associated microbiota in patients with colorectal cancer. *PLoS ONE*. 2012;7(6):e39743. doi:10.1371/journal.pone.0039743

13. Zackular JP, Baxter NT, Iverson KD, et al. The gut microbiome modulates colon tumorigenesis. *MBio*. 2013;4(6):e00692-00613. doi:10.1128/mBio.00692-13

14. Flanagan L, Schmid J, Ebert M, et al. Fusobacterium nucleatum associates with stages of colorectal neoplasia development, colorectal cancer and disease outcome. *Eur J Clin Microbiol Infect Dis*. 2014;33(8):1381-1390. doi:10.1007/s10096-014-2081-3

15. Castellarin M, Warren RL, Freeman JD, et al. Fusobacterium nucleatum infection is prevalent in human colorectal carcinoma. *Genome Res*. 2012;22(2):299-306. doi:10.1101/gr.126516.111

16. Sears CL, Geis AL, Housseau F. Bacteroides fragilis subverts mucosal biology: from symbiont to colon carcinogenesis. *J Clin Invest*. 2014;124(10):4166-4172. doi:10.1172/JCI72334

17. Wu S, Rhee K-J, Albesiano E, et al. A human colonic commensal promotes colon tumorigenesis via activation of T helper type 17 T cell responses. *Nat Med*. 2009;15(9):1016-1022. doi:10.1038/nm.2015

18. Dalmasso G, Cougnoux A, Delmas J, Darfeuille-Michaud A, Bonnet R. The bacterial genotoxin colibactin promotes colon tumor growth by modifying the tumor microenvironment. *Gut Microbes*. 2014;5(5):675-680. doi:10.4161/19490976.2014.969989

19. Uronis JM, Mühlbauer M, Herfarth HH, Rubinas TC, Jones GS, Jobin C. Modulation of the intestinal microbiota alters colitis-associated colorectal cancer susceptibility. *PLoS ONE*. 2009;4(6):e6026. doi:10.1371/journal.pone.0006026

20. Vannucci L, Stepankova R, Kozakova H, Fiserova A, Rossmann P, Tlaskalova-Hogenova H. Colorectal carcinogenesis in germ-free and conventionally reared rats: different intestinal environments affect the systemic immunity. *Int J Oncol*. 2008;32(3):609-617.

21. Kawai T, Akira S. The role of pattern-recognition receptors in innate immunity: update on Toll-like receptors. *Nat Immunol*. 2010;11(5):373-384. doi:10.1038/ni.1863

22. Kordahi MC, William DePaolo R. The Influence of the Microbiota on the Etiology of Colorectal Cancer. In: Sun J, Dudeja PK, eds. *Mechanisms Underlying Host-Microbiome Interactions in Pathophysiology of Human Diseases*. Boston, MA: Springer US; 2018:167-193. doi:10.1007/978-1-4939-7534-1_8

23. Rasmussen SB, Reinert LS, Paludan SR. Innate recognition of intracellular pathogens: detection and activation of the first line of defense. *APMIS*. 2009;117(5-6):323-337. doi:10.1111/j.1600-0463.2009.02456.x

24. Rakoff-Nahoum S, Paglino J, Eslami-Varzaneh F, Edberg S, Medzhitov R. Recognition of commensal microflora by toll-like receptors is required for intestinal homeostasis. *Cell*. 2004;118(2):229-241. doi:10.1016/j.cell.2004.07.002

25. Round JL, Lee SM, Li J, et al. The Toll-like receptor 2 pathway establishes colonization by a commensal of the human microbiota. *Science*. 2011;332(6032):974-977. doi:10.1126/science.1206095

26. Chow J, Tang H, Mazmanian SK. Pathobionts of the gastrointestinal microbiota and inflammatory disease. *Curr Opin Immunol*. 2011;23(4):473-480. doi:10.1016/j.coi.2011.07.010

27. Trinchieri G. Cancer and Inflammation: An Old Intuition with Rapidly Evolving New Concepts. *Annu Rev Immunol*. 2012;30(1):677-706. doi:10.1146/annurev-immunol-020711-075008

28. Takeuchi O, Kawai T, Mühlradt PF, et al. Discrimination of bacterial lipoproteins by Toll-like receptor 6. *Int Immunol*. 2001;13(7):933-940. doi:10.1093/intimm/13.7.933

29. Takeuchi O, Sato S, Horiuchi T, et al. Cutting edge: role of Toll-like receptor 1 in mediating immune response to microbial lipoproteins. *J Immunol*. 2002;169(1):10-14. doi:10.4049/jimmunol.169.1.10

30. Lowe EL, Crother TR, Rabizadeh S, et al. Toll-like receptor 2 signaling protects mice from tumor development in a mouse model of colitis-induced cancer. *PLoS ONE*. 2010;5(9):e13027. doi:10.1371/journal.pone.0013027

31. Kamdar K, Khakpour S, Chen J, et al. Genetic and Metabolic Signals during Acute Enteric Bacterial Infection Alter the Microbiota and Drive Progression to Chronic Inflammatory Disease. *Cell Host Microbe*. 2016;19(1):21-31. doi:10.1016/j.chom.2015.12.006

32. Janakiram NB, Rao CV. The role of inflammation in colon cancer. *Adv Exp Med Biol*. 2014;816:25-52. doi:10.1007/978-3-0348-0837-8_2

33. Bansal P, Sonnenberg A. Risk factors of colorectal cancer in inflammatory bowel disease. *Am J Gastroenterol*. 1996;91(1):44-48.

34. Bedi A, Pasricha PJ, Akhtar AJ, et al. Inhibition of apoptosis during development of colorectal cancer. *Cancer Res*. 1995;55(9):1811-1816.

35. You X, Liu L, Zeng Y, et al. Macrophage-activating lipopeptide-2 requires Mal and PI3K for efficient induction of heme oxygenase-1. *PLoS ONE*. 2014;9(7):e103433. doi:10.1371/journal.pone.0103433

36. Alessi DR, Kozlowski MT, Weng QP, Morrice N, Avruch J. 3-Phosphoinositide-dependent protein kinase 1 (PDK1) phosphorylates and activates the p70 S6 kinase in vivo and in vitro. *Curr Biol*. 1998;8(2):69-81. doi:10.1016/s0960-9822(98)70037-5

37. Ohbayashi N, Ikeda O, Taira N, et al. LIF- and IL-6-induced acetylation of STAT3 at Lys-685 through PI3K/Akt activation. *Biol Pharm Bull*. 2007;30(10):1860-1864. doi:10.1248/bpb.30.1860

38. Zushi S, Shinomura Y, Kiyohara T, et al. STAT3 mediates the survival signal in oncogenic ras-transfected intestinal epithelial cells. *Int J Cancer*. 1998;78(3):326-330. doi:10.1002/(SICI)1097-0215(19981029)78:3<326::AID-IJC12>3.0.CO;2-4

39. Leslie K, Lang C, Devgan G, et al. Cyclin D1 is transcriptionally regulated by and required for transformation by activated signal transducer and activator of transcription 3. *Cancer Res*. 2006;66(5):2544-2552. doi:10.1158/0008-5472.CAN-05-2203

40. Barton BE, Karras JG, Murphy TF, Barton A, Huang HF-S. Signal transducer and activator of transcription 3 (STAT3) activation in prostate cancer: Direct STAT3 inhibition induces apoptosis in prostate cancer lines. *Mol Cancer Ther*. 2004;3(1):11-20.

41. Faith JJ, Guruge JL, Charbonneau M, et al. The long-term stability of the human gut microbiota. *Science*. 2013;341(6141):1237439. doi:10.1126/science.1237439

42. Lee SM, Donaldson GP, Mikulski Z, Boyajian S, Ley K, Mazmanian SK. Bacterial colonization factors control specificity and stability of the gut microbiota. *Nature*. 2013;501(7467):426-429. doi:10.1038/nature12447

43. Fiorentino DF, Zlotnik A, Mosmann TR, Howard M, O'Garra A. IL-10 inhibits cytokine production by activated macrophages. *J Immunol*. 1991;147(11):3815-3822.

44. Mocellin S, Panelli MC, Wang E, Nagorsen D, Marincola FM. The dual role of IL-10. *Trends Immunol*. 2003;24(1):36-43.

45. Ballal SA, Veiga P, Fenn K, et al. Host lysozyme-mediated lysis of Lactococcus lactis facilitates delivery of colitis-attenuating superoxide dismutase to inflamed colons. *Proc Natl Acad Sci USA*. 2015;112(25):7803-7808. doi:10.1073/pnas.1501897112

46. Peña JA, Rogers AB, Ge Z, et al. Probiotic Lactobacillus spp. diminish Helicobacter hepaticus-induced inflammatory bowel disease in interleukin-10-deficient mice. *Infect Immun*. 2005;73(2):912-920. doi:10.1128/IAI.73.2.912-920.2005

47. Thirabunyanon M, Boonprasom P, Niamsup P. Probiotic potential of lactic acid bacteria isolated from fermented dairy milks on antiproliferation of colon cancer cells. *Biotechnol Lett*. 2009;31(4):571-576. doi:10.1007/s10529-008-9902-3

48. Chong ESL. A potential role of probiotics in colorectal cancer prevention: review of possible mechanisms of action. *World J Microbiol Biotechnol*. 2014;30(2):351-374. doi:10.1007/s11274-013-1499-6

49. DePaolo RW, Kamdar K, Khakpour S, Sugiura Y, Wang W, Jabri B. A specific role for TLR1 in protective TH17 immunity during mucosal infection. *Journal of Experimental Medicine*. 2012;209(8):1437-1444. doi:10.1084/jem.20112339

50. Volzing K, Borrero J, Sadowsky MJ, Kaznessis YN. Antimicrobial peptides targeting Gram-negative pathogens, produced and delivered by lactic acid bacteria. *ACS Synth Biol*. 2013;2(11):643-650. doi:10.1021/sb4000367

51. Moolenbeek C, Ruitenberg EJ. The “Swiss roll”: a simple technique for histological studies of the rodent intestine. *Lab Anim*. 1981;15(1):57-59.

52. Suzuki R, Kohno H, Sugie S, Nakagama H, Tanaka T. Strain differences in the susceptibility to azoxymethane and dextran sodium sulfate-induced colon carcinogenesis in mice. *Carcinogenesis*. 2006;27(1):162-169. doi:10.1093/carcin/bgi205

53. Kennedy RJ, Hoper M, Deodhar K, Erwin PJ, Kirk SJ, Gardiner KR. Interleukin 10-deficient colitis: new similarities to human inflammatory bowel disease. *Br J Surg*. 2000;87(10):1346-1351. doi:10.1046/j.1365-2168.2000.01615.x

54. Boivin GP, Washington K, Yang K, et al. Pathology of mouse models of intestinal cancer: consensus report and recommendations. *Gastroenterology*. 2003;124(3):762-777. doi:10.1053/gast.2003.50094

55. Schloss PD, Westcott SL, Ryabin T, et al. Introducing mothur: open-source, platform-independent, community-supported software for describing and comparing microbial communities. *Appl Environ Microbiol*. 2009;75(23):7537-7541.

56. Quince C, Lanzen A, Davenport RJ, Turnbaugh PJ. Removing noise from pyrosequenced amplicons. *BMC Bioinformatics*. 2011;12:38.

57. Pruesse E, Quast C, Knittel K, et al. SILVA: a comprehensive online resource for quality checked and aligned ribosomal RNA sequence data compatible with ARB. *Nucleic Acids Res*. 2007;35(21):7188-7196.

58. Schloss PD, Gevers D, Westcott SL. Reducing the effects of PCR amplification and sequencing artifacts on 16S rRNA-based studies. *PLoS One*. 2011;6(12):e27310.

59. Edgar RC, Haas BJ, Clemente JC, Quince C, Knight R. UCHIME improves sensitivity and speed of chimera detection. *Bioinformatics*. 2011;27(16):2194-2200.

60. Cole JR, Wang Q, Cardenas E, et al. The Ribosomal Database Project: improved alignments and new tools for rRNA analysis. *Nucleic Acids Res*. 2009;37(Database issue):D141-5.

Chapter 7. Conclusions and Perspectives

Conclusions

The interactions between host and microbe are extremely complex. Overall, this thesis elucidates the several ways in which host and microbes interact. In the first study of diet-induced non-alcoholic fatty liver disease, changes in the host physiology were accompanied with drastic changes in the microbiota. The unhealthy westernized diet found increased Firmicutes while the intervention diets had increased probiotic species such as *Bifidobacterium* and *Lactobacillus* species. Whereas other studies and perspectives suggest that treatment through fecal microbiota transplant can potentially alter disease states including NAFLD, our findings demonstrate that diet trumps the microbiota transplants. Furthermore, the study finds that altering the microbiota while maintaining the inflammatory diet could potentially impress a stressful microenvironment on an otherwise healthy-associated microbiota and exacerbate inflammation and disease. These findings emphasize the importance of the following study in which exposure to inflammation-associated omega-6 fatty acid, arachidonic acid, increased the pathogenicity and virulence of *Yersinia enterocolitica.* The study concludes that the high intake of inflammatory fatty acids in westernized diets may be correlated to the rising incidence and prevalence of the enteric pathogens. These studies of nutritional status highlight the value of studying how nutrition impacts the host and microbe individually to grasp the higher understanding of how host and microbes interact.

In addition to the environmental impacts on the microbes, this thesis investigated the mechanisms of microbe-sensing toll-like receptors (TLRs). Despite TLR1 and TLR6 being dimerization partners with TLR2, aberrant signaling in either have different consequences on the microbiota and inflammation. Disruption of TLR1 signaling drastically alters the relationship between host and microbe by diminishing the mucosal barrier, increasing mucosal-associated bacteria and allowing bacterial translocation. While these consequences were dependent on the presence of the microbiota, the TLR1-associated microbiota could not transfer any of the related inflammatory responses including IL-1β and IL-23 production in the host. On the other hand, the study of TLR6 revealed an interesting therapeutic for inflammation-associated colorectal cancer. Whereas the lack of TLR6 signaling alters colonocyte proliferation and worsened disease with

increased tumorgenesis, cohousing and sharing the microbiota between TLR6-sufficient and -deficient mice surprisingly reduced tumorgenesis in wild-type mice. This finding led to a potential therapeutic using live *Lactobacillus* species which were notably depleted during the disease. Interestingly, only the *Lactobacillus sp.* that were originally colonized in wild-type mice provided protection through the production of IL-10 and suppression of *Helicobacter*. Not only do these studies point to contrasting signaling pathways of TLR1/TLR2 and TLR6/TLR2 dimerization, these findings reveal the importance of microbiota signaling in disease. In both studies, the aberrant TLR signaling worsened disease and restoring the microbial ecology could not improve disease without the proper signaling.

In conclusion, both environmental and genetic factors play an important role in regulating the gut microbiota. The plethora of microbes within the intestines can be considered another human organ that is intimately linked to our own health. The state of the microbiota depends on the state of the host and vice versa. Studies are still unraveling if the microbiota is simply a symptom or causal factor in disease. None the less, it is abundantly clear that the microbiota is a crucial component of human health that needs to be considered when treating diseases including obesity and cancer.

Perspectives

Since the discovery of the trillions of microbes inhabiting the human body, there have been momentous progress in understanding just how these microbes affect human health. The market of probiotics and prebiotics for improved intestinal health and integrity is huge and the use of fecal microbiota transplants have considerably changed treatment of severe intestinal infections. Unfortunately, the applications of probiotics and fecal microbiota transplants are largely unregulated and can have negative consequences. Results from probiotic studies in humans have been heterogeneous, ranging from no benefits to significant reduction of symptoms in various diseases. Furthermore, the unexpected popularity of fecal microbiota transplants has led to unsupervised and outright dangerous transfers of microbial communities between individuals. In order to move forward, microbiota studies must be more rigorous and transparent. It is also important to understand that the microbiota is fluid and uniquely personalized to every individual. Additionally, the advances in sequencing has drastically improved the field of microbiology but the knowledge of known microbes in the gut is limited by the difficulty of culturing and isolating elusive microbes.

Overall, the field of microbiome research still has a long way to go with several avenues to improve on but the possibilities are endless. New technologies in sequencing and bioinformatics are constantly being discovered. Researchers and industries are endlessly innovating and inventing new ways to culture the unculturable. As for microbial therapeutics, one way to proceed can be to focus and improve on individual probiotic microbes such the ones found in this thesis. Another method would be to personalize microbiota treatments such as autologous microbiota transplants or identifying the missing or depleted microbes during disease. Whichever concept is explored, the primary aim of microbiota therapeutics is to understand how beneficial microbes interact with the host. While we have only scratched the surface of microbiota research, this field is without a doubt an endless source of scientific advancement headed towards revolutionizing human health.